UNIVERSIDAD DE CHILE
FACULTAD DE CIENCIAS FÍSICAS Y MATEMÁTICAS
DEPARTAMENTO DE INGENIERÍA MATEMÁTICA

AN INVERSE PROBLEM IN FLUID MECHANICS APPLIED IN BIOMEDICINE

TESIS PARA OPTAR AL GRADO DE
DOCTOR EN CIENCIAS DE LA INGENIERÍA,
MENCIÓN MODELACIÓN MATEMÁTICA
EN COTUTELA CON LA UNIVERSIDAD DE GRONINGEN

JORGE SEBASTIÁN AGUAYO ARANEDA

PROFESOR GUÍA:
AXEL OSSES ALVARADO
PROFESOR CO-GUÍA:
ROEL VERSTAPPEN

MIEMBROS DE LA COMISIÓN:
CRISTÓBAL BERTOGLIO BELTRÁN
MURIEL BOULAKIA
JUAN CARLOS DE LOS REYES BUENO
JAIME ORTEGA PALMA

Este trabajo ha sido parcialmente financiado por
Beca Doctorado Nacional ANID 2018 21180642
y CMM ANID BASAL FB210005.

SANTIAGO DE CHILE
2022

RESUMEN DE LA TESIS PARA OPTAR AL GRADO DE
DOCTOR EN CIENCIAS DE LA INGENIERÍA,
MENCIÓN MODELACIÓN MATEMÁTICA
POR JORGE SEBASTIÁN AGUAYO ARANEDA
FECHA: 2022
PROF. GUÍAS: AXEL OSSES ALVARADO, ROEL VERSTAPPEN

UN PROBLEMA INVERSO DE MECÁNICA DE FLUIDOS APLICADO EN BIOMEDICINA

En esta tesis se presentan nuevos avances en problemas inversos de Mecánica de Fluidos en estado estacionario, con aplicaciones directas en la recuperación de deformaciones de dominio y obstáculos, y cuyo propósito es contribuir a la detección de afecciones de la válvula aórtica (como insuficiencia o estenosis).

Como primer resultado de esta tesis, se presenta un resultado de aproximación asintótica entre los problemas de detección de obstáculos y de recuperación de un parámetro de permeabilidad no negativo que asume valores significativamente grandes en las regiones con obstáculos o el valor 0 en otras partes. Este resultado es respaldado con pruebas numéricas que confirman el resultado de aproximación.

El segundo resultado de esta tesis presenta una desigualdad logarítmica para el problema de identificación del parámetro de permeabilidad en la ecuación de Navier-Stokes a partir de mediciones locales de la velocidad del fluido. Se incluyen también pruebas numéricas sobre la recuperación de parámetros suaves y no suaves mediante algoritmos de minimización y de refinamiento adaptativo.

Finalmente, se estudia un problema de identificación de parámetros para las ecuaciones de Oseen y Navier-Stokes que permite recuperar un parámetro de permeabilidad a partir de mediciones locales o globales de la velocidad de un fluido. Varios experimentos numéricos con flujo de Navier-Stokes ilustran la aplicabilidad del método, para la localización de una válvula cardíaca 2D simulada a partir de una resonancia magnética sintética en 2D y también para la recuperación del parámetro de permeabilidad a partir de una resonancia magnética sintética en 3D.

SUMMARY OF THE THESIS TO OBTAIN THE DEGREE OF
DOCTOR EN CIENCIAS DE LA INGENIERÍA,
MENCIÓN MODELACIÓN MATEMÁTICA
BY JORGE SEBASTIÁN AGUAYO ARANEDA
DATE: 2022
ADVISORS: AXEL OSSES ALVARADO, ROEL VERSTAPPEN

AN INVERSE PROBLEM IN FLUID MECHANICS APPLIED IN BIOMEDICINE

In this thesis, new advances are presented in inverse problems of Fluid Mechanics in steady state, with direct applications in the recovery of domain deformations and obstacles, and whose purpose is to contribute to the detection of aortic valve conditions (such as insufficiency or stenosis).

The first main result of this thesis is an asymptotic approximation result between the obstacle detection problems and the recovery of a non-negative permeability parameter that assumes significantly large values in the regions with obstacles or the value 0 in other parts. This result is supported by numerical tests that confirm the approximation result.

The second result of this thesis presents a logarithmic inequality for the identification problem of the permeability parameter on Navier-Stokes equations from local measurements of fluid velocity. Numerical tests on the recovery of smooth and non-smooth parameters by a minimization problem and adaptive refinement algorithms are also included.

Finally, a parameter identification problem for the Oseen and Navier-Stokes equations is studied in order to recover a permeability parameter from local or global measurements of the fluid velocity. Several numerical experiments using Navier-Stokes flow illustrate the applicability of the method, for the localization of a simulated 2D cardiac valve from synthetic MRI and also recovering of the permeability parameter from 3D synthetic MRI.

"Sometimes, the best way to solve your own problems is to help someone else"

— Iroh to Avatar Korra, *The Legend of Korra*

"A veces, la mejor forma de resolver tus propios problemas es ayudando a alguien más"

— Iroh al Avatar Korra, *La Leyenda de Korra*

"Soms is de beste manier om je eigen problemen op te lossen, iemand anders te helpen"

— Iroh naar Avatar Korra, *De Legende van Korra*

Agradecimientos

Durante estos cuatro años, he entregado lo mejor de mí en realizar mis estudios de doctorado y esta tesis. Las circunstancias de esta tesis fueron muy particulares, donde muchos de nosotros debimos alejarnos de nuestros colegas y amigos debido a la pandemia por COVID-19, modificando los planes y perspectivas futuras constantemente. Sin embargo, no hubiese logrado todo esto sin el apoyo de diversas personas e instituciones.

En primer lugar, agradezco al Gobierno de Chile y a su Agencia Nacional de Investigación y Desarrollo (ANID) por conferirme la Beca de Doctorado Nacional 2018 21180642, la cual financió mis estudios y mi estadía en la Universidad de Groningen.

Agradezco a mi alma mater, la Universidad de Concepción, por entregarme todas las herramientas para acceder a un programa de doctorado. La guía, recomendaciones y consejos de los profesore Dr. Julio Aracena, Dr. Rodolfo Araya y Dr. Rodolfo Rodríguez fueron fundamentales para seguir un camino dentro de la academia.

A mis profesores guía de mi tesis, Dr. Axel Osses y Dr. Roel Verstappen, y al co-supervisor Dr. Cristóbal Bertoglio, les agradezco la libertad de seguir mis propias convicciones, las arduas correcciones de mis manuscritos y mis resultados, su cordialidad y disposición a trabajar en medio de una pandemia. Sin duda ustedes han dejado su huella en mí. También agradezco a todos los profesores que conforman mis comisiones de evaluación de mi tesis, tanto en la Universidad de Chile como en la Universidad de Groningen, y al Dr. Hugo Carrillo con quien trabajé en un artículo que se convirtió en uno de los capítulos de esta tesis.

A la Facultad de Ciencias Físicas y Matemáticas de la Universidad de Chile, le agradezco su cordialidad y formación científica. Desde el primer día me sentí respetado y acogido, permitiéndome crecer como científico y como persona. A Silvia Mariano y la Dra. Natacha Astromujoff, por nombrar parte del personal administrativo, les agradezco la diligencia con mis trámites y en la solución de diversos problemas de papeleo. A los profesores del Departamento de Ingeniería Matemática, por instruirme con sus clases y profundas conversaciones, tanto científicas como de la vida cotidiana. A Laura, Sebastián, Emilio, Jessica, Yamit, Daniel, Juan José y Hugo, mis compañeros de doctorado en esta universidad, les agradezco todo el apoyo emocional que me brindaron. Las conversaciones diarias con una taza de té y sus constantes bromas serán algo que atesoraré toda mi vida.

A la Universidad de Groningen y a su Instituto Bernoulli, por recibirme con los brazos abiertos en sus instalaciones. Al integrarme en CardioMath, mis compañeros Miriam, Giorgia, Jeremías y Riedmen contribuyeron notablemente en los avances de mi tesis. Les deseo lo mejor en su futuro. Agradezco también al CIT de la Universidad de Groningen por su apoyo y por proporcionar acceso al clúster HPC Peregrine.

A todos esos amigos que siguieron en mi vida, a pesar de la distancia, y a los que fui conociendo durante mis cuatro años de doctorado, les agradezco de todo corazón su compañía, su empatía y aliento en los tiempos difíciles. A Cristian, Joaquín y Felipe, les agradezco por darme las más entretenidas partidas de Magic: el encuentro, acompañadas por las conversaciones de todo tipo. A Paz, Catalina, Nathalie, Natalia, Daniel, Alejandro, Rodrigo, Felipe y Jorge, por acompañarme en diversas etapas de mi doctorado, entregándome consuelo en momentos de atribulación, risas variadas y un abrazo fraterno en cada momento. A Cala, Isa, Claudia, Rafael, Juan, Rodrigo y muchos otros amigos que conocí en Groningen, les agradezco por acogerme en otro país y empaparme con sus vivencias y su vibrante energía. En especial, le agradezco a Elena, quien se convirtió en una hermanita menor durante esos 6 meses en Groningen. Sin duda serás una gran científica.

A Natalia Soto, por aparecer en un momento muy especial de mi vida y darle un matiz especial, convirtiéndose en una amiga que me acompañó en toda circunstancia rompiendo la barrera de la distancia, siendo confidente y consejera. Te agradezco todos esos momentos compartidos, las conversaciones diarias y la oportunidad de conocer y compartir con tu familia. Las rebeliones se empiezan con esperanza, Natalia, nunca lo olvides.

Finalmente, a toda mi familia por su compañía y apoyo incondicional. A mis padres, Jorge e Isis, a mi hermana Isis Camila y mi prima Sigrid (que en el fondo es como mi hermana mayor) y al pequeño Facundo. Gracias por comprender mi sacrificio, mi dolor físico y del alma, por ensalzar mis pequeños éxitos y por motivarme a conseguir muchos más. Por su cariño, su confianza y el eterno amor que nos tenemos, muchas e infinitas gracias.

Table of Content

Chapter 1

Introduction

In this thesis, new advances are presented in inverse problems of Fluid Mechanics in steady state, with direct applications in the recovery of domain deformations and obstacles, and whose purpose is to contribute to the detection of aortic valve conditions (such as insufficiency or stenosis).

The partial differential equations (PDEs) are equations where the unknowns are functions and where not only the functions themselves appear in the equations but also their derivatives. PDEs are used in the mathematical modelling, distributed in space and time, of processes in engineering, physics and other sciences such that propagation of heat, electrodynamics, fluid dynamics, elasticity and many others. In the analysis of PDEs, a problem is considered direct when, knowing the domain, smoothness conditions and all the parameters of an equation or system of equations, the solution of the equation or system of equations is obtained in response. A problem is considered inverse when, knowing total or partial information of the solution of the equation or system of equations, some of the required data (generally one of these data) are unknown.

The human blood is a body fluid that delivers necessary substances such as nutrients and oxygen to the cells and transports metabolic waste products away from those same cells. Blood is circulated around the body through blood vessels by the pumping action of the heart. The aortic valve is one of the four valves of the human heart located between the left ventricle and the aorta. It usually has three leaflets, however in 1-2% of the population it is found that it has two leaflets due to congenital conditions. This valve is the last heart structure that blood travels through before stopping flow through the systemic circulation. A proper aortic valve closure helps maintain high pressure in the systemic circulation while lowering ventricular pressure and allowing blood flow from the lungs to fill the left ventricle. An inadequate closure produces diastolic pressure losses and aortic regurgitation, with the possibility of developing heart failure and pulmonary edema. Inadequate opening of the aortic valve, often due to calcification, results in higher velocities through the valve and higher pressure gradients. The diagnosis of aortic stenosis depends on the quantification of this gradient. The insuffiency and stenosis can lead to left ventricular hypertrophy.

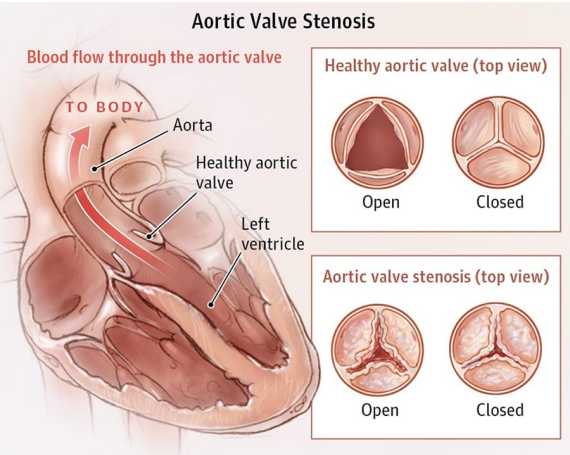

Figure 1.1: Aortic Valve Stenosis

One of the medical challenges about aortic valve malfunctions is early detection of them. In this context, it is desirable to obtain an estimate of the valve shape when the valve is fully open, where it is possible to consider that the blood is a Newtonian fluid following a steady state. Then, the aortic valve can be modeled as an obstacle or a domain deformation from a control domain. For instance, the aortic valve is very thin (0.5 mm), and therefore its shape can be imaged nowadays using only two modalities: computerized tomography (CT) and transesophageal echocardiography (TEE). Since CT is based on X-rays, it is only used in patients that are selected for valvular replacement in order to obtain the aortic root dimensions for sizing the prosthesis. Such CT images are usually obtained when the valve is closed. Obtaining the image at open valve position requires about 5 times larger radiation dose since the complete cardiac cycle has to be imaged. This is equivalent to the annual recommended total radiation dose. TEE is a newer technique, but highly invasive: a wire is inserted through the esophagus of the patient involving a cumbersome procedure. TEE is most of the time applied to monitor valve surgeries, and is therefore rarely applied in a diagnostic phase.

Magnetic resonance imaging (MRI) allows to image anatomical structures in a non-invasive and nonionising way. Unfortunately, the aortic valve geometry is not directly visible with MRI, since the valve thickness is smaller than the image voxel size. However, visual inspection of 3D Flow MRI Imaging data sets clearly shows that the valvular shape could be retrieved from the flow pattern in the valve surroundings. This fact motivates to formulate, analyze and numerically assess the inverse problem of inferring rigid obstacles from interior velocity measurements, with the ultimate goal of recovering the shape of cardiac valves at the opening position from velocity images.

One of the difficulties of this problem is the mathematical modeling as a parameter identification problem. Although the problem consists of recovering the shape of an obstacle or domain deformations, which is the explicit problem, this problem can be asymptotically approximated to a problem of recovery of a permeability parameter (also called porosity parameter) that follows Brinkham's law, which is the implicit problem. Then, the focuses of this thesis are the deduction of the asymptotic approximation between the explicit and implicit problems using homogenization techniques and the analysis of the inverse problem of recovering the permeability coefficient, presenting stability estimates and a technique to

find numerical approximations of this permeability coefficient from synthetic data.

1.1 Research objectives

The objectives of this thesis are the following

1. Establish equivalences between the explicit and the implicit problem. In Chapter 2, results are presented that allow the explicit problem to be approximated asymptotically by one where the obstacles or domain deformations are represented by a permeability parameter. For this, this parameter is a non-negative function that is equal to a sufficiently large constant $R > 0$ in regions where there are obstacles or domain deformations or equal to 0 otherwise.
2. Establish uniqueness and stability results for the implicit problem from local measurements of the velocity. In Chapter 3, a stability result for the inverse problem of recovering a smooth scalar permeability parameter given by the Brinkman's law applied on steady Navier-Stokes equations with local observations of the fluid velocity on a fixed domain is studied and deducted from Carleman inequalities. This logarithmic estimate requieres a weaker version of a non-degeneracy condition, but it is based in a strategy that does not require pressure observations, showing a new way to deduce Carleman estimates for the linearized Navier-Stokes equations.
3. Model the inverse problem using the Oseen and Navier-Stokes equations, designing an approximated problem that allow us to reconstruct a realistic estimate of the valve. In Chapters 4 and 5, a penalization parameter method for obstacle identification in an incompressible fluid flow for modified versions of the Oseen equations and the Navier-Stokes equations is presented. The proposed method consists in adding a permeability term following the Brinkman's law to the system such that some subset of its boundary support represents the obstacle. This allows to work in a fixed domain and highly simplify the solution of the inverse problem via some suitable cost functional. Existence of minimizers and first and second order optimality conditions are derived through the differentiability of the solutions of the Oseen and Navier-Stokes equations with respect to the permeability coefficient. Finally, several numerical experiments using Navier-Stokes flow illustrate the applicability of the method, for the localization of a simulated 2D cardiac valve from synthetic MRI and also recovering of the permeability parameter from 3D synthetic MRI.

1.2 A review of Navier-Stokes equations with some variations

The Navier-Stokes equations are nonlinear PDEs which describe expressions for the conservation of momentum and mass for Newtonian viscous fluids as a function of fluid velocity and pressure, knowing the permeability of the media, viscosity and density of the fluid. These equations are elliptic in space and parabolic in time. These equations are very useful for

describing physics and engineering phenomena, with applications in meteorology, aerodynamics and ocean currents, among others. In their simplified variational formulation, the Navier-Stokes equations contribute, for example, to the design of vehicles, chemical and metallurgical reactors, and the study of hemodynamics. In this section, notations and the Navier-Stokes equations with the respective boundary conditions are presented, emphasizing the results of existence and uniqueness of solution with non-homogenous Dirichlet and directional do-nothing boundary conditions.

1.2.1 Notations

Consider a non-empty bounded domain $\Omega \subseteq \mathbb{R}^d$, with $d \in \{2, 3\}$. The Lebesgue measure of Ω is denoted by $|\Omega|$, which extends to lesser dimension spaces. The norm and seminorms for Sobolev spaces $W^{m,p}(\Omega)$ is denoted by $\|\cdot\|_{m,p,\Omega}$ and $|\cdot|_{m,p,\Omega}$, respectively. For $p = 2$, the norm, seminorms and inner product of the space $W^{m,2}(\Omega) = H^m(\Omega)$ are denoted by $\|\cdot\|_{m,\Omega}$, $|\cdot|_{m,\Omega}$ and $(\cdot,\cdot)_{m,\Omega}$, respectively. Also, $\mathcal{C}^m(\Omega)$ and $\mathcal{C}^\infty(\Omega)$ denote the space of functions with m continuous derivatives and all continuous derivatives, respectively. For Ω_1 and Ω_2 two open subsets of $\mathbb{R}^3$, we denote $\Omega_1 \Subset \Omega_2$ when there exists a compact set K such that $\Omega_1 \subseteq K \subseteq \Omega_2$. The spaces $\boldsymbol{H}^m(\Omega)$, $\boldsymbol{W}^{m,p}(\Omega)$, $\boldsymbol{C}^m(\Omega)$ and $\boldsymbol{C}^\infty(\Omega)$ are defined by $\boldsymbol{H}^m(\Omega) = [H^m(\Omega)]^d$, $\boldsymbol{W}^{m,p}(\Omega) = [W^{m,p}(\Omega)]^d$, $\boldsymbol{C}^m(\Omega) = [\mathcal{C}^m(\Omega)]^d$ and $\boldsymbol{C}^\infty(\Omega) = [\mathcal{C}^\infty(\Omega)]^d$. The notation for norms, seminorms and inner products will be extended from $W^{m,p}(\Omega)$ or $H^m(\Omega)$. Given $\boldsymbol{a}, \boldsymbol{b} \in \mathbb{R}^3$, $[\boldsymbol{a}]_j$ denotes the $j-$th component of vector $\boldsymbol{a}$, $\boldsymbol{a}^T$ denotes the transpose vector of $\boldsymbol{a}$ and $\boldsymbol{a} \times \boldsymbol{b}$ denotes the cross product given by

$$\boldsymbol{a} \times \boldsymbol{b} = \left([\boldsymbol{a}]_2 [\boldsymbol{b}]_3 - [\boldsymbol{a}]_3 [\boldsymbol{b}]_2, [\boldsymbol{a}]_3 [\boldsymbol{b}]_1 - [\boldsymbol{a}]_1 [\boldsymbol{b}]_3, [\boldsymbol{a}]_1 [\boldsymbol{b}]_2 - [\boldsymbol{a}]_2 [\boldsymbol{b}]_1\right)^T$$

Also, $\nabla \times \boldsymbol{u}$ (or $\operatorname{curl} \boldsymbol{u}$) denotes the curl of $\boldsymbol{u}$, given by

$$\nabla \times \boldsymbol{u} = \left(\frac{\partial [\boldsymbol{u}]_3}{\partial x_2} - \frac{\partial [\boldsymbol{u}]_2}{\partial x_3}, \frac{\partial [\boldsymbol{u}]_1}{\partial x_3} - \frac{\partial [\boldsymbol{u}]_3}{\partial x_1}, \frac{\partial [\boldsymbol{u}]_2}{\partial x_1} - \frac{\partial [\boldsymbol{u}]_1}{\partial x_2}\right)^T$$

For $\boldsymbol{a}, \boldsymbol{b} \in \mathbb{R}^2$, $w \in H^1(\Omega)$ and $\boldsymbol{w} \in \boldsymbol{H}^1(\Omega)$, we define

$$\begin{aligned} \boldsymbol{a} \times \boldsymbol{b} &= [\boldsymbol{a}]_1 [\boldsymbol{b}]_2 - [\boldsymbol{a}]_2 [\boldsymbol{b}]_1 \\ \operatorname{curl} w &= \left(\frac{\partial w}{\partial x_2}, \frac{\partial w}{\partial x_1}\right)^T \\ \operatorname{curl} \boldsymbol{w} &= \frac{\partial [\boldsymbol{w}]_2}{\partial x_1} - \frac{\partial [\boldsymbol{w}]_1}{\partial x_2} \end{aligned}$$

1.2.2 The equations for the direct problem

This thesis studies the steady state Navier-Stokes equations following the Brinkman's law for imcompressible fluids, where the density is constant, which are given by

$$\begin{aligned} -\nu \triangle \boldsymbol{u} + (\nabla \boldsymbol{u})\, \boldsymbol{u} + \nabla \boldsymbol{p} + \gamma \boldsymbol{u} &= \boldsymbol{f} \\ \operatorname{div} \boldsymbol{u} &= 0 \end{aligned}$$

where the unknowns are the pair $(\boldsymbol{u}, p)$, where $\boldsymbol{u}$ is the velocity and p is pressure of the fluid, resepctively. The parameters of this equations are the kinematic viscosity of the fluid ν, the permeability media coefficient γ and the external source $\boldsymbol{f}$.

The first equation is the convective form of the conservation of momentum equation. The term $\gamma\boldsymbol{u}$ is given by the Brinkman's law, where a porous media offers some resistance to fluid movement. The coefficient γ is non-negative. When $\gamma = 0$, the media is completely porous and we can recover the original version of the Navier-Stokes equations. The fluid movement is damped in regions where γ assumes large values. The second equation represents the conservation of mass.

Defining a suitable control volume given by a bounded domain Ω and defining appropriate boundary conditions on $\partial\Omega$, it is possible to study some characteristics of the solutions of the Navier-Stokes equations and model some specific phenomena. If Ω has a Lipschitz boundary $\partial\Omega = \Gamma_D \cup \Gamma_N$ with a outer normal vector $\boldsymbol{n}$, where $\text{int}(\Gamma_D) \cap \text{int}(\Gamma_N) = \emptyset$ and $|\Gamma_D| \neq 0 \neq |\Gamma_N|$, the equations with the respective boundary condition can be written as

$$\begin{aligned} -\nu\triangle\boldsymbol{u} + (\nabla\boldsymbol{u})\,\boldsymbol{u} + \nabla\boldsymbol{p} + \gamma\boldsymbol{u} &= \boldsymbol{f} && \text{in } \Omega \\ \operatorname{div}\boldsymbol{u} &= 0 && \text{in } \Omega \\ \boldsymbol{u} &= \boldsymbol{g} && \text{on } \Gamma_D \\ -\nu\frac{\partial\boldsymbol{u}}{\partial\boldsymbol{n}} + p\boldsymbol{n} + \frac{1}{2}(\boldsymbol{u}\cdot\boldsymbol{n})_-\,\boldsymbol{u} &= \boldsymbol{0} && \text{on } \Gamma_N \end{aligned} \tag{1.1}$$

where $\boldsymbol{f} \in \boldsymbol{H}^{-1}(\Omega)$, $\boldsymbol{g} \in \boldsymbol{H}^{1/2}(\Gamma_D)$ and

$$(\forall x \in \mathbb{R}) \quad (x)_- = \begin{cases} 0 & \text{if } x \geq 0 \\ x & \text{if } x < 0 \end{cases}$$

for all $x \in \mathbb{R}$. The boundary condition $\boldsymbol{u} = \boldsymbol{g}$ on Γ_D is a classical Dirichlet condition. Particularly, in some subsets of Γ_D where $\boldsymbol{g} = \boldsymbol{0}$ it is called no-slip condition. The boundary condition $-\nu\frac{\partial\boldsymbol{u}}{\partial\boldsymbol{n}} + p\boldsymbol{n} + \frac{1}{2}(\boldsymbol{u}\cdot\boldsymbol{n})_-\,\boldsymbol{u} = \boldsymbol{0}$ on Γ_N is known as directional do nothing condition. In comparison with the traditional do nothing condition given by $-\nu\frac{\partial\boldsymbol{u}}{\partial\boldsymbol{n}} + p\boldsymbol{n} = \boldsymbol{0}$ on Γ_N, the directional do nothing condition imposed on Γ_N allows to prove the existence of solution using energy estimates (see [22]) for stable backflow on the open boundary.

1.2.3 Existence and uniqueness of weak solutions for the direct problem

The study of existence and uniqueness of weak solutions to the Navier-Stokes equations has been analyzed for two general cases: and directional do-nothing condition on $\Gamma_N \subseteq \partial\Omega$ with homogenous Dirichlet boundary condition on $\partial\Omega \setminus \Gamma_N$ (see [22]), and inhomogenous Dirichlet boundary conditions (see Section IX.4 in [48]). Then, it is necessary to establish the existence and uniqueness of weak solutions of Equations (1.1). In order to simplifying this analysis, an equivalent formulation with homogeneous Dirichlet boundary condition is proposed. First, it is necessary to cite a version of Trace Theorem and other auxiliary results.

Theorem 1.2.1. *Let $\Omega \subseteq \mathbb{R}^N$ be a bounded domain with locally Lipschitz boundary $\partial\Omega$. There exists a linear operator $T : H^1(\Omega) \to H^{1/2}(\partial\Omega)$ such that there exists a constant $c_T > 0$ only depending of Ω such that*

$$(\forall u \in H^1(\Omega)) \quad \|T(u)\|_{1/2,\partial\Omega} \leq c_T \|u\|_{1,\Omega} \qquad \|u\|_{1,\Omega} \leq c_T \|T(u)\|_{1/2,\Omega}$$

and $T(u) = u$ on $\partial\Omega$ when u is also a continuous function in $\overline{\Omega}$.

Proof. See Theorem II.4.1 in [48] □

Lemma 1.2.1. *Let $\eta > 0$ and $M > 0$ such that $\|\boldsymbol{g}\|_{1/2,\Gamma_N} \leq M$. There exists $\boldsymbol{h} \in \boldsymbol{H}^1(\Omega)$ such that $\operatorname{div} \boldsymbol{h} = 0$, $\boldsymbol{h} = \boldsymbol{u}_D$ on Γ_D and*

$$\left(\forall \boldsymbol{v} \in \boldsymbol{H}^1(\Omega)\right) \quad |((\nabla \boldsymbol{h})\boldsymbol{v}, \boldsymbol{v})| \leq \eta |\boldsymbol{v}|^2_{1,\Omega}$$

and a constant $c_1 > 0$, that only depends of Ω, Γ_N, ε and M such that

$$\|\boldsymbol{h}\|_{1,\Omega} \leq c \|\boldsymbol{u}_D\|_{1/2,\Gamma_N}$$

Proof. Let $\varepsilon > 0$ and $\boldsymbol{g}^* \in \boldsymbol{H}^{1/2}(\partial\Omega)$, with $\boldsymbol{g}^*$ an extension of $\boldsymbol{g}$ such that $\|\boldsymbol{g}^*\|_{1/2,\Gamma_N} \leq 2\|\boldsymbol{g}\|_{1/2,\Gamma_D}$ and

$$\int_{\partial\Omega} \boldsymbol{g}^* \cdot \boldsymbol{n} \, dS = 0$$

Applying Lemma IV.2.3 in [50], we obtain the existence of $\boldsymbol{h} \in \boldsymbol{H}^1(\Omega)$ such that $\operatorname{div} \boldsymbol{h} = 0$, $\boldsymbol{h} = \boldsymbol{g}^*$ on $\partial\Omega$ and

$$\left(\forall \boldsymbol{v} \in \boldsymbol{H}^1(\Omega)\right) \quad |((\nabla \boldsymbol{h})\boldsymbol{v}, \boldsymbol{v})| \leq \varepsilon |\boldsymbol{v}|^2_{1,\Omega}$$

In particular, $\boldsymbol{h} = \boldsymbol{g}$ on Γ_D, proving the first part of the lemma. The existence of c is obtained using Lemma IX.4.2 in [48]. □

Let $\boldsymbol{h} \in \boldsymbol{H}^1(\Omega)$ constructed in Lemma 1.2.1 for $\eta = \dfrac{\nu}{4\beta}$, taking $\boldsymbol{v} = \boldsymbol{u} - \boldsymbol{h}$ and $\boldsymbol{F} = \boldsymbol{f} + \nu\triangle\boldsymbol{h} - (\nabla \boldsymbol{h})\boldsymbol{h} - \gamma\boldsymbol{h}$ in $\boldsymbol{H}^{-1}(\Omega)$, the model problem can be written in a new equivalent form.

$$\begin{aligned} -\nu\triangle\boldsymbol{v} + (\nabla\boldsymbol{v})\boldsymbol{v} + ((\nabla\boldsymbol{v})\boldsymbol{h} + (\nabla\boldsymbol{h})\boldsymbol{v}) + \nabla p + \gamma\boldsymbol{v} &= \boldsymbol{F} && \text{in } \Omega \\ \operatorname{div}\boldsymbol{v} &= 0 && \text{in } \Omega \\ \boldsymbol{v} &= \boldsymbol{0} && \text{on } \Gamma_D \\ -\nu\frac{\partial\boldsymbol{v}}{\partial\boldsymbol{n}} + p\boldsymbol{n} + \frac{1}{2}((\boldsymbol{v}+\boldsymbol{h})\cdot\boldsymbol{n})_-(\boldsymbol{v}+\boldsymbol{h}) &= \nu\frac{\partial\boldsymbol{h}}{\partial\boldsymbol{n}} && \text{on } \Gamma_N \end{aligned} \tag{1.2}$$

A first step is to introduce some helpful notations.

Definition 1.2.1. *The space $\boldsymbol{H}^1_{\Gamma_D}(\Omega)$, subspace of $\boldsymbol{H}^1(\Omega)$, is defined by*

$$\boldsymbol{H}^1_{\Gamma_D}(\Omega) = \left\{\boldsymbol{v} \in \boldsymbol{H}^1(\Omega) \mid \boldsymbol{v} = \boldsymbol{0} \text{ on } \Gamma_D\right\}.$$

Analogously, the space $L_0^2(\Omega)$ *is defined by*

$$L_0^2(\Omega) = \left\{ p \in L^2(\Omega) \mid (p,1)_{0,\Omega} = 0 \right\}.$$

Also, it is denoted $\mathcal{H} = \boldsymbol{H}^1_{\Gamma_D}(\Omega) \times L_0^2(\Omega)$*, which is a Banach space behind the norm*

$$\|[\boldsymbol{v}, p]\|_{\mathcal{H}} = \nu \, |\boldsymbol{v}|_{1,\Omega} + \|p\|_{0,\Omega}$$

Theorem 1.2.2. *Let* $\Gamma \subseteq \partial\Omega$ *with* $|\Gamma| > 0$*. There exists* $C_{FP} > 0$*, only dependent of* Ω*, such that*

$$\begin{aligned} \left(\forall \boldsymbol{v} \in \boldsymbol{H}^1_{\Gamma_D}(\Omega)\right) \quad & \|\boldsymbol{v}\|_{1,\Omega} \leq C_{FP} \, |\boldsymbol{v}|_{1,\Omega} \\ \left(\forall \boldsymbol{v} \in \boldsymbol{H}^1(\Omega)\right) \quad & \|\boldsymbol{v}\|^2_{1,\Omega} \leq C_{FP} \left(|\boldsymbol{v}|^2_{1,\Omega} + \|\boldsymbol{v}\|^2_{0,\Gamma} \right) \end{aligned}$$

Proof. See Section 6.6 in [36]. □

Lemma 1.2.2. *The application* $a : \boldsymbol{H}^1(\Omega) \times \boldsymbol{H}^1(\Omega) \times \boldsymbol{H}^1_{\Gamma_D}(\Omega) \to \mathbb{R}$*, defined by*

$$a(\boldsymbol{u}, \boldsymbol{v}, \boldsymbol{w}) = ((\nabla \boldsymbol{v})\, \boldsymbol{u}, \boldsymbol{w})_{0,\Omega}$$

is continuous and there exists a constant $\kappa_1 > 0$*, only depending of* Ω*, such that*

$$(\forall (\boldsymbol{u}, \boldsymbol{v}, \boldsymbol{w}) \in \boldsymbol{H}^1(\Omega) \times \boldsymbol{H}^1(\Omega) \times \boldsymbol{H}^1_{\Gamma_D}(\Omega)) \quad |a(\boldsymbol{u}, \boldsymbol{v}, \boldsymbol{w})| \leq \kappa_1 \, \|\boldsymbol{u}\|_{1,\Omega} \, |\boldsymbol{v}|_{1,\Omega} \, |\boldsymbol{w}|_{1,\Omega}$$

Proof. See Lemma IX.1.1 in [48]. □

Lemma 1.2.3. *The application* $b : \boldsymbol{H}^{1/2}(\partial\Omega) \times \boldsymbol{H}^{1/2}(\partial\Omega) \times \boldsymbol{H}^{1/2}(\partial\Omega) \to \mathbb{R}$*, defined by*

$$b(\boldsymbol{u}, \boldsymbol{v}, \boldsymbol{w}) = \int_{\Gamma_N} (\boldsymbol{u} \cdot \boldsymbol{n})\, (\boldsymbol{v} \cdot \boldsymbol{w}) \; dS,$$

is continuous and there exists a constant $\kappa_2 > 0$*, only depending of* Ω*, such that*

$$\left(\forall \boldsymbol{u}, \boldsymbol{v}, \boldsymbol{w} \in \boldsymbol{H}^{1/2}(\partial\Omega)\right) \qquad |b(\boldsymbol{u}, \boldsymbol{v}, \boldsymbol{w})| \leq \kappa_2 \, \|\boldsymbol{u}\|_{1/2,\Gamma_N} \, \|\boldsymbol{v}\|_{1/2,\Gamma_N} \, \|\boldsymbol{w}\|_{1/2,\Gamma_N}$$

Proof. From Hölder inequality, we obtain

$$|b(\boldsymbol{u}, \boldsymbol{v}, \boldsymbol{w})| \leq \kappa_2 \, \|\boldsymbol{u}\|_{0,\Gamma_N} \, \|\boldsymbol{v}\|_{0,4,\Gamma_N} \, \|\boldsymbol{w}\|_{0,4,\Gamma_N}$$

Applying Sobolev Embedding Theorem, Theorems 1.2.2 and 1.2.1, the embedding from $\boldsymbol{H}^{1/2}(\Omega)$ to $\boldsymbol{L}^q(\Gamma_N)$ is continuous for $q \in [2,4]$ and there exists a constant $c_1 > 0$, only depending of Ω, such that

$$\begin{aligned} |b(\boldsymbol{u}, \boldsymbol{v}, \boldsymbol{w})| &\leq \|\boldsymbol{u}\|_{0,\Gamma_N} \, \|\boldsymbol{v}\|_{0,4,\Gamma_N} \, \|\boldsymbol{w}\|_{0,4,\Gamma_N} \\ &\leq \|\boldsymbol{u}\|_{0,\Gamma_N} \left(c_1 \, \|\boldsymbol{v}\|_{1/2,\Gamma_N} \right) \left(c_1 \, \|\boldsymbol{w}\|_{1/2,\Gamma_N} \right) \\ &\leq c_1^2 \, \|\boldsymbol{u}\|_{1/2,\Gamma_N} \, \|\boldsymbol{v}\|_{1/2,\Gamma_N} \, \|\boldsymbol{w}\|_{1/2,\Gamma_N} \end{aligned}$$

Taking $\kappa_2 = c_1^2 > 0$, the lemma is proved. □

Definition 1.2.2. *We define* $\kappa = \max_{j,k\in\{0,1,2,3\}} \left\{\kappa_1 C_{FP}, \kappa_2 c_T^j C_{FP}^k\right\}$.

The existence and uniqueness of weak solutions is proved in [22] in the case where $\boldsymbol{u}_D = \boldsymbol{0}$. However, the difference between Equation (1.2) and the equation analyzed in [22] is given by a modification on the "directional do nothing condition". Then, it is necessary to repeat the analysis of existence and uniqueness of solution.

Theorem 1.2.3. *Let* $\boldsymbol{u}_D \in \boldsymbol{H}^{1/2}(\Gamma_D)$. *If* $2\kappa \|\boldsymbol{u}_D\|_{1/2,\Omega} \leq \nu$, *then Equation* (1.2) *has at least one weak solution* $(\boldsymbol{u}, p) \in \mathcal{H}$ *and there exist* $C_1, C_2 > 0$, *such that*

$$\nu |\boldsymbol{u}|_{1,\Omega} \leq C_1 \left(\|\boldsymbol{f}\|_{-1,\Omega} + \|\boldsymbol{g}\|_{1/2,\Gamma_D} + \|\boldsymbol{g}\|_{1/2,\Gamma_D}^2 \right)$$
$$\|p\|_{0,\Omega} \leq C_1 C_2 \left(\|\boldsymbol{f}\|_{-1,\Omega} + |\boldsymbol{u}|_{1,\Omega} + \|\boldsymbol{g}\|_{1/2,\Gamma_D} + \left(\|\boldsymbol{f}\|_{-1,\Omega} + \|\boldsymbol{g}\|_{1/2,\Gamma_D} + \|\boldsymbol{g}\|_{1/2,\Gamma_D}^2 \right)^2 \right)$$

Furthermore, if $\dfrac{3\kappa C_1}{2\nu^2} \left(\|\boldsymbol{f}\|_{-1,\Omega} + \|\boldsymbol{g}\|_{1/2,\Gamma_D} + \|\boldsymbol{g}\|_{1/2,\Gamma_D}^2 \right) < 1$, *then Equation* (1.2) *has a unique weak solution.*

Proof. First, testing the equations of (1.2) with $\boldsymbol{w} \in \boldsymbol{H}^1_{\Gamma_D}(\Omega)$ and $q \in L^2_0(\Omega)$, respectively, and applying integration by parts, we obtain

$$\begin{aligned} \nu (\nabla \boldsymbol{v}, \nabla \boldsymbol{w})_{0,\Omega} + ((\nabla \boldsymbol{v})\, \boldsymbol{v}, \boldsymbol{w})_{0,\Omega} + ((\nabla \boldsymbol{v})\, \boldsymbol{h}, \boldsymbol{w})_{0,\Omega} + ((\nabla \boldsymbol{h})\, \boldsymbol{v}, \boldsymbol{w})_{0,\Omega} \\ - (p, \operatorname{div} \boldsymbol{w}) + (\gamma \boldsymbol{v}, \boldsymbol{w})_{0,\Omega} - \frac{1}{2} \left(((\boldsymbol{v} + \boldsymbol{h}) \cdot \boldsymbol{n})_- (\boldsymbol{v} + \boldsymbol{h}), \boldsymbol{w} \right)_{0,\Gamma_N} = \langle \boldsymbol{F}, \boldsymbol{w} \rangle \\ (q, \operatorname{div} \boldsymbol{v}) = 0 \end{aligned}$$

where $\langle \cdot, \cdot \rangle$ denotes the duality product between $\boldsymbol{H}^{-1}(\Omega)$ and $\boldsymbol{H}^1(\Omega)$. Taking $\boldsymbol{w} = \boldsymbol{v}$ and $q = p$, we obtain

$$\begin{aligned} &\nu |\boldsymbol{v}|_{1,\Omega}^2 + ((\nabla \boldsymbol{v})\, \boldsymbol{v}, \boldsymbol{v})_{0,\Omega} + ((\nabla \boldsymbol{v})\, \boldsymbol{h}, \boldsymbol{v})_{0,\Omega} + ((\nabla \boldsymbol{h})\, \boldsymbol{v}, \boldsymbol{v})_{0,\Omega} + (\gamma \boldsymbol{v}, \boldsymbol{v})_{0,\Omega} \\ &- \frac{1}{2} \left(((\boldsymbol{v} + \boldsymbol{h}) \cdot \boldsymbol{n})_- \boldsymbol{v}, \boldsymbol{v} \right)_{0,\Gamma_N} - \frac{1}{2} \left(\left[((\boldsymbol{v} + \boldsymbol{h}) \cdot \boldsymbol{n})_- - (\boldsymbol{h} \cdot \boldsymbol{n})_- \right] \boldsymbol{h}, \boldsymbol{v} \right)_{0,\Gamma_N} \\ &= \langle \boldsymbol{F}, \boldsymbol{v} \rangle + \frac{1}{2} \left((\boldsymbol{h} \cdot \boldsymbol{n})_- \boldsymbol{h}, \boldsymbol{v} \right)_{0,\Gamma_N} \end{aligned}$$

where

$$\begin{aligned} &((\nabla \boldsymbol{v})\, \boldsymbol{v}, \boldsymbol{v})_{0,\Omega} + ((\nabla \boldsymbol{v})\, \boldsymbol{h}, \boldsymbol{v})_{0,\Omega} - \frac{1}{2} \left(((\boldsymbol{v} + \boldsymbol{h}) \cdot \boldsymbol{n})_- \boldsymbol{v}, \boldsymbol{v} \right)_{0,\Gamma_N} \\ =& \frac{1}{2} \left(((\boldsymbol{v} + \boldsymbol{h}) \cdot \boldsymbol{n})_+, |\boldsymbol{v}|^2 \right)_{0,\Gamma_N} \geq 0 \end{aligned}$$

and

$$\begin{aligned} \left| -\frac{1}{2} \left(\left[((\boldsymbol{v} + \boldsymbol{h}) \cdot \boldsymbol{n})_- - (\boldsymbol{h} \cdot \boldsymbol{n})_- \right] \boldsymbol{h}, \boldsymbol{v} \right)_{0,\Gamma_N} \right| &\leq \frac{1}{2} \kappa \|\boldsymbol{h}\|_{1/2,\Gamma_D} |\boldsymbol{v}|_{1,\Omega}^2 \\ &\leq \frac{1}{2} \kappa \|\boldsymbol{g}\|_{1/2,\Gamma_D} |\boldsymbol{v}|_{1,\Omega}^2 \end{aligned}$$

If $2\kappa \|\boldsymbol{g}\|_{1/2,\Gamma_D} \leq \nu$, then

$$-\frac{1}{2}\left(\left[((\boldsymbol{v}+\boldsymbol{h})\cdot\boldsymbol{n})_- - (\boldsymbol{h}\cdot\boldsymbol{n})_-\right]\boldsymbol{h},\boldsymbol{v}\right)_{0,\Gamma_N} \geq -\frac{\nu}{4}|\boldsymbol{v}|^2_{1,\Omega}$$
$$((\nabla\boldsymbol{h})\,\boldsymbol{v},\boldsymbol{v}) \geq -\frac{\nu}{4}|\boldsymbol{v}|^2_{1,\Omega}$$

In consequence, there exists $c_1 > 0$, only depending of Γ_N and Ω, such that

$$\begin{aligned}\frac{\nu}{4}|\boldsymbol{v}|^2_{1,\Omega} &\leq \langle \boldsymbol{F},\boldsymbol{v}\rangle_{\boldsymbol{H}^{-1}(\Omega)} + \frac{1}{2}\left((\boldsymbol{h}\cdot\boldsymbol{n})_-(\boldsymbol{h}),\boldsymbol{v}\right)_{0,\Gamma_N}\\ &\leq \left(\|\boldsymbol{f}\|_{-1,\Omega} + \left(\nu + c_1\|\gamma\|_{0,\Omega}\right)\|\boldsymbol{g}\|_{1,\Omega} + \kappa_1\|\boldsymbol{g}\|^2_{1,\Omega} + \frac{1}{2}\kappa_2 c_T C_{FP}\|\boldsymbol{g}\|^2_{1/2,\Omega}\right)|\boldsymbol{v}|_{1,\Omega}\end{aligned}$$

Then, due to $\|\boldsymbol{h}\|_{1,\Omega} \leq c\|\boldsymbol{g}\|_{1/2,\Gamma_N}$ there exist a constant $C > 0$, independent of $\boldsymbol{v}$, such that

$$\nu|\boldsymbol{v}|_{1,\Omega} \leq C\left(\|\boldsymbol{f}\|_{-1,\Omega} + \|\boldsymbol{g}\|_{1/2,\Gamma_D} + \|\boldsymbol{g}\|^2_{1/2,\Gamma_D}\right)$$

and

$$\begin{aligned}\nu|\boldsymbol{u}|_{1,\Omega} &\leq \nu\left(|\boldsymbol{v}|_{1,\Omega} + M_1 c\|\boldsymbol{g}\|_{1/2,\Gamma_D}\right)\\ &\leq C_1\left(\|\boldsymbol{f}\|_{-1,\Omega} + \|\boldsymbol{g}\|_{1/2,\Gamma_D} + \|\boldsymbol{g}\|^2_{1/2,\Gamma_D}\right)\end{aligned}$$

when $C_1 = C + \nu c$. Furthermore, there exists $\beta > 0$, depending at most of Ω and Γ_N, such that

$$\begin{aligned}\|p\|_{0,\Omega} &= \beta\sup_{|\boldsymbol{w}|_{1,\Omega}=1}\left|(p,\operatorname{div}\boldsymbol{w})_{0,\Omega}\right|\\ &\leq \beta C_1\left(\|\boldsymbol{f}\|_{-1,\Omega} + \|\boldsymbol{g}\|_{1/2,\Gamma_D} + \|\boldsymbol{g}\|^2_{1/2,\Gamma_D} + \left(\|\boldsymbol{f}\|_{-1,\Omega} + \|\boldsymbol{g}\|_{1/2,\Gamma_D} + \|\boldsymbol{g}\|^2_{1/2,\Gamma_D}\right)^2\right)\end{aligned}$$

The deduction of existence of weak solutions is similar to the proof of Theorem 3.1 in [22]. The following step is to deduce the uniqueness of solution.

Denoting $\boldsymbol{H} = \left\{\boldsymbol{v} \in \boldsymbol{H}^1_{\Gamma_D}(\Omega) \mid \operatorname{div}\boldsymbol{v} = 0\right\}$, consider the mapping $\mathcal{O} : \boldsymbol{H} \to \boldsymbol{H}$ given by $\mathcal{O}(\boldsymbol{a}) = \boldsymbol{v}$, where $(\boldsymbol{v},p) \in \mathcal{H}$ is the unique solution of the linear variational formulation

$$\begin{aligned}(\forall \boldsymbol{w} \in \boldsymbol{H}) \qquad &\nu(\nabla\boldsymbol{v},\nabla\boldsymbol{w})_{0,\Omega} + ((\nabla\boldsymbol{v})(\boldsymbol{a}+\boldsymbol{h},\boldsymbol{w})_{0,\Omega} + ((\nabla\boldsymbol{h})\,\boldsymbol{v},\boldsymbol{w})_{0,\Omega}\\ &+ (\gamma\boldsymbol{v},\boldsymbol{w})_{0,\Omega} - \frac{1}{2}\left(((\boldsymbol{a}+\boldsymbol{h})\cdot\boldsymbol{n})_-\boldsymbol{v},\boldsymbol{w}\right)_{0,\Gamma_N}\\ &= \langle\boldsymbol{F},\boldsymbol{w}\rangle - \frac{1}{2}\left(((\boldsymbol{a}+\boldsymbol{h})\cdot\boldsymbol{n})_-\boldsymbol{h},\boldsymbol{w}\right)_{0,\Gamma_N}\end{aligned}$$

Then,

$$\nu|\boldsymbol{v}|_{1,\Omega} \leq C_1\left(\|\boldsymbol{f}\|_{-1,\Omega} + \|\boldsymbol{g}\|_{1,\Omega} + \|\boldsymbol{g}\|^2_{1,\Omega}\right)$$

Choosing $\boldsymbol{a}_1,\boldsymbol{a}_2 \in \boldsymbol{H}$, $\boldsymbol{v}_1 = \mathcal{O}(\boldsymbol{a}_1)$, $\boldsymbol{v}_2 = \mathcal{O}(\boldsymbol{a}_2)$ and $\boldsymbol{w} = \boldsymbol{v}_1 - \boldsymbol{v}_2$, it follows that

$$\nu|\boldsymbol{w}|^2_{1,\Omega} + ((\nabla\boldsymbol{w})\,\boldsymbol{h},\boldsymbol{w})_{0,\Omega} + ((\nabla\boldsymbol{h})\,\boldsymbol{w},\boldsymbol{w})_{0,\Omega}$$

$$\leq \left(\left(\nabla \boldsymbol{v}_1 \right) \left(\boldsymbol{a}_2 - \boldsymbol{a}_1 \right), \boldsymbol{w} \right)_{0,\Omega} + \frac{1}{2} \left(\left[\left(\left(\boldsymbol{a}_1 + \boldsymbol{h} \right) \cdot \boldsymbol{n} \right)_- - \left(\left(\boldsymbol{a}_2 + \boldsymbol{h} \right) \cdot \boldsymbol{n} \right)_- \right] \boldsymbol{v}_1, \boldsymbol{w} \right)_{0,\Gamma_N}$$

Then,

$$\frac{\nu}{2} \left| \boldsymbol{w} \right|_{1,\Omega}^2 \leq \left(\kappa_1 C_{FP} + \frac{\kappa_2}{2} c_T^3 C_{FP}^3 \right) \left| \boldsymbol{v}_1 \right|_{1,\Omega} \left| \boldsymbol{a}_2 - \boldsymbol{a}_1 \right|_{1,\Omega} \left| \boldsymbol{w} \right|_{1,\Omega}$$

$$\left| \boldsymbol{w} \right|_{1,\Omega} \leq \frac{3\kappa C_1}{\nu^2} \left(\left\| \boldsymbol{f} \right\|_{-1,\Omega} + \left\| \boldsymbol{g} \right\|_{1,\Omega} + \left\| \boldsymbol{g} \right\|_{1,\Omega}^2 \right) \left| \boldsymbol{a}_2 - \boldsymbol{a}_1 \right|_{1,\Omega}$$

Since $\frac{3\kappa C_1}{\nu^2} \left(\left\| \boldsymbol{f} \right\|_{-1,\Omega} + \left\| \boldsymbol{g} \right\|_{1/2,\Gamma_D} + \left\| \boldsymbol{g} \right\|_{1/2,\Gamma_D}^2 \right) < 1$, then

$$\left| \boldsymbol{w} \right|_{1,\Omega} = \left| \boldsymbol{v}_1 - \boldsymbol{v}_2 \right|_{1,\Omega} < \left| \boldsymbol{a}_2 - \boldsymbol{a}_1 \right|_{1,\Omega} = \left| \mathcal{O} \left(\boldsymbol{v}_1 \right) - \mathcal{O} \left(\boldsymbol{v}_2 \right) \right|_{1,\Omega}$$

proving that $\mathcal{O}$ is a contraction. Applying Banach Fixed Point Theorem, we deduce the existence and uniqueness of solution. □

Then, supposing that $\boldsymbol{g}$ verifies the hypotheses of Theorem 1.2.3, the Equation (1.2) has a unique solution. Similar results can be obtained when $\Gamma_N = \emptyset$. Then, $\partial\Omega = \Gamma_D$ and $\boldsymbol{g} \in \boldsymbol{H}^{1/2} \left(\Gamma_D \right)$ must verify the compatibility condition

$$\int_{\partial\Omega} \boldsymbol{g} \cdot \boldsymbol{n} \, dS = 0$$

Chapter 2

Analysis of obstacles immersed in viscous fluids using Brinkman's law for steady Stokes and Navier-Stokes equations

The content of this chapter was published in J. Aguayo and H. Carrillo. "Analysis of obstacles immersed in viscous fluids using Brinkman's law for steady Stokes and Navier-Stokes equations" in SIAM Journal on Applied Mathematics, 2022. [4].

From the steady Stokes and Navier-Stokes models, a penalization method has been considered by several authors for approximating those fluid equations around obstacles. In this chapter, we present a justification for using fictitious domains to study obstacles immersed in incompressible viscous fluids through a simplified version of Brinkman's law for porous media. If the scalar function ψ is considered as the inverse of permeability, it is possible to study the singularities of ψ as approximations of obstacles (when ψ tends to ∞) or of the domain corresponding to the fluid (when $\psi = 0$ or is very close to 0). The strong convergence of the solution of the perturbed problem to the solution of the strong problem is studied, also considering error estimates that depend on the penalty parameter, both for fluids modeled with the Stokes and Navier-Stokes equations with inhomogeneous boundary conditions. A numerical experiment is presented that validates this result and allows to study the application of this perturbed problem simulation of flows and the identification of obstacles.

2.1 Introduction

When modeling flows containing obstacles or enclosed by solid walls with a complex geometry, there are at least two main approaches: using body-fitted unstructured meshes to simulate the geometries or using a simplified mesh adding a penalization term in the differential equations.

In numerical methods relying on the discretization with body-fitted geometry, solid walls are treated by Dirichlet boundary conditions on a mesh refined in the neighborhood of the wall. However, in this methods it is necessary to rebuild the meshes whenever the geometry

changes, which could be a disadvantage for the computing performance.

The approach given by the addition of penalization terms has been reported in the pioneering work of Angot [10] and [64], where the authors in addition show a numerical validation of the model. Instead of considering Dirichlet boundary conditions on solid walls, in these methods the addition of a penalization or forcing term is considered in order to make the flow immovable inside the obstacles. The additional term can be seen as porosity Brinkman's law for imposing porous wall conditions [24] and it corresponds to the limit to null porosity. This method is versatile in terms of geometry: the mesh does not need to depend on the shape of the solid body, so that several geometries can be simulated in a simpler way.

Several extensions for Brinkman's penalty method have been studied, for example, the penalization was used to model the interface of multiphase flows [17, 20], to study gas-particle flows coupling weakly compressible formulation of the Navier-Stokes equations with mass and heat transfer [53], moving obstacles [77], and penalizing Dirichlet or Neumann conditions applied on obstacle boundaries [79, 80]. In [27] the authors propose an extension to Brinkman penalization for generalized Neumann and Robin boundary conditions by introducing hyperbolic penalization terms with characteristics pointing inward on solid obstacles. In [81] the authors also study the Brinkman penalization method for Neumann and Robin boundary conditions. This method has been extended even for other equations, see for example [63] and [78].

In addition, beyond the simulation of flows, the inverse problem of the obstacles or wall shapes estimation also can be studied considering the approaches mentioned above, that is, body-fitted unstructured meshes or the addition of a penalization term. For the first approach, we can find, for example, works of [15] and [37], where the authors provide identifiability and stability results, and [7] where the authors use shape derivatives arguments for the reconstruction. However, those methods need the geometry of the obstacle is not too complex, usually assuming a circular nature. For the second approach we can find works of [3] and [46] not depending on the geometry. However, either we study the direct or inverse problem, the penalized problem is seen as an approximation, so it is necessary to establish how accurate it is.

In the literature, there are several works showing numerical validations of the approximation between the penalized problem and the problem with the simulated geometry, for example [61] and references above. However, there are not much works showing in a theoretical way the effectiveness of the method as an approximation of obstacles. We mention previous works in [8, 9], where the authors formally established $\boldsymbol{H}^1$ error bounds for the approximate and exact problem in the steady Stokes system and unsteady Stokes, respectively. In both works, only Dirichlet conditions are considered for the entire domain boundary.

In this chapter, we study the modeling of obstacles immersed in viscous fluids that satisfy the Stokes and Navier-Stokes equations for inhomogeneous boundary conditions, by the approximation of the fluid equations with the addition of a penalization term. For the stationary Stokes problem the boundary conditions consist on: a known velocity entry, no-slip conditions in the walls and a Neumann boundary condition in the outlet, while for the stationary Navier-Stokes we consider known velocities of entry and outlet, and no-slip conditions for the walls. We establish new convergence results, consisting in the steady Stokes and Navier-Stokes equations in the fluid domain, approximated by the respective penalized equations in a bigger domain containing both the fluid and solid part. We follow techniques

of [8, 9], that is, we make problems to have homogeneous boundary conditions and we study the weak convergence of a sequence of functions depending on the penalization term in order to establish the strong convergence with rates depending on the penalization term going to infinite.

The results presented in this chapter have not been reported before in these particular settings, which have been chosen motivated by the applied problem of modeling blood flow in the presence of heart valves. In particular, this work justifies the use of a penalizing term in [3], where the authors study the inverse problem of determining the geometry of heart valves given velocity measurements in the whole virtual domain, using as model the equations we present in this work. An important aspect to mention is that in such work the authors assume the velocity measurements consist of one snapshot obtained from magnetic resonance imaging (MRI) measurements using a technique known as phase-contrast MRI [26, 65], in which the time derivative of the velocity is assumed to be negligible due to the very short timescale of the data acquisition.

This chapter is organized as follows. In Section 2, we provide the reader the basic notations of the fluid and solid domains, and the functional spaces involved in the main theorems. In Sections 3 and 4, we show estimates of the error in norm $\boldsymbol{H}^1$ induced by the penalization. In Section 3, we show the analysis for the Stokes equations with mixed boundary conditions, which are the conditions usually considered in problems such that parts of the boundary are not walls. In Section 4, we show the analysis for the Navier-Stokes case with inhomogeneous Dirichlet boundary conditions, which is also an extension of [8] to the nonlinear case. We closely follow ideas of [8, 9]. Finally, in Section 5, we show numerical tests to validate our theoretical findings.

2.2 Preliminaries and notations

Consider a non-empty bounded domain $\Omega \subseteq \mathbb{R}^d$, $d \in \{2, 3\}$. The Lebesgue measure of Ω is denoted by $|\Omega|$, which extends to lesser dimension spaces. The norm and seminorms for Sobolev spaces $W^{m,p}(\Omega)$ is denoted by $\|\cdot\|_{m,p,\Omega}$ and $|\cdot|_{m,p,\Omega}$, respectively. For $p = 2$, the norm, seminorms and inner product of the space $W^{m,2}(\Omega) = H^m(\Omega)$ are denoted by $\|\cdot\|_{m,\Omega}$, $|\cdot|_{m,\Omega}$ and $(\cdot,\cdot)_{m,\Omega}$, respectively. Also, $\|\cdot\|_{\infty,\Omega}$ denotes the norm of $L^\infty(\Omega)$. The spaces $\boldsymbol{H}^m(\Omega)$ and $\boldsymbol{W}^{m,p}(\Omega)$ are defined by $\boldsymbol{H}^m(\Omega) = [H^m(\Omega)]^d$ and $\boldsymbol{W}^{m,p}(\Omega) = [W^{m,p}(\Omega)]^d$. The notation for norms, seminorms and inner products will be extended from $W^{m,p}(\Omega)$ or $H^m(\Omega)$.

We assume that $\Gamma = \partial\Omega$ is piecewise $\mathcal{C}^1$ and Ω contains N regular obstacles given by nonempty open sets $\Omega_S^j \subseteq \Omega$ for $j \in \{1, \ldots, N\}$.

Definition 2.2.1. *The sets Ω_S, Ω_F, Σ_S^j (for $j \in \{1, \ldots, N\}$) are defined by*

$$\Omega_S = \bigcup_{j=1}^{N} \Omega_S^j, \quad \Omega_F = \Omega \setminus \overline{\Omega}_s$$

$$\Sigma_s^i = \partial\Omega_S^j, \quad \Gamma = \partial\Omega$$

We also define $\Gamma_I, \Gamma_W, \Gamma_O \subset \Gamma$, disjoint subsets of Γ, such that

$$\overline{\Gamma}_I \cup \overline{\Gamma}_W \cup \overline{\Gamma}_O = \Gamma,$$

$$\Gamma_I \subset \partial\Omega_F \cap \partial\Omega, \quad \Gamma_O \subset \partial\Omega_F \cap \partial\Omega$$

Finally, we define $\Gamma_{F,W} = \partial\Omega_F \setminus (\Gamma_I \cup \Gamma_O)$

The set Ω_F models a fluid domain where the Stokes or Navier-Stokes equations is fulfilled.

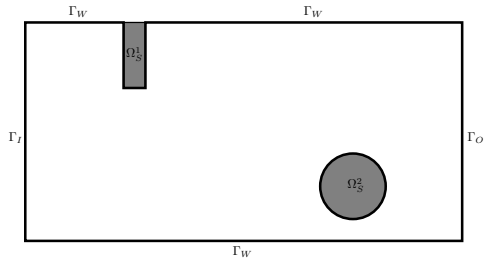

Figure 2.1: Example of Ω with two obstacles Ω_S^1 and Ω_S^2.

Definition 2.2.2. *Let $\gamma \subseteq \partial\Omega$. We define the following spaces*

$$\begin{aligned}
\boldsymbol{H}_0^1(\Omega) &= \left\{\boldsymbol{v} \in \boldsymbol{H}^1(\Omega) \mid \boldsymbol{v} = \boldsymbol{0} \text{ on } \partial\Omega\right\} \\
\boldsymbol{H}_\gamma^1(\Omega) &= \left\{\boldsymbol{v} \in \boldsymbol{H}^1(\Omega) \mid \boldsymbol{v} = \boldsymbol{0} \text{ on } \partial\Omega \setminus \gamma\right\} \\
\boldsymbol{H}_{\mathrm{div}}(\Omega) &= \left\{\boldsymbol{v} \in \boldsymbol{H}^1(\Omega) \mid \operatorname{div}\boldsymbol{v} = \boldsymbol{0} \text{ on } \Omega\right\} \\
\boldsymbol{V}_\gamma(\Omega) &= \boldsymbol{H}_\gamma^1(\Omega) \cap \boldsymbol{H}_{\mathrm{div}}(\Omega) \\
\boldsymbol{V}(\Omega) &= \boldsymbol{H}_0^1(\Omega) \cap \boldsymbol{H}_{\mathrm{div}}(\Omega) \\
L_0^2(\Omega) &= \left\{p \in L^2(\Omega) \mid (p,1)_{0,\Omega} = 0\right\} \\
\mathcal{H}_\gamma(\Omega) &= \boldsymbol{V}_\gamma(\Omega) \times L_0^2(\Omega) \\
\mathcal{H}(\Omega) &= \boldsymbol{V}(\Omega) \times L_0^2(\Omega)
\end{aligned}$$

We extend these definitions to Ω_F and Ω_S.

2.3 Stokes system with mixed boundary conditions

Let $\nu > 0$, $\boldsymbol{u}_D \in \boldsymbol{H}^{1/2}(\Gamma_I)$ such that $\boldsymbol{u}_D = \boldsymbol{0}$ on $\overline{\Gamma}_I \cap \overline{\Gamma}_W$ and $(\boldsymbol{u}, p) \in \mathcal{H}(\Omega)$ the unique solution of the Stokes system with mixed boundary conditions over Ω_F given by

$$\begin{aligned}
-\nu\triangle\boldsymbol{u} + \nabla p &= \boldsymbol{0} && \text{in } \Omega_F \\
\operatorname{div}\boldsymbol{u} &= 0 && \text{in } \Omega_F \\
\boldsymbol{u} &= \boldsymbol{u}_D && \text{on } \Gamma_I \\
\boldsymbol{u} &= \boldsymbol{0} && \text{on } \Gamma_{F,W} \\
-\nu\frac{\partial\boldsymbol{u}}{\partial n} + p\boldsymbol{n} &= \boldsymbol{0} && \text{on } \Gamma_O
\end{aligned} \tag{2.1}$$

extended by $(\boldsymbol{0}, 0)$ in Ω_S.

On the other hand, for each $R > 0$, let $(\boldsymbol{u}_R, p_R) \in \mathcal{H}(\Omega)$ the unique solution of the modified Stokes system with a L^2 penalization term over Ω given by

$$\begin{aligned} -\nu\triangle\boldsymbol{u}_R + \nabla p_R + \psi_R\boldsymbol{u}_R &= \boldsymbol{0} && \text{in } \Omega \\ \operatorname{div}\boldsymbol{u}_R &= 0 && \text{in } \Omega \\ \boldsymbol{u}_R &= \boldsymbol{u}_D && \text{on } \Gamma_I \\ \boldsymbol{u}_R &= \boldsymbol{0} && \text{on } \Gamma_W \\ -\nu\frac{\partial\boldsymbol{u}_R}{\partial n} + p_R\boldsymbol{n} &= \boldsymbol{0} && \text{on } \Gamma_O \end{aligned} \tag{2.2}$$

where $\psi_R = R\chi_{\Omega_S}$, and

$$\chi_{\Omega_S}(x) = \begin{cases} 1 & \text{if } x \in \Omega_S, \\ 0 & \text{otherwise.} \end{cases}$$

2.3.1 Preliminary results

We start stating some previous results in order to use them in the proof of Theorems 2.3.1 and 2.3.2.

Lemma 2.3.1. *Let $\eta > 0$ and $M > 0$ such that $\|\boldsymbol{u}_D\|_{1/2,\Gamma_I} \leq M$. There exists $\boldsymbol{g} \in \boldsymbol{H}^1(\Omega_F)$ such that $\operatorname{div}\boldsymbol{g} = 0$, $\boldsymbol{g} = \boldsymbol{u}_D$ on Γ_I, $\boldsymbol{g} = \boldsymbol{0}$ on $\Gamma_{F,W}$ and*

$$\left(\forall \boldsymbol{v} \in \boldsymbol{H}^1(\Omega_F)\right) \qquad \left|((\nabla\boldsymbol{g})\,\boldsymbol{v}, \boldsymbol{v})_{0,\Omega_F}\right| \leq \eta\,|\boldsymbol{v}|^2_{1,\Omega_F}$$

and a constant $c > 0$, that only depends of Ω, Γ_I, Γ_W and M such that

$$\|\boldsymbol{g}\|_{1,\Omega} \leq c\,\|\boldsymbol{u}_D\|_{1/2,\Gamma_I}$$

Proof. Let $\boldsymbol{u}_D^* \in \boldsymbol{H}^{1/2}(\partial\Omega_F)$, with $\boldsymbol{u}_D^*$ an extension of $\boldsymbol{u}_D$ such that $\|\boldsymbol{u}_D^*\|_{1/2,\partial\Omega_F} \leq 2\,\|\boldsymbol{u}_D\|_{1/2,\Gamma_I}$ and

$$\int_{\partial\Omega_F} \boldsymbol{u}_D^* \cdot \boldsymbol{n}\; dS = 0$$

Applying Lemma IV.2.3 in [50], there exists $\boldsymbol{g} \in \boldsymbol{H}^1(\Omega_F)$ such that $\operatorname{div}\boldsymbol{g} = 0$ in Ω_F, $\boldsymbol{g} = \boldsymbol{u}_D^*$ on $\partial\Omega_F$ and

$$\left(\forall \boldsymbol{v} \in \boldsymbol{H}^1(\Omega_F)\right) \qquad \left|((\nabla\boldsymbol{g})\,\boldsymbol{v}, \boldsymbol{v})_{0,\Omega_F}\right| \leq \eta\,|\boldsymbol{v}|^2_{1,\Omega_F}$$

In particular, $\boldsymbol{g} = \boldsymbol{u}_D$ on Γ_I and $\boldsymbol{g} = \boldsymbol{0}$ on Γ_W, proving the first part of the lemma. Using Lemma IX.4.2 in [48], we can deduce the existence of c. □

Remark 2.3.1. *Since $\boldsymbol{g} = \boldsymbol{0}$ on $\Gamma_{F,W}$, it is possible to extend $\boldsymbol{g} \in \boldsymbol{H}^1(\Omega_F)$ to $\boldsymbol{g} \in \boldsymbol{H}^1(\Omega)$ such that $\boldsymbol{g} = \boldsymbol{u}_D$ on Γ_I and $\boldsymbol{g} = \boldsymbol{0}$ on Γ_W.*

Proposition 2.3.1. *Let $\boldsymbol{v}_R = \boldsymbol{u}_R - \boldsymbol{g}$, where $\boldsymbol{g}$ is given by Lemma 2.3.1. Then*

$$|\boldsymbol{v}_R|_{1,\Omega} \leq |\boldsymbol{g}|_{1,\Omega} \quad \text{and} \quad \|\boldsymbol{v}_R\|_{0,\Omega_S} \leq \frac{\nu}{R}|\boldsymbol{g}|_{1,\Omega}$$

Proof. Consider the penalized equation (2.2) after introducing $\boldsymbol{v}_R$ given by

$$\begin{aligned} -\nu\triangle\boldsymbol{v}_R + \nabla p_R + \psi_R\boldsymbol{v}_R &= \nu\triangle\boldsymbol{g} && \text{in } \Omega \\ \operatorname{div}(\boldsymbol{v}_R) &= 0 && \text{in } \Omega \\ \boldsymbol{v}_R &= 0 && \text{on } \Gamma_I \cup \Gamma_W \\ -\nu\frac{\partial \boldsymbol{v}_R}{\partial n} + p_R\boldsymbol{n} &= \nu\frac{\partial \boldsymbol{g}}{\partial \boldsymbol{n}} && \text{on } \Gamma_O \end{aligned}$$

Testing this equations by $\boldsymbol{w} \in \boldsymbol{V}_{\Gamma_O}(\Omega)$ and $q \in L^2_0(\Omega)$, we obtain

$$\nu(\nabla\boldsymbol{v}_R, \nabla\boldsymbol{w})_{0,\Omega} + R(\boldsymbol{v}_R, \boldsymbol{w})_{0,\Omega_S} = -\nu(\nabla\boldsymbol{g}, \nabla\boldsymbol{w})_{0,\Omega} \tag{2.3}$$

Taking $\boldsymbol{w} = \boldsymbol{v}_R$, we deduce

$$\nu|\boldsymbol{v}_R|^2_{1,\Omega} + R\|\boldsymbol{v}_R\|^2_{0,\Omega_S} = -\nu(\nabla\boldsymbol{g}, \nabla\boldsymbol{v}_R)_{0,\Omega} \leq \nu|\boldsymbol{g}|_{1,\Omega}|\boldsymbol{v}_R|_{1,\Omega}$$

and then we conclude. □

Proposition 2.3.2. *$\boldsymbol{v}_R$ converges weakly to $\boldsymbol{v}$ in $\boldsymbol{V}_{\Gamma_O}(\Omega)$.*

Proof. By the result of Proposition 2.3.1, we see that there exists a subsequence $\boldsymbol{v}_R$ (we call it the same way) weakly convergent in $\boldsymbol{H}^1(\Omega)$ to $\tilde{\boldsymbol{v}}$. Since $\tilde{\boldsymbol{v}} = 0$ in Ω_S, applying Trace Theorem (see Theorem II.4.1 in [48]), we can see that $\tilde{\boldsymbol{v}} = 0$ on $\partial\Omega_S$. Later, for all $\boldsymbol{w} \in \boldsymbol{V}_{\Gamma_O}(\Omega)$ we have

$$\begin{aligned} (\psi_R\boldsymbol{v}_R, \boldsymbol{w})_{0,\Omega} &= -\Big(\nu(\nabla\boldsymbol{g}, \nabla\boldsymbol{w})_{0,\Omega} + \nu(\nabla\boldsymbol{v}_R, \nabla\boldsymbol{w})_{0,\Omega}\Big) \\ &\to -\Big(\nu(\nabla\boldsymbol{g}, \nabla\boldsymbol{w})_{0,\Omega} + \nu(\nabla\tilde{\boldsymbol{v}}, \nabla\boldsymbol{w})_{0,\Omega}\Big) \end{aligned}$$

Hence $\psi_R\boldsymbol{v}_R$ converges weakly to some $\boldsymbol{h} \in [\boldsymbol{V}_{\Gamma_O}(\Omega)]'$, where $\operatorname{supp}(\boldsymbol{h}) \subseteq \Omega$. Then,

$$\nu(\nabla\tilde{\boldsymbol{v}}, \nabla\boldsymbol{w})_{0,\Omega} + \langle\boldsymbol{h}, \boldsymbol{w}\rangle_{\boldsymbol{H}^{-1}(\Omega),\boldsymbol{H}^1(\Omega)} = -\nu(\nabla\boldsymbol{g}, \nabla\boldsymbol{w})_{0,\Omega} \tag{2.4}$$

Since $\boldsymbol{v}_R = 0$ on $\Gamma_I \cup \Gamma_W$, we have $\tilde{\boldsymbol{v}} = 0$ on $\Gamma_I \cup \Gamma_W$ as well, by the continuity of the trace operator. Now, applying the De Rham's Theorem (see Theorem I.2.3 in [50]), there exists $\tilde{p} \in L^2_0(\Omega)$ such that

$$\begin{aligned} -\nu\triangle\tilde{\boldsymbol{v}} + \nabla\tilde{p} + \boldsymbol{h} &= \nu\triangle\boldsymbol{g} && \text{in } \Omega \\ \operatorname{div}\tilde{\boldsymbol{v}} &= 0 && \text{in } \Omega \\ \tilde{\boldsymbol{v}} &= \boldsymbol{0} && \text{on } (\Gamma_I \cup \Gamma_W) \cap \partial\Omega_F \end{aligned}$$

Taking $(\boldsymbol{w}, q) \in \mathcal{H}(\Omega)$ such that $(\boldsymbol{w}, q) = (\boldsymbol{0}, 0)$ in Ω_S, we have

$$\nu(\nabla\tilde{\boldsymbol{v}}, \nabla\boldsymbol{w})_{0,\Omega_F} + \Big(-\nu\frac{\partial(\tilde{\boldsymbol{v}} + \boldsymbol{g})}{\partial\boldsymbol{n}} + \tilde{p}\boldsymbol{n}, \boldsymbol{w}\Big)_{0,\Gamma_O} = -\nu(\nabla\boldsymbol{g}, \nabla\boldsymbol{w})_{0,\Omega_F} \tag{2.5}$$

and then

$$-\frac{\partial(\tilde{\boldsymbol{v}} + \boldsymbol{g})}{\partial\boldsymbol{n}} + p\boldsymbol{n} = \boldsymbol{0}$$

on Γ_O. Hence, $(\tilde{\boldsymbol{v}}, \tilde{p})$ is a weak solution for Equation (2.1). Since Equation (2.1) has a unique solution, we conclude $(\tilde{\boldsymbol{v}}, \tilde{p}) = (\boldsymbol{v}, p)$. Finally, extending the solution by $(\boldsymbol{0}, 0)$ in Ω_S, we have that for all $(\boldsymbol{w}, q) \in \mathcal{H}(\Omega)$,

$$\nu(\nabla\tilde{\boldsymbol{v}}, \nabla\boldsymbol{w})_{0,\Omega} = -\nu(\nabla\boldsymbol{g}, \nabla\boldsymbol{w})_{0,\Omega}$$

In conclusion, $(\tilde{\boldsymbol{v}}, \tilde{p}) = (\boldsymbol{v}, p)$ in Ω and $\tilde{\boldsymbol{v}}_R \rightharpoonup \boldsymbol{v}$ in $\boldsymbol{H}^1_{\Gamma_O}(\Omega)$ as $R \to \infty$. □

2.3.2 Main results

Now we can establish the first convergence result.

Theorem 2.3.1. *Let $R > 0$, $\boldsymbol{u}$ be solution of (2.1) and $\boldsymbol{u}_R$ solution of (2.2). With the previous assumptions, there is strong convergence of $\{\boldsymbol{u}_R\}_{R>0}$, that is*

$$\lim_{R\to\infty} |\boldsymbol{u}_R - \boldsymbol{u}|_{1,\Omega} = 0$$

and there there exists a constant $C > 0$ independent such that for all $R > 0$

$$\|\boldsymbol{u} - \boldsymbol{u}_R\|_{0,\Omega_S} \leq \frac{C}{R^{1/2}}$$

Proof. Let $\boldsymbol{w}_R = \boldsymbol{v}_R - \boldsymbol{v}$. Subtracting the variational formulations (2.3) and (2.4) for $\boldsymbol{v}_R$ and $\tilde{\boldsymbol{v}}$, respectively, we obtain for all $\boldsymbol{w} \in \boldsymbol{V}$

$$\nu(\nabla \boldsymbol{w}_R, \nabla \boldsymbol{w})_{0,\Omega} + R(\boldsymbol{w}_R, \boldsymbol{w})_{0,\Omega_S} = \langle \boldsymbol{h}, \boldsymbol{w}\rangle_{\boldsymbol{V}',\boldsymbol{V}} \tag{2.6}$$

since $\boldsymbol{v} = \boldsymbol{g} = \boldsymbol{0}$ in Ω_S. Taking $\boldsymbol{w} = \boldsymbol{w}_R$ and using that $\boldsymbol{w}_R \rightharpoonup 0$ in $\boldsymbol{V}$ as $R \to \infty$, we obtain

$$\nu|\boldsymbol{w}_R|^2_{1,\Omega} + R\|\boldsymbol{w}_R\|^2_{0,\Omega_S} = \langle \boldsymbol{h}, \boldsymbol{w}_R\rangle_{\boldsymbol{V}',\boldsymbol{V}} \to 0$$

proving the theorem. □

Imposing more regularity to $\boldsymbol{u}_D$ and $\partial\Omega_F$, the first convergence theorem can be upgraded to this new result.

Theorem 2.3.2. *Let $R > 0$, $\boldsymbol{u}$ be solution of (2.1) and $\boldsymbol{u}_R$ solution of (2.2). With the previous assumptions, where we assume in addition that $\partial\Omega_F$ is piecewise $\mathcal{C}^2$ class and $\boldsymbol{u}_D \in H^{3/2}(\Gamma_I)$, then there is strong convergence of $\{\boldsymbol{u}_R\}_{R>0}$ in $\boldsymbol{H}^1(\Omega)$ when $R \to \infty$. Furthermore, there exists a constant $C > 0$ independent of R such that for all $R > 0$*

$$|\boldsymbol{u} - \boldsymbol{u}_R|_{1,\Omega} \leq \frac{C}{R^{1/4}}, \qquad \|\boldsymbol{u} - \boldsymbol{u}_R\|_{0,\Omega_S} \leq \frac{C}{R^{3/4}}.$$

Proof. We can assume that the function $\boldsymbol{g}$ given by Lemma 2.3.1 is now in $\boldsymbol{H}^2(\Omega)$. Hence, results about regularity of solution to the Stokes equations (see Theorem IV.6.1 in [48]) allow us to consider $(\boldsymbol{v}, p) \in \boldsymbol{H}^2(\Omega) \times \boldsymbol{H}^1(\Omega)$. Let us replace the Dirichlet condition of $\boldsymbol{u}$ in (6) on $\partial\Omega_S \setminus \Gamma$ by

$$-\nu\frac{\partial \boldsymbol{u}}{\partial \boldsymbol{n}} + p\boldsymbol{n} = \boldsymbol{k}.$$

Then, for $\boldsymbol{v} = \boldsymbol{u} - \boldsymbol{g}$,

$$\boldsymbol{k} = -\nu\frac{\partial \boldsymbol{v} + \boldsymbol{g}}{\partial \boldsymbol{n}} + p\boldsymbol{n} \quad \text{on } \partial\Omega_S \setminus \Gamma.$$

where $\boldsymbol{k} \in \boldsymbol{H}^{1/2}(\Gamma_O)$. For all $\boldsymbol{w} \in \boldsymbol{H}^1_{(\partial\Omega_S\setminus\Gamma)\cup\Gamma_O}(\Omega_F)$:

$$\nu\left(\nabla \boldsymbol{v}, \nabla \boldsymbol{w}\right)_{0,\Omega_F} + \left(\boldsymbol{k}, \boldsymbol{w}\right)_{0,\partial\Omega_S} = -\nu\left(\nabla \boldsymbol{g}, \nabla \boldsymbol{w}\right)_{0,\Omega_F}$$

Since

$$\left(\forall \boldsymbol{w} \in \boldsymbol{H}^1_{\Gamma_O}(\Omega)\right) \qquad \nu\left(\nabla \boldsymbol{v}, \nabla \boldsymbol{w}\right)_{0,\Omega} + \langle \boldsymbol{h}, \boldsymbol{w}\rangle_{V',V} = -\nu\left(\nabla \boldsymbol{g}, \nabla \boldsymbol{w}\right)_{0,\Omega}$$

and considering $\boldsymbol{v} = \boldsymbol{g} = \mathbf{0}$ in Ω_S, then we have

$$\left(\forall \boldsymbol{w} \in \boldsymbol{H}^1_{\Gamma_O}(\Omega)\right) \qquad \langle \boldsymbol{h}, \boldsymbol{w} \rangle_{V',V} = (\boldsymbol{k}, \boldsymbol{w})_{0,\partial\Omega_S \setminus \Gamma} \tag{2.7}$$

Then, from (2.6) and (2.7), applying Hölder and Cauchy-Schwartz inequalities, we have

$$\begin{aligned} \nu \left|\boldsymbol{w}_R\right|^2_{1,\Omega} + R \left\|\boldsymbol{w}_R\right\|^2_{0,\Omega_S} &= (\boldsymbol{k}, \boldsymbol{w}_R)_{0,\partial\Omega_S} \\ &\leq C \left\|\boldsymbol{k}\right\|_{0,\partial\Omega_S} \left|\boldsymbol{w}_R\right|^{1/2}_{1,\Omega_S} \left\|\boldsymbol{w}_R\right\|^{1/2}_{0,\Omega_S} \\ &\leq \frac{\left(C \left\|\boldsymbol{k}\right\|_{0,\partial\Omega_S}\right)^2}{2\left(\nu R\right)^{1/2}} + \frac{1}{4}\left(\nu \left|\boldsymbol{w}_R\right|^2_{1,\Omega} + R \left\|\boldsymbol{w}_R\right\|^2_{0,\Omega_S}\right) \end{aligned}$$

where $C > 0$ is a constant independent of R. Then,

$$\nu \left|\boldsymbol{w}_R\right|^2_{1,\Omega} + R \left\|\boldsymbol{w}_R\right\|^2_{0,\Omega_S} \leq \frac{2\left(C \left\|\boldsymbol{k}\right\|_{0,\partial\Omega_S}\right)^2}{3\left(\nu R\right)^{1/2}}$$

In conclusion, $\left|\boldsymbol{w}_R\right|_{1,\Omega} = \mathcal{O}\left(R^{-1/4}\right)$ and $\left\|\boldsymbol{w}_R\right\|_{0,\Omega_S} = \mathcal{O}\left(R^{-3/4}\right)$, proving this theorem. □

2.4 Navier-Stokes equation with Dirichlet boundary conditions

2.4.1 Preliminary results

Let us consider Ω, Ω_F and Ω_S as described in Section 2.3. Let $(\boldsymbol{u}, p) \in \mathcal{H}(\Omega_F)$ a solution of the Navier-Stokes system with Dirichlet boundary conditions over Ω_F

$$\begin{aligned} -\nu \triangle \boldsymbol{u} + (\nabla \boldsymbol{u})\, \boldsymbol{u} + \nabla p &= \mathbf{0} && \text{in } \Omega_F \\ \operatorname{div} \boldsymbol{u} &= 0 && \text{in } \Omega_F \\ \boldsymbol{u} &= \boldsymbol{u}_D && \text{on } \Gamma_I \cup \Gamma_O \\ \boldsymbol{u} &= \mathbf{0} && \text{on } \partial\Omega_F \setminus (\Gamma_I \cup \Gamma_O) \end{aligned} \tag{2.8}$$

and for all $R > 0$, let $(\boldsymbol{u}_R, p_R) \in \mathcal{H}(\Omega)$ a solution of the following modified Navier-Stokes system over Ω, with a L^2 penalization term, given by

$$\begin{aligned} -\nu \triangle \boldsymbol{u}_R + (\nabla \boldsymbol{u}_R)\, \boldsymbol{u}_R + \nabla p_R + R\chi_{\Omega_S} \boldsymbol{u}_R &= \mathbf{0} && \text{in } \Omega \\ \operatorname{div} \boldsymbol{u}_R &= 0 && \text{in } \Omega_F \\ \boldsymbol{u}_R &= \boldsymbol{u}_D && \text{on } \Gamma_I \cup \Gamma_O \\ \boldsymbol{u}_R &= \mathbf{0} && \text{on } \Gamma_W \end{aligned} \tag{2.9}$$

provided $\boldsymbol{u}_D \in \boldsymbol{H}^{1/2}(\Omega)$ and

$$\int_{\Gamma_I} \boldsymbol{u}_D \cdot \boldsymbol{n}\, dS + \int_{\Gamma_O} \boldsymbol{u}_D \cdot \boldsymbol{n}\, dS = 0$$

The uniqueness of solution of both problems is guaranteed under certain additional hypotheses. In order to establish those hypotheses, it is necessary to cite the following results.

Theorem 2.4.1. *There exists* $\boldsymbol{g} \in H^1(\Omega_f)$ *such that* $\operatorname{div} \boldsymbol{g} = 0$, $\boldsymbol{g} = \boldsymbol{u}_D$ *on* $\Gamma_I \cup \Gamma_0$, $\boldsymbol{g} = \boldsymbol{0}$ *on* $\Gamma_f \setminus (\Gamma_I \cup \Gamma_O)$ *and*

$$\left(\forall \boldsymbol{w} \in \boldsymbol{H}_0^1(\Omega)\right) \qquad |((\nabla \boldsymbol{g})\,\boldsymbol{w}, \boldsymbol{w})| \leq \alpha\, |\boldsymbol{w}|_{1,\Omega}^2$$

for all $\alpha \in (0, \nu)$.

Proof. See Lemma IV.2.3 in [50] and Lemma IX.4.2 in [48]. □

Theorem 2.4.2. *There exists a constant* $\kappa > 0$ *only depending on* Ω, *such that*

$$\left(\forall (\boldsymbol{u}, \boldsymbol{v}, \boldsymbol{w}) \in \boldsymbol{H}_0^1(\Omega) \times \boldsymbol{H}^1(\Omega) \times \boldsymbol{H}_0^1(\Omega)\right) \qquad |((\nabla \boldsymbol{v})\,\boldsymbol{u}, \boldsymbol{w})| \leq \kappa\, |\boldsymbol{u}|_{1,\Omega}\, |\boldsymbol{v}|_{1,\Omega}\, |\boldsymbol{w}|_{1,\Omega}$$
$$\left(\forall (\boldsymbol{u}, \boldsymbol{v}, \boldsymbol{w}) \in \boldsymbol{H}^1(\Omega) \times \boldsymbol{H}^1(\Omega) \times \boldsymbol{H}_0^1(\Omega)\right) \qquad |((\nabla \boldsymbol{v})\,\boldsymbol{u}, \boldsymbol{w})| \leq \kappa\, \|\boldsymbol{u}\|_{1,\Omega}\, |\boldsymbol{v}|_{1,\Omega}\, |\boldsymbol{w}|_{1,\Omega}$$

Proof. Direct consequence of Hölder inequalty and Sobolev Embedding Theorem. □

Then, as for the Stokes problem, we consider the extension of $\boldsymbol{g}$ to $\boldsymbol{H}^1(\Omega)$ such that $\boldsymbol{g} = \boldsymbol{0}$ en Ω_S. Let us define $\boldsymbol{v} = \boldsymbol{u} - \boldsymbol{g}$, so we have the following equation

$$\begin{aligned} -\nu \triangle \boldsymbol{v} + (\nabla \boldsymbol{v})\,\boldsymbol{v} + (\nabla \boldsymbol{v})\,\boldsymbol{g} + (\nabla \boldsymbol{g})\,\boldsymbol{v} + \nabla p &= \nu \triangle \boldsymbol{g} - (\nabla \boldsymbol{g})\,\boldsymbol{g} && \text{in } \Omega_F \\ \operatorname{div} \boldsymbol{v} &= 0 && \text{in } \Omega_F \\ \boldsymbol{v} &= \boldsymbol{0} && \text{on } \partial\Omega_F \end{aligned} \tag{2.10}$$

where we extend $(\boldsymbol{v}, p) \in \mathcal{H}(\Omega)$ by $(\boldsymbol{0}, 0)$. In addition, let $\boldsymbol{v}_R = \boldsymbol{u}_R - \boldsymbol{g}$, so we have

$$\begin{aligned} -\nu \triangle \boldsymbol{v}_R + (\nabla \boldsymbol{v}_R)\,\boldsymbol{v}_R + (\nabla \boldsymbol{v}_R)\,\boldsymbol{g} + (\nabla \boldsymbol{g})\,\boldsymbol{v}_R + \nabla p_R + R\chi_\Omega \boldsymbol{v}_R &= \nu \triangle \boldsymbol{g} - (\nabla \boldsymbol{g})\,\boldsymbol{g} && \text{in } \Omega \\ \operatorname{div} \boldsymbol{v}_R &= 0 && \text{in } \Omega \\ \boldsymbol{v}_R &= \boldsymbol{0} && \text{on } \partial\Omega \end{aligned} \tag{2.11}$$

Remark 2.4.1. *Defining the constant* $C \geq 0$ *given by*

$$C = \nu\, \|\boldsymbol{g}\|_{1,\Omega_F} + \kappa\, \|\boldsymbol{g}\|_{1,\Omega_F}^2$$

we can proceed similarly than Section IV.2 in [50] and conclude that the solutions of (2.8) *and* (2.10) *are unique provided*

$$\frac{C\kappa}{(\nu - \alpha)^2} < 1.$$

Repeating the same arguments as in Section 2.3, it is possible to obtain the same convergence results deduced in Theorems (2.3.1) and (2.3.2). The first step is the uniformly boundedness of $\{\boldsymbol{v}_R\}_{R>0}$

Proposition 2.4.1. *There exists a constant* $C > 0$ *only depending of* $\boldsymbol{g}$ *such that*

$$|\boldsymbol{v}_R|_{1,\Omega} \leq \frac{C}{\nu - \alpha} \qquad R\, \|\boldsymbol{v}_R\|_{0,\Omega_S}^2 \leq \frac{C^2}{\nu - \alpha}$$

Proof. Let us testing first equation of (2.10) by $\boldsymbol{w} \in \boldsymbol{V}(\Omega_F)$. Then,

$$\begin{aligned}&\nu\left(\nabla \boldsymbol{v}, \nabla \boldsymbol{w}\right)_{0,\Omega_F} + \left(\left(\nabla \boldsymbol{v}\right)\boldsymbol{v}, \boldsymbol{w}\right)_{0,\Omega_F} + \left(\left(\nabla \boldsymbol{v}\right)\boldsymbol{g}, \boldsymbol{w}\right)_{0,\Omega_F} + \left(\left(\nabla \boldsymbol{g}\right)\boldsymbol{v}, \boldsymbol{w}\right)_{0,\Omega_F}\\ =& -\nu\left(\nabla \boldsymbol{g}, \nabla \boldsymbol{w}\right)_{0,\Omega_F} - \left(\left(\nabla \boldsymbol{g}\right)\boldsymbol{g}, \boldsymbol{w}\right)_{0,\Omega_F}\end{aligned}$$

Considering the extension to Ω, we have that for all $\boldsymbol{w} \in \boldsymbol{V}(\Omega)$

$$\begin{aligned}&\nu\left(\nabla \boldsymbol{v}, \nabla \boldsymbol{w}\right)_{0,\Omega} + \left(\left(\nabla \boldsymbol{v}\right)\boldsymbol{v}, \boldsymbol{w}\right)_{0,\Omega} + \left(\left(\nabla \boldsymbol{v}\right)\boldsymbol{g}, \boldsymbol{w}\right)_{0,\Omega} + \left(\left(\nabla \boldsymbol{g}\right)\boldsymbol{v}, \boldsymbol{w}\right)_{0,\Omega}\\ =& -\nu\left(\nabla \boldsymbol{g}, \nabla \boldsymbol{w}\right)_{0,\Omega_F} - \left(\left(\nabla \boldsymbol{g}\right)\boldsymbol{g}, \boldsymbol{w}\right)_{0,\Omega_F}\end{aligned}$$

Testing the penalized equation (2.11) by $\boldsymbol{w} \in \boldsymbol{V}(\Omega)$, we obtain

$$\begin{aligned}&\nu\left(\nabla \boldsymbol{v}_R, \nabla \boldsymbol{w}\right)_{0,\Omega} + R\left(\boldsymbol{v}_R, \boldsymbol{w}\right)_{0,\Omega_S} + \left(\left(\nabla \boldsymbol{v}_R\right)\boldsymbol{v}_R, \boldsymbol{w}\right)_{0,\Omega}\\ &+ \left(\left(\nabla \boldsymbol{v}_R\right)\boldsymbol{g}, \boldsymbol{w}\right)_{0,\Omega} + \left(\left(\nabla \boldsymbol{g}\right)\boldsymbol{v}_R, \boldsymbol{w}\right)_{0,\Omega}\\ =& -\nu\left(\nabla \boldsymbol{g}, \nabla \boldsymbol{w}\right)_{0,\Omega_F} - \left(\left(\nabla \boldsymbol{g}\right)\boldsymbol{g}, \boldsymbol{w}\right)_{0,\Omega_F}\end{aligned} \tag{2.12}$$

Taking $\boldsymbol{w} = \boldsymbol{v}_R$, we have

$$\left(\left(\nabla \boldsymbol{v}_R\right)\boldsymbol{g}, \boldsymbol{v}_R\right)_{0,\Omega} = \left(\left(\nabla \boldsymbol{v}_R\right)\boldsymbol{v}_R, \boldsymbol{v}_R\right)_{0,\Omega} = 0$$

since $\operatorname{div} \boldsymbol{g} = 0$, and then

$$\nu\left|\boldsymbol{v}_R\right|_{1,\Omega}^2 + \left(\left(\nabla \boldsymbol{g}\right)\boldsymbol{v}_R, \boldsymbol{v}_R\right)_{0,\Omega} + R\left\|\boldsymbol{v}_R\right\|_{0,\Omega_S}^2 = -\nu\left(\nabla \boldsymbol{g}, \nabla \boldsymbol{v}_R\right)_{0,\Omega_F} - \left(\left(\nabla \boldsymbol{g}\right)\boldsymbol{g}, \boldsymbol{v}_R\right)_{0,\Omega_F}$$

and due to Theorems 2.4.1 and 2.4.2,

$$\left(\nu - \alpha\right)\left|\boldsymbol{v}_R\right|_{1,\Omega}^2 + R\left\|\boldsymbol{v}_R\right\|_{0,\Omega_S}^2 \leq \left(\nu\left\|\boldsymbol{g}\right\|_{1,\Omega_F} + \kappa\left\|\boldsymbol{g}\right\|_{1,\Omega_F}^2\right)\left|\boldsymbol{v}_R\right|_{1,\Omega}$$

Hence, defining

$$C = \nu\left\|\boldsymbol{g}\right\|_{1,\Omega_F} + \kappa\left\|\boldsymbol{g}\right\|_{1,\Omega_F}^2$$

we conclude

$$\left|\boldsymbol{v}_R\right|_{1,\Omega} \leq \frac{C}{\nu - \alpha} \qquad R\left\|\boldsymbol{v}_R\right\|_{0,\Omega_S}^2 \leq \frac{C^2}{\nu - \alpha}$$

□

The second step is to prove the weakly convergence of $\{\boldsymbol{v}_R\}_{R>0}$

Proposition 2.4.2. *$\boldsymbol{v}_R$ converges weakly to $\boldsymbol{v}$ in $\boldsymbol{V}(\Omega)$.*

Proof. From Proposition 2.4.1, we see that $\boldsymbol{v}_R$ is bounded in $\boldsymbol{H}_{\Gamma_D}^1(\Omega) = V$ and $\chi_{\Omega_S}\boldsymbol{v}_R \to 0$ as $R \to +\infty$. Then there exists a subsequence of $\boldsymbol{v}_R$ (denoted by the same way) that converges weakly in $\boldsymbol{H}^1(\Omega)$ to a function $\tilde{\boldsymbol{v}} \in \boldsymbol{H}^1(\Omega)$. In particular, $\tilde{\boldsymbol{v}} = \boldsymbol{0}$ in Ω_S. Moreover, by Trace Theorem, $\tilde{\boldsymbol{v}} = \boldsymbol{0}$ on $\partial\Omega_S$. On the other hand, applying (2.12), we have that for all $\boldsymbol{w} \in \boldsymbol{V}(\Omega)$:

$$\begin{aligned}\left(R\chi_{\Omega_S}\boldsymbol{v}_R, \boldsymbol{w}\right)_{0,\Omega} &= -\left[\nu\left(\nabla\left(\boldsymbol{v}_R + \boldsymbol{g}\right), \nabla \boldsymbol{w}\right)_{0,\Omega} + \nu\left(\left(\nabla\left(\boldsymbol{v}_R + \boldsymbol{g}\right)\right)\left(\boldsymbol{v}_R + \boldsymbol{g}\right), \nabla \boldsymbol{w}\right)_{0,\Omega}\right]\\ &\to -\left[\nu\left(\nabla\left(\tilde{\boldsymbol{v}} + \boldsymbol{g}\right), \nabla \boldsymbol{w}\right)_{0,\Omega} + \nu\left(\left(\nabla\left(\tilde{\boldsymbol{v}} + \boldsymbol{g}\right)\right)\left(\tilde{\boldsymbol{v}} + \boldsymbol{g}\right), \nabla \boldsymbol{w}\right)_{0,\Omega}\right]\end{aligned}$$

as $R \to \infty$, since $\boldsymbol{v}_R \to \tilde{\boldsymbol{v}}$ in $\boldsymbol{L}^p(\Omega)$, for $p \in [2,6)$. Then $R\chi_{\Omega_S}\boldsymbol{v}_R$ converges weakly to a function $\boldsymbol{h} \in [\boldsymbol{V}(\Omega)]'$ such that $\operatorname{supp}\boldsymbol{h} \subseteq \Omega_S$. Then, taking the limit $R \to \infty$ in (2.12), we have that for all $\boldsymbol{w} \in \boldsymbol{V}(\Omega)$:

$$\begin{aligned} &\nu(\nabla\tilde{\boldsymbol{v}}, \nabla\boldsymbol{w})_{0,\Omega} + ((\nabla\tilde{\boldsymbol{v}})\,\tilde{\boldsymbol{v}}, \boldsymbol{w})_{0,\Omega} + ((\nabla\tilde{\boldsymbol{v}})\,\boldsymbol{g}, \boldsymbol{w})_{0,\Omega} + ((\nabla\boldsymbol{g})\,\tilde{\boldsymbol{v}}, \boldsymbol{w})_{0,\Omega} + \langle\boldsymbol{h}, \boldsymbol{w}\rangle_{V',V} \\ &= -\nu(\nabla\boldsymbol{g}, \nabla\boldsymbol{w})_{0,\Omega_F} - ((\nabla\boldsymbol{g})\,\boldsymbol{g}, \boldsymbol{w})_{0,\Omega_F} \end{aligned} \tag{2.13}$$

Since $\boldsymbol{v}_R = 0$ on $\partial\Omega$, we have $\tilde{\boldsymbol{v}} = \boldsymbol{0}$ on $\partial\Omega$ due the continuity of the trace operator. By the De Rham's Theorem, there exists $\tilde{p} \in L^2_0(\Omega)$ such that

$$\begin{aligned} -\nu\triangle\tilde{\boldsymbol{v}} + (\nabla\tilde{\boldsymbol{v}})\,\tilde{\boldsymbol{v}} + (\nabla\tilde{\boldsymbol{v}})\,\boldsymbol{g} + (\nabla\boldsymbol{g})\,\tilde{\boldsymbol{v}} + \nabla\tilde{\boldsymbol{p}} + \boldsymbol{h} &= \nu\triangle\boldsymbol{g} - (\nabla\boldsymbol{g})\,\boldsymbol{g} && \text{in } \Omega \\ \operatorname{div}\tilde{\boldsymbol{v}} &= 0 && \text{in } \Omega \\ \tilde{\boldsymbol{v}} &= \boldsymbol{0} && \text{on } \partial\Omega \end{aligned}$$

And since $\operatorname{supp}\boldsymbol{h} \subseteq \Omega_S$, we have that for all $\boldsymbol{w} \in \boldsymbol{V}(\Omega)$ such that $\boldsymbol{w} = \boldsymbol{0}$ on Ω_S,

$$\begin{aligned} &\nu(\nabla\tilde{\boldsymbol{v}}, \nabla\boldsymbol{w})_{0,\Omega_F} + ((\nabla\tilde{\boldsymbol{v}})\,\tilde{\boldsymbol{v}}, \boldsymbol{w})_{0,\Omega_F} + ((\nabla\tilde{\boldsymbol{v}})\,\boldsymbol{g}, \boldsymbol{w})_{0,\Omega_F} + ((\nabla\boldsymbol{g})\,\tilde{\boldsymbol{v}}, \boldsymbol{w})_{0,\Omega_F} \\ &= -\nu(\nabla\boldsymbol{g}, \nabla\boldsymbol{w})_{0,\Omega_F} - ((\nabla\boldsymbol{g})\,\boldsymbol{g}, \boldsymbol{w})_{0,\Omega_F} \end{aligned}$$

so $(\tilde{\boldsymbol{v}}|_{\Omega_F}, \tilde{p}|_{\Omega_F})$ is a weak solution for (2.8). Since such a solution is unique, $(\tilde{\boldsymbol{v}}, \tilde{p}) = (\boldsymbol{v}, p)$ in Ω_F. Therefore, $(\tilde{\boldsymbol{v}}, \tilde{p}) = (v, p)$ in Ω and $\boldsymbol{v}_R \rightharpoonup \boldsymbol{v}$ in $\boldsymbol{H}^1_0(\Omega)$. □

2.4.2 Main results

Finally, we can enunciate and prove the strong convergence results.

Theorem 2.4.3. *Let $R > 0$, $\boldsymbol{u}$ be solution of (2.10) and $\boldsymbol{u}_R$ solution of (2.11). With the previous assumptions, there is strong convergence of $\{\boldsymbol{u}_R\}_{R>0}$, i.e.,*

$$\lim_{R\to\infty} |\boldsymbol{u}_R - \boldsymbol{u}|_{1,\Omega} = 0$$

and there exists $C > 0$ such that for all $R > 0$

$$\|\boldsymbol{u} - \boldsymbol{u}_R\|_{0,\Omega_S} \leq \frac{C}{R^{1/2}}$$

Proof. Let $\boldsymbol{w}_R = \boldsymbol{v}_R - \boldsymbol{v}$. From the variational formulations (2.12) and (2.13) we obtain that for all $\boldsymbol{w} \in \boldsymbol{V}(\Omega)$

$$\begin{aligned} &\nu(\nabla\boldsymbol{w}_R, \nabla\boldsymbol{w})_{0,\Omega} + ((\nabla\boldsymbol{v}_R)\,\boldsymbol{v}_R, \boldsymbol{w})_{0,\Omega} - ((\nabla\tilde{\boldsymbol{v}})\,\tilde{\boldsymbol{v}}, \boldsymbol{w})_{0,\Omega} + ((\nabla\boldsymbol{w}_R)\,\boldsymbol{g}, \boldsymbol{w})_{0,\Omega_F} \\ &+ ((\nabla\boldsymbol{g})\,\boldsymbol{w}_R, \boldsymbol{w})_{0,\Omega_F} - \langle\boldsymbol{h}, \boldsymbol{w}\rangle_{V',V} + R(\boldsymbol{v}_R, \boldsymbol{w})_{0,\Omega_S} = 0 \end{aligned}$$

Writing in terms of $\boldsymbol{w}_R$,

$$\begin{aligned} \nu(\nabla\boldsymbol{w}_R, \nabla\boldsymbol{w})_{0,\Omega} + ((\nabla\boldsymbol{w}_R)\,\boldsymbol{v}_R, \boldsymbol{w})_{0,\Omega} + ((\nabla\tilde{\boldsymbol{v}})\,\boldsymbol{w}_R, \boldsymbol{w})_{0,\Omega} + ((\nabla\boldsymbol{w}_R)\,\boldsymbol{g}, \boldsymbol{w})_{0,\Omega_F} \\ + ((\nabla\boldsymbol{g})\,\boldsymbol{w}_R, \boldsymbol{w})_{0,\Omega_F} + R(\boldsymbol{w}_R, \boldsymbol{w})_{0,\Omega_S} = \langle\boldsymbol{h}, \boldsymbol{w}\rangle_{V',V} \end{aligned}$$

Then we take $\boldsymbol{w} = \boldsymbol{w}_R$, and thus

$$\nu \left|\boldsymbol{w}_R\right|_{1,\Omega}^2 + \left(\left(\nabla\left(\tilde{\boldsymbol{v}} + \boldsymbol{g}\right)\right)\boldsymbol{w}_R, \boldsymbol{w}_R\right)_{0,\Omega} + R\left\|\boldsymbol{w}_R\right\|_{0,\Omega_S}^2 = \left\langle \boldsymbol{h}, \boldsymbol{w}_R\right\rangle_{V',V} \tag{2.14}$$

Let $c_2 = \alpha + \dfrac{C\kappa}{\nu - \alpha}$, then

$$0 < c_2 = \alpha + \frac{C\kappa}{\nu - \alpha} < \alpha + \nu - \alpha = \nu$$

Hence, from Theorems 2.4.1 and 2.4.2,

$$\begin{aligned}\left(\left(\nabla\left(\tilde{\boldsymbol{v}} + \boldsymbol{g}\right)\right)\boldsymbol{w}_R, \boldsymbol{w}_R\right)_{0,\Omega} &\leq \left(\alpha + \kappa\left|\tilde{\boldsymbol{v}}\right|_{1,\Omega}\right)\left|\boldsymbol{w}_R\right|_{1,\Omega}^2 \\ &\leq \left(\alpha + \frac{C\kappa}{\nu - \alpha}\right)\left|\boldsymbol{w}_R\right|_{1,\Omega}^2 = c_2\left|\boldsymbol{w}_R\right|_{1,\Omega}^2\end{aligned}$$

and using this inequality in (2.14), we have

$$\left(\nu - c_2\right)\left|\boldsymbol{w}_R\right|_{1,\Omega}^2 + R\left\|\boldsymbol{w}_R\right\|_{0,\Omega_S}^2 \leq \left\langle \boldsymbol{h}, \boldsymbol{w}_R\right\rangle_{V',V}$$

Also we have,

$$\left\langle \boldsymbol{h}, \boldsymbol{w}_R\right\rangle_{V',V} = -\left[\nu\left(\nabla\left(\tilde{\boldsymbol{v}} + \boldsymbol{g}\right), \nabla\boldsymbol{w}_R\right)_{0,\Omega} + \nu\left(\left(\nabla\left(\tilde{\boldsymbol{v}} + \boldsymbol{g}\right)\right)\left(\tilde{\boldsymbol{v}} + \boldsymbol{g}\right), \nabla\boldsymbol{w}_R\right)_{0,\Omega}\right] \to 0$$

as $R \to \infty$. Therefore

$$\left(\nu - c_2\right)\left|\boldsymbol{w}_R\right|_{1,\Omega}^2 + R\left\|\boldsymbol{w}_R\right\|_{0,\Omega_S}^2 = \left\langle \boldsymbol{h}, \boldsymbol{w}_R\right\rangle_{V',V} \to 0$$

so we have proved that $\left|\boldsymbol{w}_R\right|_{1,\Omega} \to 0$ and $\left\|\boldsymbol{w}_R\right\|_{0,\Omega_S} = \mathcal{O}\left(R^{-1/2}\right)$. □

Theorem 2.4.4. *Let $R > 0$, $\boldsymbol{u}$ be solution of (2.10) and $\boldsymbol{u}_R$ solution of (2.11). With the previous assumptions, where we assume in addition that $\partial\Omega_F$ is piecewise $\mathcal{C}^2$ and $\boldsymbol{u}_D \in H^{3/2}(\Omega)$, then there is strong convergence of $\{u_R\}$ in $H^1(\Omega)$ and moreover there exists a constant $C > 0$ such that for all $R > 0$*

$$\left|\boldsymbol{u} - \boldsymbol{u}_R\right|_{1,\Omega} \leq \frac{C}{R^{1/4}}, \qquad \left\|\boldsymbol{u} - \boldsymbol{u}_R\right\|_{0,\Omega_S} \leq \frac{C}{R^{3/4}}$$

Proof. We can assume that $\boldsymbol{g} \in \boldsymbol{H}^2\left(\Omega\right)$ because $\boldsymbol{u}_D \in H^{3/2}(\Omega)$, then there is strong convergence of $\{u_R\}$ in $H^1(\Omega)$. Reasoning as in Theorem 2.3.2, we can apply a regularity result (see Theorem IX.5.2 in [48]) and consider $(\boldsymbol{v}, p) \in \boldsymbol{H}^2\left(\Omega\right) \times \boldsymbol{H}^1\left(\Omega\right)$. Defining $\boldsymbol{k} \in H^{1/2}\left(\Omega\right)$ by

$$\boldsymbol{k} = -\nu\frac{\partial\boldsymbol{v} + \boldsymbol{g}}{\partial\boldsymbol{n}} + p\boldsymbol{n} + \frac{1}{2}\left(\left(\boldsymbol{v} + \boldsymbol{g}\right)\cdot\boldsymbol{n}\right)\left(\boldsymbol{v} + \boldsymbol{g}\right) = -\nu\frac{\partial\boldsymbol{v} + \boldsymbol{g}}{\partial\boldsymbol{n}} + p\boldsymbol{n}$$

and taking $\boldsymbol{w} \in \boldsymbol{V}_{\partial\Omega_S\setminus\Gamma}\left(\Omega_F\right)$ extended by $\boldsymbol{0}$ to Ω_S, we have

$$\begin{aligned}&\nu\left(\nabla\boldsymbol{v}, \nabla\boldsymbol{w}\right)_{0,\Omega} + \left(\left(\nabla\boldsymbol{v}\right)\boldsymbol{v}, \boldsymbol{w}\right)_{0,\Omega} + \left(\left(\nabla\boldsymbol{v}\right)\boldsymbol{g}, \boldsymbol{w}\right)_{0,\Omega} + \left(\left(\nabla\boldsymbol{g}\right)\boldsymbol{v}, \boldsymbol{w}\right)_{0,\Omega} + \left(\boldsymbol{k}, \boldsymbol{w}\right)_{0,\partial\Omega_S\setminus\Gamma} \\ &= -\nu\left(\nabla\boldsymbol{g}, \nabla\boldsymbol{w}\right)_{0,\Omega_F} - \left(\left(\nabla\boldsymbol{g}\right)\boldsymbol{g}, \boldsymbol{w}\right)_{0,\Omega_F}\end{aligned}$$

Since

$$\begin{aligned}&\nu\left(\nabla \boldsymbol{v}, \nabla \boldsymbol{w}\right)_{0,\Omega} + \left(\left(\nabla \boldsymbol{v}\right)\boldsymbol{v}, \boldsymbol{w}\right)_{0,\Omega} + \left(\left(\nabla \boldsymbol{v}\right)\boldsymbol{g}, \boldsymbol{w}\right)_{0,\Omega} + \left(\left(\nabla \boldsymbol{g}\right)\boldsymbol{v}, \boldsymbol{w}\right)_{0,\Omega} + \left\langle \boldsymbol{h}, \boldsymbol{w}\right\rangle_{V',V}\\ =& -\nu\left(\nabla \boldsymbol{g}, \nabla \boldsymbol{w}\right)_{0,\Omega_F} - \left(\left(\nabla \boldsymbol{g}\right)\boldsymbol{g}, \boldsymbol{w}\right)_{0,\Omega_F}\end{aligned}$$

we have

$$\left(\forall \boldsymbol{w} \in \boldsymbol{V}_{\partial\Omega_S\setminus\Gamma}\left(\Omega\right)\right) \qquad \left\langle \boldsymbol{h}, \boldsymbol{w}\right\rangle_{V',V} = \left(\boldsymbol{k}, \boldsymbol{w}\right)_{0,\partial\Omega_S\setminus\Gamma}$$

Hence, applying Trace Theorem, Hölder inequality and Sobolev Embedding Theorem (see Section 6.6 in [36]), there exists a constant $C > 0$, independent of $R > 0$, such that

$$\begin{aligned}\left(\nu - c_2\right)\left|\boldsymbol{w}_R\right|^2_{1,\Omega} + R\left\|\boldsymbol{w}_R\right\|^2_{0,\Omega_S} &\leq \left(\boldsymbol{k}, \boldsymbol{w}_R\right)_{0,\partial\Omega_S\setminus\Gamma}\\ &\leq C\left\|\boldsymbol{k}\right\|_{0,\partial\Omega_S}\left|\boldsymbol{w}_R\right|^{1/2}_{1,\Omega_S}\left\|\boldsymbol{w}_R\right\|^{1/2}_{0,\Omega_S}\\ &\leq \frac{\left(C\left\|\boldsymbol{k}\right\|_{0,\partial\Omega_S\setminus\Gamma}\right)^2}{2\left(\nu R\right)^{1/2}} + \frac{1}{4}\left(\nu\left|\boldsymbol{w}_R\right|^2_{1,\Omega} + R\left\|\boldsymbol{w}_R\right\|^2_{0,\Omega_S}\right)\end{aligned}$$

which can be rewritten as

$$\nu\left|\boldsymbol{w}_R\right|^2_{1,\Omega} + R\left\|\boldsymbol{w}_R\right\|^2_{0,\Omega_S} \leq \frac{2\left(C\left\|\boldsymbol{k}\right\|_{0,\partial\Omega_S\setminus\Gamma}\right)^2}{3\left(\nu R\right)^{1/2}}$$

Therefore, $\left|\boldsymbol{w}_R\right|_{1,\Omega} = \mathcal{O}\left(R^{-1/4}\right)$ and $\left\|\boldsymbol{w}_R\right\|_{0,\Omega_S} = \mathcal{O}\left(R^{-3/4}\right)$, proving this result. □

2.5 Numerical examples

In this section, we report a simple 2D numerical experiment to validate the use of fictitious domains in the study of obstacles, to verify the convergence orders obtained in Sections 2.3 and 2.4. We also present numerical estimates in this experiment, although our theory does not consider an error estimate for the pressure p in Ω_F. This experiment is motivated for numerical implementations performed in [3], where the approach consists in reconstructing a potential via the minimization of a least-squares functional with a regularization term in order to reconstruct obstacles which could be either immersed or added to the virtual boundary domain.

First, we consider the domain $\Omega = \Omega_F \cup \overline{\Omega}_S = (-2, 2) \times (-1, 1)$ given in Figure 2.2 where $\Omega_F \cap \Omega_S = \emptyset$ and Ω_S is given by

$$\Omega_S = (-1.1, -0.9) \times (0.4, 1) \cup \{(x, y) \in \mathbb{R}^2 \mid (x-1)^2 + (y-0.5)^2 = (0.3)^2\}$$

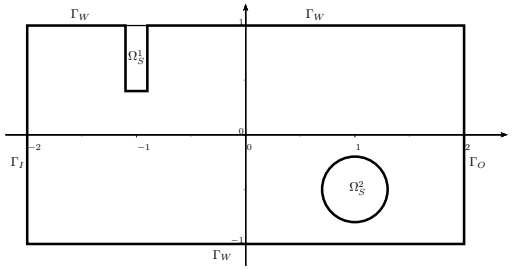

Figure 2.2: Fictitious domain Ω with obstacles Ω_S^1 and Ω_S^2.

This example is representative for our purposes, since it consists of a domain with two types of obstacles: the first one, Ω_S^1 is added to the boundary of the whole virtual domain, while the other obstacle, Ω_S^2 is such that its closure is totally embedded in the fluid.

In order to determine the reference solutions $(\boldsymbol{u}, p)$ for Stokes and Navier-Stokes equations, we consider the following boundary conditions for the domain Ω_F:

- The inflow $\Gamma_I = -2 \times [-1, 1]$ has a parabolic profile following Poiseuille's Law given by

$$\boldsymbol{u}_D\,(x, y) = -U(1 + y)(1 - y)\boldsymbol{n},$$

  where $U > 0$, $\boldsymbol{x} = (x, y)$ are the Cartesian coordinates of the domain and $\boldsymbol{n}$ is the outer normal vector.

- The do-nothing conditions are imposed on the outflow $\Gamma_O = 2 \times [-1, 1]$, given by

$$-\nu \frac{\partial \boldsymbol{u}}{\partial \boldsymbol{n}} + p\boldsymbol{n} = \boldsymbol{0}.$$

- No-slip boundary condition for $\Gamma_{F,W} = \partial\Omega_S \setminus (\Gamma_I \cup \Gamma_O)$.

Given $R > 0$, we use the same boundary conditions for $\Gamma_I = -2 \times [-1, 1]$ and $\Gamma_O = 2 \times [-1, 1]$ to calculate the penalized solutions $(\boldsymbol{u}_R, p_R)$. The no-slip boundary condition is now applied to $\Gamma_F = [-2, 2] \times \{-1, 1\}$.

The numerical solutions of Stokes and Navier-Stokes equations are computed by the Finite Element Method (FEM) with Taylor-Hood elements ($\mathbb{P}_2$ for velocity and $\mathbb{P}_1$ for pressure) on an unstructured triangular mesh generated for Ω by domain triangulation with $h = 0.05$, which corresponds to 8416 elements and 4329 nodes. The mesh was designed to approach obstacles Ω_S as smoothly as possible.

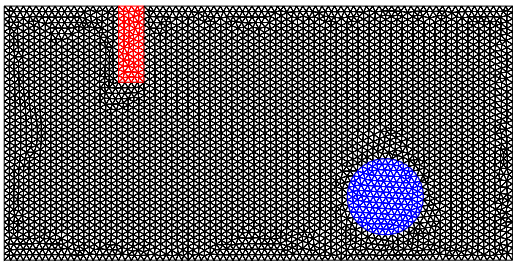

Figure 2.3: Plots of structure mesh of Ω_F (black), Ω_S^1 (red) and Ω_S^2 (blue).

The mesh is generated by Gmsh [49] and the numerical solvers are implemented using the Finite element library FEniCS [5] with the default configuration. To solve the nonlinear problems, a Newton's method was used.

The parameters $\nu = 1$ and $U = 100$ will be used for the Stokes and Navier-Stokes equations. Considering $d = 2$ as the length of Γ_I, the peak Reynolds number on the inflow is

$$\mathrm{Re} = \frac{Ud}{\nu} = 200.$$

2.5.1 Stokes equation

First, we consider the reference solution $(\boldsymbol{u}, p)$ as the solution computed on the real domain Ω_F. Then, for $R \in \{10^n \mid n \in \{0, 1, \ldots, 10\}\}$, the solution $(\boldsymbol{u}_R, p_R)$ is calculated on the fictitious domain Ω. Finally, we compute the errors $\|\boldsymbol{u}_R\|_{0,\Omega_S}$, $|\boldsymbol{u} - \boldsymbol{u}_R|_{1,\Omega}$, $|\boldsymbol{u} - \boldsymbol{u}_R|_{1,\Omega}$ and $\|p - p_R\|_{0,\Omega_F}$, where $\boldsymbol{u}$ is extended by $\mathbf{0}$ on Ω_S.

	$\|\boldsymbol{u}_R\|_{0,\Omega_S}$		$\|\boldsymbol{u} - \boldsymbol{u}_R\|_{0,\Omega_F}$		$\|p - p_R\|_{0,\Omega_F}$	
R	Error	Rate	Error	Rate	Error	Rate
10^0	$4.2961 \cdot 10^1$	–	$4.2961 \cdot 10^2$	–	$2.5866 \cdot 10^3$	–
10^1	$3.7983 \cdot 10^1$	0.0535	$3.9663 \cdot 10^2$	0.0347	$2.3619 \cdot 10^3$	0.0395
10^2	$1.9419 \cdot 10^1$	0.2914	$2.6400 \cdot 10^2$	0.1768	$1.4234 \cdot 10^3$	0.2199
10^3	$4.4546 \cdot 10^0$	0.6394	$1.2827 \cdot 10^2$	0.3135	$4.6572 \cdot 10^2$	0.4852
10^4	$7.6739 \cdot 10^{-1}$	0.7638	$6.2586 \cdot 10^1$	0.3116	$1.1085 \cdot 10^2$	0.6234
10^5	$1.2696 \cdot 10^{-1}$	0.7813	$1.8038 \cdot 10^1$	0.5403	$1.6119 \cdot 10^1$	0.8374
10^6	$1.5054 \cdot 10^{-2}$	0.9260	$2.3898 \cdot 10^0$	0.8778	$1.7153 \cdot 10^0$	0.9730
10^7	$1.5396 \cdot 10^{-3}$	0.9902	$2.4761 \cdot 10^{-1}$	0.9846	$1.7268 \cdot 10^{-1}$	0.9971
10^8	$1.5432 \cdot 10^{-4}$	0.9990	$2.4851 \cdot 10^{-2}$	0.9984	$1.7280 \cdot 10^{-2}$	0.9997
10^9	$1.5436 \cdot 10^{-5}$	0.9999	$2.4860 \cdot 10^{-3}$	0.9998	$1.7281 \cdot 10^{-3}$	1.0000
10^{10}	$1.5436 \cdot 10^{-6}$	1.0000	$2.4861 \cdot 10^{-4}$	1.0000	$1.7281 \cdot 10^{-4}$	1.0000

Table 2.1: History of convergence for Stokes equations.

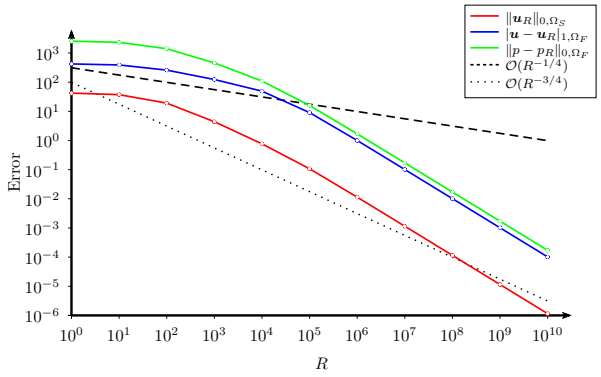

Figure 2.4: History of convergence for Stokes equations.

Table 2.1 and Figure 2.4 show that in this experiment the numerical error orders are better than we deduced in Theorem 2.3.2. When R is going to $+\infty$, the errors $\|\boldsymbol{u}_R\|_{0,\Omega_S}$ and $|\boldsymbol{u} - \boldsymbol{u}_R|_{1,\Omega}$ decrease with order $\mathcal{O}(R^{-1})$. The error orders are similar to $\mathcal{O}(R^{-3/4})$ and $\mathcal{O}(R^{-1/4})$ for $\|\boldsymbol{u}_R\|_{0,\Omega_S}$ and $|\boldsymbol{u} - \boldsymbol{u}_R|_{1,\Omega}$, respectively, until $R = 10^4$. For higher values of R, the error order grows up to $\mathcal{O}(R^{-1})$. Hence these results suggest that the obtained error estimates might not be optimal. The error $\|p - p_R\|_{0,\Omega_F}$ follows a behavior very similar to the errors $\|\boldsymbol{u}_R\|_{0,\Omega_S}$ and $|\boldsymbol{u} - \boldsymbol{u}_R|_{1,\Omega}$.

From the isovalues and streamlines plots for $\boldsymbol{u}$ and $\boldsymbol{u}_R$ in Figures 2.5, 2.6 and 2.7, we observe that the numerical solution of $\boldsymbol{u}_R$ effectively approximates the reference velocity $\boldsymbol{u}$ for large values of R.

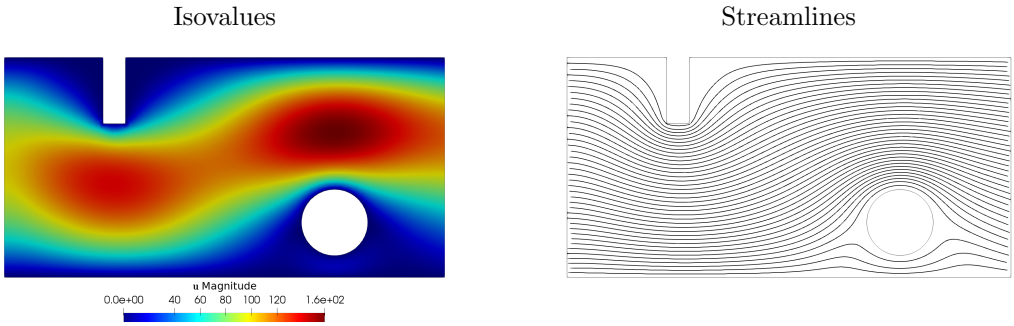

Figure 2.5: Reference solution, Stokes equations on Ω_F.

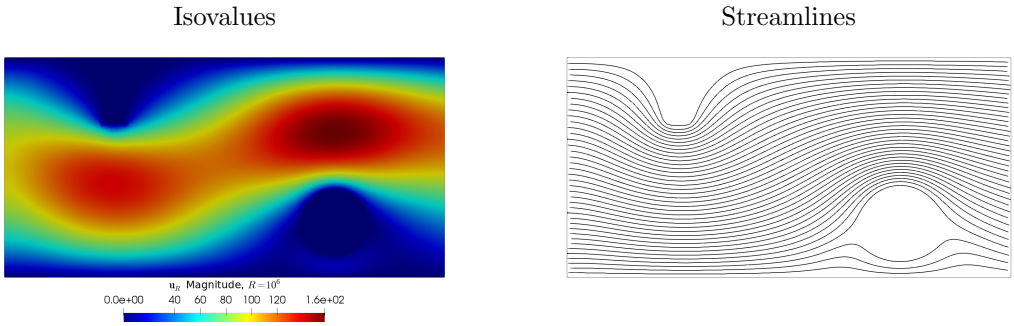

Figure 2.6: Solution for penalized Stokes equations for $R = 10^6$ on Ω.

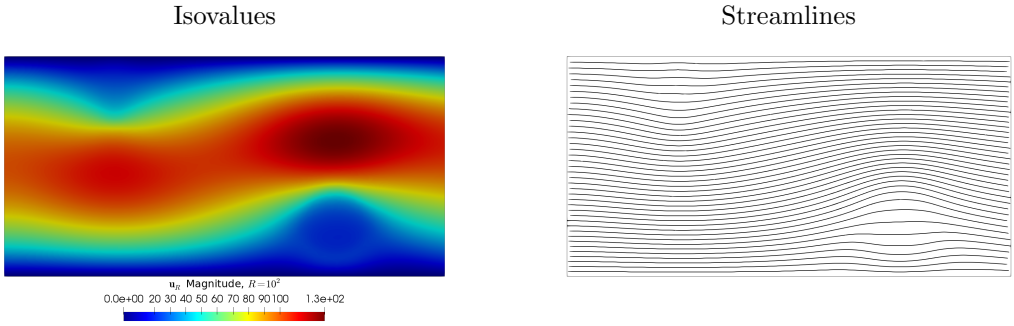

Figure 2.7: Solution for penalized Stokes equations for $R = 10^2$ on Ω.

2.5.2 Navier-Stokes equation

We repeat the same calculations now for the Navier-Stokes equations. We consider the reference solution $(\boldsymbol{u}, p)$ as the solution computed on the real domain Ω_F and the solution $(\boldsymbol{u}_R, p_R)$ on the fictitious domain Ω for $R \in \{10^n \mid n \in \{0, 1, \ldots, 10\}\}$. The errors $\|\boldsymbol{u}_R\|_{0,\Omega_S}$, $|\boldsymbol{u} - \boldsymbol{u}_R|_{1,\Omega}$ and $\|p - p_R\|_{0,\Omega_F}$ are computed the same way as in Stokes equations.

R	$\|\boldsymbol{u}_R\|_{0,\Omega_S}$ Error	Rate	$\|\boldsymbol{u}-\boldsymbol{u}_R\|_{1,\Omega}$ Error	Rate	$\|p-p_R\|_{0,\Omega_F}$ Error	Rate
10^0	$4.3520 \cdot 10^1$	–	$7.0881 \cdot 10^2$	–	$1.5482 \cdot 10^4$	–
10^1	$4.2667 \cdot 10^1$	0.0086	$7.0356 \cdot 10^2$	0.0032	$1.5227 \cdot 10^4$	0.0072
10^2	$3.5656 \cdot 10^1$	0.0780	$6.5737 \cdot 10^2$	0.0295	$1.2880 \cdot 10^4$	0.0727
10^3	$1.5385 \cdot 10^1$	0.3650	$4.5125 \cdot 10^2$	0.1364	$4.8714 \cdot 10^3$	0.4223
10^4	$3.0413 \cdot 10^0$	0.7040	$2.0814 \cdot 10^1$	0.3361	$9.4603 \cdot 10^2$	0.7117
10^5	$4.6066 \cdot 10^{-1}$	0.8197	$6.0166 \cdot 10^1$	0.5390	$1.5174 \cdot 10^2$	0.7948
10^6	$5.3538 \cdot 10^{-2}$	0.9347	$8.0308 \cdot 10^0$	0.8746	$1.7796 \cdot 10^1$	0.9308
10^7	$5.4639 \cdot 10^{-3}$	0.9912	$8.3281 \cdot 10^{-1}$	0.9842	$1.8164 \cdot 10^0$	0.9911
10^8	$5.4755 \cdot 10^{-4}$	0.9991	$8.3593 \cdot 10^{-2}$	0.9984	$1.8202 \cdot 10^{-1}$	0.9991
10^9	$5.4767 \cdot 10^{-5}$	0.9999	$8.3625 \cdot 10^{-3}$	0.9998	$1.8206 \cdot 10^{-2}$	0.9999
10^{10}	$5.4768 \cdot 10^{-6}$	1.0000	$8.3628 \cdot 10^{-4}$	1.0000	$1.8203 \cdot 10^{-3}$	1.0001

Table 2.2: History of convergence for Navier-Stokes equations.

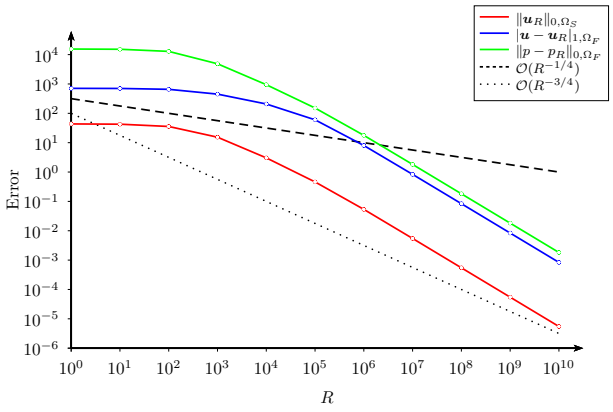

Figure 2.8: History of convergence for Navier-Stokes equations.

While the theory developed in Section 2.4 considers only inhomogeneous Dirichlet boundary conditions, we obtain similar results as in Stokes equations using mixed boundary conditions (Dirichlet and Neumann). Indeed, Table (2.2) and Figure 2.8 show that in this experiment the numerical error orders are better than $\mathcal{O}(R^{-3/4})$ and $\mathcal{O}(R^{-1/4})$ for $\|\boldsymbol{u}_R\|_{0,\Omega_S}$ and $|\boldsymbol{u}-\boldsymbol{u}_R|_{1,\Omega}$ when R is going to $+\infty$, obtaining an order $\mathcal{O}(R^{-1})$ for both errors. Similar result were obtained for the error $\|p-p_R\|_{0,\Omega_F}$ with a behavior very similar to the errors $\|\boldsymbol{u}_R\|_{0,\Omega_S}$ and $|\boldsymbol{u}-\boldsymbol{u}_R|_{1,\Omega}$. Again, the error estimates obtained in Theorem 2.4.4 might not be optimal, with similar conclusions as in the Stokes problem.

From the isovalues and streamlines plots for $\boldsymbol{u}$ and $\boldsymbol{u}_R$ in Figures 2.9, 2.10 and 2.11, we observe that the numerical solution of $\boldsymbol{u}_R$ effectively approximates the reference velocity $\boldsymbol{u}$, including the vortex after the upper obstacle, for large values of R.

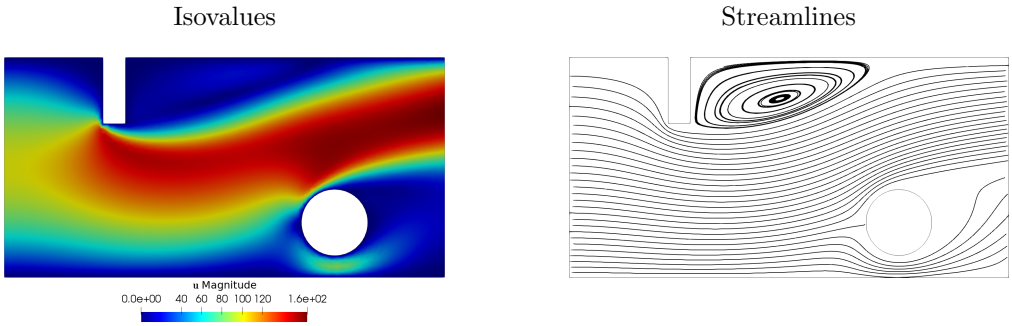

Figure 2.9: Reference solution, Navier-Stokes equations on Ω_F.

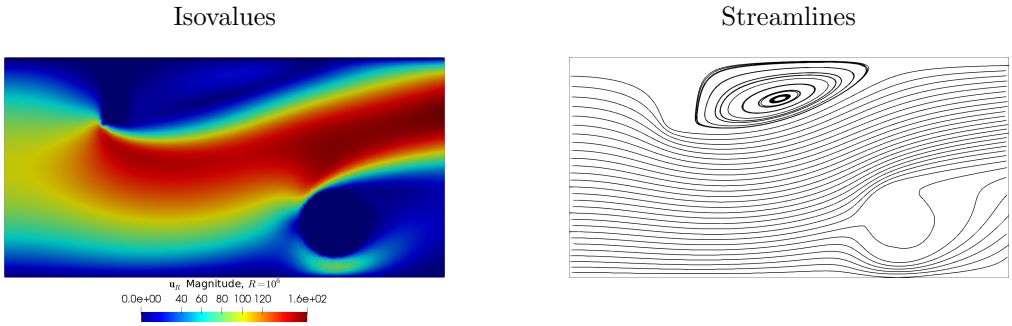

Figure 2.10: Solution for penalized Navier-Stokes equations for $R = 10^6$ on Ω.

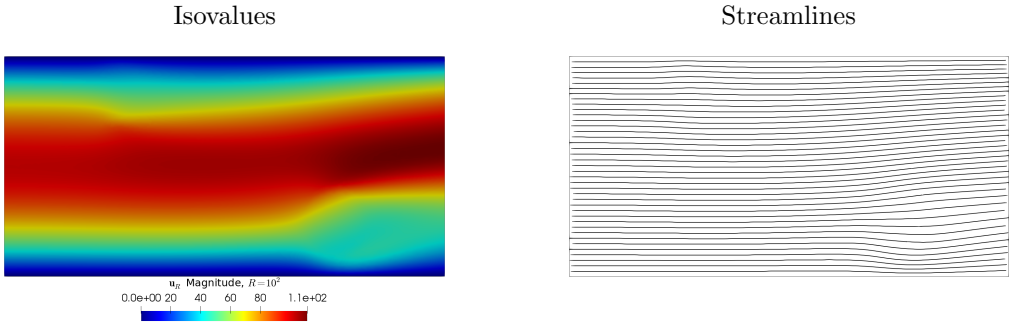

Figure 2.11: Solution for penalized Navier-Stokes equations for $R = 10^2$ on Ω.

2.6 Conclusions

We have rigorously established and analyzed a penalization method for steady Stokes and Navier-Stokes equations to approximate the fluid equations around obstacles. The error estimations obtained in Sections 2.3 and 2.4 allow us to consider the penalization parameter R as large as necessary to reduce the penalty error, verifying the robustness of the method.

The numerical test proves that this method is easy to implement and is a way to analyze obstacles that does not change the domain when working with a fictitious domain. Hence,

we have shown both theoretically and with numerical experiments that the equations presented constitute a valid model for fluids going through obstacles in which the numerical implementation is much simpler and cheap for computations since it will not depend on the geometry of the obstacles. As a consequence, it is possible to avoid shape optimization methods and work with this penalization term and thus to simplify the models and their numerical implementation.

About future work, the numerical experiments developed in this work allows us to conjecture that it would be possible to improve theoretically the penalty error from $R^{-3/4}$ to R^{-1} and possible estimate for the pressure error $\|p - p_R\|_{0,\Omega_F}$. In addition, for the time dependent setting, it would be possible to prove similar estimates, and if we use similar techniques, we expect to find the penalty error observed in [9], since here we obtained the penalty error observed in [8].

Chapter 3

A stability result for the identification of a permeability parameter on Navier-Stokes equations

The content of this chapter was published in J. Aguayo and A. Osses. "A stability result for the identification of a permeability parameter on Navier-Stokes equations" in Inverse Problems, 2022. [4].

In this chapter, we present a stability result for the inverse problem of recovering a smooth scalar permeability parameter given by the Brinkman's law applied to the steady Navier-Stokes equations from local observations of the fluid velocity on a fixed domain. In comparison with [34], we prove a logarithmic estimate under weaker assumptions, since our proof is based in a strategy that does not require pressure observations. This kind of results are useful for inverse problems in soft tissue elastography (see [54]). Finally, we present some numerical tests that validate our theoretical findings. All the results presented in this chapter are also valid when $\Omega \subseteq \mathbb{R}^2$, adapting the definitions of cross product and curl to the two dimensional case.

3.1 An historic introduction to Carleman inequalities and its applications

In 1939, a new method for proving uniqueness of solution for 2D elliptic equations were presented by Torsten Carleman in [30]. One of the principal advantages of this new method is the relaxation of some hypothesis, where the previous results require that the solutions of the elliptic equation must be analytical. Particularly, Carleman established a L^2 weighted inequality similar to the following one:

$$\|e^{s\varphi}u\|_{0,\Omega} \leq C \|e^{s\varphi}Pu\|_{0,\Omega}$$

for all $u \in \mathcal{C}_0^\infty(\Omega)$ and $s \geq s_0 > 1$, where P is an elliptic differential operator, φ is a suitable non-negative function and $s_0, C \in \mathbb{R}$ are positive constants independent on φ, s and u, to prove the unique continuation property given by:

Let Ω be a connected open non-empty subset of $\mathbb{R}^2$ and $V \in L^\infty(\Omega)$. If $u \in H^2(\Omega)$ is a solution to

$$-\triangle u + Vu = 0 \text{ in } \Omega$$

such that $u = 0$ in a non-empty open subset $\omega \Subset \Omega$, then $u = 0$ in Ω.

The use of Carleman estimate has allowed to relax hypotheses of smoothness of solutions of different PDEs to verify or deduce some energy estimates, allowing to establish the stability of the solution of some direct, inverse and ill-posed problems.

3.2 Introduction and main model

Let Ω be a $\mathcal{C}^2-$bounded domain in $\mathbb{R}^3$ with boundary $\partial\Omega$ and outer normal vector $\boldsymbol{n}$, $\nu \in \mathbb{R}$ with $\nu > 0$, $M \in \mathbb{R}$ with $M > 0$, $\gamma_j \in H^1(\Omega)$ such that $0 \leq \gamma_j \leq M$ for $j \in \{1, 2\}$ and $\boldsymbol{u}_D \in \boldsymbol{H}^{3/2}(\partial\Omega)$. The model problem

$$\begin{aligned} -\nu\triangle \boldsymbol{u}_j + (\nabla \boldsymbol{u}_j)\,\boldsymbol{u}_j + \nabla p_j + \gamma_j \boldsymbol{u}_j &= \boldsymbol{0} \quad \text{in } \Omega \\ \operatorname{div} \boldsymbol{u}_j &= 0 \quad \text{in } \Omega \\ \boldsymbol{u}_j &= \boldsymbol{u}_D \quad \text{on } \partial\Omega \end{aligned} \tag{3.1}$$

admits an unique solution $(\boldsymbol{u}_j, p_j) \in \boldsymbol{H}^2(\Omega) \times H^1(\Omega)$ with $(p_j, 1)_\Omega = 0$. For $\varepsilon > 0$, we define

$$\Omega_\varepsilon = \{\boldsymbol{x} \in \Omega \mid d(\boldsymbol{x}, \partial\Omega) \geq \varepsilon\}.$$

We suppose

$$\gamma_j \in H(\Omega) = \left\{f \in H_0^1(\Omega) \mid f = 0 \text{ in } \Omega \setminus \Omega_\varepsilon\right\}.$$

Then, there exists a constant $c_1 > 0$ only dependent on Ω and M such that.

$$\|\boldsymbol{u}_j\|_{2,\Omega}^2 + \|p_j\|_{1,\Omega}^2 \leq c_1 \|\boldsymbol{u}_D\|_{1/2,\partial\Omega}^2.$$

Defining $\gamma = \gamma_1 - \gamma_2$, $\boldsymbol{u} = \boldsymbol{u}_1 - \boldsymbol{u}_2$ and $p = p_1 - p_2$, $(\boldsymbol{u}, p)$ is the unique solution of the Oseen equations given by

$$\begin{aligned} -\nu\triangle \boldsymbol{u} + (\nabla \boldsymbol{u})\,\boldsymbol{u}_1 + (\nabla \boldsymbol{u}_2)\,\boldsymbol{u} + \nabla p + \gamma_1 \boldsymbol{u} &= -\boldsymbol{f} \quad \text{in } \Omega \\ \operatorname{div} \boldsymbol{u} &= 0 \quad \text{in } \Omega \\ \boldsymbol{u} &= \boldsymbol{0} \quad \text{on } \partial\Omega, \end{aligned} \tag{3.2}$$

where $\boldsymbol{f} = \gamma \boldsymbol{u}_2$. In this case, we have a constant $c_{NS} > 0$ such that

$$\|\boldsymbol{u}\|_{2,\Omega}^2 + \|p\|_{1,\Omega}^2 \leq c_{NS} \|\gamma\|_{0,\Omega}^2.$$

We pose the following assumptions:

1. There exists a constant $K > 0$ such that $\|\gamma\|_{1,\Omega} \leq K$.
2. There exist constants $M_2 > 0$ and $c_{NS} > 0$ such that $\|\boldsymbol{u}\|_{2,\Omega}^2 + \|p\|_{1,\Omega}^2 \leq M_2^2 \leq c_{NS} K^2$.
3. There exists a constant $M_3 > 0$ such that $\|\boldsymbol{u}\|_{3,\Omega} \leq M_3$

4. The velocity $\boldsymbol{u}_2$ verifies $\operatorname{curl} \boldsymbol{u}_2 \in \boldsymbol{L}^\infty(\Omega)$.

Remark 3.2.1. *Assumption 1 is usual in problems where the permeability coefficient is studied. Assumptions 2 and 3 are similar to the one used in [14]. Finally, assumption 4 is similar to smoothness assumptions in [14] and [34].*

In order to avoid an analysis of the gradient of the pressure p we eliminate this variable using the curl operator. If we define $\boldsymbol{z} = \operatorname{curl} \boldsymbol{u}$, where $\boldsymbol{u}$ is the solution of Equation (3.2), then $\boldsymbol{u}$ verifies the following second-order elliptical equation:

$$\begin{aligned} -\triangle \boldsymbol{u} = \operatorname{curl}(\operatorname{curl} \boldsymbol{u}) - \nabla(\operatorname{div} \boldsymbol{u}) = \operatorname{curl} \boldsymbol{z} \quad & \text{in } \Omega \\ \boldsymbol{u} = \boldsymbol{0} \quad & \text{on } \partial\Omega. \end{aligned} \tag{3.3}$$

Thanks to $\operatorname{curl}(\nabla p) = \boldsymbol{0}$, the vector field $\boldsymbol{z}$ verifies the following equations

$$\begin{aligned} -\nu \triangle \boldsymbol{z} + (\nabla \boldsymbol{z})\, \boldsymbol{u}_1 + \gamma_1 \boldsymbol{z} = -(\operatorname{curl} \boldsymbol{f} + \boldsymbol{h}) \quad & \text{in } \Omega \\ \operatorname{div} \boldsymbol{z} = 0 \quad & \text{in } \Omega \\ \boldsymbol{z} = \operatorname{curl} \boldsymbol{u} \quad & \text{on } \partial\Omega, \end{aligned} \tag{3.4}$$

where $\boldsymbol{h} \in \boldsymbol{L}^2(\Omega)$ is defined by

$$\boldsymbol{h} = \nabla \gamma_1 \times \boldsymbol{u} + (\nabla \operatorname{curl}(\boldsymbol{u}_2))\, \boldsymbol{u} + \sum_{j=1}^{3} \nabla [\boldsymbol{u}_1]_j \times \frac{\partial \boldsymbol{u}}{\partial x_j} + \nabla [\boldsymbol{u}]_j \times \frac{\partial \boldsymbol{u}_2}{\partial x_j}.$$

From an open connected non-empty subset $\omega \subseteq \Omega$, the inverse problem we studied here is to determinate $\gamma = \gamma_1 - \gamma_2$ in Ω from the observation data $\boldsymbol{u}|_\omega = (\boldsymbol{u}_1 - \boldsymbol{u}_2)|_\omega$, where $\boldsymbol{u}_1$ and $\boldsymbol{u}_2$ verify the Navier-Stokes equations given in (3.1) for γ_1 and γ_2, respectively.

The main objective of this work is to obtain a stability result for this parameter identification problem, where we search a permeability parameter γ from a measured velocity $\boldsymbol{u}$. This problem was already studied in [3] by minimizing a quadratic functional for a model based in Oseen equations, so this article validates the strategy by ensuring the uniqueness of the quadratic functional minimizer in those cases where the hypotheses of this article are verified. A first approach to this problem is given in [14] and [34]. In [14], the authors describe Carleman inequalities for steady Oseen equations applied to find stability results for Navier and Robin boundary coefficients in a compact subset $K \subseteq \partial\Omega$ such that $|\boldsymbol{u}_2| \geq m$ in K, where $m > 0$ is a constant. That estimates need an analysis of pressure to be computed. In [34], the authors obtain a Lipschitz stability result for the right-hand side of a unsteady linearized Navier-Stokes equation, recovering a source scalar term f using a global observation of $\boldsymbol{u}$ and $\operatorname{curl} \boldsymbol{u}$ in a fixed time and local observations of $\boldsymbol{u}$ in a time interval. The source term represent the density of external force with a form $f\boldsymbol{R}$, where $\boldsymbol{R}$ is a vector field that verifies a non-degeneracy condition. Both ideas can be adapted to this new problem, obtaining a Carleman inequality and a stability result with no observation data of p.

This chapter is structured as follows. In Section 3, we have adapted the technique used to prove Theorem 2.3 in [14] to obtain an improved version of a Carleman inequality for weak solutions of Equation (3.2). In Section 4, we present a modified version of the non-degeneracy condition introduced in [34] that allow us to prove a logarithmic stability result

using a Carleman estimate obtained in Section 3 and a similar Carleman estimate obtained for strong solutions of Equation (3.3). Finally, in Section 5 we present two numerical test that validates the main result recovering a smooth and a discontinuous parameter solving a minimization problem. The second test, inspired in [3], is not covered by our main result. However, we add an adaptive refinement algorithm that improves the numerical results.

3.3 A Carleman estimate

This first result allows us to define the Carleman weights for our estimates.

Lemma 3.3.1. *Let $c_0 \geq 0$. There exists a function $\varphi \in \mathcal{C}^\infty\left(\overline{\Omega}\right)$ such that $\varphi = c_0$ on $\partial\Omega$, $\varphi > c_0$ in Ω and $\nabla\varphi \neq \mathbf{0}$ in $\overline{\Omega \setminus \omega}$.*

Proof. See Lemma 1.1 in [47]. □

The following lemma is the Carleman inequality for weak solutions of linear second-order elliptic PDE with homogenous Dirichlet boundary conditions.

Lemma 3.3.2. *Let $f \in L^2(\Omega)$, $\boldsymbol{F} \in \boldsymbol{H}^1(\Omega)$, $\nu \in \mathbb{R}$ with $\nu > 0$, $\boldsymbol{a}, \boldsymbol{b} \in \boldsymbol{L}^\infty(\Omega)$, $c \in L^\infty(\Omega)$ and $u \in H^2(\Omega)$ solution of*

$$\begin{aligned} -\nu\triangle u + \boldsymbol{a}\cdot\nabla u + \operatorname{div}(u\boldsymbol{b}) + cu &= f + \operatorname{div}\boldsymbol{F} && \text{in } \Omega \\ u &= 0 && \text{on } \partial\Omega. \end{aligned}$$

Then, there exist $C > 0$, $\tilde{\lambda} > 1$ and $\tilde{s} > 1$, independent on u, such that for all $k \in \{0, 1\}$, $\lambda \geq \tilde{\lambda}$ and $s \geq \tilde{s}$,

$$\begin{aligned} &\int_\Omega \left(e^{(k-1)\lambda\varphi}\left|\nabla u\right|^2 + s^2\lambda^2 e^{(k+1)\lambda\varphi}\left|u\right|^2\right) e^{2se^{\lambda\varphi}} dx \\ \leq & C\left(\int_\Omega \frac{1}{s\lambda^2} e^{(k-2)\lambda\varphi}\left|f\right|^2 e^{2se^{\lambda\varphi}} dx + \int_\Omega s e^{k\lambda\varphi}\left|\boldsymbol{F}\right|^2 e^{2se^{\lambda\varphi}} dx\right. \\ &\left. + \int_\omega s^2\lambda^2 e^{(k+1)\lambda\varphi}\left|u\right|^2 e^{2se^{\lambda\varphi}} dx\right). \end{aligned}$$

Proof. For $k = 1$, the result is given by Theorem A.1 in [57] . When $k = 0$, define $z = e^{-\lambda\varphi/2}u$ and use the result for $k = 1$. □

To determine a Carleman estimate for our problem, a first step is to analyze the Equation (3.3). Each component of $\operatorname{curl}\boldsymbol{z}$ can be written as a divergence of a vector field resulting from a linear transformation of $\boldsymbol{u}$. Applying Lemma 3.3.2 with $k = 1$ in each component, we can obtain that there exist $C > 0$, $\tilde{\lambda} > 1$ and $\tilde{s} > 1$, such that for all $\lambda \geq \tilde{\lambda}$ and $s \geq \tilde{s}$,

$$\begin{aligned} \int_\Omega \left(\left|\nabla\boldsymbol{u}\right|^2 + s^2\lambda^2 e^{2\lambda\varphi}\left|\boldsymbol{u}\right|^2\right) e^{2se^{\lambda\varphi}} dx \leq & C\left(\int_\Omega s e^{\lambda\varphi}\left|\boldsymbol{z}\right|^2 e^{2se^{\lambda\varphi}} dx\right. \\ & \left. \leq \int_\omega s^2\lambda^2 e^{2\lambda\varphi}\left|\boldsymbol{u}\right|^2 e^{2se^{\lambda\varphi}} dx\right). \end{aligned} \tag{3.5}$$

Later, it is clear that we need an upper bound for the first term on the right-hand side of Equation (3.3) in terms of $\boldsymbol{u}$. A second step is to establish a similar result from Equation (3.4), rewriting each component of the right-hand side of that equation to the form $f+\operatorname{div}\boldsymbol{F}$. Because of the counts are analogous, we only show the analysis of the first component of $\operatorname{curl}\boldsymbol{f}+\boldsymbol{h}$.

$$
\begin{aligned}
h_1 =& \sum_{j=1}^{3} \frac{\partial\left[\boldsymbol{u}_1\right]_j}{\partial x_2}\frac{\partial\left[\boldsymbol{u}\right]_3}{\partial x_j} - \frac{\partial\left[\boldsymbol{u}_1\right]_j}{\partial x_3}\frac{\partial\left[\boldsymbol{u}\right]_2}{\partial x_j} + \sum_{j=1}^{3} \frac{\partial\left[\boldsymbol{u}\right]_j}{\partial x_2}\frac{\partial\left[\boldsymbol{u}_2\right]_3}{\partial x_j} - \frac{\partial\left[\boldsymbol{u}\right]_j}{\partial x_3}\frac{\partial\left[\boldsymbol{u}_2\right]_2}{\partial x_j} \\
&+ \sum_{j=1}^{3} \frac{\partial}{\partial x_j}\left(\frac{\partial\left[\boldsymbol{u}_2\right]_3}{\partial x_2} - \frac{\partial\left[\boldsymbol{u}_2\right]_2}{\partial x_3}\right)\left[\boldsymbol{u}\right]_j + \frac{\partial\gamma_1}{\partial x_2}\left[\boldsymbol{u}\right]_3 - \frac{\partial\gamma_1}{\partial x_3}\left[\boldsymbol{u}\right]_2 + \frac{\partial\left[\boldsymbol{f}\right]_3}{\partial x_2} - \frac{\partial\left[\boldsymbol{f}\right]_2}{\partial x_3} \\
=& \frac{\partial\gamma_1}{\partial x_2}\left[\boldsymbol{u}\right]_3 - \frac{\partial\gamma_1}{\partial x_3}\left[\boldsymbol{u}\right]_2 + \frac{\partial\left[\boldsymbol{f}\right]_3}{\partial x_2} - \frac{\partial\left[\boldsymbol{f}\right]_2}{\partial x_3} \\
&+ \sum_{j=1}^{3} \frac{\partial}{\partial x_j}\left(\left[\boldsymbol{u}\right]_3\frac{\partial\left[\boldsymbol{u_1}\right]_j}{\partial x_2} - \left[\boldsymbol{u}\right]_2\frac{\partial\left[\boldsymbol{u_1}\right]_j}{\partial x_3}\right) \\
&+ \sum_{j=1}^{3} \frac{\partial}{\partial x_2}\left(\left[\boldsymbol{u}\right]_j\frac{\partial\left[\boldsymbol{u}_2\right]_3}{\partial x_j}\right) - \frac{\partial}{\partial x_3}\left(\left[\boldsymbol{u}\right]_j\frac{\partial\left[\boldsymbol{u}_2\right]_2}{\partial x_j}\right) \\
&- \sum_{j=1}^{3}\left(\left[\boldsymbol{u}\right]_3\frac{\partial^2\left[\boldsymbol{u}_1\right]_j}{\partial x_j\partial x_2} - \left[\boldsymbol{u}\right]_2\frac{\partial^2\left[\boldsymbol{u}_1\right]_j}{\partial x_j\partial x_3} + \left[\boldsymbol{u}\right]_j\frac{\partial^2\left[\boldsymbol{u}_2\right]_3}{\partial x_j\partial x_2} - \left[\boldsymbol{u}\right]_j\frac{\partial^2\left[\boldsymbol{u}_2\right]_2}{\partial x_j\partial x_3}\right) \\
=& \frac{\partial\gamma_1}{\partial x_2}\left[\boldsymbol{u}\right]_3 - \frac{\partial\gamma_1}{\partial x_3}\left[\boldsymbol{u}\right]_2 \\
&- \sum_{j=1}^{3}\left(\left[\boldsymbol{u}\right]_3\frac{\partial^2\left[\boldsymbol{u}_1\right]_j}{\partial x_j\partial x_2} - \left[\boldsymbol{u}\right]_2\frac{\partial^2\left[\boldsymbol{u}_1\right]_j}{\partial x_j\partial x_3} + \left[\boldsymbol{u}\right]_j\frac{\partial^2\left[\boldsymbol{u}_2\right]_3}{\partial x_j\partial x_2} - \left[\boldsymbol{u}\right]_j\frac{\partial^2\left[\boldsymbol{u}_2\right]_2}{\partial x_j\partial x_3}\right) \\
&+ \frac{\partial}{\partial x_1}\left(\left[\boldsymbol{u}\right]_3\frac{\partial\left[\boldsymbol{u}_1\right]_1}{\partial x_2} - \left[\boldsymbol{u}\right]_2\frac{\partial\left[\boldsymbol{u}_1\right]_1}{\partial x_3}\right) \\
&+ \frac{\partial}{\partial x_2}\left(\left[\boldsymbol{u}\right]_3\frac{\partial\left[\boldsymbol{u}_1\right]_2}{\partial x_2} - \left[\boldsymbol{u}\right]_2\frac{\partial\left[\boldsymbol{u}_1\right]_2}{\partial x_3} + \left[\boldsymbol{f}\right]_3 + \sum_{j=1}^{3}\left[\boldsymbol{u}\right]_j\frac{\partial\left[\boldsymbol{u}_2\right]_3}{\partial x_j}\right) \\
&+ \frac{\partial}{\partial x_3}\left(\left[\boldsymbol{u}\right]_3\frac{\partial\left[\boldsymbol{u}_1\right]_3}{\partial x_2} - \left[\boldsymbol{u}\right]_2\frac{\partial\left[\boldsymbol{u}_1\right]_3}{\partial x_3} - \left[\boldsymbol{f}\right]_2 - \sum_{j=1}^{3}\left[\boldsymbol{u}\right]_j\frac{\partial\left[\boldsymbol{u}_2\right]_2}{\partial x_j}\right)
\end{aligned}
$$

However, Equation (3.4) does not have homogenous Dirichlet boundary conditions. A Carleman inequality in the case of non-homogeneous boundary data can be obtained following the same arguments that in Section 2.2 in [14]. In the following, we consider a function $\varphi\in\mathcal{C}^{\infty}\left(\overline{\Omega}\right)$ that verifies Lemma 3.3.1 for a constant $c_0>0$.

Definition 3.3.1. *We define the following space*

$$
\boldsymbol{H}_0^2\left(\Omega\right) = \left\{\boldsymbol{u}\in\boldsymbol{H}^2\left(\Omega\right) \mid \boldsymbol{u}=\boldsymbol{0} \text{ and } \nabla\boldsymbol{u}=\boldsymbol{0} \text{ on } \partial\Omega\right\}
$$

In order to simplify the proof of our Carleman inequality, we present the following technical result. We present a similar proof to the one for Theorem 2.2 in [14] for the sake of self-containedness.

Lemma 3.3.3. *Let $(\boldsymbol{u}, p) \in \boldsymbol{H}_0^2(\Omega_0) \times H_0^1(\Omega_0)$ solutions of (3.2). There exist $C > 0$, $\tilde{s} > 1$ and $\tilde{\lambda} > 1$ such that for every $s \geq \tilde{s}$ and $\lambda \geq \tilde{\lambda}$*

$$\begin{aligned}&\int_\Omega \left(se^{\lambda\varphi}\left|\operatorname{curl}\boldsymbol{u}\right|^2 + \left|\nabla\boldsymbol{u}\right|^2 + s^2\lambda^2 e^{2\lambda\varphi}\left|\boldsymbol{u}\right|^2\right) e^{2se^{\lambda\varphi}}dx\\ \leq& C\left(\int_\Omega \frac{1}{\lambda^2}\left|-\nu\triangle\boldsymbol{u} + \nabla p\right|^2 e^{2se^{\lambda\varphi}}dx + \int_\omega s^3\lambda^2 e^{3\lambda\varphi}\left|\boldsymbol{u}\right|^2 e^{2se^{\lambda\varphi}}\ dx\right).\end{aligned}$$

Proof. First, we define $\boldsymbol{g} = -\nu\triangle\boldsymbol{u} + \nabla p$. Then, we have

$$-\nu\triangle\left(\operatorname{curl}\boldsymbol{u}\right) = \operatorname{curl}\boldsymbol{g}$$

Let $\omega_0 \Subset \omega$ a non-empty open subset. Applying Lemma 3.3.2 with $k = 0$, there exist $C_1 > 0$, $\tilde{s} > 1$ and $\tilde{\lambda} > 1$ such that for every, $s \geq \tilde{s}$ and $\lambda \geq \tilde{\lambda}$, we obtain

$$\begin{aligned}&\int_\Omega \left(\frac{e^{-\lambda\varphi}}{s\lambda^2}\left|\nabla\operatorname{curl}\boldsymbol{u}\right|^2 + se^{\lambda\varphi}\left|\operatorname{curl}\boldsymbol{u}\right|^2\right) e^{2se^{\lambda\varphi}}dx\\ \leq& C_1\left(\int_\Omega \frac{1}{\lambda^2}\left|\boldsymbol{g}\right|^2 e^{2se^{\lambda\varphi}}dx + \int_{\omega_0} se^{\lambda\varphi}e^{2se^{\lambda\varphi}}\left|\operatorname{curl}\boldsymbol{u}\right|^2\ dx\right)\end{aligned}$$

Let $\rho \in \mathcal{C}_0^\infty(\omega)$ such that $0 \leq \rho \leq 1$ and $\rho = 1$ in ω_0. Then, for all $s > 0$, we obtain

$$\int_{\omega_0} se^{\lambda\varphi}e^{2se^{\lambda\varphi}}\left|\operatorname{curl}\boldsymbol{u}\right|^2 dx = \int_{\omega_0} se^{\lambda\varphi}\rho\left|\operatorname{curl}\boldsymbol{u}\right|^2 e^{2se^{\lambda\varphi}}dx \leq \int_\omega se^{\lambda\varphi}\rho\left|\operatorname{curl}\boldsymbol{u}\right|^2 e^{2se^{\lambda\varphi}}dx$$

Applying integration by parts and triangular inequality, there exists a constant $C_2 > 0$ only dependent of ρ such that

$$\begin{aligned}&\int_\omega se^{\lambda\varphi}\rho\left|\operatorname{curl}\boldsymbol{u}\right|^2 e^{2se^{\lambda\varphi}}dx \qquad (3.6)\\ =&\int_\omega \left(se^{\lambda\varphi}\rho e^{2se^{\lambda\varphi}}\operatorname{curl}\boldsymbol{u}\right)\cdot\operatorname{curl}\boldsymbol{u}\ dx\\ =&\int_\omega \boldsymbol{u}\cdot\operatorname{curl}\left(se^{\lambda\varphi}\rho e^{2se^{\lambda\varphi}}\operatorname{curl}\boldsymbol{u}\right)\ dx - \int_{\partial\omega} se^{\lambda\varphi}\rho e^{2se^{\lambda\varphi}}\operatorname{curl}\boldsymbol{u}\times\boldsymbol{u}\ dx\\ =&\int_\omega \boldsymbol{u}\cdot\operatorname{curl}\left(se^{\lambda\varphi}\rho e^{2se^{\lambda\varphi}}\operatorname{curl}\boldsymbol{u}\right)\ dx\\ \leq& C_2\left(\int_\omega s^2\lambda e^{2\lambda\varphi}e^{2se^{\lambda\varphi}}\left|\operatorname{curl}\boldsymbol{u}\right|\left|\boldsymbol{u}\right|\ dx + \int_\omega se^{\lambda\varphi}e^{2se^{\lambda\varphi}}\left|\nabla\operatorname{curl}\boldsymbol{u}\right|\left|\boldsymbol{u}\right|\ dx\right) \qquad (3.7)\end{aligned}$$

Using Hölder inequality, there exists a constant $C_3 > 0$ independent of $\boldsymbol{u}$ such that for all $\varepsilon > 0$,

$$\begin{aligned}&\int_{\omega_0} se^{\lambda\varphi}\left|\operatorname{curl}\boldsymbol{u}\right|^2 e^{2se^{\lambda\varphi}}dx\\ \leq& C_2\left(\int_\omega s^2\lambda e^{2\lambda\varphi}e^{2se^{\lambda\varphi}}\left|\operatorname{curl}\boldsymbol{u}\right|\left|\boldsymbol{u}\right|\ dx + \int_\omega se^{\lambda\varphi}e^{2se^{\lambda\varphi}}\left|\nabla\operatorname{curl}\boldsymbol{u}\right|\left|\boldsymbol{u}\right|\ dx\right)\\ \leq& \varepsilon\left(s\int_{\Omega_0} e^{\lambda\varphi}e^{2se^{\lambda\varphi}}\left|\operatorname{curl}\boldsymbol{u}\right|^2\ dx + \frac{1}{s\lambda^2}\int_{\Omega_0} e^{-\lambda\varphi}e^{2se^{\lambda\varphi}}\left|\nabla\operatorname{curl}\boldsymbol{u}\right|^2\ dx\right)\end{aligned}$$

$$+\frac{C_3}{\varepsilon}\int_\omega s^3\lambda^2 e^{3\lambda\varphi}e^{2se^{\lambda\varphi}}\left|\boldsymbol{u}\right|^2\ dx$$

Then,

$$\begin{aligned}&\int_\Omega\left(\frac{e^{-\lambda\varphi}}{s\lambda^2}\left|\nabla\operatorname{curl}\boldsymbol{u}\right|^2+se^{\lambda\varphi}\left|\operatorname{curl}\boldsymbol{u}\right|^2\right)e^{2se^{\lambda\varphi}}dx\\ \leq& C_3\left(\int_\Omega\frac{1}{\lambda^2}\left|\boldsymbol{g}\right|^2e^{2se^{\lambda\varphi}}dx+\frac{1}{\varepsilon}\int_\omega s^3\lambda^2e^{3\lambda\varphi}e^{2se^{\lambda\varphi}}\left|\boldsymbol{u}\right|^2\ dx\right.\\ &\left.+\frac{\varepsilon}{C_3}\left(s\int_{\Omega_0}e^{\lambda\varphi}e^{2se^{\lambda\varphi}}\left|\operatorname{curl}\boldsymbol{u}\right|^2\ dx+\frac{1}{s\lambda^2}\int_{\Omega_0}e^{-\lambda\varphi}e^{2se^{\lambda\varphi}}\left|\nabla\operatorname{curl}\boldsymbol{u}\right|^2\ dx\right)\right)\end{aligned}$$

Choosing $\varepsilon>0$ small enough, we can absorb the first term of the right-hand side with the terms of the left-hand side. Thus, there exists $C_4>0$ such that

$$\int_\Omega se^{\lambda\varphi}\left|\operatorname{curl}\boldsymbol{u}\right|^2e^{2se^{\lambda\varphi}}dx\leq C_4\left(\int_\Omega\frac{1}{\lambda^2}\left|\boldsymbol{g}\right|^2e^{2se^{\lambda\varphi}}dx+\int_\omega s^3\lambda^2e^{3\lambda\varphi}e^{2se^{\lambda\varphi}}\left|\boldsymbol{u}\right|^2\ dx\right)$$

Applying this result to (3.5), we finally obtain

$$\begin{aligned}&\int_\Omega\left(se^{\lambda\varphi}\left|\operatorname{curl}\boldsymbol{u}\right|^2+\left|\nabla\boldsymbol{u}\right|^2+s^2\lambda^2e^{2\lambda\varphi}\left|\boldsymbol{u}\right|^2\right)e^{2se^{\lambda\varphi}}dx\\ \leq& C\left(\int_\Omega\frac{1}{\lambda^2}\left|\boldsymbol{g}\right|^2e^{2se^{\lambda\varphi}}dx+\int_\omega s^3\lambda^2e^{3\lambda\varphi}\left|\boldsymbol{u}\right|^2e^{2se^{\lambda\varphi}}\ dx\right)\end{aligned}$$

proving this lemma. □

Now we can formulate our new Carleman estimate.

Theorem 3.3.1. *There exist $C>0$, $\tilde{s}>1$ and $\tilde{\lambda}>1$ such that for every $s\geq\tilde{s}$ and $\lambda\geq\tilde{\lambda}$*

$$\begin{aligned}&\int_\Omega\left(se^{\lambda\varphi}\left|\boldsymbol{z}\right|^2+\left|\nabla\boldsymbol{u}\right|^2+s^2\lambda^2e^{2\lambda\varphi}\left|\boldsymbol{u}\right|^2\right)e^{2se^{\lambda\varphi}}dx\\ \leq& C\left(\frac{e^{2se^{\lambda c_0}}}{\lambda^2}\left(\left\|\boldsymbol{u}\right\|_{2,\Omega}^2+\left\|p\right\|_{1,\Omega}^2\right)+\int_\Omega\frac{1}{\lambda^2}\left|\boldsymbol{f}\right|^2e^{2se^{\lambda\varphi}}dx+\int_\omega s^3e^{3\lambda\varphi}e^{2se^{\lambda\varphi}}\left|\boldsymbol{u}\right|^2\ dx\right).\end{aligned}$$

where $(\boldsymbol{u},p)$ are the solutions of Equation (3.2) and $\boldsymbol{z}=\operatorname{curl}\boldsymbol{u}$.

Proof. The proof is similar to the proof of Theorem 2.3 from [14] with some modifications due to the permeability term. Let $\Omega_0\subseteq\mathbb{R}^3$ be a bounded domain with a $\mathcal{C}^2$ boundary $\partial\Omega_0$ such that $\Omega\Subset\Omega_0$. We can extend φ to Ω_0 (keeping the same name) such that $\varphi\in\mathcal{C}^2\left(\overline{\Omega_0}\right)$,

$$\varphi>0\text{ in }\Omega_0\qquad\varphi=0\text{ on }\partial\Omega_0\qquad\varphi=c_0\text{ on }\partial\Omega$$

$$0<\varphi<c_0\text{ in }\Omega_0\setminus\overline{\Omega}\qquad\varphi>c_0\text{ in }\Omega\qquad\nabla\varphi\neq\boldsymbol{0}\text{ in }\overline{\Omega_0\setminus\omega}.$$

It is easy to see that that this extension exists thanks to the regularity of the domain and Lemma 3.3.1. Taking the extension operator $\boldsymbol{A}:\boldsymbol{H}^2(\Omega)\times H^1(\Omega)\to\boldsymbol{H}_0^2(\Omega_0)\times H_0^1(\Omega_0)$ given by the Stein's theorem (see [2]) such that $\boldsymbol{A}(\boldsymbol{u},p)=(\boldsymbol{u},p)$ in Ω, we define $(\tilde{\boldsymbol{u}},\tilde{p})=\boldsymbol{A}(\boldsymbol{u},p)$. We also denote by $\tilde{\boldsymbol{u}}_1$, $\tilde{\boldsymbol{u}}_2$, $\tilde{\gamma}_1$ and $\tilde{\boldsymbol{f}}$ the continuous extensions of $\boldsymbol{u}_1$, $\boldsymbol{u}_2$, γ and $\boldsymbol{f}$ in the

$\boldsymbol{H}^2(\Omega_0)$, $L^\infty(\Omega_0) \cap \boldsymbol{H}_0^1(\Omega_0)$ and $\boldsymbol{L}^2(\Omega_0)$ spaces, respectively, where γ is extended by 0 in $\Omega_0 \setminus \Omega$. Then, $(\tilde{\boldsymbol{u}}, \tilde{p})$ is solution to the system

$$\begin{aligned} -\nu\triangle\tilde{\boldsymbol{u}} + (\nabla\tilde{\boldsymbol{u}})\,\tilde{\boldsymbol{u}}_1 + (\nabla\tilde{\boldsymbol{u}}_2)\,\tilde{\boldsymbol{u}} + \nabla\tilde{p} + \tilde{\gamma}_1\tilde{\boldsymbol{u}} &= \tilde{\boldsymbol{f}} \quad \text{in } \Omega_0 \\ \operatorname{div}\tilde{\boldsymbol{u}} &= 0 \quad \text{in } \Omega_0 \\ \tilde{\boldsymbol{u}} &= \boldsymbol{0} \quad \text{on } \partial\Omega_0 \\ \frac{\partial\tilde{\boldsymbol{u}}}{\partial\boldsymbol{n}} &= \boldsymbol{0} \quad \text{on } \partial\Omega_0 \\ \tilde{p} &= 0 \quad \text{on } \partial\Omega_0, \end{aligned} \tag{3.8}$$

where $\tilde{\boldsymbol{f}} \in \boldsymbol{L}^2(\Omega_0)$ is given by

$$\tilde{\boldsymbol{f}} = \begin{cases} -\boldsymbol{f} & \text{in } \Omega \\ -\nu\triangle\tilde{\boldsymbol{u}} + (\nabla\tilde{\boldsymbol{u}})\,\tilde{\boldsymbol{u}}_1 + (\nabla\tilde{\boldsymbol{u}}_2)\,\tilde{\boldsymbol{u}} + \nabla\tilde{p} + \tilde{\gamma}_1\tilde{\boldsymbol{u}} & \text{in } \Omega_0 \setminus \overline{\Omega} \end{cases}$$

Using the continuity of $\boldsymbol{A}$, there exists a constant $C_1 > 0$ depending only on $\tilde{\boldsymbol{u}}_1$, $\tilde{\boldsymbol{u}}_2$, $\tilde{\gamma}_1$, ν and the continuity constant of $\boldsymbol{A}$ such that

$$\left\|\tilde{\boldsymbol{f}}\right\|_{0,\Omega_0}^2 \leq C_1\left(\|\boldsymbol{u}\|_{2,\Omega}^2 + \|p\|_{1,\Omega}^2\right).$$

Now, taking $\tilde{\boldsymbol{z}} = \operatorname{curl}\tilde{\boldsymbol{u}}$ and applying Lemma 3.3.3, we obtain

$$\begin{aligned} &\int_{\Omega_0}\left(se^{\lambda\varphi}\,|\tilde{\boldsymbol{z}}|^2 + |\nabla\tilde{\boldsymbol{u}}|^2 + s^2\lambda^2e^{2\lambda\varphi}\,|\tilde{\boldsymbol{u}}|^2\right)e^{2se^{\lambda\varphi}}dx \\ \leq& C_2\left(\int_{\Omega_0}\frac{1}{\lambda^2}\,|-\nu\triangle\tilde{\boldsymbol{u}} + \nabla\tilde{p}|^2\,e^{2se^{\lambda\varphi}}dx + \int_\omega\left(s^3\lambda^2e^{3\lambda\varphi}\,|\boldsymbol{u}|^2\right)e^{2se^{\lambda\varphi}}dx\right) \\ \leq& C_2\left(\int_{\Omega_0}\frac{1}{\lambda^2}\left|\tilde{\boldsymbol{f}} - \left((\nabla\tilde{\boldsymbol{u}})\,\tilde{\boldsymbol{u}}_1 + (\nabla\tilde{\boldsymbol{u}}_2)\,\tilde{\boldsymbol{u}} + \tilde{\gamma}_1\tilde{\boldsymbol{u}}\right)\right|^2 e^{2se^{\lambda\varphi}}dx \right. \qquad (3.9) \\ &\left. + \int_\omega\left(s^3\lambda^2e^{3\lambda\varphi}\,|\boldsymbol{u}|^2\right)e^{2se^{\lambda\varphi}}dx\right) \qquad (3.10) \end{aligned}$$

for all $\lambda \geq \tilde{\lambda}$ and $s \geq \tilde{s}$, where $C_2 > 0$, $\tilde{\lambda} > 1$ and $\tilde{s} > 1$ are independent of $\boldsymbol{u}$. Applying the Sobolev Embedding Theorem, we can see that $\tilde{\boldsymbol{u}}_1 \in \boldsymbol{L}^\infty(\Omega_0)$. Since $\tilde{\gamma} \in L^\infty(\Omega_0)$, we have

$$\int_{\Omega_0}|(\nabla\tilde{\boldsymbol{u}})\,\tilde{\boldsymbol{u}}_1|^2\,e^{2se^{\lambda\varphi}}dx \leq \|\tilde{\boldsymbol{u}}_1\|_{0,\infty,\Omega_0}^2\int_{\Omega_0}|(\nabla\tilde{\boldsymbol{u}})|^2\,e^{2se^{\lambda\varphi}}dx$$

Now, applying again Sobolev Embedding Theorem and Hölder inequality, there exist a constant $C_3 > 0$ independent of $\boldsymbol{u}$ such that

$$\begin{aligned} \int_{\Omega_0}|(\nabla\tilde{\boldsymbol{u}}_2)\,\tilde{\boldsymbol{u}}|^2\,e^{2se^{\lambda\varphi}}dx &\leq \int_{\Omega_0}|(\nabla\tilde{\boldsymbol{u}}_2)|^2\left|e^{se^{\lambda\varphi}}\tilde{\boldsymbol{u}}\right|^2dx \\ &\leq \|\tilde{\boldsymbol{u}}_2\|_{1,3,\Omega_0}^2\left\|e^{se^{\lambda\varphi}}\tilde{\boldsymbol{u}}\right\|_{0,6,\Omega_0}^2 \\ &\leq \|\tilde{\boldsymbol{u}}_2\|_{1,3,\Omega_0}^2\left\|\nabla\left(e^{se^{\lambda\varphi}}\tilde{\boldsymbol{u}}\right)\right\|_{0,2,\Omega_0}^2 \\ &\leq C_3\,\|\tilde{\boldsymbol{u}}_2\|_{1,3,\Omega_0}^2\int\left(|\nabla\tilde{\boldsymbol{u}}|^2 + s^2\lambda^2e^{2\lambda\varphi}\,|\boldsymbol{u}|^2\right)e^{2se^{\lambda\varphi}}dx. \end{aligned}$$

Analogously, we have

$$\int_{\Omega_0} |\tilde{\gamma}_1 \tilde{\boldsymbol{u}}|^2 e^{2se^{\lambda\varphi}} dx \leq C_4 \|\tilde{\gamma}_1\|^2_{0,3,\Omega_0} \int \left(|\nabla \tilde{\boldsymbol{u}}|^2 + s^2\lambda^2 e^{2\lambda\varphi} |\boldsymbol{u}|^2 \right) e^{2se^{\lambda\varphi}} dx$$

for a constant $C_4 > 0$ independent on $\boldsymbol{u}$. Hence, there is a constant $C_5 > 0$ independent on $\boldsymbol{u}$ such that the integral term with $\tilde{\boldsymbol{f}}$ verifies

$$\begin{aligned}
&\int_{\Omega_0} \frac{1}{\lambda^2} \left| \tilde{\boldsymbol{f}} - \left((\nabla \tilde{\boldsymbol{u}})\, \tilde{\boldsymbol{u}}_1 + (\nabla \tilde{\boldsymbol{u}}_2)\, \tilde{\boldsymbol{u}} + \tilde{\gamma}_1 \tilde{\boldsymbol{u}} \right) \right|^2 e^{2se^{\lambda\varphi}} dx \\
\leq &\int_{\Omega_0} \frac{1}{\lambda^2} \left(\left| \tilde{\boldsymbol{f}} \right|^2 + C_5 \left(|\nabla \tilde{\boldsymbol{u}}|^2 + s^2\lambda^2 e^{2\lambda\varphi} |\boldsymbol{u}|^2 \right) \right) e^{2se^{\lambda\varphi}} dx,
\end{aligned}$$

where the last terms can be absorbed by the left-hand side of Inequality (3.9) for $\lambda \geq \lambda_2$, with λ_2 large enough and independent on $\boldsymbol{u}$. Then, there exists a constant $C_6 > 0$ such that

$$\begin{aligned}
&\int_{\Omega_0} \left(se^{\lambda\varphi} |\tilde{\boldsymbol{z}}|^2 + |\nabla \tilde{\boldsymbol{u}}|^2 + s^2\lambda^2 e^{2\lambda\varphi} |\tilde{\boldsymbol{u}}|^2 \right) e^{2se^{\lambda\varphi}} dx \\
\leq &C_6 \left(\int_{\Omega_0} \frac{1}{\lambda^2} \left| \tilde{\boldsymbol{f}} \right|^2 e^{2se^{\lambda\varphi}} dx + \int_{\omega} \left(s^3\lambda^2 e^{3\lambda\varphi} |\boldsymbol{u}|^2 \right) e^{2se^{\lambda\varphi}} dx \right)
\end{aligned}$$

Finally, we have

$$\begin{aligned}
\int_{\Omega_0} \frac{1}{\lambda^2} \left| \tilde{\boldsymbol{f}} \right|^2 e^{2se^{\lambda\varphi}} dx &= \int_{\Omega} \frac{1}{\lambda^2} |\boldsymbol{f}|^2 e^{2se^{\lambda\varphi}} dx + \int_{\Omega_0 \setminus \Omega} \frac{1}{\lambda^2} \left| \tilde{\boldsymbol{f}} \right|^2 e^{2se^{\lambda\varphi}} dx \\
&\leq \int_{\Omega} \frac{1}{\lambda^2} |\boldsymbol{f}|^2 e^{2se^{\lambda\varphi}} dx + C_1 \frac{e^{2se^{\lambda c_0}}}{\lambda^2} \left(\|\boldsymbol{u}\|^2_{2,\Omega} + \|p\|^2_{1,\Omega} \right),
\end{aligned}$$

proving that there exist $C > 0$, $\tilde{s} > 1$ and $\tilde{\lambda} > 1$ such that for every $s \geq \tilde{s}$ and $\lambda \geq \tilde{\lambda}$

$$\begin{aligned}
&\int_{\Omega} \left(se^{\lambda\varphi} |\boldsymbol{z}|^2 + |\nabla \boldsymbol{u}|^2 + s^2\lambda^2 e^{2\lambda\varphi} |\boldsymbol{u}|^2 \right) e^{2se^{\lambda\varphi}} dx \\
\leq &\int_{\Omega_0} \left(se^{\lambda\varphi} |\tilde{\boldsymbol{z}}|^2 + |\nabla \tilde{\boldsymbol{u}}|^2 + s^2\lambda^2 e^{2\lambda\varphi} |\tilde{\boldsymbol{u}}|^2 \right) e^{2se^{\lambda\varphi}} dx \\
\leq &C_6 \left(\int_{\Omega} \frac{1}{\lambda^2} |\boldsymbol{f}|^2 e^{2se^{\lambda\varphi}} dx + \frac{e^{2se^{\lambda c_0}}}{\lambda^2} \left(\|\boldsymbol{u}\|^2_{2,\Omega} + \|p\|^2_{1,\Omega} \right) + \int_{\omega} \left(s^3\lambda^2 e^{3\lambda\varphi} |\boldsymbol{u}|^2 \right) e^{2se^{\lambda\varphi}} dx \right),
\end{aligned}$$

concluding the proof of the theorem. □

3.4 Main result

In this section, we present a logarithmic local stability result for our inverse problem. Unlike [14], the right-hand side is more complex and requires a special treatment. We need to prove the following result as a preliminary step.

Theorem 3.4.1. *Let $\beta \in \mathcal{C}^2(\overline{\Omega})$, $\boldsymbol{a} \in \boldsymbol{C}^1(\overline{\Omega})$. There exist $s_0 > 1$ and $C > 0$ such that for all $g \in H(\Omega)$, $\lambda > \lambda_0$ and $s > s_0$*

$$s^2 \int_{\Omega} \left(|\boldsymbol{a} \cdot \nabla \beta|^2 - \frac{C}{s} \right) |g|^2 e^{2s\beta} dx \leq C \int_{\Omega} |\boldsymbol{a} \cdot \nabla g|^2 e^{2s\beta}\, dx.$$

Proof. Let us consider $s > 0$ and define $w = e^{s\beta} g$. Then,

$$e^{s\beta} \boldsymbol{a} \cdot \nabla g = e^{s\beta} \boldsymbol{a} \cdot \nabla \left(e^{-s\beta} w \right) = \boldsymbol{a} \cdot \nabla w - sw \left(\boldsymbol{a} \cdot \nabla \beta \right).$$

Later,

$$\begin{aligned}
&\int_\Omega e^{2s\beta} \left| \boldsymbol{a} \cdot \nabla g \right| \, dx \\
=&\int_\Omega \left| \boldsymbol{a} \cdot \nabla w \right|^2 \, dx + s^2 \int_\Omega e^{2s\beta} \left| g \right|^2 \left| \boldsymbol{a} \cdot \nabla \beta \right|^2 \, dx - 2s \int_\Omega w \left(\boldsymbol{a} \cdot \nabla \beta \right) \left(\boldsymbol{a} \cdot \nabla w \right) \, dx \\
\geq& s^2 \int_\Omega e^{2s\beta} \left| g \right|^2 \left| \boldsymbol{a} \cdot \nabla \beta \right|^2 \, dx - 2s \int_\Omega w \left(\boldsymbol{a} \cdot \nabla \beta \right) \left(\boldsymbol{a} \cdot \nabla w \right) \, dx
\end{aligned}$$

Integrating by parts,

$$\begin{aligned}
2s \int_\Omega w \left(\boldsymbol{a} \cdot \nabla \beta \right) \left(\boldsymbol{a} \cdot \nabla w \right) \, dx =& s \int_\Omega \nabla \left(w^2 \right) \cdot \left(\boldsymbol{a} \cdot \nabla \beta \right) \, dx \\
=& s \int_{\partial\Omega} e^{2s\beta} g \left(\boldsymbol{a} \cdot \nabla \beta \right) \left(\boldsymbol{a} \cdot \boldsymbol{n} \right) \, dx \\
&- s \int_\Omega w^2 \operatorname{div} \left(\left(\boldsymbol{a} \cdot \nabla \beta \right) \boldsymbol{a} \right) \, dx \\
=& - s \int_\Omega e^{2s\beta} \left| g \right|^2 \operatorname{div} \left(\left(\boldsymbol{a} \cdot \nabla \beta \right) \boldsymbol{a} \right) \, dx
\end{aligned}$$

because $g = 0$ on $\partial\Omega$. Also, $\operatorname{div} \left(\left(\boldsymbol{a} \cdot \nabla \beta \right) \boldsymbol{a} \right)$ is bounded in $\overline{\Omega}$. Then, there exists a constant $C_1 > 0$ only dependent of $\boldsymbol{a}$, β and $\overline{\Omega}$ such that

$$2s \int_\Omega w \left(\boldsymbol{a} \cdot \nabla \beta \right) \left(\boldsymbol{a} \cdot \nabla w \right) \, dx \geq -C_1 s \int_\Omega e^{2s\beta} \left| g \right|^2 \, dx$$

Thus, there exist $s_0 > 1$ and $C > 0$ such that for all $s > s_0$

$$C \int_\Omega e^{2s\beta} \left| \boldsymbol{a} \cdot \nabla g \right| \, dx \geq s^2 \int_\Omega e^{2s\beta} \left(\left| \boldsymbol{a} \cdot \nabla \beta \right|^2 - \frac{C}{s} \right) \left| g \right|^2 e^{2s\beta} \, dx$$

proving the theorem. □

The previous theorem reduces the study of $\operatorname{curl} \boldsymbol{f}$ recovering a non-degeneracy condition very similar to Theorem 1 in [34] given by $|\nabla\varphi \times \boldsymbol{u}_2| \neq 0$ in $\overline{\Omega}$ or $\overline{\Omega \setminus \omega}$.

Remark 3.4.1. *Despite the fact that $\nabla\varphi$ vanishes at some points of ω, we can always consider two regions of the observation zone, a small open subset ω_0 included in $\Omega \setminus \bar{\Omega}_\varepsilon$ containing the critical points of φ and another open subset of Ω_ε with absence of them. Velocity and vorticity measurements are required in both sets.*

Now, we have

$$\operatorname{curl} \left(\boldsymbol{f} \right) = \gamma \operatorname{curl} \boldsymbol{u}_2 + \nabla\gamma \times \boldsymbol{u}_2$$

Taking $\boldsymbol{a}_1 = \left(0, \left[\boldsymbol{u}_2 \right]_3, - \left[\boldsymbol{u}_2 \right]_2 \right)^T$, $g = \gamma$ and $\beta = e^{\lambda\varphi}$ in Theorem 3.4.1, we obtain

$$s^2 \int_\Omega \left(\lambda^2 e^{2\lambda\varphi} \left| \boldsymbol{a}_1 \cdot \nabla\varphi \right|^2 - \frac{C_1}{s} \right) \left| \gamma \right|^2 e^{2se^{\lambda\varphi}} dx \leq C \int_\Omega \left| \boldsymbol{a}_1 \cdot \nabla\gamma \right|^2 e^{2se^{\lambda\varphi}} dx$$

We can repeat this with $\boldsymbol{a}_2 = (-[\boldsymbol{u}_2]_3, 0, [\boldsymbol{u}_2]_1)^T$ and $\boldsymbol{a}_3 = ([\boldsymbol{u}_2]_2, -[\boldsymbol{u}_2]_2, 0)^T$ obtaining

$$s^2 \int_\Omega \left(\lambda^2 e^{2\lambda\varphi} |\boldsymbol{a}_2 \cdot \nabla\varphi|^2 - \frac{C_1}{s}\right) |\gamma|^2 e^{2se^{\lambda\varphi}} dx \leq C_1 \int_\Omega |\boldsymbol{a}_2 \cdot \nabla\gamma|^2 e^{2se^{\lambda\varphi}} dx$$
$$s^2 \int_\Omega \left(\lambda^2 e^{2\lambda\varphi} |\boldsymbol{a}_3 \cdot \nabla\varphi|^2 - \frac{C_1}{s}\right) |\gamma|^2 e^{2se^{\lambda\varphi}} dx \leq C_1 \int_\Omega |\boldsymbol{a}_3 \cdot \nabla\gamma|^2 e^{2se^{\lambda\varphi}}\ dx$$

where

$$(\boldsymbol{a}_1 \cdot \nabla\varphi, \boldsymbol{a}_2 \cdot \nabla\varphi, \boldsymbol{a}_3 \cdot \nabla\varphi)^T = \nabla\varphi \times \boldsymbol{u}_2$$
$$(\boldsymbol{a}_1 \cdot \nabla\gamma, \boldsymbol{a}_2 \cdot \nabla\gamma, \boldsymbol{a}_3 \cdot \nabla\gamma)^T = \nabla\gamma \times \boldsymbol{u}_2$$

In conclusion, adding the three inequalities, we can obtain that

$$\begin{aligned} & s^2 \int_\Omega \left(\lambda^2 e^{2\lambda\varphi} |\nabla\varphi \times \boldsymbol{u}_2|^2 - \frac{3C_1}{s}\right) |\gamma|^2 e^{2se^{\lambda\varphi}} dx \\ \leq & C_1 \int_\Omega |\nabla\gamma \times \boldsymbol{u}_2|^2 e^{2se^{\lambda\varphi}} dx \\ \leq & C_1 \int_\Omega \left(|\operatorname{curl}(\boldsymbol{f})|^2 + |\gamma \operatorname{curl} \boldsymbol{u}_2|^2\right) e^{2se^{\lambda\varphi}} dx \end{aligned} \tag{3.11}$$

recovering the term $|\nabla\gamma \times \boldsymbol{u}_2|$ on the left-hand side of this inequality. Furthermore, the left-hand side of this inequality can be simplified thanks to the following lemma.

Lemma 3.4.1. *Let $f \in \mathcal{C}(\overline{\Omega})$ such that $f(\boldsymbol{x}) \neq 0$ for all $\boldsymbol{x} \in \Omega$. There exist constants $R > 0$, $\lambda_1 > 0$ and $s_1 > 0$ such that for all $g \in L^2(\Omega)$, $s > s_1$ and $\lambda > \lambda_1$,*

$$\int_\Omega \left(\lambda^2 |f(x)|^2 - \frac{1}{s}\right) |g(x)|^2 dx \geq R\lambda^2 \int |g(x)|^2\ dx.$$

Proof. The property is fulfilled when $\|g\|_{0,\Omega} = 0$. Then, we suppose that $\|g\|_{0,\Omega} \neq 0$. Since $f \in \mathcal{C}(\overline{\Omega})$ and $f \neq 0$, there exists $R_1 > 0$ such that $|f(\boldsymbol{x})| \geq R_1$ for all $\boldsymbol{x} \in \Omega$. Then,

$$\int_\Omega \left(\lambda^2 |f(x)|^2 - \frac{1}{s}\right) |g(x)|^2 dx \geq \left(\lambda^2 R_1 - \frac{1}{s}\right) \int_\Omega |g(x)|^2 dx.$$

Now, choosing $\lambda_1 = 1$, $s_1 = \dfrac{2}{R_1}$ and $R = \dfrac{R_1}{2}$, we obtain that for all $s > s_1$ and $\lambda > \lambda_1$,

$$\begin{aligned} \int_\Omega \left(\lambda^2 |f(x)|^2 - \frac{1}{s}\right) |g(x)|^2 dx &\geq \left(R_1\lambda^2 - \frac{1}{s}\right) \int_\Omega |g(x)|^2 dx \\ &\geq \left(R_1\lambda^2 - \frac{R_1}{2}\right) \int_\Omega |g(x)|^2 dx \\ &\geq \frac{R_1}{2}\lambda^2 \int_\Omega |g(x)|^2 dx = R\lambda^2 \int_\Omega |g(x)|^2 dx. \end{aligned}$$

proving the lemma. □

Remark 3.4.2. *Note that there exist $R>0$, $s_1>1$ and $\lambda_1>1$ such that, for all $s>s_1$ and $\lambda>\lambda_1$,*

$$\int_{\Omega_\varepsilon}\left(\lambda^2 e^{2\lambda\varphi}\left|\nabla\varphi\times\boldsymbol{u}_2\right|^2-\frac{3C_1}{s}\right)|\gamma|^2 e^{2se^{\lambda\varphi}}dx\geq R\int_{\Omega_\varepsilon}\lambda^2|\gamma|^2 e^{2se^{\lambda\varphi}}dx. \tag{3.12}$$

Since $\boldsymbol{u}_2\in\boldsymbol{H}^2(\Omega)$, Theorem 5.8.4 in [41] states that $\boldsymbol{u}_2\in\boldsymbol{C}(\Omega)$. Then, $|\nabla\varphi\times\boldsymbol{u}_2|\in\mathcal{C}(\Omega)$ and $|\nabla\varphi\times\boldsymbol{u}_2|\neq 0$ in $\overline{\Omega_\varepsilon}$ almost everywhere. Then, choosing $f(x)=e^{\lambda\varphi}|\nabla\varphi(x)\times\boldsymbol{u}_2(x)|$ and $g(x)=e^{se^{\lambda\varphi}}|\gamma(x)|$ on Lemma 3.4.1, we can deduce the Inequality (3.12).

It is possible to prove, similar to Lemma 3.3.2 and Theorem 3.3.1 in Section 3.3, the following Carleman estimates for strong solutions of linear second-order elliptic PDE with homogenous and nonhomogeneous Dirichlet boundary conditions.

Lemma 3.4.2. *Let $f\in L^2(\Omega)$, $\nu\in\mathbb{R}$ with $\nu>0$, $\boldsymbol{a},\boldsymbol{b}\in\boldsymbol{L}^\infty(\Omega)$, $c\in L^\infty(\Omega)$ and $u\in H^2(\Omega)$ solution of*

$$\begin{aligned}-\nu\triangle u+\boldsymbol{a}\cdot\nabla u+\operatorname{div}(u\boldsymbol{b})+cu&=f \quad \text{in } \Omega\\ u&=0 \quad \text{on } \partial\Omega.\end{aligned}$$

Then, there exist $C>0$, $\tilde{\lambda}>1$ and $\tilde{s}>1$, independent on u, such that for all $k\in\mathbb{N}\cup\{0\}$, $\lambda\geq\tilde{\lambda}$ and $s\geq\tilde{s}$,

$$\begin{aligned}&\int_\Omega\left(\left(s\lambda e^{\lambda\varphi}\right)^{k-2}|\triangle u|^2+\left(s\lambda e^{\lambda\varphi}\right)^k|\nabla u|^2+\left(s\lambda e^{\lambda\varphi}\right)^{k+2}|u|^2\right)e^{2se^{\lambda\varphi}}dx\\ \leq& C\left(\int_\Omega\frac{1}{\lambda}\left(s\lambda e^{\lambda\varphi}\right)^{k-1}|f|^2 e^{2se^{\lambda\varphi}}dx+\int_\omega\left(s\lambda e^{\lambda\varphi}\right)^{k+2}|u|^2 e^{2se^{\lambda\varphi}}dx\right).\end{aligned} \tag{3.13}$$

Proof. See Theorem A.1 in [57]. □

Lemma 3.4.3. *Let $f\in L^2(\Omega)$, $\boldsymbol{F}\in\boldsymbol{L}^2(\Omega)$, $\nu\in\mathbb{R}$ with $\nu>0$, $\boldsymbol{a},\boldsymbol{b}\in\boldsymbol{L}^\infty(\Omega)$, $c\in L^\infty(\Omega)$, $g\in H^{3/2}(\partial\Omega)$ and $u\in H^2(\Omega)$ solution of*

$$\begin{aligned}-\nu\triangle u+\boldsymbol{a}\cdot\nabla u+\operatorname{div}(u\boldsymbol{b})+cu&=f+\operatorname{div}\boldsymbol{F} \quad \text{in } \Omega\\ u&=g \quad \text{on } \partial\Omega.\end{aligned}$$

Then, there exist $C>0$, $\tilde{\lambda}>1$ and $\tilde{s}>1$, independent on u, such that for all $k\in\mathbb{N}\cup\{0\}$, $\lambda\geq\tilde{\lambda}$ and $s\geq\tilde{s}$,

$$\begin{aligned}&\int_\Omega\left(\left(s\lambda e^{\lambda\varphi}\right)^{k-2}|\triangle u|^2+\left(s\lambda e^{\lambda\varphi}\right)^k|\nabla u|^2+\left(s\lambda e^{\lambda\varphi}\right)^{k+2}|u|^2\right)e^{2se^{\lambda\varphi}}dx\\ \leq& C\left(\frac{e^{2se^{\lambda c_0}}}{\lambda}\left(s\lambda e^{\lambda c_0}\right)^{k-1}\|u\|_{2,\Omega}^2+\int_\Omega\frac{1}{\lambda}\left(s\lambda e^{\lambda\varphi}\right)^{k-1}|f|^2 e^{2se^{\lambda\varphi}}dx\right.\\ &\left.+\int_\Omega\frac{1}{\lambda}\left(s\lambda e^{\lambda\varphi}\right)^{k+1}|\boldsymbol{F}|^2 e^{2se^{\lambda\varphi}}dx+\int_\omega\left(s\lambda e^{\lambda\varphi}\right)^{k+2}|u|^2 e^{2se^{\lambda\varphi}}dx\right).\end{aligned} \tag{3.14}$$

Proof. See Theorem 2.2 in [57]. □

Then, we can present our local stability result.

Theorem 3.4.2. *Consider an non-empty open subset $\omega \subseteq \Omega$ such that $|\nabla\varphi(\boldsymbol{x}) \times \boldsymbol{u}_2(\boldsymbol{x})| \neq 0$ for all $\boldsymbol{x} \in \overline{\Omega_\varepsilon}$. Then, defining a constant $M_4 = (M_3^2 + K^2)^{1/2} > 0$, there exists a constant $C > 0$ independent on $\boldsymbol{u}_1$ and $\boldsymbol{u}_2$ such that*

$$\|\gamma\|_{0,\Omega_\varepsilon} \leq \frac{CM_4}{\left[\ln\left(1 + \dfrac{M_4}{\|\boldsymbol{u}\|_{0,\omega} + \|\operatorname{curl}\boldsymbol{u}\|_{0,\omega}}\right)\right]^{1/2}},$$

Proof. Let us consider $c = \|\varphi\|_{0,\infty,\Omega}$ and $\boldsymbol{z} = \operatorname{curl}\boldsymbol{u}$. From the equation

$$-\nu\triangle\boldsymbol{z} + (\nabla\boldsymbol{z})\,\boldsymbol{u}_1 + \gamma_1\boldsymbol{z} = -(\operatorname{curl}\boldsymbol{f} + \boldsymbol{h})$$

there exists a constant $C_2 > 0$ that only depends of $\boldsymbol{u}_1$, $\boldsymbol{u}_2$ and M such that

$$|\operatorname{curl}\boldsymbol{f}|^2 e^{2se^{\lambda\varphi}} \leq C_2\left(|\triangle\boldsymbol{z}|^2 + |\nabla\boldsymbol{z}|^2 + |\boldsymbol{z}|^2 + |\nabla\boldsymbol{u}|^2 + |\boldsymbol{u}|^2\right)e^{2se^{\lambda\varphi}}$$

Applying Theorem 3.4.3 with $k = 2$, then there exist constants $C_3 > 0$, $\tilde{\lambda} \geq 1$ and $\tilde{s} \geq 1$ such that for all $\lambda \geq \tilde{\lambda}$ and $s \geq \tilde{s}$

$$\begin{aligned}
&\int_\Omega \left(|\triangle\boldsymbol{z}|^2 + |\nabla\boldsymbol{z}|^2\right)e^{2se^{\lambda\varphi}}dx\\
\leq& C_3\left(se^{\lambda c_0}e^{2se^{\lambda c_0}}\|\boldsymbol{z}\|_{2,\Omega}^2 + \int_\Omega se^{\lambda\varphi}|(\operatorname{curl}\boldsymbol{f} + \boldsymbol{h})|^2 e^{2se^{\lambda\varphi}}dx\right.\\
&\left.\int_\omega \left(s\lambda e^{\lambda\varphi}\right)^4|\boldsymbol{z}|^2 e^{2se^{\lambda\varphi}}dx\right)\\
\leq& C_3\left(se^{\lambda c_0}e^{2se^{\lambda c_0}}\|\boldsymbol{u}\|_{3,\Omega}^2 + \int_\Omega se^{\lambda\varphi}\left(|\operatorname{curl}\boldsymbol{f}|^2 + |\boldsymbol{u}|^2 + |\nabla\boldsymbol{u}|^2\right)e^{2se^{\lambda\varphi}}dx\right.\\
&\left.+\int_\omega \left(s\lambda e^{\lambda\varphi}\right)^4|\boldsymbol{z}|^2 e^{2se^{\lambda\varphi}}dx\right)\\
\leq& C_3\left(se^{\lambda c_0}e^{2se^{\lambda c_0}}\|\boldsymbol{u}\|_{3,\Omega}^2 + \int_\Omega se^{\lambda\varphi}\left(|\nabla\gamma| + |\gamma|^2 + |\boldsymbol{u}|^2 + |\nabla\boldsymbol{u}|^2\right)e^{2se^{\lambda\varphi}}dx\right.\\
&\left.+\int_\omega \left(s\lambda e^{\lambda\varphi}\right)^4|\boldsymbol{z}|^2 e^{2se^{\lambda\varphi}}dx\right)\\
\leq& C_3\left(se^{\lambda c_0}e^{2se^{\lambda c_0}}M_3^2 + se^{\lambda c}e^{2se^{\lambda c}}K^2 + \int_\Omega se^{\lambda\varphi}\left(|\gamma|^2 + |\boldsymbol{u}|^2 + |\nabla\boldsymbol{u}|^2\right)e^{2se^{\lambda\varphi}}dx\right.\\
&\left.+\int_\omega \left(s\lambda e^{\lambda\varphi}\right)^4|\boldsymbol{z}|^2 e^{2se^{\lambda\varphi}}dx\right),
\end{aligned}$$

where we use that $\boldsymbol{u}_1, \boldsymbol{u}_2, \operatorname{curl}\boldsymbol{u}_2 \in \boldsymbol{L}^\infty(\Omega)$ and the Assumption 1. Now, applying Theorem 3.3.1, there exists a constant $C_4 > 0$ such that for all $\lambda \geq \tilde{\lambda}$ and $s \geq \tilde{s}$

$$\begin{aligned}
&\int_\Omega \left(|\boldsymbol{z}|^2 + |\nabla\boldsymbol{u}|^2 + |\boldsymbol{u}|^2\right)e^{2se^{\lambda\varphi}}dx\\
\leq& \int_\Omega \left(se^{\lambda\varphi}|\boldsymbol{z}|^2 + |\nabla\boldsymbol{u}|^2 + \left(s\lambda e^{\lambda\varphi}\right)^2|\boldsymbol{u}|^2\right)e^{2se^{\lambda\varphi}}dx
\end{aligned}$$

$$\leq C_4 \left(\frac{e^{2se^{\lambda c_0}}}{\lambda^2} M_2^2 + \int_\Omega \frac{1}{\lambda^2} |\gamma|^2 e^{2se^{\lambda\varphi}} dx + \int_\omega s^3 e^{3\lambda\varphi} e^{2se^{\lambda\varphi}} |\boldsymbol{u}|^2 \ dx \right)$$

Then, there exists a constant $C_5 > 0$ such that for all $\lambda \geq \tilde{\lambda}$ and $s \geq \tilde{s}$

$$\begin{aligned}
&\int_\Omega |\operatorname{curl} \boldsymbol{f}|^2 e^{2se^{\lambda\varphi}} dx \\
\leq & C_2 \int_\Omega \left(|\triangle \boldsymbol{z}|^2 + |\nabla \boldsymbol{z}|^2 + |\boldsymbol{z}|^2 + |\nabla \boldsymbol{u}|^2 + |\boldsymbol{u}|^2 \right) e^{2se^{\lambda\varphi}} dx \\
\leq & C_5 \left(se^{\lambda c} e^{2se^{\lambda c}} M_4^2 + \int_\Omega se^{\lambda\varphi} |\gamma|^2 e^{2se^{\lambda\varphi}} dx + \int_\omega \left(s\lambda e^{\lambda\varphi} \right)^4 e^{2se^{\lambda\varphi}} \left(|\boldsymbol{u}|^2 + |\boldsymbol{z}|^2 \right) \ dx \right)
\end{aligned}$$

Replacing this in Inequality (3.11) and using that $\operatorname{curl} \boldsymbol{u}_2 \in \boldsymbol{L}^\infty(\Omega)$, we deduce that there exists a constant $C_6 > 0$ such that

$$\begin{aligned}
& Rs^2 \int_{\Omega_\varepsilon} |\gamma|^2 e^{2se^{\lambda\varphi}} dx \\
\leq & s^2 \int_{\Omega_\varepsilon} \left(\lambda^2 e^{2\lambda\varphi} |\nabla\varphi \times \boldsymbol{u}_2|^2 - \frac{3C_1}{s} \right) |\gamma|^2 e^{2se^{\lambda\varphi}} dx \\
\leq & C_1 \int_\Omega \left(|\operatorname{curl} \boldsymbol{f}|^2 + |\gamma \operatorname{curl} \boldsymbol{u}_2|^2 \right) e^{2se^{\lambda\varphi}} \ dx \\
\leq & C_6 \left(se^{\lambda c} e^{2se^{\lambda c}} M_4^2 + \int_\Omega se^{\lambda\varphi} |\gamma|^2 e^{2se^{\lambda\varphi}} dx \right. \\
& \left. \int_\omega \left(s\lambda e^{\lambda\varphi} \right)^4 e^{2se^{\lambda\varphi}} \left(|\boldsymbol{u}|^2 + |\boldsymbol{z}|^2 \right) \ dx \right)
\end{aligned}$$

where $|\nabla\varphi \times \boldsymbol{u}_2| \in \boldsymbol{C}(\Omega)$ and $|\nabla\varphi \times \boldsymbol{u}_2| \neq 0$. Then, taking $s > 0$ sufficiently large and fixing $\lambda = \tilde{\lambda}$, we can absorb the second term of the right-hand side by the left-hand side. Thus, there exist constants $C_7 > 0$, $\hat{s} > 0$ and $c^* > 1$ such that for all $s \geq \hat{s}$

$$\begin{aligned}
s^2 \int_{\Omega_\varepsilon} |\gamma|^2 e^{2se^{\lambda\varphi}} dx \leq C_7 \left(se^{\tilde{\lambda}c} e^{2se^{\tilde{\lambda}c}} M_4^2 + \int_\omega \left(s\tilde{\lambda} e^{\tilde{\lambda}\varphi} \right)^4 e^{2se^{\tilde{\lambda}\varphi}} \left(|\boldsymbol{u}|^2 + |\boldsymbol{z}|^2 \right) \ dx \right) \\
\|\gamma\|_{0,\Omega_\varepsilon}^2 \leq \frac{M_4^2}{s} + e^{2sc^*} \left(\|\boldsymbol{u}\|_{0,\omega} + \|\boldsymbol{z}\|_{0,\omega} \right)^2 \qquad (3.15)
\end{aligned}$$

If $\|\boldsymbol{u}\|_{0,\omega} + \|\boldsymbol{z}\|_{0,\omega} = 0$, then for all $s \geq \hat{s}$ we have $\|\gamma\|_{0,\Omega_\varepsilon} \leq \dfrac{M_4}{s^{1/2}}$ for all $s \geq \hat{s}$. Later, $\|\gamma\|_{0,\Omega_\varepsilon} = 0$.

Now, we assume that $\|\boldsymbol{u}\|_{0,\omega} + \|\boldsymbol{z}\|_{0,\omega} \neq 0$. We have two cases. In the first case, if we suppose that

$$\frac{1}{2c^*} \ln \left(1 + \tfrac{M_4}{\|\boldsymbol{u}\|_{0,\omega} + \|\boldsymbol{z}\|_{0,\omega}} \right) \leq \hat{s}$$

Later,

$$M_4 \leq e^{2\hat{s}c^*} \left(\|\boldsymbol{u}\|_{0,\omega} + \|\boldsymbol{z}\|_{0,\omega} \right)$$

Then, taking $s = \hat{s}$ in Inequality (3.15), and using $\|\boldsymbol{u}\|_{0,\omega} + \|\boldsymbol{z}\|_{0,\omega} \leq M_4$ and $\dfrac{1}{x} \leq \dfrac{1}{\ln(x+1)}$ for all $x > 0$, we obtain

$$\|\gamma\|_{0,\Omega_\varepsilon}^2 \leq \frac{M_4^2}{\hat{s}} + e^{2\hat{s}c^*} \left(\|\boldsymbol{u}\|_{0,\omega} + \|\boldsymbol{z}\|_{0,\omega} \right)^2$$

$$\leq \frac{e^{4\hat{s}c^*}}{\hat{s}}\left(\|\boldsymbol{u}\|_{0,\omega}+\|\boldsymbol{z}\|_{0,\omega}\right)^2+e^{4\hat{s}c^*}\left(\|\boldsymbol{u}\|_{0,\omega}+\|\boldsymbol{z}\|_{0,\omega}\right)^2$$
$$\leq 2e^{4\hat{s}c^*}\left(\|\boldsymbol{u}\|_{0,\omega}+\|\boldsymbol{z}\|_{0,\omega}\right)^2$$
$$\leq 2e^{4\hat{s}c^*}M_4\left(\|\boldsymbol{u}\|_{0,\omega}+\|\boldsymbol{z}\|_{0,\omega}\right)$$
$$\leq 2e^{4\hat{s}c^*}M_4^2\frac{\left(\|\boldsymbol{u}\|_{0,\omega}+\|\boldsymbol{z}\|_{0,\omega}\right)}{M_4}\leq \frac{2e^{4\hat{s}c^*}M_4^2}{\left[\ln\left(1+\frac{M_4}{\|\boldsymbol{u}\|_{0,\omega}+\|\boldsymbol{z}\|_{0,\omega}}\right)\right]} \tag{3.16}$$

In the second case, if we suppose that

$$\frac{1}{2c^*}\ln\left(1+\frac{M_4}{\|\boldsymbol{u}\|_{0,\omega}+\|\boldsymbol{z}\|_{0,\omega}}\right)\geq \hat{s}$$

Taking $s=\dfrac{1}{2c^*}\ln\left(1+\dfrac{M_4}{\|\boldsymbol{u}\|_{0,\omega}+\|\boldsymbol{z}\|_{0,\omega}}\right)$ in Inequality (3.15), using $\|\boldsymbol{u}\|_{0,\omega}+\|\boldsymbol{z}\|_{0,\omega}\leq M_4$ and

$$\frac{(x+1)\ln(1+x)}{x^2}\leq 2$$

for all $x>1$, we obtain

$$e^{2sc^*}=1+\frac{M_4}{\|\boldsymbol{u}\|_{0,\omega}+\|\boldsymbol{z}\|_{0,\omega}}$$

and

$$\|\gamma\|_{0,\Omega_\varepsilon}^2\leq \frac{M_4^2}{s}+e^{2sc^*}\left(\|\boldsymbol{u}\|_{0,\omega}+\|\boldsymbol{z}\|_{0,\omega}\right)^2$$
$$\leq \frac{M_4^2}{s}\left(1+\left[\frac{1}{2c^*}\ln\left(1+\frac{M_4}{\|\boldsymbol{u}\|_{0,\omega}+\|\boldsymbol{z}\|_{0,\omega}}\right)\right]\left(1+\frac{M_4}{\|\boldsymbol{u}\|_{0,\omega}+\|\boldsymbol{z}\|_{0,\omega}}\right)\frac{\left(\|\boldsymbol{u}\|_{0,\omega}+\|\boldsymbol{z}\|_{0,\omega}\right)^2}{M_4^2}\right)$$
$$\leq \frac{M_4^2}{s}\left(1+\frac{1}{c^*}\right)=\frac{(2c^*+1)M_4^2}{\ln\left(1+\frac{M_4}{\|\boldsymbol{u}\|_{0,\omega}+\|\boldsymbol{z}\|_{0,\omega}}\right)} \tag{3.17}$$

From (3.16) and (3.17), we can deduce that there exists a constant $C>0$ such that

$$\|\gamma\|_{0,\Omega_\varepsilon}\leq \frac{CM_4}{\left[\ln\left(1+\dfrac{M_4}{\|\boldsymbol{u}\|_{0,\omega}+\|\operatorname{curl}\boldsymbol{u}\|_{0,\omega}}\right)\right]^{1/2}}$$

proving the theorem.

□

Remark 3.4.3. *The result obtained in Theorem 3.4.2 allows us to conclude a stability result for the problem of recovering the permeability coefficient from local observations of the velocity and vorticity of a fluid. However, those velocity and vorticity measurements must be highly precise in order to recover an accurate permeability coefficient due to the logarithmic estimate. This stability result is similar to the result obtained in [14] (see Theorem 1.4) for the stability of the problem of recovering a Robin coefficient. In general, logarithmic estimates are often obtained in steady problems, while it is possible to obtain Hölder estimates in unsteady problems (see Theorem 1 in [34]).*

3.5 Numerical results

In this section, we present two numerical tests that support the stability result proved in Theorem 3.4.2. We perform numerical experiments in 2D, but the theory of the previous sections is valid both in 2 and 3 dimensions. In both examples will use the sames 2D domain $\Omega = [-1,1]^2$, subset $\Omega_\varepsilon = [-0.9,0.9]^2$ (with a $\varepsilon = 0.1$), and observation region $\omega = [-0.5,0.5]^2$, similar Dirichlet boundary conditions, and a different function γ_R (R for reference) such that $\gamma_R = 0$ in $\Omega \setminus \Omega_\varepsilon$. We obtain numerical approximations for the solutions $(\boldsymbol{u}_R; p_R)$ of Equation (3.1) with $\gamma = \gamma_R$ using the Finite Element method with Taylor-Hood elements ($\mathbb{P}_2$ for the velocity $\boldsymbol{u}_R$ and $\mathbb{P}_1$ for the pressure p_R) on an unstructured hyperfine triangular mesh (with mesh size $h = 0.01$.) We recover the coefficient γ_R as the solution of the following minimization problem

$$\text{minimize} \quad J(\gamma, \boldsymbol{u}) = \frac{1}{2}\|\boldsymbol{u} - \boldsymbol{u}_R\|^2_{0,\omega} + \frac{1}{2}\|\operatorname{curl}\boldsymbol{u} - \operatorname{curl}\boldsymbol{u}_R\|^2_{0,\omega} \tag{3.18}$$

$$\begin{aligned} \text{subject to} \quad -\nu\triangle\boldsymbol{u} + (\nabla\boldsymbol{u})\,\boldsymbol{u} + \nabla p + \gamma\boldsymbol{u} &= \boldsymbol{0} \quad \text{in } \Omega \\ \operatorname{div}\boldsymbol{u} &= 0 \quad \text{in } \Omega \\ \boldsymbol{u} &= \boldsymbol{u}_D \quad \text{on } \partial\Omega \\ \boldsymbol{u} \in \boldsymbol{H}^1(\Omega),\ \gamma \in H^1(\Omega) & \\ 0 \le \gamma \le M \text{ a.e. in } \Omega, & \end{aligned} \tag{3.19}$$

where $M = \max_{\boldsymbol{x}\in\Omega} \gamma_R(\boldsymbol{x})$. The functional J was chosen because it is differentiable with respect to γ and is equivalent to $\|\boldsymbol{u} - \boldsymbol{u}_R\|_{0,\omega} + \|\operatorname{curl}\boldsymbol{u} - \operatorname{curl}\boldsymbol{u}_R\|_{0,\omega}$. This problem is numerically solved approximating the Navier-Stokes equations with Finite Element method using stable pairs of spaces (in terms of the inf-sup condition, see Section 3.6 in [62]) in a coarse structured mesh, where γ is approximated by $\mathbb{P}_1$ elements. It should be noted that the second example is based on recovering a discontinuous coefficient γ_R, which is not covered by Theorem 3.4.2, but it complements the work of Aguayo et al [3]. The FEM solver is implemented using the finite element library FEniCS 2019.1.0 [5] with the default configuration. The nonlinear problems were solved using the Newton method with a relaxation parameter $\alpha \in [0.9999, 1]$. The dolfin-adjoint library [71] were used to numerically solve the optimization problems with the L-BFGS-B algorithm (see Section 4.3 in [39]). Furthermore, we explain more details of the parameters, domains, meshes, numerical methods and tolerances used on each example.

3.5.1 Recovering a smooth function

In this first test, we consider $\nu = 1$, $\boldsymbol{f} = \boldsymbol{0}$, Dirichlet boundary conditions given by a function $\boldsymbol{u}_D$ such that

$$\boldsymbol{u}_D(x,y) = \begin{cases} (5(1-y^2), 0)^T & \text{if } x \in \{-1,1\} \\ 0 & \text{if } y \in \{-1,1\} \end{cases}$$

and a function $\gamma_R \in H(\Omega)$ such that

$$\gamma_R(x,y) = \begin{cases} \frac{100}{16}\left(1+\cos\left(\frac{\pi x}{0.9}\right)\right)^2\left(1+\cos\left(\frac{\pi y}{0.9}\right)\right)^2 & \text{if } \boldsymbol{x} = (x,y) \in \Omega_\varepsilon \\ 0 & \text{if } \boldsymbol{x} = (x,y) \in \Omega \setminus \Omega_\varepsilon \end{cases}$$

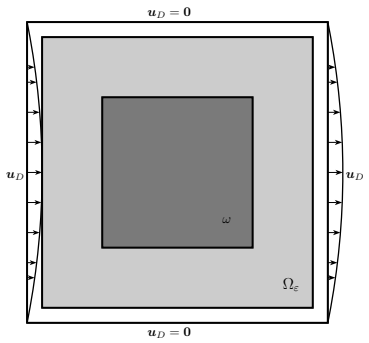

Figure 3.1: Domain Ω for the numerical tests and boundary conditions.

The reference solutions are the numerical solutions $(\boldsymbol{u_R}; p_R)$ of Equation (3.1), obtained by Finite Element Method with Taylor-Hood elements ($\mathbb{P}_2$ for the velocity $\boldsymbol{u}$ and $\mathbb{P}_1$ for the pressure p) in a hyperfine unstructured triangular mesh (mesh size $h = 0.01$, 53649 nodes and 107296 elements), using the function γ_R defined previously.

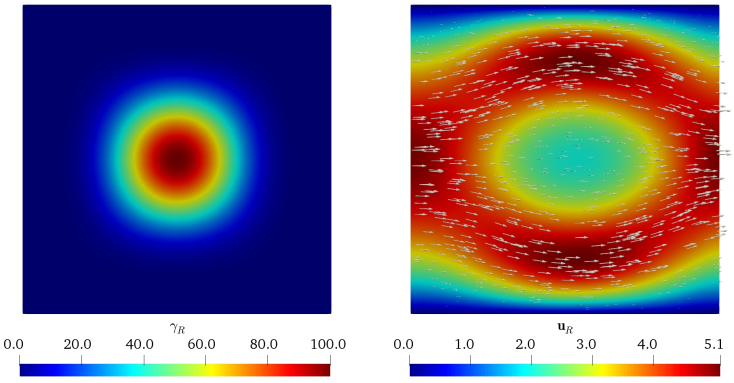

Figure 3.2: Plots of the Brinkman's law reference permeability parameter γ_R and the correspondent reference isovalues and flow $\boldsymbol{u}_R$.

The optimization problem was discretized with the same FEM scheme for a coarse structured triangular mesh. The function γ was discretized using $\mathbb{P}_1$ elements. The discretized Navier-Stokes equations were solved using Newton method with a tolerance of 10^{-7} for the discrete ℓ_2 residual norm. The tolerance criterion for the L-BFGS-B algorithm was $5 \cdot 10^{-9}$ for consecutive evaluations of functional J or approximations of the Riesz representant of ∇J, the Fréchet derivative of J, in norms $L^2(\Omega)$ or ℓ_2. We used $\gamma_0 = 0$ as a initial guess for the L-BFGS-B algorithm. If we denote γ_k and $\boldsymbol{u}_k$ as the optimal control and their respective state on the k iteration of the L-BFGS-B algorithm, we can define the errors $\gamma_{E,k} = \gamma_k - \gamma_R$ and $\boldsymbol{u}_{E,k} = \boldsymbol{u}_k - \boldsymbol{u}_R$. Also we define γ^* as the optimal function obtained by the L-BFGS-B algorithm and $(\boldsymbol{u}^*, p^*)$ as the optimal states. Table 3.1 and Figures 3.3 and 3.4 summarize the numerical results obtained.

Comparing Figures 3.2 and 3.3, we can see that there is a fast convergence of the velocity at the optimal $\boldsymbol{u}_R$, both in the measurement region ω and in the rest of Ω. However, the convergence rate of γ is low, according to the Theorem3.4.2. In the measurement region ω, γ^* has a similar shape to γ_R, with differences of less than 4% in L^∞ norm. Outside the

measurement region ω, γ^* presents some noise, as can be seen in Figures 3.3 and 3.4, which is mainly associated with the measurement region, the chosen objective function J and the Finite Element approximation.

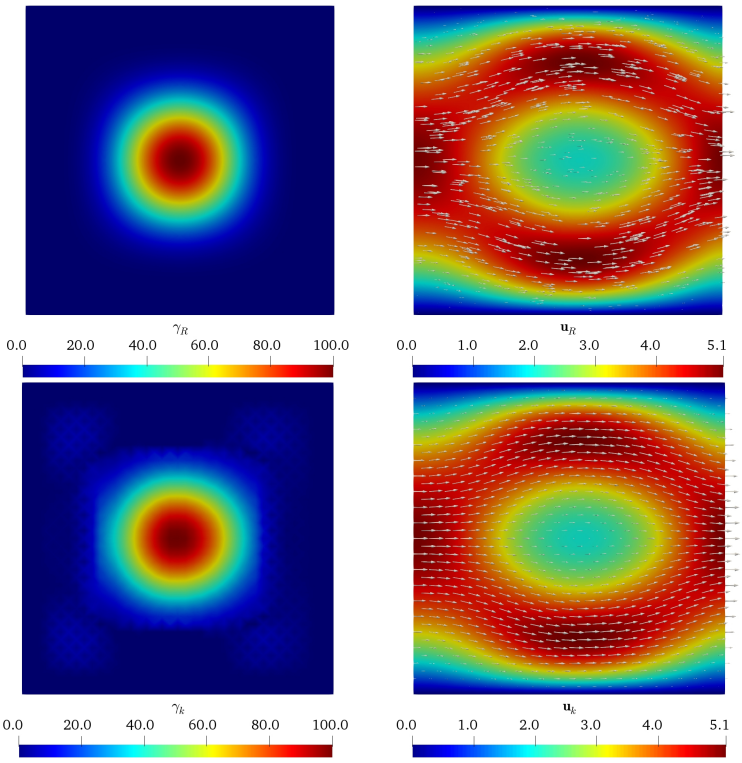

Figure 3.3: Plots of reference parameters and velocity (top), recovered permeability parameter γ_k and velocity $\boldsymbol{u}_k$ on iteration 198 (bottom).

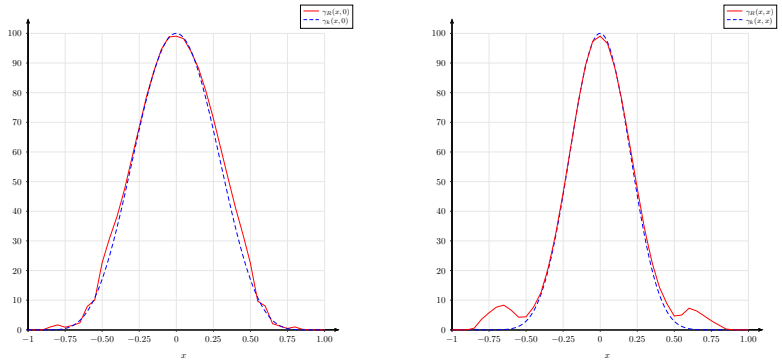

Figure 3.4: Cut lines of the optimal γ_k on iteration 198 and γ_R on $y = 0$ (left) and $y = x$ (right).

k	$J(\gamma_k)$	$\|\nabla J(\gamma_k)\|_{0,\Omega}$	$\|\boldsymbol{u}_{E,k}\|_{0,\omega} + \|\mathrm{curl}\,\boldsymbol{u}_{E,k}\|_{0,\omega}$	$\|\gamma_{E,k}\|_{0,\Omega_\varepsilon}$
0	$4.8156 \cdot 10^{1}$	$1.7378 \cdot 10^{-2}$	$1.1536 \cdot 10^{1}$	$4.9219 \cdot 10^{1}$
3	$8.9908 \cdot 10^{0}$	$4.6005 \cdot 10^{-3}$	$5.0507 \cdot 10^{0}$	$3.6516 \cdot 10^{1}$
5	$1.3860 \cdot 10^{0}$	$1.1846 \cdot 10^{-3}$	$2.0324 \cdot 10^{0}$	$2.5782 \cdot 10^{1}$
8	$1.5234 \cdot 10^{-1}$	$1.8093 \cdot 10^{-4}$	$6.9552 \cdot 10^{-1}$	$1.6227 \cdot 10^{1}$
14	$1.0747 \cdot 10^{-2}$	$1.1264 \cdot 10^{-5}$	$2.0450 \cdot 10^{-1}$	$1.1485 \cdot 10^{1}$
41	$1.0969 \cdot 10^{-3}$	$2.0214 \cdot 10^{-6}$	$6.1340 \cdot 10^{-2}$	$6.1686 \cdot 10^{0}$
68	$1.0095 \cdot 10^{-4}$	$4.0138 \cdot 10^{-7}$	$1.9318 \cdot 10^{-2}$	$5.0834 \cdot 10^{0}$
196	$5.0897 \cdot 10^{-5}$	$3.3451 \cdot 10^{-8}$	$1.0601 \cdot 10^{-2}$	$4.6065 \cdot 10^{0}$

Table 3.1: Evolution of L-BFGS-B algorithm.

3.5.2 Recovering a non-smooth function

Unlike the previous test, in this one we are looking for recovering a function $\gamma_R \in L^2(\Omega)$ with $\gamma_R = 0$ in $\Omega \setminus \Omega_\varepsilon$ such that $\gamma_R \notin H^1(\Omega)$. Then, in this test we do not expect to recover the theoretical results, since the hypothesis of the main theorem is not fulfilled, but rather to present a strategy that allows recovering a discontinuous coefficient γ. This example is motivated by [3], where the authors solved numerically an inverse problem to recover a discontinuous coefficient that represent an obstacle.

We consider the sames domains Ω and Ω_ε as in the first test and the same the parameters $\nu = 1$ and $\boldsymbol{f} = \boldsymbol{0}$. The Dirichlet boundary condition is given by a function $\boldsymbol{u}_D$ such that

$$\boldsymbol{u}_D(x,y) = \begin{cases} (30(1-y^2),0)^T & \text{if } x \in \{-1,1\} \\ 0 & \text{if } y \in \{-1,1\} \end{cases}$$

and a function $\gamma_R \in H(\Omega)$ such that

$$\gamma_R(x,y) = \begin{cases} 10000 & \text{if } (x,y) \in B \\ 0 & \text{if } (x,y) \in \Omega \setminus B \end{cases}$$

where $B = \{(x,y) \in \mathbb{R}^2 \mid x^2 + y^2 \leq 0.2^2\}$

The reference solutions are the numerical solutions $(\boldsymbol{u_R}; p_R)$ of Equation (3.1), obtained by Finite Element Method with the Taylor-Hood elements ($\mathbb{P}_2$ for the velocity $\boldsymbol{u_R}$ and $\mathbb{P}_1$ for the pressure p_R) in a hyperfine unstructured triangular mesh (mesh size $h = 0.01$, 53649 nodes and 106496 elements), using the function γ_R defined previously.

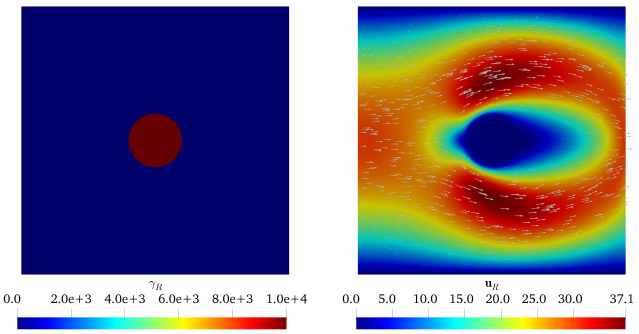

Figure 3.5: Plots of γ_R and $\boldsymbol{u}_R$.

The optimization problem were discretized with the MINI element ($\mathbb{P}_1 \oplus V_{\text{bub}}$ for the velocity $\boldsymbol{u}$ and $\mathbb{P}_1$ for the pressure p, where V_{bub} is the space of the bubble functions, see Section 3.6.1 in [62]) for a coarse structured triangular mesh. The discretized Navier-Stokes equations were solved using Newton method with a tolerance of 10^{-7} for the discrete ℓ_2 residual norm. Thanks to we can recover a discontinuous L^2 function, we decided to use $\mathbb{P}_1$ elements for γ discretization combined with a new algorithm for this optimization problem based in adaptive refinement. If $\mathcal{T}_h$ is a triangulation for $\overline{\Omega}$, we denote by T the elements of $\mathcal{T}_h$ and by $\mathcal{E}_h$ the set of all edges $\mathcal{T}_h$. Also $\mathcal{E}_h = \mathcal{E}_\Omega \cup \mathcal{E}_\partial$, where $\mathcal{E}_\Omega$ and $\mathcal{E}_\partial$ are the sets of edges lying in the interior and the boundary of $\overline{\Omega}$, respectively. We use h_T as the diameter of T and $h_F = |F|$ for each $F \in \mathcal{E}_\Omega$. Then, for each $T \in \mathcal{T}_h$, we define $\eta_{\gamma,T} > 0$ and $\eta_T > 0$ such that

$$
\begin{aligned}
\eta_{\gamma,T}^2 &= \sum_{F \in \partial T \cap \mathcal{E}_\Omega} h_F \left\| [\![\nabla \gamma_F]\!]_F \right\|_{0,F}^2 \\
\eta_T^2 &= h_T^2 \left\| -\nu \triangle \boldsymbol{u} + (\nabla \boldsymbol{u})\, \boldsymbol{u} + \gamma \boldsymbol{u} + \nabla p \right\|_{0,T}^2 + \left\| \operatorname{div} \boldsymbol{u} \right\|_{0,T}^2 \\
&\quad + \sum_{F \in \partial T \cap \mathcal{E}_\Omega} h_F \left\| \left[\!\!\left[\nu \frac{\partial \boldsymbol{u}}{\partial \boldsymbol{n}} - p\boldsymbol{n} \right]\!\!\right] \right\|_{0,F}^2
\end{aligned}
$$

where $[\![\cdot]\!]_F$ denotes the vectorial jump operator on the edge $F \in \mathcal{E}_\Omega$. The term $\eta_{\gamma,T}$ corresponds to a quantification of the jumps of γ for the element T, which we want to reduce in order to obtain a better resolution The expression η_T is the a-posteriori error estimator presented by Verfürth calculated in the element T (see Section 8 in [83]).

At each stage of the algorithm, we partially solve the optimization problem until reaching a maximum number of iterations or a convergence criterion of the L-BFGS-B algorithm. Next, we quantify the error estimators, mark some elements and refine the marked elements following the algorithm. The next stage uses the Lagrange interpolation of the optimal control obtained in the last stage. Also we increment the maximum number of iterations for L-BFGS-B algorithm for the next stage because the descent directions of that algorithm are not compatible with the discrete spaces obtained after the adaptive refinement.

Algorithm 1 Algorithm of each adaptive refinement stage.

Require: A coarse mesh $\mathcal{T}_h$, $N, \Delta \in \mathbb{N}$, $\gamma = 0$.

1: Run N iterations of the L-BFGS-B algorithm for the problem (3.18) on the current mesh.
2: For each $T \in \mathcal{T}_h$, compute the estimators $\eta_{\gamma,T}$ and η_T using the optimal function and the optimal states.
3: Given $T \in \mathcal{T}_h$ such that $\eta_{\gamma,T} \geq 0.8 \max_{K \in \mathcal{T}_h} \eta_{\gamma,K}$ or $\eta_T \geq 0.5 \max_{K \in \mathcal{T}_h} \eta_K$, mark T and generate a new mesh $\mathcal{T}_h$ refining the marked elements.
4: If the stop criterion is not satisfied, choose γ as the Lagrange interpolation of the optimal control in the new finite element space obtained in the step 1, increase N to $N + \Delta$ and go to the step 1.

The tolerance criterion for the L-BFGS-B algorithm were $2 \cdot 10^{-5}$ for consecutive evaluations of functional J or approximations of the Riesz representant of ∇J, the Fréchet derivative of J, in norms $L^2(\Omega)$ or ℓ_2. We used $\gamma_0 = 0$ as a initial prediction for the L-BFGS-B algorithm. We choose $N = 60$ as the maximum number of iterations for the first stage, with increments of 30 iterations for the following stages. If we denote γ_k and $\boldsymbol{u}_k$ as the optimal control and their respective state on the k stage of the refinement algorithm, we define the errors $\gamma_{E,k} = \gamma_k - \gamma_R$ and $\boldsymbol{u}_{E,k} = \boldsymbol{u}_k - \boldsymbol{u}_R$, and γ^* as the optimal function obtained by the L-BFGS-B algorithm withe the optimal state $(\boldsymbol{u}^*, p^*)$ as in the previous test. Figures 3.7 and 3.6, and Table 3.2 summarize the numerical results obtained.

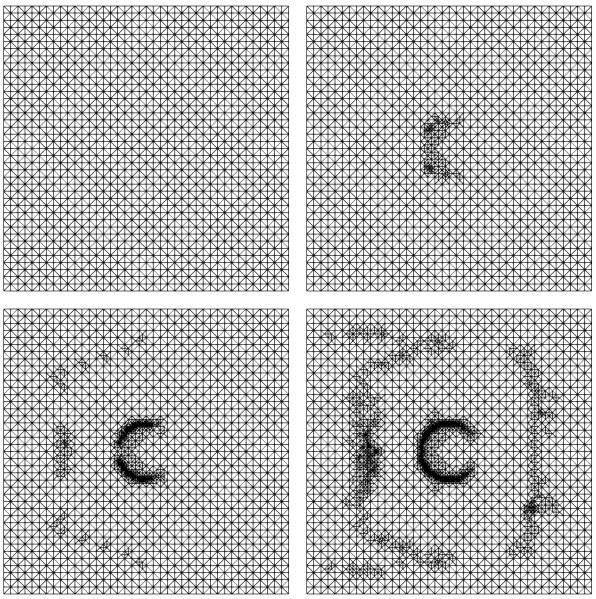

Figure 3.6: Plots of refined meshes on stages 1 (top left), 3 (top right), 7 (bottom left) and 13 (bottom right).

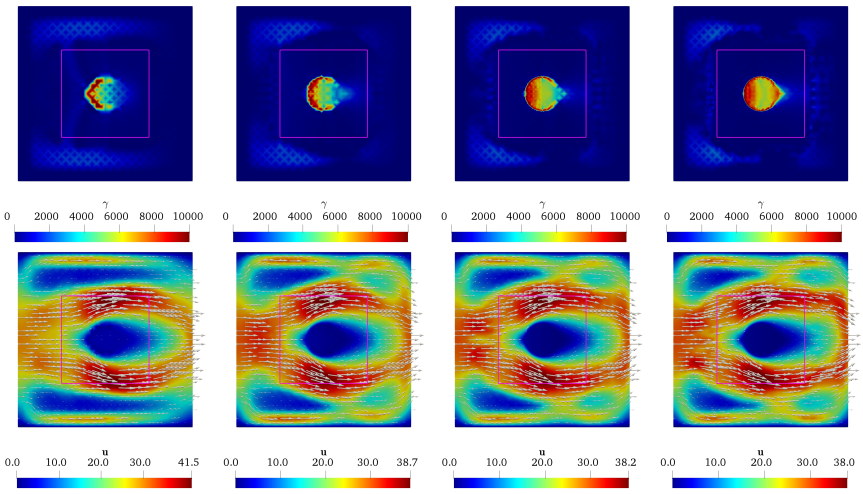

Figure 3.7: Plots of γ_k (first row) and $\boldsymbol{u}_k$ (second row) after stages 1, 3, 7 and 13 (from left to right).

k	It.	$J(\gamma_k)$	$\|\nabla J(\gamma_k)\|_{0,\Omega}$	$\|\boldsymbol{u}_{E,k}\|_{0,\omega} + \|\mathrm{curl}\,\boldsymbol{u}_{E,k}\|_{0,\omega}$	$\|\gamma_{E,k}\|_{0,\Omega_\varepsilon}$
0	0	$7.3218 \cdot 10^3$	$6.8677 \cdot 10^{-1}$	$1.3714 \cdot 10^2$	$3.4662 \cdot 10^3$
1	60	$2.4691 \cdot 10^2$	$1.0367 \cdot 10^{-3}$	$2.5022 \cdot 10^1$	$2.1659 \cdot 10^3$
3	270	$8.4010 \cdot 10^1$	$2.6439 \cdot 10^{-4}$	$1.4178 \cdot 10^1$	$1.8784 \cdot 10^3$
5	600	$5.0553 \cdot 10^1$	$8.4971 \cdot 10^{-5}$	$1.0996 \cdot 10^1$	$1.7416 \cdot 10^3$
7	1050	$2.9497 \cdot 10^1$	$4.3242 \cdot 10^{-5}$	$8.4704 \cdot 10^0$	$1.6257 \cdot 10^3$
9	1620	$2.5874 \cdot 10^1$	$3.6794 \cdot 10^{-5}$	$7.9048 \cdot 10^0$	$1.5348 \cdot 10^3$
11	2310	$2.0731 \cdot 10^1$	$2.4171 \cdot 10^{-5}$	$7.0901 \cdot 10^0$	$1.5229 \cdot 10^3$
13	2848	$1.9714 \cdot 10^1$	$1.9335 \cdot 10^{-5}$	$6.9145 \cdot 10^0$	$1.5304 \cdot 10^3$

Table 3.2: Evolution of the adaptive refinement algorithm.

We appreciate that the convergence of the numerical solution to the real solution is slow, similar to the previous test, which is benefited by the adaptive refinement strategy. The adaptive refinement strategy allows to recover smoothly the boundary of the set B, where $\gamma_R = 10000$. However, we can obtain numerical noise in the boundary of ω, drawn with magenta lines in Figure 3.7. Indeed, we can see that the prediction of γ is not accurate outside ω due to the same explanations of the previous test: the measurement region, the chosen objective function J and the Finite Element approximation. Furthermore, the values of the numerical noise are sufficient to significantly modify the magnitude of $\boldsymbol{u}$ outside ω with respect to the reference $\boldsymbol{u}_R$, but that noise is slightly attenuated by the effect of the optimization solver and the adaptive refinement algorithm.

3.6 Conclusions

We have presented a new stability result for the inverse problem of recovering a smooth scalar permeability parameter for a steady Navier-Stokes equations with permeability modeled by

Brinkman's law from local observations of the fluid velocity and vorticity in a fixed subdomain. Our main result is a logarithmic estimate obtained from H^1 and H^2 global Carleman inequalities for second-order elliptical equations. We followed similar extension technique used as the one used in [14] under an analogous non-degeneracy condition as the one introduced in [34]. The approach of eliminating the pressure and measuring only velocity $\boldsymbol{u}$ is useful not only for fluids, but also in some problems appearing in elastography (see [31]).

Our numerical test for recovering a smooth parameter shows a slow convergence of the optimization solver, which is directly related to our stability result. Likewise, the numerical test that recovers a discontinuous coefficient with an adaptive refinement strategy follows a similar behavior to the first test, which allows us to observe that we could relax the regularity hypotheses of our main theorem. Also, one of the problems was the numerical noise generated by the discrete scheme. An alternative is to consider the vorticity $\operatorname{curl} \boldsymbol{u}$ as a new unknown in the finite element system.

In [4], authors describe that an obstacle immersed in a fluid can be represented asymptotically by a discontinuous permeability coefficient. The adaptive refinement strategy is effective to recover discontinuous coefficients with greater precision, facilitating the detection of obstacles with better resolution. However, the use of error estimators may not be appropriate. Then, one of the future improvements for this work is to apply new techniques, for example the one explained in [38] based in basis adaptation, as a new strategy of mesh adaptivity.

Chapter 4

A distributed resistance inverse method for flow obstacle identification from internal velocity measurements: the Oseen problem

The content of this chapter was published in J. Aguayo, C. Bertoglio and A. Osses. "A distributed resistance inverse method for flow obstacle identification from internal velocity measurements" in Inverse Problems, 2021. [3].

We present a penalization parameter method for obstacle identification in an incompressible fluid flow for a modified version of the Oseen equations. The proposed method consist in adding a high resistance potential to the system such that some subset of its boundary support represents the obstacle. This allows to work in a fixed domain and highly simplify the solution of the inverse problem via some suitable cost functional. Existence of minimizers and first and second order optimality conditions are derived through the differentiability of the solutions of the Oseen equation with respect to the potential. Finally, several numerical experiments using Navier-Stokes flow illustrate the applicability of the method, for the localization of a bi-dimensional cardiac valve from MRI and ultrasound flow type imaging data.

4.1 Introduction

The pathway of blood flow through the heart is regulated by four membrane structures or valves, opening and closing by differential blood pressures. Valvular heart diseases affect 20% of the population. Among them, aortic valve stenosis is the most prevalent one in developed countries [60].

Imaging the 3D shape of the valves is a challenging task. For instance, the aortic valve is very thin (0.5 mm), and therefore its shape can be imaged nowadays using only two modalities: computerized tomography (CT) and transesophageal echocardiography (TEE). Since CT is based on X-rays, it is only used in patients that are selected for valvular replacement in order to obtain the aortic root dimensions for sizing the prosthesis. Such CT images are

usually obtained when the valve is closed. Obtaining the image at open valve position requires about 5 times larger radiation dose since the complete cardiac cycle has to be imaged. This is equivalent to the annual recommended total radiation dose (see [69]). TEE is a newer technique, but highly invasive: a wire is inserted through the esophagus of the patient involving a cumbersome procedure. TEE is most of the time applied to monitor valve surgeries (see [43]), and is therefore rarely applied in a diagnostic phase.

Magnetic resonance imaging (MRI) allows to image anatomical structures in a non-invasive and non-ionising way. Unfortunately, the aortic valve geometry is not directly visible with MRI, since the valve thickness is smaller than the image voxel size.

However, visual inspection of 3D Flow MRI Imaging (4D Flow, see [40]) data sets clearly shows that the valvular shape could be retrieved from the flow pattern in the valve surroundings. This fact motivates to formulate, analyze and numerically assess the inverse problem of inferring rigid obstacles from interior velocity measurements, with the ultimate goal of recovering the shape of cardiac valves at the opening position from velocity images.

Available approaches studied and reported in the mathematical literature are limited to the detection of obstacles in viscous fluid flows using boundary stress measurements, which limits the inverse problem to oversimplified shapes, usually of circular nature [6, 15, 32, 33]. Noteworthy, boundary stress measurements would mean in practice to introduce a catheter close to the valve.

The novelty of this work is the identification of flow obstacles by a distributed resistance inverse method. That is, we propose the incorporation of a large resistance term that allows to model the effect of an obstacle in the viscous fluid. This method reduces the obstacle identification to a simpler potential inverse problem. This idea is inspired by [29, 12, 44], who model cardiac valves using a resistive immerse surface (RIS) given by a Dirac distribution. The problem of using RIS for valve identification would be the need of modifying the discretization of the domain at every iteration of the identification procedure. In contrast, the distributed resistance term that we propose here allows us to work in a fixed domain to solve the valve shape identification problem. This distributed resistance method can also be useful to estimate porosity in porous media flows following Brinkman's law [24, 13].

The paper is structured as follows. In Section 2, a parameter identification problem is defined for the Oseen equations (as a linearization of Navier-Stokes equations) adding a resistive potential term with the form $\gamma \boldsymbol{u}$, where $\boldsymbol{u}$ is the velocity field and $\gamma \geq 0$ is a function that takes large values in zones where is the obstacle should be located, or 0. In Section 3, a proof of the existence of minimizers using appropriate techniques is presented. In Sections 4 and 5, first and second order optimality conditions for some suitable cost functions are established, motivating the choice of suitable spaces for the parameter and the feasibility of implementing optimization algorithms to numerically solve this problem. Section 6 presents numerical examples that illustrate the feasibility of the proposed penalty method using Navier-Stokes equations from a 2D reference case representing the blood flow passing through the aortic valve. We reconstruct the position of the valve from global or local velocity field measurements. For this purpose, synthetic images based on MRI and ultrasound type measurements are used. Finally, conclusions and future work are presented in Section 7.

4.2 Model problem

Consider a non-empty bounded domain $\Omega \subseteq \mathbb{R}^N$, $N \in \{2, 3\}$. The Lebesgue measure of Ω is denoted by $|\Omega|$, which extends to lesser dimension spaces. The norm and seminorms for Sobolev spaces $W^{m,p}(\Omega)$ is denoted by $\|\cdot\|_{m,p,\Omega}$ and $|\cdot|_{m,p,\Omega}$, respectively. For $p = 2$, the norm, seminorms and inner product of the space $W^{m,2}(\Omega) = H^m(\Omega)$ are denoted by $\|\cdot\|_{m,\Omega}$, $|\cdot|_{m,\Omega}$ and $(\cdot,\cdot)_{m,\Omega}$, respectively. Also, $\|\cdot\|_{\infty,\Omega}$ denotes the norm of $L^\infty(\Omega)$. The spaces $\boldsymbol{H}^m(\Omega)$ and $\boldsymbol{W}^{m,p}(\Omega)$ are defined by $\boldsymbol{H}^m(\Omega) = [H^m(\Omega)]^N$ and $\boldsymbol{W}^{m,p}(\Omega) = [W^{m,p}(\Omega)]^N$. The notation for norms, seminorms and inner products will be extended from $W^{m,p}(\Omega)$ or $H^m(\Omega)$.

Consider $\alpha > 0$, $\nu > 0$, $s \geq 0$, $M > 0$, Ω with a Lipschitz boundary $\partial\Omega = \Gamma_D \cup \Gamma_N$ such that $\operatorname{int}(\Gamma_D) \cap \operatorname{int}(\Gamma_N) = \emptyset$, an open subset $\omega \subseteq \Omega$, $\boldsymbol{u}_R \in \boldsymbol{H}^1(\omega)^d$, $\boldsymbol{u}_D \in \boldsymbol{H}^{1/2}(\Gamma_D)$ and $\boldsymbol{a} \in \boldsymbol{W}^{1,\infty}(\Omega)$ such that $\operatorname{div}\boldsymbol{a} = 0$ and $\boldsymbol{a}\cdot\boldsymbol{n} \geq 0$ on Γ_N, where $\boldsymbol{n}$ is the outer normal vector. The model problem is defined by

$$\text{minimize} \quad J(\gamma, \boldsymbol{u}) = \frac{1}{2}\|\boldsymbol{u} - \boldsymbol{u}_R\|_{0,\omega}^2 + \frac{\alpha}{2}\|\gamma\|_{s,\Omega}^2 \tag{4.1}$$

$$\begin{aligned} \text{subject to} \quad -\nu\triangle\boldsymbol{u} + (\nabla\boldsymbol{u})\,\boldsymbol{a} + \nabla p + \gamma\boldsymbol{u} &= \boldsymbol{0} \quad \text{in } \Omega \\ \operatorname{div}\boldsymbol{u} &= 0 \quad \text{in } \Omega \\ \boldsymbol{u} &= \boldsymbol{u}_D \quad \text{on } \Gamma_D \\ -\nu\frac{\partial\boldsymbol{u}}{\partial\boldsymbol{n}} + p\boldsymbol{n} &= \boldsymbol{0} \quad \text{on } \Gamma_N \\ \boldsymbol{u} \in \boldsymbol{H}^1(\Omega),\ \gamma \in H^s(\Omega) & \\ 0 \leq \gamma \leq M \text{ a.e. in } \Omega. & \end{aligned} \tag{4.2}$$

The modified version of Oseen equations given by Equation (4.2) models the velocity $\boldsymbol{u}$ and pressure p of a fluid that passes through the control volume Ω. The term $\gamma\boldsymbol{u}$, with $\gamma \geq 0$, represents the distributed resistance that Ω imposes to the fluid. A zero value of γ represents that the fluid follows the Oseen equations. As the γ values increases in a certain area, the magnitude of $\boldsymbol{u}$ tends to decrease to 0. According to Brinkman's law [24, 13], $1/\gamma$ is an indicator of permeability. The media is completly permeable when $\gamma = 0$, while γ tends to $+\infty$ in zones where there are obstacles. Bounded values of γ model porous media, where porosity decreases as γ increases.

In order to simplifying the analysis of this problem, an equivalent formulation with homogeneous Dirichlet boundary condition is proposed. Let $\boldsymbol{G} \in \boldsymbol{H}^1(\Omega)$ such that $\boldsymbol{G} = \boldsymbol{u}_D$ on Γ_D. Taking $\boldsymbol{v} = \boldsymbol{u} - \boldsymbol{G}$, $\boldsymbol{f} = \nu\triangle\boldsymbol{G} - (\nabla\boldsymbol{G})\,\boldsymbol{a} - \gamma\boldsymbol{G}$ in $\boldsymbol{H}^{-1}(\Omega)$, $g = -\operatorname{div}\boldsymbol{G}$ in $L^2(\Omega)$ and $\boldsymbol{h} = \nu\dfrac{\partial\boldsymbol{G}}{\partial\boldsymbol{n}}$ in $\boldsymbol{H}^{1/2}(\Gamma_N)$, the model problem can be written in a new equivalent form.

$$\text{minimize} \quad J(\gamma, \boldsymbol{v}) = \frac{1}{2}\|\boldsymbol{v} + \boldsymbol{G} - \boldsymbol{u}_R\|_{0,\omega}^2 + \frac{\alpha}{2}\|\gamma\|_{s,\Omega}^2 \tag{4.3}$$

$$\begin{aligned} \text{subject to} \quad -\nu\triangle\boldsymbol{v} + (\nabla\boldsymbol{v})\,\boldsymbol{a} + \nabla p + \gamma\boldsymbol{v} &= \boldsymbol{f} \quad \text{in } \boldsymbol{H}^{-1}(\Omega) \\ \operatorname{div}\boldsymbol{v} &= g \quad \text{in } \Omega \\ \boldsymbol{v} &= \boldsymbol{0} \quad \text{on } \Gamma_D \end{aligned} \tag{4.4}$$

$$-\nu\frac{\partial \boldsymbol{v}}{\partial \boldsymbol{n}} + p\boldsymbol{n} = \boldsymbol{h} \quad \text{on } \Gamma_N$$
$$\boldsymbol{v} \in \boldsymbol{H}^1(\Omega),\ \gamma \in H^s(\Omega)$$
$$0 \leq \gamma \leq M \text{ a.e. in } \Omega.$$

Remark 4.2.1. *The boundary condition imposed in Γ_N strongly depends of $\boldsymbol{a}\cdot\boldsymbol{n} \geq 0$, but that hypothesis can be restrictive for some existing phenomena in the applied case. For example, if a vortex crosses the outlet, there may be a region where the flow returns to the domain. To overcome this problem, the so called "backflow" stabilization techniques [18] can be applied. For example, directional do-nothing condition can be used for this problem. This condition verifies*

$$-\nu\frac{\partial \boldsymbol{u}}{\partial \boldsymbol{n}} + p\boldsymbol{n} + \frac{1}{2}(\boldsymbol{a}\cdot\boldsymbol{n})_{-}\boldsymbol{u} = 0$$

where $(x)_{-} = \min\{x, 0\}$. For this case, the existence of a solution of the Oseen equations is verified [22].

4.3 Existence of solution

The demonstration of the existence of an optimal solution presented follows the same scheme as [11]. A first step is to introduce some helpful notations.

Definition 4.3.1. *Let $s \geq 0$. The set of admissible parameter functions is defined by*

$$\mathcal{A} = \{\gamma \in H^s(\Omega) \mid 0 \leq \gamma \leq M\}.$$

Definition 4.3.2. *The space $\boldsymbol{H}^1_{\Gamma_D}(\Omega)$, subspace of $\boldsymbol{H}^1(\Omega)$, is defined by*

$$\boldsymbol{H}^1_{\Gamma_D}(\Omega) = \left\{\boldsymbol{v} \in \boldsymbol{H}^1(\Omega) \mid \boldsymbol{v} = \boldsymbol{0} \text{ on } \Gamma_D\right\}.$$

Definition 4.3.3. *Let $\gamma \in L^\infty(\Omega)$, the map $A : L^\infty(\Omega) \to \boldsymbol{H}^1_{\Gamma_D}(\Omega) \times L^2_0(\Omega)$ is defined by $A(\gamma) = [A_1(\gamma), A_2(\gamma)] = [\boldsymbol{v}, p]$, where $\boldsymbol{v} \in \boldsymbol{H}^1_{\Gamma_D}(\Omega)$ and $p \in L^2_0(\Omega)$ are the unique variational solutions of the Problem (4.4). In what follows, it is denoted $\mathcal{H} = \boldsymbol{H}^1_{\Gamma_D}(\Omega) \times L^2_0(\Omega)$, which is a Banach space behind the norm*

$$\|[\boldsymbol{v}, p]\|_{\mathcal{H}} = \nu\,|\boldsymbol{v}|_{1,\Omega} + \|p\|_{0,\Omega}$$

Remark 4.3.1. *It is possible to ensure that A is well defined, because (4.4) has an unique solution for every $\gamma \in \mathcal{A}$ (see Lemma 5.8 on [62]). Futhermore, there exists a constant $C > 0$, independent of γ, ν, $\boldsymbol{u}_D$ and $\boldsymbol{G}$, such that*

$$\nu\,|\boldsymbol{v}|^2_{1,\Omega} + (\gamma\boldsymbol{v}, \boldsymbol{v})_{0,\Omega} \leq C\max\left\{\nu, \frac{\|\boldsymbol{a}\|^2_\infty}{\nu}, \|\gamma\|_{\infty,\Omega}\right\}\|\boldsymbol{G}\|^2_{1,\Omega}$$
$$\|p\|^2_{0,\Omega} \leq C\max\left\{\nu, \|\boldsymbol{a}\|_{\infty,\Omega}, \frac{\|\boldsymbol{a}\|^2_{\infty,\Omega}}{\nu}, \|\gamma\|_{\infty,\Omega}\right\}\|\boldsymbol{G}\|_{1,\Omega}.$$

The uniformly boundedness of $\|\boldsymbol{v}\|_{1,\Omega}$ and $\|p\|_{0,\Omega}$ are obtained because $\|\gamma\|_{\infty,\Omega} \leq M$.

Theorem 4.3.1. *Problem* (4.3) *has at least one solution* $\gamma^* \in \mathcal{A}$ *with optimal states* $A(\gamma^*) = [\boldsymbol{v}^*, p^*]$, *i.e.*

$$(\forall \gamma \in \mathcal{A}) \qquad J(\gamma, A_1(\gamma)) \geq J(\gamma^*, \boldsymbol{v}^*).$$

Proof. First, $J(\gamma) = J(\gamma, A(\gamma))$ is bounded below by 0 and

$$(\forall \gamma \in \mathcal{A}) \quad J(\gamma) \geq \frac{\alpha}{2} \|\gamma\|_{s,\Omega}^2.$$

Thus, $m = \inf_{\gamma \in \mathcal{A}} J(\gamma)$ is well defined. Let $\{\gamma_n\}_{n\in\mathbb{N}} \subseteq \mathcal{A}$ and $\{[\boldsymbol{v}_n, p_n]\}_{n\in\mathbb{N}} \subseteq \boldsymbol{H}^1_{\Gamma_D}(\Omega) \times L^2_0(\Omega)$ such that $A(\gamma_n) = [\boldsymbol{v}_n, p_n]$, $\{J(\gamma_n)\}$ is decreasing and $J(\gamma_n) \to m$. It is clear that

$$(\forall n \in \mathbb{N}) \qquad J(\gamma_n) \leq J(\gamma_1).$$

Then, $\{\gamma_n\}_{n\in\mathbb{N}}$ is uniformly bounded in $H^s(\Omega)$. Since $\mathcal{A}$ is weakly closed, there exists a subsequence (denoted by $\{\gamma_n\}_{n\in\mathbb{N}}$) such that $\gamma_n \rightharpoonup \gamma^*$ in $H^s(\Omega)$, with $\gamma^* \in \mathcal{A}$. In particular, $\gamma_n \rightharpoonup \gamma^*$ in $L^2(\Omega)$. By the same way, $\{\boldsymbol{v}_n\}_{n\in\mathbb{N}}$ and $\{p_n\}_{n\in\mathbb{N}}$ are also uniformly bounded (see Remark 4.3.1) on $\boldsymbol{H}^1_{\Gamma_D}(\Omega)$ and $L^2_0(\Omega)$, respectively. Applying the Sobolev embedding Theorem (see Section 6.6 in [36]), there exists a subsequence (also denoted by $\{\boldsymbol{v}_n\}_{n\in\mathbb{N}}$) such that $\boldsymbol{v}_n \rightharpoonup \boldsymbol{v}^*$ weakly in $\boldsymbol{H}^1_{\Gamma_D}(\Omega)$, with $\boldsymbol{v}^* \in \boldsymbol{H}^1_{\Gamma_D}(\Omega)$, and $\boldsymbol{v}_n \to \boldsymbol{v}^*$ in $\boldsymbol{L}^p(\Omega)$ for $p \in [2, 6)$ when $N \geq 3$, or for $p \geq 2$ when $N = 2$. In particular,

$$\boldsymbol{v}_n \to \boldsymbol{v}^* \text{ in } \boldsymbol{L}^4(\Omega) \text{ and } \boldsymbol{L}^2(\Omega).$$

Let $\boldsymbol{w} \in \boldsymbol{H}^1_{\Gamma_D}(\Omega)$. Since $d \in \{2, 3\}$, then $\boldsymbol{w} \in \boldsymbol{L}^4(\Omega)$. Later, $\boldsymbol{v}_n \cdot \boldsymbol{w} \to \boldsymbol{v}^* \cdot \boldsymbol{w}$ in $L^2(\Omega)$ and $(\nabla \boldsymbol{v}_n)\boldsymbol{a} \rightharpoonup (\nabla \boldsymbol{v})\boldsymbol{a}$ weakly in $L^2(\Omega)$. Thus, for every $\boldsymbol{w} \in \boldsymbol{H}^1_{\Gamma_D}(\Omega)$

$$(\gamma_n \boldsymbol{v}_n, \boldsymbol{w})_{0,\Omega} \to (\gamma^* \boldsymbol{v}^*, \boldsymbol{w})_{0,\Omega} \qquad ((\nabla \boldsymbol{v}_n)\boldsymbol{a}, \boldsymbol{w})_{0,\Omega} \to ((\nabla \boldsymbol{v}^*)\boldsymbol{a}, \boldsymbol{w})_{0,\Omega}.$$

Repeating this argument, there exists a subsequence also denoted by $\{p_n\}_{n\in\mathbb{N}}$ such that

$$p_n \rightharpoonup p^* \text{ in } L^2_0(\Omega).$$

In conclusion, $(\boldsymbol{v}^*, p^*) \in \mathcal{H}$ is the variational solution of Equation (4.4). In other words, $A(\gamma^*) = [\boldsymbol{v}^*, p^*]$. Now, γ^* is optimal. Indeed,

$$\begin{aligned} m &= \lim_{n\to\infty} J(\gamma_n) \\ &\geq \lim_{n\to\infty} \frac{1}{2} \|\boldsymbol{v}_n + \boldsymbol{G} - \boldsymbol{u}_R\|_{0,\omega}^2 + \frac{\alpha}{2} \liminf_{n\to\infty} \|\gamma_n\|_{s,\Omega}^2 \\ &\geq \frac{1}{2} \|\boldsymbol{v}^* + \boldsymbol{G} - \boldsymbol{u}_R\|_{0,\omega}^2 + \frac{\alpha}{2} \|\gamma^*\|_{s,\Omega}^2 = J(\gamma^*) \geq m. \end{aligned}$$

Hence, $J(\gamma, A_1(\gamma)) \geq J(\gamma^*, \boldsymbol{v}^*)$ for every $\gamma \in \mathcal{A}$, proving this theorem. □

4.4 First order necessary optimality condition

In order to implement a descent method to numerically solve this problem, it is necessary to establish the differentiability of functional J. However, this directly depends on the differentiability of map A. From this result, it is possible to establish necessary optimality conditions.

Theorem 4.4.1. *The map A is Fréchet-differentiable. For each $\gamma, \gamma_1 \in \mathcal{A}$, if $A(\gamma) = [\boldsymbol{v}, p]$, then the Fréchet derivative $A'(\gamma)[\gamma_1] = [\boldsymbol{v}_1', p_1']$ can be described by the weak solution of the following problem*

$$\begin{aligned} -\nu\triangle\boldsymbol{v}_1' + (\nabla\boldsymbol{v}_1')\,\boldsymbol{a} + \nabla p_1' + \gamma\boldsymbol{v}_1' &= -\gamma_1(\boldsymbol{v}+\boldsymbol{G}) && \text{in } \Omega \\ \operatorname{div}\boldsymbol{v}_1' &= 0 && \text{in } \Omega \\ \boldsymbol{v}_1' &= \boldsymbol{0} && \text{on } \Gamma_D \\ -\nu\frac{\partial\boldsymbol{v}_1'}{\partial\boldsymbol{n}} + p_1'\boldsymbol{n} &= \boldsymbol{0} && \text{on } \Gamma_N. \end{aligned} \tag{4.5}$$

Proof. Let $\gamma, \gamma_1 \in \mathcal{A}$, it will be proved that there is a linear application $D : L^\infty(\Omega) \to \mathcal{H}$ such that

$$A(\gamma+\gamma_1) - A(\gamma) = D(\gamma_1) + r(\gamma, \gamma_1),$$

where

$$\|\gamma_1\|_{\infty,\Omega} \to 0 \Rightarrow \frac{\|r(\gamma,\gamma_1)\|_{\mathcal{H}}}{\|\gamma_1\|_{\infty,\Omega}} \to 0.$$

Let $[\boldsymbol{v}_1, p_1] = A(\gamma+\gamma_1)$. Taking $D(\gamma_1) = [\boldsymbol{v}_1', p_1']$ and $r(\gamma,\gamma_1) = [\delta\boldsymbol{v}, \delta p] = [\boldsymbol{v}_1 - \boldsymbol{v} - \boldsymbol{v}_1', p_1 - p - p_1']$, it is possible to see that $D(\gamma_1)$ is linear. Also, $r(\gamma,\gamma_1)$ is solution of the problem

$$\begin{aligned} -\nu\triangle(\delta\boldsymbol{v}) + (\nabla\delta\boldsymbol{v}_1)\,\boldsymbol{a} + \nabla(\delta p) + \gamma(\delta\boldsymbol{v}) &= \gamma_1(v - v_1) && \text{in } \Omega \\ \operatorname{div}(\delta\boldsymbol{v}) &= 0 && \text{in } \Omega \\ (\delta\boldsymbol{v}) &= \boldsymbol{0} && \text{on } \Gamma_D \\ -\nu\frac{\partial(\delta\boldsymbol{v})}{\partial\boldsymbol{n}} + (\delta p)\,\boldsymbol{n} &= \boldsymbol{0} && \text{on } \Gamma_N. \end{aligned}$$

Thus, there exists a constant $c_1 > 0$, independent of γ and γ_1 (see Lemma 5.8 on [62]), such that

$$\|r(\gamma,\gamma_1)\|_{\mathcal{H}} = \nu|\delta\boldsymbol{v}|_{1,\Omega} + \|\delta p\|_{0,\Omega} \le c_1\|\gamma_1\|_{0,\Omega}\|\boldsymbol{v}-\boldsymbol{v}_1\|_{0,\Omega}.$$

subtracting the equations of $\boldsymbol{v}$ y $\boldsymbol{v}_1$ and using integration by parts,

$$\nu|\boldsymbol{v}-\boldsymbol{v}_1|_{1,\Omega}^2 + (\gamma(\boldsymbol{v}-\boldsymbol{v}_1), \boldsymbol{v}-\boldsymbol{v}_1)_{0,\Omega} = (\gamma_1(\boldsymbol{G}+\boldsymbol{v}_1), \boldsymbol{v}-\boldsymbol{v}_1)_{0,\Omega}.$$

Applying Cauchy-Schwarz and Friedrichs-Poincaré inequalities, there exists $c_2 > 0$ such that

$$\begin{aligned} \nu|\boldsymbol{v}-\boldsymbol{v}_1|_{1,\Omega}^2 &\le (\gamma_1(\boldsymbol{G}+\boldsymbol{v}_1), \boldsymbol{v}-\boldsymbol{v}_1)_{0,\Omega} \\ &\le \|\gamma_1\|_{\infty,\Omega}\|\boldsymbol{G}+\boldsymbol{v}_1\|_{0,\Omega}\|\boldsymbol{v}-\boldsymbol{v}_1\|_{0,\Omega} \\ &\le c_2\|\gamma_1\|_{\infty,\Omega}\|\boldsymbol{G}+\boldsymbol{v}_1\|_{0,\Omega}|\boldsymbol{v}-\boldsymbol{v}_1|_{1,\Omega}. \end{aligned}$$

But, using Friedrichs-Poincaré inequality again, there exists $c_3 > 0$ such that $\|\boldsymbol{G}+\boldsymbol{v}_1\|_{0,\Omega} \le c_3\|\boldsymbol{G}\|_{1,\Omega}$ (see Remark 4.3.1). Then, there exists $C_1 > 0$ such that

$$\nu|\boldsymbol{v}-\boldsymbol{v}_1|_{1,\Omega} \le C_1\|\gamma_1\|_{\infty,\Omega}\|\boldsymbol{G}\|_{0,\Omega}.$$

Finally, applying Friedrichs-Poincaré inequality, there exists a constant $C > 0$ such that

$$\|r(\gamma,\gamma_1)\|_{\mathcal{H}} = \nu|\delta\boldsymbol{v}|_{1,\Omega} + \|\delta p\|_{0,\Omega} \le C\|\gamma_1\|_{\infty,\Omega}^2\|\boldsymbol{G}\|_{0,\Omega}.$$

Thus,

$$\frac{\|r(\gamma,\gamma_1)\|_{\mathcal{H}}}{\|\gamma_1\|_{\infty,\Omega}} \leq C\,\|\gamma_1\|_{0,\Omega}\,\|\boldsymbol{G}\|_{0,\Omega} \overset{\|\gamma_1\|_{\infty,\Omega}\to 0}{\longrightarrow} 0,$$

proving the theorem. □

Defining $B(\boldsymbol{v}) = \frac{1}{2}\|\boldsymbol{v}+\boldsymbol{G}-\boldsymbol{u}_R\|^2_{0,\omega}$ and $C(\gamma) = \frac{\alpha}{2}\|\gamma\|^2_{s,\Omega}$, an expression for Frechét derivatives of B and C is given by

$$B'(\boldsymbol{v})[w] = (\boldsymbol{v}+\boldsymbol{G}-\boldsymbol{u}_R,\boldsymbol{w})_{0,\omega} \qquad C'(\gamma)[\beta] = \alpha(\gamma,\beta)_{s,\Omega}.$$

Applying chain rule, it is obtained that

$$\begin{aligned} J'(\gamma)[\gamma_1] &= B'(\boldsymbol{v})[A_1'(\gamma)[\gamma_1]] + C'(\gamma)[\gamma_1] \\ &= (\boldsymbol{v}+\boldsymbol{G}-\boldsymbol{u}_R,\boldsymbol{v}_1')_{0,\omega} + \alpha(\gamma,\gamma_1)_{s,\Omega}. \end{aligned}$$

In order to reduce this expression, the following definition is introduced similarly to [1].

Definition 4.4.1. *Let $\gamma \in \mathcal{A}$ and $A(\gamma) = [\boldsymbol{v},p]$. The adjoint states $A^*(\gamma) = [\boldsymbol{\varphi},\xi]$ are defined as the unique weak solution of the problem*

$$\begin{aligned} -\nu\triangle\boldsymbol{\varphi} - (\nabla\boldsymbol{\varphi})\,\boldsymbol{a} + \nabla\xi + \gamma\boldsymbol{\varphi} &= \chi_\omega(\boldsymbol{v}+\boldsymbol{G}-\boldsymbol{u}_R) && \text{in } \boldsymbol{\Omega} \\ \operatorname{div}\boldsymbol{\varphi} &= 0 && \text{in } \Omega \\ \boldsymbol{\varphi} &= \boldsymbol{0} && \text{on } \Gamma_D \\ -\nu\frac{\partial\boldsymbol{\varphi}}{\partial\boldsymbol{n}} + \xi\boldsymbol{n} - (\boldsymbol{a}\cdot\boldsymbol{n})\,\boldsymbol{\varphi} &= \boldsymbol{0} && \text{on } \Gamma_N. \end{aligned} \tag{4.6}$$

where χ_ω is the indicator function of ω.

Using this defintion, it is possible to rewrite $J'(\gamma_1)$ depending of the adjoint state. That expression is simpler to analyze, since it depends on the adjoint state, allowing a simple form of a first order optimality condition using a variational inequality.

Theorem 4.4.2. *Let $\gamma,\gamma_1 \in \mathcal{A}$ and $s \geq 0$. Then,*

$$J'(\gamma)[\gamma_1] = -(\gamma_1(\boldsymbol{v}+\boldsymbol{G}),\boldsymbol{\varphi})_{0,\Omega} + \alpha(\gamma,\gamma_1)_{s,\Omega},$$

where $A(\gamma) = [\boldsymbol{v},p]$. If $\gamma^* \in \mathcal{A}$ is an optimal for Problem (4.3), then

$$(\forall\gamma\in\mathcal{A}) \qquad -((\gamma-\gamma^*)(\boldsymbol{v}^*+\boldsymbol{G}),\boldsymbol{\varphi})_{0,\Omega} + \alpha(\gamma^*,\gamma-\gamma^*)_{s,\Omega} \geq 0$$

where $A(\gamma^*) = [\boldsymbol{v}^*,p^*]$ and $A^*(\gamma^*) = [\boldsymbol{\varphi},\xi]$ are the states and adjont states of γ^*, respectively.

Proof. First, using integration by parts with the adjoint states $[\boldsymbol{\varphi},\xi]$ as tests functions, it is obtained that

$$\begin{aligned} -\nu\int_\Omega \triangle\boldsymbol{v}_1'\cdot\boldsymbol{\varphi}\,d\boldsymbol{x} &= -\nu\int_\Omega \triangle\boldsymbol{\varphi}\cdot\boldsymbol{v}_1'\,d\boldsymbol{x} + \int_{\partial\Omega}\boldsymbol{\varphi}\cdot\left(-\nu\frac{\partial\boldsymbol{v}_1'}{\partial\boldsymbol{n}}\right) - \boldsymbol{v}_1'\cdot\left(-\nu\frac{\partial\boldsymbol{\varphi}}{\partial\boldsymbol{n}}\right)\,dS \\ \int_\Omega[(\nabla\boldsymbol{v}_1')\,\boldsymbol{a}]\cdot\boldsymbol{\varphi}\,d\boldsymbol{x} &= -\int_\Omega[(\nabla\boldsymbol{a})\,\boldsymbol{v}_1']\cdot\boldsymbol{\varphi}\,d\boldsymbol{x} + \int_{\partial\Omega}(\boldsymbol{a}\cdot\boldsymbol{n})(\boldsymbol{\varphi}\cdot\boldsymbol{v}_1')\,dS \end{aligned}$$

$$\int_\Omega \nabla p_1' \cdot \boldsymbol{\varphi}\ d\boldsymbol{x} = -\int_\Omega p_1' \operatorname{div} \boldsymbol{\varphi}\ d\boldsymbol{x} + \int_{\partial\Omega} \boldsymbol{\varphi} \cdot (p_1' \boldsymbol{n})\ dS$$
$$-\int_\Omega \xi \operatorname{div} \boldsymbol{v}_1'\ d\boldsymbol{x} = \int_\Omega \nabla\xi \cdot \boldsymbol{v}_1'\ d\boldsymbol{x} - \int_{\partial\Omega} \boldsymbol{v}_1' \cdot (\xi \boldsymbol{n})\ dS.$$

Then,

$$\begin{aligned}
&-\left(\gamma_1 (\boldsymbol{v}+\boldsymbol{G}), \boldsymbol{\varphi}\right)_{0,\Omega} \\
=&-\nu\int_\Omega \triangle \boldsymbol{v}_1' \cdot \boldsymbol{\varphi}\ d\boldsymbol{x} + \int_\Omega [(\nabla \boldsymbol{v}_1')\,\boldsymbol{a}] \cdot \boldsymbol{\varphi}\ d\boldsymbol{x} + \int_\Omega \nabla p_1' \cdot \boldsymbol{\varphi}\ d\boldsymbol{x} + \int_\Omega \gamma \boldsymbol{v}_1' \cdot \boldsymbol{\varphi}\ d\boldsymbol{x} \\
&-\int_\Omega \xi \operatorname{div} \boldsymbol{v}_1'\ d\boldsymbol{x} \\
=&-\nu\int_\Omega \triangle \boldsymbol{\varphi} \cdot \boldsymbol{v}_1'\ d\boldsymbol{x} - \int_\Omega [(\nabla \boldsymbol{\varphi})\,\boldsymbol{a}] \cdot \boldsymbol{v}_1' d\boldsymbol{x} + \int_\Omega \nabla\xi \cdot \boldsymbol{v}_1'\ d\boldsymbol{x} + \int_\Omega \gamma \boldsymbol{v}_1' \cdot \boldsymbol{\varphi}\ d\boldsymbol{x} \\
&-\int_\Omega p_1' \operatorname{div} \boldsymbol{\varphi}\ d\boldsymbol{x} + \int_{\Gamma_N} \boldsymbol{\varphi} \cdot \left(-\nu \frac{\partial \boldsymbol{v}_1'}{\partial \boldsymbol{n}} + p_1' \boldsymbol{n}\right) - \int_{\Gamma_N} \boldsymbol{v}_1' \cdot \left(-\nu \frac{\partial \boldsymbol{\varphi}}{\partial \boldsymbol{n}} + \xi \boldsymbol{n} - (\boldsymbol{a}\cdot\boldsymbol{n})\,\boldsymbol{\varphi}\right)\ dS \\
=&-\nu\int_\Omega \triangle \boldsymbol{\varphi} \cdot \boldsymbol{v}_1'\ d\boldsymbol{x} - \int_\Omega [(\nabla \boldsymbol{v}_1')\,\boldsymbol{a}] \cdot \boldsymbol{\varphi}\ d\boldsymbol{x} + \int_\Omega \nabla\xi \cdot \boldsymbol{v}_1'\ d\boldsymbol{x} + \int_\Omega \gamma \boldsymbol{v}_1' \cdot \boldsymbol{\varphi}\ d\boldsymbol{x} \\
&-\int_\Omega p_1' \operatorname{div} \boldsymbol{\varphi}\ d\boldsymbol{x} \\
=&\left((\boldsymbol{v}+\boldsymbol{G}-\boldsymbol{u}_D), \boldsymbol{v}_1'\right)_{0,\omega}
\end{aligned}$$

Thus,

$$J'(\gamma)[\gamma_1] = -\left(\gamma_1 (\boldsymbol{v}+\boldsymbol{G}), \boldsymbol{\varphi}\right)_{0,\Omega} + \alpha(\gamma, \gamma_1)_{s,\Omega}$$

Later, if $\gamma^* \in \mathcal{A}$ is optimal for the problem, then

$$(\forall \gamma \in \mathcal{A}) \quad J(\gamma) \geq J(\gamma^*),$$

Finally, it is obtained that

$$J'(\gamma^*)[\gamma - \gamma^*] = \lim_{\varepsilon \to 0^+} \frac{J(\gamma^* + \varepsilon(\gamma - \gamma^*)) - J(\gamma^*)}{\varepsilon} \geq 0,$$

proving this theorem. □

4.5 Second order sufficient optimality condition.

The stability results of the optimization algorithms depend, for the most part, on the existence of the second derivative of J. Likewise, it is possible to establish second order sufficient optimality conditions.

In first place, it is necesary to introduce new forms of emebedding inequalties.

Theorem 4.5.1. *There exists a constant $q^* > 2$, dependent only of Ω, such that for each $p \in [2, q^*]$ there exists a constant $C > 0$, dependent only of Ω, M, ν and p such that*

$$\|\boldsymbol{v}\|_{1,p,\Omega} \leq C \|G\|_{-1,p,\Omega}$$

where $G \in W^{-1,p}(\Omega)$ *(the dual of* $W_0^{1,q}(\Omega)$*) is defined by*

$$\left(\forall \boldsymbol{w} \in W_0^{1,q}(\Omega)\right) \qquad \langle G(\boldsymbol{v}), \boldsymbol{w}\rangle = \langle \boldsymbol{f}, \boldsymbol{w}\rangle_{\boldsymbol{H}^{-1}(\Omega),\boldsymbol{H}^1(\Omega)} + (\boldsymbol{h}, \boldsymbol{w})_{0,\Gamma_N}$$

with $q \geq 2$ *such that* $\dfrac{1}{p} + \dfrac{1}{q} = 1$.

Proof. See Theorem 1 in [51]. □

Remark 4.5.1. *The hypotheses* $\boldsymbol{u}_R \in L^\infty(\omega)$ *and* $\boldsymbol{u}_D \in L^\infty(\Gamma_D)$ *appear frequently. Asumming* $\boldsymbol{u}_R \in L^\infty(\omega)$ *and* $\boldsymbol{u}_D \in L^\infty(\Gamma_D)$*, it is clear that* $\boldsymbol{G} \in \boldsymbol{W}^{1,\infty}(\Omega)$*. Then, there exists a constant* $C_p > 0$*, depending only of* p *and* Ω*, such that*

$$\|G\|_{-1,p,\Omega} \leq C_p \max\left\{\nu, \|\boldsymbol{a}\|_{\infty,\Omega}, \|\gamma\|_{\infty,\Omega}\right\} \|\boldsymbol{G}\|_{1,\infty,\Omega}.$$

Futhermore, using Theorem 4.5.1,

$$\|\boldsymbol{v}\|_{1,p,\Omega} \leq C C_p \max\left\{\nu, \|\boldsymbol{a}\|_{\infty,\Omega}, M\right\} \|\boldsymbol{G}\|_{1,\infty,\Omega}$$

So, $\|\boldsymbol{v}\|_{1,p,\Omega}$ *is uniformly bounded for each* $p \in [2, q^*]$*. Also, Theorem 1 in [51] allows us to be more precise about the asymptotic behavior of* q^**. Indeed, if the value of* $\|\gamma\|_{\infty,\Omega}$ *increases,* q^* *decreases to* 2*.*

Lemma 4.5.1. *Let* $s > 0$ *and* $p \in [1, N]$*.*

1. *If* $N > sp$*, then the embedding from* $W^{s,p}(\Omega)$ *to* $L^r(\Omega)$ *is continuous for* $r \in \left[p, \dfrac{d}{d - sp}\right]$*.*
2. *If* $N = sp$*, then the embedding from* $W^{s,p}(\Omega)$ *to* $L^r(\Omega)$ *is continuous for* $r \in [p, +\infty)$*.*

Proof. See Section 6.6 in [36] □

Remark 4.5.2. *Using this embedding result with* $s \geq \dfrac{N}{q^*}$ *and* $p = 2$*, Lemma 4.5.1 can be written by*

1. *If* $q^* > 2$*, then the embedding from* $H^{d/q^*}(\Omega)$ *to* $L^r(\Omega)$ *is compact for* $r \in \left[2, \dfrac{1}{\frac{1}{p} - \frac{1}{q^*}}\right]$*.*
2. *If* $q^* = 2$*, then the embedding from* $H^{d/q^*}(\Omega)$ *to* $L^r(\Omega)$ *is compact for* $r \in [2, +\infty)$*.*

Then, for $2 \leq p \leq \dfrac{1}{\frac{1}{2} - \frac{1}{q^*}}$ there exists $C > 0$ such that

$$(\forall \gamma \in \mathcal{A}) \quad \|\gamma\|_{0,p,\Omega} \leq C \|\gamma\|_{s,\Omega}.$$

In order to establish and prove second order optimality conditions, a first step is to show that the map A is twice Fréchet-differentiable.

Theorem 4.5.2. *The map $\gamma \longmapsto A'(\gamma)[\gamma_1]$ from $L^\infty(\Omega)$ to $\mathcal{H}$ for each $\gamma_1 \in \mathcal{A}$ is Fréchet-differentiable. Let $\gamma, \gamma_1, \gamma_2 \in\in \mathcal{A}$, the Fréchet derivative of $A'(\gamma)[\gamma_1]$ on γ_2 direction is given by $A''(\gamma)[\gamma_1, \gamma_2] = [\boldsymbol{v}'', p'']$, where $[\boldsymbol{v}'', p'']$ is the unique weak solution of the problem*

$$\begin{aligned} -\nu\triangle \boldsymbol{v}'' + (\nabla \boldsymbol{v}'')\,\boldsymbol{a} + \nabla p'' + \gamma \boldsymbol{v}'' &= -(\gamma_2 \boldsymbol{v}_1' + \gamma_1 \boldsymbol{v}_2') && \text{in } \Omega \\ \operatorname{div} \boldsymbol{v}'' &= 0 && \text{in } \Omega \\ \boldsymbol{v}'' &= \boldsymbol{0} && \text{on } \Gamma_D \\ -\nu \frac{\partial \boldsymbol{v}''}{\partial \boldsymbol{n}} + p''\boldsymbol{n} &= \boldsymbol{0} && \text{on } \Gamma_N. \end{aligned} \tag{4.7}$$

and $A'(\gamma)\gamma_j = \left[\boldsymbol{v}_j', p_j'\right]$, for $j \in \{1, 2\}$.

Proof. Let $\gamma, \gamma_1 \in \mathcal{A}$, it will be proved that there is a linear application $D_2 : L^\infty(\Omega) \to \mathcal{H}$ such that

$$A'(\gamma + \gamma_2)[\gamma_1] - A'(\gamma)[\gamma_1] = D_2(\gamma, \gamma_1)[\gamma_2] + r(\gamma, \gamma_1, \gamma_2),$$

where

$$\|\gamma_2\|_{\infty,\Omega} \to 0 \Rightarrow \frac{\|r(\gamma, \gamma_1, \gamma_2)\|_{\mathcal{H}}}{\|\gamma_2\|_{\infty,\Omega}} \to 0.$$

Let $A'(\gamma + \gamma_2)[\gamma_1] = [\boldsymbol{w}_1', q_1']$, $A'(\gamma)[\gamma_1] = [\boldsymbol{v}_1', p_1']$ (see Theorem 4.4.1), $A(\gamma) = [\boldsymbol{v}, p]$ and $A(\gamma + \gamma_2) = [\boldsymbol{w}, q]$ (see Definition 4.3.3). Defining $D(\gamma, \gamma_1)[\gamma_2] = [\boldsymbol{v}'', p'']$ as function of γ_2 and

$$r(\gamma, \gamma_1, \gamma_2) = [\delta\boldsymbol{v}, \delta p] = [\boldsymbol{w}_1' - \boldsymbol{v}_1' - \boldsymbol{v}'', q_1' - p_1' - p''],$$

it is possible to see that $D(\gamma, \gamma_1)$ is linear and $r(\gamma, \gamma_1, \gamma_2)$ is solution of the problem

$$\begin{aligned} -\nu\triangle(\delta\boldsymbol{v}) + (\nabla\delta\boldsymbol{v})\,\boldsymbol{a} + \nabla(\delta p) + \gamma(\delta\boldsymbol{v}) &= \gamma_2(\boldsymbol{v}_1' - \boldsymbol{w}_1') + \gamma_1(\boldsymbol{v}_2' + \boldsymbol{v} - \boldsymbol{w}) && \text{in } \Omega \\ \operatorname{div}(\delta\boldsymbol{v}) &= 0 && \text{in } \Omega \\ (\delta\boldsymbol{v}) &= \boldsymbol{0} && \text{on } \Gamma_D \\ -\nu\frac{\partial(\delta\boldsymbol{v})}{\partial\boldsymbol{n}} + (\delta p)\,\boldsymbol{n} &= \boldsymbol{0} && \text{on } \Gamma_N. \end{aligned}$$

Then, applying Friedrichs-Poincaré inequality, there exists $c_1 > 0$, independent of $\gamma, \gamma_1, \gamma_2$ such that

$$\nu|\delta\boldsymbol{v}|_{1,\Omega} + \|\delta p\|_{0,\Omega} \leq c_1\left(\|\gamma_2\|_{\infty,\Omega}|\boldsymbol{v}_1' - \boldsymbol{w}_1'|_{1,\Omega} + \|\gamma_1\|_{\infty,\Omega}|\boldsymbol{v}_2' + \boldsymbol{v} - \boldsymbol{w}|_{1,\Omega}\right).$$

Later, subtracting the equations of $\boldsymbol{v}_1'$ and $\boldsymbol{w}_1'$, testing with $\boldsymbol{v}_1' - \boldsymbol{w}_1'$ and $p_1' - q_1$, respectively, and applying Friedrichs-Poincaré inequality, there exists $c_2 > 0$ such that

$$\begin{aligned} \nu|\boldsymbol{v}_1' - \boldsymbol{w}_1'|_{1,\Omega}^2 &\leq (\gamma_2\boldsymbol{w}_1', \boldsymbol{v}_1' - \boldsymbol{w}_1')_{0,\Omega} + (\gamma_1(\boldsymbol{w} - \boldsymbol{v}), \boldsymbol{v}_1' - \boldsymbol{w}_1')_{0,\Omega} \\ &\leq \|\gamma_2\|_{\infty,\Omega}\|\boldsymbol{w}_1'\|_{0,\Omega}\|\boldsymbol{v}_1' - \boldsymbol{w}_1'\|_{0,\Omega} + \|\gamma_1\|_{\infty,\Omega}\|\boldsymbol{w} - \boldsymbol{v}\|_{0,\Omega}\|\boldsymbol{v}_1' - \boldsymbol{w}_1'\|_{0,\Omega} \\ &\leq c_2\left(\|\gamma_2\|_{\infty,\Omega}|\boldsymbol{w}_1'|_{1,\Omega} + \|\gamma_1\|_{\infty,\Omega}|\boldsymbol{w} - \boldsymbol{v}|_{1,\Omega}\right)|\boldsymbol{v}_1' - \boldsymbol{w}_1'|_{1,\Omega}. \end{aligned}$$

Hence,

$$\nu|\boldsymbol{v}_1' - \boldsymbol{w}_1'|_{1,\Omega} \leq c_2\left(\|\gamma_2\|_{\infty,\Omega}|\boldsymbol{w}_1'|_{1,\Omega} + \|\gamma_1\|_{\infty,\Omega}|\boldsymbol{w} - \boldsymbol{v}|_{1,\Omega}\right).$$

Analogously, from the equations of $\boldsymbol{w}$ and $\boldsymbol{v}$, there exists $c_2 > 0$ such that

$$\begin{aligned}\nu \left|\boldsymbol{w}-\boldsymbol{v}\right|_{1,\Omega}^2 &\leq -\left(\gamma_2\left(\boldsymbol{v}+\boldsymbol{G}\right),\boldsymbol{w}-\boldsymbol{v}\right)_{0,\Omega}\\ &\leq \left\|\gamma_2\right\|_{\infty,\Omega}\left\|\boldsymbol{v}+\boldsymbol{G}\right\|_{0,\Omega}\left\|\boldsymbol{w}-\boldsymbol{v}\right\|_{0,\Omega}\\ &\leq c_2\left\|\gamma_2\right\|_{\infty,\Omega}\left|\boldsymbol{v}+\boldsymbol{G}\right|_{1,\Omega}\left|\boldsymbol{w}-\boldsymbol{v}\right|_{1,\Omega},\end{aligned}$$

but there exists $c_3 > 0$ such that $\left|\boldsymbol{v}\right|_{1,\Omega} \leq c_3\left\|\boldsymbol{G}\right\|_{1,\Omega}$ (see Remark 4.3.1). Then,

$$\nu\left|\boldsymbol{w}-\boldsymbol{v}\right|_{1,\Omega} \leq c_2c_3\left\|\gamma_2\right\|_{\infty,\Omega}\left\|\boldsymbol{G}\right\|_{1,\Omega}.$$

Futhermore, there exists $c_4 > 0$ such that

$$\nu\left|\boldsymbol{w}_1'\right|_{1,\Omega} \leq c_4\left\|\boldsymbol{G}\right\|_{1,\Omega}.$$

In conclusion, there exists $C_1 > 0$ such that

$$\nu\left|\boldsymbol{v}_1'-\boldsymbol{w}_1'\right|_{1,\Omega} \leq C_1\left\|\gamma_1\right\|_{\infty,\Omega}\left\|\gamma_2\right\|_{\infty,\Omega}\left\|\boldsymbol{G}\right\|_{1,\Omega}.$$

Repeating this analysis for the term $\boldsymbol{v}_2'+\boldsymbol{v}-\boldsymbol{w}$, there exists $c_5 > 0$ such that

$$\begin{aligned}\nu\left|\boldsymbol{v}_2'+\boldsymbol{v}-\boldsymbol{w}\right|_{0,\Omega} &\leq c_5\left\|\gamma_2\right\|_{\infty,\Omega}\left|\boldsymbol{w}-\boldsymbol{v}\right|_{1,\Omega}\\ &\leq c_5\left\|\gamma_2\right\|_{\infty,\Omega}^2\left\|\boldsymbol{G}\right\|_{1,\Omega}.\end{aligned}$$

Then, there exists $C_2 > 0$ such that

$$\begin{aligned}\left\|r\left(\gamma,\gamma_1,\gamma_2\right)\right\|_{\mathcal{H}} &= \nu\left|\delta\boldsymbol{v}\right|_{1,\Omega}+\left\|\delta p\right\|_{0,\Omega}\\ &\leq c_1\left(\left\|\gamma_2\right\|_{\infty,\Omega}\left|\boldsymbol{v}_1'-\boldsymbol{w}_1'\right|_{0,\Omega}+\left\|\gamma_1\right\|_{\infty,\Omega}\left|\boldsymbol{v}_2'+\boldsymbol{v}-\boldsymbol{w}\right|_{1,\Omega}\right)\\ &\leq c_1\left(c_2\left\|\gamma_1\right\|_{\infty,\Omega}\left\|\gamma_2\right\|_{\infty,\Omega}^2\left\|\boldsymbol{G}\right\|_{1,\Omega}+c_5c_2\left\|\gamma_1\right\|_{\infty,\Omega}\left\|\gamma_2\right\|_{\infty,\Omega}^2\left\|\boldsymbol{G}\right\|_{1,\Omega}\right)\\ &\leq C_2\left\|\gamma_1\right\|_{\infty,\Omega}\left\|\gamma_2\right\|_{\infty,\Omega}^2\left\|\boldsymbol{G}\right\|_{1,\Omega}.\end{aligned}$$

In conclusion,

$$\frac{\left\|r\left(\gamma,\gamma_1,\gamma_2\right)\right\|_{\mathcal{H}}}{\left\|\gamma_2\right\|_{\infty,\Omega}} \leq C_2\left\|\gamma_1\right\|_{\infty,\Omega}\left\|\gamma_2\right\|_{\infty,\Omega}\left\|\boldsymbol{G}\right\|_{0,\Omega} \overset{\left\|\gamma_2\right\|_{\infty,\Omega}\to 0}{\longrightarrow} 0,$$

proving the theorem □

Let $\gamma,\gamma_1,\gamma_2 \in \mathcal{A}$. An expresion for the Fréchet second derivative of $J\left(\gamma\right)$ on directions γ_1 and γ_2 is given by

$$\begin{aligned}J''\left(\gamma\right)\left[\gamma_1,\gamma_2\right] &= B''\left(A\left(\gamma\right)\right)\left[A_1'\left(\gamma_1\right),A'\left(\gamma_2\right)\right]+B'\left(\left(A\left(\gamma\right)\right)\right)\left[A_1''\left(\gamma\right)\left[\gamma_1,\gamma_2\right]\right]+C''\left(\gamma\right)\left[\gamma_1,\gamma_2\right]\\ &= \left(\boldsymbol{v}_1',\boldsymbol{v}_2'\right)_{0,\Omega}+\left(\boldsymbol{v}+\boldsymbol{G}-\boldsymbol{u}_D,\boldsymbol{v}''\right)_{0,\omega}+\alpha\left(\gamma_1,\gamma_2\right)_{s,\Omega},\end{aligned}$$

where, reasoning as in the proof of Theorem 4.4.2,

$$\left(\boldsymbol{v}+\boldsymbol{G}-\boldsymbol{u}_D,\boldsymbol{v}''\right)_{0,\omega} = -\left(\gamma_1\boldsymbol{v}_2'+\gamma_2\boldsymbol{v}_1',\boldsymbol{\varphi}\right)_{0,\Omega}.$$

In consequence,

$$\begin{aligned} J''(\gamma)[\gamma_1,\gamma_2] &= B''(A(\gamma))[A_1'(\gamma_1), A'(\gamma_2)] + B'((A(\gamma)))[A_1''(\gamma)[\gamma_1,\gamma_2]] + C''(\gamma)[\gamma_1,\gamma_2] \\ &= (\boldsymbol{v}_1', \boldsymbol{v}_2')_{0,\Omega} - (\gamma_1 \boldsymbol{v}_2' + \gamma_2 \boldsymbol{v}_1', \boldsymbol{\varphi})_{0,\Omega} + \alpha(\gamma_1,\gamma_2)_{s,\Omega}. \end{aligned}$$

In what follows, a second order optimality condition is proved. For this, a series of technical results are required. Consider r such that $\frac{1}{q^*} + \frac{1}{r} = \frac{1}{2}$. For $\gamma, \gamma_1, \gamma_2, h \in \mathcal{A}$, consider $A(\gamma) = [\boldsymbol{v}, p]$, $A(\gamma + h) = [\boldsymbol{v}_h, p_h]$, with respective adjoint states $[\boldsymbol{\varphi}, \xi]$ and $[\boldsymbol{\varphi}_h, \xi_h]$, $A'(\gamma)[\gamma_k] = [\boldsymbol{v}_k', p_k']$ and $[\boldsymbol{v}_{h,k}', p_{h,k}'] = A'(\gamma + h)[\gamma_k]$ for $k \in \{1,2\}$. Using this, it is possible to obtain the following estimations.

Lemma 4.5.2. *For each $q \in [2, q^*]$, there exists $C > 0$, independent of $\boldsymbol{v}$, γ, γ_1, γ_2 and h such that $\|\boldsymbol{v}_h - \boldsymbol{v}\|_{1,q,\Omega} \leq C \|h\|_{\infty,\Omega}$,*

Proof. subtracting the equations of $A(\gamma + h)$ and $A(\gamma)$, it is obtained

$$-\nu \triangle(\boldsymbol{v}_h - \boldsymbol{v}) + [\nabla(\boldsymbol{v}_h - \boldsymbol{v})]\boldsymbol{a} + \nabla(p_h - p) + \gamma(\boldsymbol{v}_h - \boldsymbol{v}) = -h(\boldsymbol{G} + \boldsymbol{v}_h).$$

Using Theorem 4.5.1 twice and triangular inequality, there exist $c_1, c_2 > 0$ such that

$$\begin{aligned} \|\boldsymbol{v}\|_{1,q,\Omega} &\leq c_1 \|h(\boldsymbol{G} + \boldsymbol{v}_h)\|_{-1,q,\Omega} \\ &\leq c_1 \|h\|_{\infty,\Omega} \|(\boldsymbol{G} + \boldsymbol{v}_h)\|_{1,q,\Omega} \\ &\leq c_2 \|h\|_{\infty,\Omega} \|\boldsymbol{G}\|_{1,\infty,\Omega}. \end{aligned}$$

Taking $C = c_2 \|\boldsymbol{G}\|_{1,\infty,\Omega}$, the estimation is proved. □

Lemma 4.5.3. *Let $k \in \{1,2\}$. There exists $C > 0$ independent of $\boldsymbol{v}$, γ, γ_1, γ_2 and h such that $|\boldsymbol{v}_{h,k}'|_{1,\Omega} \leq C \|\gamma_k\|_{s,\Omega}$.*

Proof. First, testing the equation of $\boldsymbol{v}_{h,k}'$ with $\boldsymbol{v}_{h,k}'$ and appliying Friedichs-Poincaré and Hölder inequalities, there exists a constant $c_1 > 0$ such that

$$\begin{aligned} \nu |\boldsymbol{v}_{h,k}'|_{1,\Omega} &\leq c_1 \|\gamma_k(\boldsymbol{G} + \boldsymbol{v}_{k,h})\|_{0,\Omega} \\ &\leq c_1 \|\gamma_k\|_{0,r,\Omega} \|(\boldsymbol{G} + \boldsymbol{v}_{k,h})\|_{0,q^*,\Omega} \end{aligned}$$

From Remark 4.5.1, $\|(\boldsymbol{G} + \boldsymbol{v}_{k,h})\|_{0,q^*,\Omega}$ is uniformly bounded by $c_2 > 0$. Also, due to $r = \frac{1}{\frac{1}{2} - \frac{1}{q^*}}$, Remark 4.5.2 points out that there exists $c_3 > 0$ such that $\|\gamma_k\|_{0,r,\Omega} \leq c_3 \|\gamma_k\|_{s,\Omega}$. In conclusion,

$$\nu |\boldsymbol{v}_{h,k}'|_{1,\Omega} \leq c_2 c_3 \|\gamma_k\|_{s,\Omega},$$

proving this estimation. □

Lemma 4.5.4. *There exists $C > 0$ such that*

$$\begin{aligned} \left|(\boldsymbol{v}_{h,1}' - \boldsymbol{v}_1', \boldsymbol{v}_2')_{0,\Omega}\right| &\leq C \|\gamma_1\|_{s,\Omega} \|\gamma_2\|_{s,\Omega} \|h\|_{\infty,\Omega} \\ \left|(\boldsymbol{v}_{h,1}', \boldsymbol{v}_{h,2}' - \boldsymbol{v}_2')_{0,\Omega}\right| &\leq C \|h\|_{\infty,\Omega} \|\gamma_1\|_{s,\Omega} \|\gamma_2\|_{s,\Omega}. \end{aligned}$$

Proof. Using Cauchy-Schwartz and Friedrichs-Poincaré inequalities, there exist $c_1, c_2 > 0$ such that

$$\left|\left(\boldsymbol{v}'_{h,1} - \boldsymbol{v}'_1, \boldsymbol{v}'_2\right)_{0,\Omega}\right| \leq c_1 \left|\boldsymbol{v}'_2\right|_{1,\Omega} \left|\boldsymbol{v}'_{h,1} - \boldsymbol{v}'_1\right|_{1,\Omega} \leq c_2 \left\|\gamma_2\right\|_{s,\Omega} \left|\boldsymbol{v}'_{h,1} - \boldsymbol{v}'_1\right|_{1,\Omega}$$

Using previous lemmas, Friedrichs-Poincaré inequality and Remark 4.5.2, there exist $c_3, c_4, c_5, c_6 > 0$ such that

$$\begin{aligned}
\nu \left|\boldsymbol{v}'_{h,1} - \boldsymbol{v}'_1\right|_{1,\Omega} &\leq c_3 \left(\left\|h\right\|_{\infty,\Omega} \left|\boldsymbol{v}'_{h,1}\right|_{1,\Omega} + \left\|\gamma_1 \left(\boldsymbol{v}_h - \boldsymbol{v}\right)\right\|_{1,\Omega}\right) \\
&\leq c_3 \left(c_4 \left\|h\right\|_{\infty,\Omega} \left\|\gamma_1\right\|_{s,\Omega} + c_5 \left\|\gamma_1\right\|_{0,r,\Omega} \left\|\left(\boldsymbol{v}_h - \boldsymbol{v}\right)\right\|_{1,q^*,\Omega}\right) \\
&\leq c_3 \left(c_4 + c_6\right) \left\|h\right\|_{\infty,\Omega} \left\|\gamma_1\right\|_{s,\Omega},
\end{aligned}$$

concluding that

$$\left|\left(\boldsymbol{v}'_{h,1}, \boldsymbol{v}'_{h,2} - \boldsymbol{v}'_2\right)_{0,\Omega}\right| \leq C \left\|h\right\|_{\infty,\Omega} \left\|\gamma_1\right\|_{s,\Omega} \left\|\gamma_2\right\|_{s,\Omega}.$$

The proof of the second inequality is similar.

□

Lemma 4.5.5. *Let $k, j \in \{1, 2\}$, with $j \neq k$. There exists $C > 0$ such that*

$$\left|\left(\gamma_j \boldsymbol{v}'_{h,k}, \boldsymbol{\varphi}_h - \boldsymbol{\varphi}\right)_{0,\Omega}\right| \leq C \left\|h\right\|_{\infty,\Omega} \left\|\gamma_1\right\|_{s,\Omega} \left\|\gamma_2\right\|_{s,\Omega}.$$

Proof. First, applying Hölder and Friedrichs-Poincaré inequalties, there exist $c_1, c_2 > 0$ such that

$$\begin{aligned}
\left|\left(\gamma_j \boldsymbol{v}'_{h,k}, \boldsymbol{\varphi}_h - \boldsymbol{\varphi}\right)_{0,\Omega}\right| &\leq c_1 \left\|\gamma_j\right\|_{0,r,\Omega} \left\|\boldsymbol{v}'_{h,k}\right\|_{1,q^*,\Omega} \left|\boldsymbol{\varphi}_h - \boldsymbol{\varphi}\right|_{1,\Omega} \\
&\leq c_2 \left\|\gamma_j\right\|_{s,\Omega} \left\|\gamma_k\right\|_{s,\Omega} \left|\boldsymbol{\varphi}_h - \boldsymbol{\varphi}\right|_{1,\Omega},
\end{aligned}$$

where $[\boldsymbol{\varphi}_h - \boldsymbol{\varphi}, \xi_h - \xi]$ verifies

$$\begin{aligned}
-\nu \triangle \left(\boldsymbol{\varphi}_h - \boldsymbol{\varphi}\right) - \left[\nabla \left(\boldsymbol{\varphi}_h - \boldsymbol{\varphi}\right)\right] \boldsymbol{a} + \nabla \left(\xi_h - \xi\right) + \gamma \left(\boldsymbol{\varphi}_h - \boldsymbol{\varphi}\right) &= \boldsymbol{v}_h - \boldsymbol{v} - h\boldsymbol{\varphi}_h \\
\operatorname{div} \left(\boldsymbol{\varphi}_h - \boldsymbol{\varphi}\right) &= 0.
\end{aligned}$$

By repeating the previous procedures, since $\left|\boldsymbol{\varphi}_h\right|_{1,\Omega}$ is uniformly bounded, there exist $c_2, c_3 > 0$ such that

$$\begin{aligned}
\nu \left|\boldsymbol{\varphi}_h - \boldsymbol{\varphi}\right|_{1,\Omega} &\leq c_2 \left(\left\|\boldsymbol{v}_h - \boldsymbol{v}\right\|_{1,q,\Omega} + \left\|h\right\|_{\infty,\Omega} \left|\boldsymbol{\varphi}_h\right|_{1,\Omega}\right) \\
&\leq c_3 \left\|h\right\|_{\infty,\Omega}.
\end{aligned}$$

Thus, there exists $C > 0$ such that $\left|\left(\gamma_j \boldsymbol{v}'_{h,k}, \boldsymbol{\varphi}_h - \boldsymbol{\varphi}\right)_{0,\Omega}\right| \leq C \left\|h\right\|_{\infty,\Omega} \left|\gamma_j\right|_{s,\Omega} \left|\gamma_k\right|_{s,\Omega}$. □

Theorem 4.5.3. *Let $\gamma, \gamma_1, \gamma_2, h \in L^\infty(\Omega)$. There exists $L > 0$ such that*

$$\left|\left(J''(\gamma + h) - J''(\gamma)\right)[\gamma_1, \gamma_2]\right| \leq L \left\|h\right\|_{\infty,\Omega} \left|\gamma_1\right|_{s,\Omega} \left|\gamma_2\right|_{s,\Omega}.$$

Proof. Applying triangular inequality, we obtain

$$\begin{aligned}|\left(J''\left(\gamma+h\right)-J''\left(\gamma\right)\right)\left[\gamma_1,\gamma_2\right]| \leq & \left|\left(\boldsymbol{v}'_{h,1},\boldsymbol{v}'_{h,2}-\boldsymbol{v}'_2\right)_{0,\Omega}\right|+\left|\left(\boldsymbol{v}'_{h,1}-\boldsymbol{v}'_1,\boldsymbol{v}'_2\right)_{0,\Omega}\right| \\ & +\left|\left(\gamma_1\boldsymbol{v}'_{h,2},\boldsymbol{\varphi}_h-\boldsymbol{\varphi}\right)_{0,\Omega}\right|+\left|\left(\gamma_1\left(\boldsymbol{v}'_{h,2}-\boldsymbol{v}'_2\right),\boldsymbol{\varphi}\right)_{0,\Omega}\right| \\ & +\left|\left(\gamma_2\boldsymbol{v}'_{h,1},\boldsymbol{\varphi}_h-\boldsymbol{\varphi}\right)_{0,\Omega}\right|+\left|\left(\gamma_2\left(\boldsymbol{v}'_{h,1}-\boldsymbol{v}'_1\right),\boldsymbol{\varphi}\right)_{0,\Omega}\right|,\end{aligned}$$

where every term were bounded with estimations of the form $C\left\|h\right\|_{\infty,\Omega}\left|\gamma_1\right|_{s,\Omega}\left|\gamma_2\right|_{s,\Omega}$ (see Lemmas 4.5.4 and 4.5.5). In conclusion, there exists $L>0$ such that

$$|\left(J''\left(\gamma+h\right)-J''\left(\gamma\right)\right)\left[\gamma_1,\gamma_2\right]| \leq L\left\|h\right\|_{\infty,\Omega}\left|\gamma_1\right|_{s,\Omega}\left|\gamma_2\right|_{s,\Omega}.$$

□

Corollary 4.5.1. *There exists $L>0$ such that, for every $\theta\in[0,1]$*

$$|\left(J''\left(\theta\gamma^*+\left(1-\theta\right)\gamma\right)-J''\left(\gamma^*\right)\right)\left[\gamma-\gamma^*,\gamma-\gamma^*\right]| \leq L\left\|\gamma-\gamma^*\right\|_{\infty,\Omega}\left|\gamma-\gamma^*\right|_{s,\Omega}^2.$$

Finally, a second order sufficent optimality condition is presented and proved.

Theorem 4.5.4. *Let $s\geq\dfrac{N}{q^*}$ and $\gamma^*\in\mathcal{A}$ such that γ^* verifies the first orden optimality condition. If there exists $\delta>0$ such that*

$$\left(\forall\gamma\in\mathcal{A}\right)\qquad J''\left(\gamma^*\right)\left[\gamma-\gamma^*,\gamma-\gamma^*\right]\geq\delta\left\|\gamma-\gamma^*\right\|_{s,\Omega}^2$$

Then, there exist $\sigma,\varepsilon>0$, independent of γ and γ^*, such that

$$\left(\forall\gamma\in\mathcal{A}\right)\qquad \left\|\gamma-\gamma^*\right\|_{\infty,\Omega}\leq\varepsilon\Rightarrow J\left(\gamma\right)\geq J\left(\gamma^*\right)+\sigma\left\|\gamma-\gamma^*\right\|_{s,\Omega}^2.$$

In consequence, J has a local minimum at γ^*.

Proof. Applying a Taylor expansion, there exists $\theta\in(0,1)$ such that

$$J\left(\gamma\right)=J\left(\gamma^*\right)+J'\left(\gamma^*\right)\left[\gamma-\gamma^*\right]+\frac{1}{2}J''\left(\theta\gamma^*+\left(1-\theta\right)\gamma\right)\left[\gamma-\gamma^*,\gamma-\gamma^*\right].$$

Using Corollary 4.5.1, if $\varepsilon\leq\dfrac{\delta}{2L}$, $\sigma=\dfrac{\delta}{4}$ and $\left\|\gamma-\gamma^*\right\|_{\infty,\Omega}\leq\varepsilon$, then

$$\begin{aligned}J\left(\gamma\right)=&J\left(\gamma^*\right)+J'\left(\gamma^*\right)\left[\gamma-\gamma^*\right]+\frac{1}{2}J''\left(\theta\gamma^*+\left(1-\theta\right)\gamma\right)\left[\gamma-\gamma^*,\gamma-\gamma^*\right] \\ \geq&J\left(\gamma^*\right)+\frac{1}{2}J''\left(\theta\gamma^*+\left(1-\theta\right)\gamma\right)\left[\gamma-\gamma^*,\gamma-\gamma^*\right] \\ \geq&J\left(\gamma^*\right)+\frac{1}{2}\left(J''\left(\theta\gamma^*+\left(1-\theta\right)\gamma\right)-J''\left(\gamma^*\right)\right)\left[\gamma-\gamma^*,\gamma-\gamma^*\right] \\ &+\frac{1}{2}J''\left(\gamma^*\right)\left[\gamma-\gamma^*,\gamma-\gamma^*\right] \\ \geq&J\left(\gamma^*\right)+\frac{\delta}{2}\left\|\gamma-\gamma^*\right\|_{s,\Omega}^2-\frac{L}{2}\left\|\gamma-\gamma^*\right\|_{\infty,\Omega}\left\|\gamma-\gamma^*\right\|_{s,\Omega}^2 \\ \geq&J\left(\gamma^*\right)+\frac{\delta}{2}\left\|\gamma-\gamma^*\right\|_{s,\Omega}^2-\frac{\delta}{4}\left\|\gamma-\gamma^*\right\|_{s,\Omega}^2=J\left(\gamma^*\right)+\sigma\left\|\gamma-\gamma^*\right\|_{s,\Omega}^2,\end{aligned}$$

proving the theorem. □

Remark 4.5.3. *The result obtained in Theorem 4.5.4 is conditioned to* $s \geq \dfrac{N}{q^*}$. *Considering the most pessimistic case, when* $q^* = 2$, *it is possible to establish that the simplest spaces for* γ^*, *where Theorem 4.5.4 is valid, are* $H^1(\Omega)$ *and* $H^2(\Omega)$ *when* $N = 2$ *and* $N = 3$, *respectively.*

4.6 Numerical results

In this section, the previous analysis is complemented by numerical experiments for the new parameter identification problem. Realistic synthetic cases are analyzed in 2D, which represent a longitudinal section of the structure of a cardiac valve in an arbitrary position. However, the numerical results presented below were obtained using the Navier-Stokes equation. So, the numerical problem to be solved is given by

$$\text{minimize} \quad J(\gamma, \boldsymbol{u}) = \frac{1}{2}\|\boldsymbol{u} - \boldsymbol{u}_R\|^2_{0,\omega} + \frac{\alpha}{2}\|\gamma\|^2_{1,\Omega} \tag{4.8}$$

$$\begin{aligned} \text{subject to} \quad -\nu\triangle\boldsymbol{u} + (\nabla\boldsymbol{u})\,\boldsymbol{u} + \nabla p + \gamma\boldsymbol{u} &= \boldsymbol{0} \quad \text{in } \Omega \\ \operatorname{div}\boldsymbol{u} &= 0 \quad \text{in } \Omega \\ \boldsymbol{u} &= \boldsymbol{u}_D \quad \text{on } \Gamma_D \\ -\nu\frac{\partial\boldsymbol{u}}{\partial\boldsymbol{n}} + p\boldsymbol{n} &= \boldsymbol{0} \quad \text{on } \Gamma_N \\ \boldsymbol{u} \in \boldsymbol{H}^1(\Omega),\ \gamma \in H^1(\Omega) & \\ 0 \leq \gamma \leq M \text{ a.e. in } \Omega & \end{aligned} \tag{4.9}$$

This special formulation of (4.9) is similar to (4.2) in terms of the resistance term. In the following subsections, the configurations of the reference case is explained, as well as the numerical solutions of the inverse problems associated with MRI images or Doppler ultrasound. Due to our lack of real images, our experiments are fully synthetic.

4.6.1 Reference test

First, a reference geometry is defined. This geometry Ω represents the area around the aortic valve. The inflow Γ_I has a parabolic profile following Poiseuille's Law given by

$$\boldsymbol{u}_D(x, y) = -Ux(d - x)\,\boldsymbol{n},$$

where $\boldsymbol{x} = (x, y)$ are the cartesian coordinates of the domain, $\boldsymbol{n}$ is the outer normal vector and d is the diameter of the inflow, while do-nothing conditions are imposed on the outflow Γ_O given by

$$-\nu\frac{\partial\boldsymbol{u}}{\partial\boldsymbol{n}} + p\boldsymbol{n} = \boldsymbol{0}.$$

In the walls of the structure, represented by Γ_W, the fluid has no-slip conditions given by $\boldsymbol{u} = \boldsymbol{0}$.

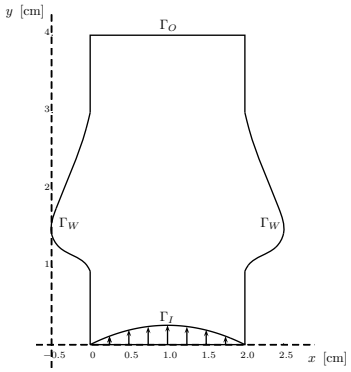

Figure 4.1: Domain for the numerical tests.

The valves are modeled on the resistance term $\gamma \boldsymbol{u}$ using the function γ. This function assumes a constant value $M \gg 1$ in the regions where the valve is and assumes the value 0 where the valve is not. In order to define γ, a parabolic figure is drawn on each side Ω with an approximate thickness of 1 mm. When the valves are fully closed, they are symmetrical with respect to the vertical axis of symmetry. When the valves are open, these parabolas are rotated with respect to a reference system whose origin is at the point where the valve coincides with the walls of the structure given by Γ_W. Since blood flow is modeled, the kinematic viscosity is considered equal to $\nu = 0.035\,\mathrm{cm}^2\,/\,\mathrm{s}$, the density is assumed as $\rho = 1\,\mathrm{g}\,/\,\mathrm{cm}^3$, and the dimensions $d = 2\,\mathrm{cm}$ and $U = 30\,\mathrm{cm}\,/\,\mathrm{s}$, resulting in a peak Reynolds number on the inlet of

$$\mathrm{Re} = \frac{Ud}{\nu} = 1714.$$

The Navier-Stokes equations are discretized using the finite element method (FEM) with Taylor-Hood elements ($\mathbb{P}_2$ for the velocity $\boldsymbol{u}$ and $\mathbb{P}_1$ for the pressure) on an unstructured triangular mesh. The mesh used was generated by domain triangulation with $h = 0.05\,\mathrm{cm}$, which corresponds to 9950 elements and 4976 nodes. The solver is implemented using the finite element library FEniCS [5] with the default configuration. To solve the nonlinear problems, a Newton's method was used. The resistance γ is defined as a discontinuous function with discrete values in each element, assuming the value of $M = 10^8$ if the element intersects the valve or, otherwise, assumes the value 0. We define the set $\mathcal{O}$, that represents the valve inside of Ω, by

$$\mathcal{O} = \left\{ \boldsymbol{x} \in \Omega \mid \gamma(\boldsymbol{x}) = 10^8 \right\}.$$

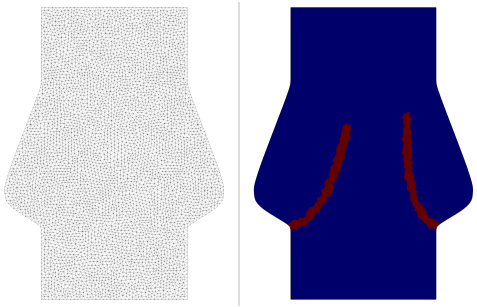

Figure 4.2: Plots of unstructured mesh (left) and γ (right).

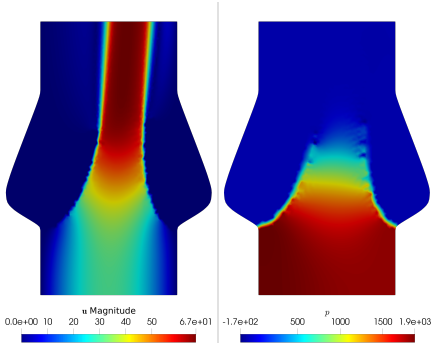

Figure 4.3: Reference solutions $\boldsymbol{u}$ and p.

4.6.2 Numerical solution of the inverse problem

Using the solution of the reference test as reference solution $\boldsymbol{u}_R$, the following version of the model problem is solved numerically using FEniCS and dolfin-adjoint

$$\text{minimize} \quad J(\gamma, \boldsymbol{u}) = \frac{1}{2}\|\boldsymbol{u} - \boldsymbol{u}_R\|^2_{0,\omega} + \frac{\alpha}{2}\|\gamma\|^2_{0,\Omega} + \frac{\beta}{2}|\gamma|^2_{1,\Omega} \tag{4.10}$$

$$\begin{aligned} \text{subject to} \quad -\nu\triangle\boldsymbol{u} + (\nabla\boldsymbol{u})\,\boldsymbol{u} + \nabla p + \gamma\boldsymbol{u} &= \boldsymbol{0} && \text{in } \Omega \\ \operatorname{div}\boldsymbol{u} &= 0 && \text{in } \Omega \\ \boldsymbol{u} &= \boldsymbol{u}_D && \text{on } \Gamma_I \\ \boldsymbol{u} &= \boldsymbol{0} && \text{on } \Gamma_W \\ -\nu\frac{\partial\boldsymbol{u}}{\partial\boldsymbol{n}} + p\boldsymbol{n} &= \boldsymbol{0} && \text{on } \Gamma_N \\ \boldsymbol{u} \in \boldsymbol{H}^1(\Omega),\ \gamma \in H^1(\Omega) & \\ 0 \le \gamma \le C \text{ a.e. in } \Omega. & \end{aligned} \tag{4.11}$$

For this example, we considered a measurement area $\omega = \Omega$ and the values $C = 10^3$, $\alpha = 10^{-4}$ and $\beta = 10^{-8}$. The use of two different weights for the norm and seminorm is consistent with the theoretical analysis of the previous sections, so this problem has a solution. The dolfin-adjoint library [71] allows to implement automatic derivation of the discrete adjoint equations for pde models and implement minimization algorithms from the Python 3 libraries. In particular, the L-BFGS-B algorithm (see Section 4.3 in [39]) was used with the following stopping criteria on the step k

$$\frac{|J(\gamma_k) - J(\gamma_{k+1})|}{\max\{|J(\gamma_k)|, |J(\gamma_{k+1})|, 1\}} \le 10^{-6} \qquad \text{or} \qquad \max_{j\in\{1,\dots,n\}}\left\{\left|(\nabla J_k)_j\right|\right\} \le 10^{-6}$$

where $(\nabla J_k)_j$ is the $j-$th component of the projected gradient on the step k. To start the algorithm, $\gamma_0 = 0$ was used as the initial solution.

As a way to define a valve reconstruction algorithm sketch, we follow these steps.

1. We defined an axis that crosses the domain from the inflow to the outflow.
2. For a uniform discretization of the axis, we defined perpendicular lines.

3. The solution γ^* obtained by the algorithm is interpolated on each of the lines. Three points are selected on each side of the axis. The first and second point are the limits of an interval where $\nabla\gamma^* \cdot \boldsymbol{n}$ has the maximim positive values with 1% of tolerance. The third point is the local maximum closest to the interval.
4. An average is obtained between the three points.
5. A polyline is drawn on each side of the axis. Each polyline passes through all the average points.

Numerical results are presented in Figure 4.4. The polyline is drawn in white, which presents a great approximation to the interface between the different values of the reference given by γ.

The optimal γ^* has values close to 0 in the areas before and after the valves. On the other hand, in the interior area where there are no valves, the optimal solution takes values close to 0. Likewise, the magnitude and direction of $\boldsymbol{u}^*$ is similar to $\boldsymbol{u_R}$, where $\boldsymbol{u}^*$ corresponds to the optimal state.

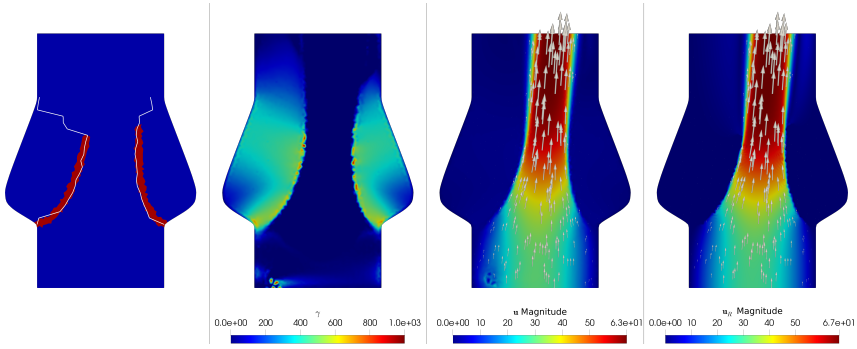

Figure 4.4: Real γ and reconstructed valve, optimal γ, optimal $\boldsymbol{u}$, and reference solution $\boldsymbol{u}_R$ (from left to right). Reference test, 148 iterations.

It is necessary to corroborate that this algorithm is able to solve the inverse problem measuring only a part of $\boldsymbol{u}_R$ given by the reference velocity. In this case, choosing ω as the area where the valves should be (see Figure 4.5 right), given by

$$\omega = \Omega \cap \left\{(x, y) \in \mathbb{R}^2 \mid 1 \leq y \leq 3\right\},$$

the expected result should be similar to that found above.

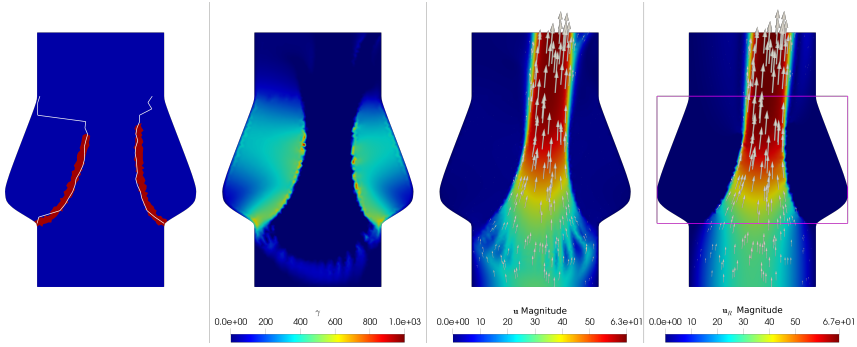

Figure 4.5: Real γ and reconstructed valve, optimal γ, optimal $\boldsymbol{u}$, and reference solution $\boldsymbol{u}_R$ (from left to right). Reference test with subdomain, 240 iterations.

Figure 4.5 presents the numerical results, the polyline and the references. In the case of the reference solution $\boldsymbol{u}_R$, a pink rectangle was drawn that allows delimiting the measurement area ω. In particular, this problem required more iterations than the case with measurements on Ω, obtaining very similar results.

4.6.3 Measurements of MRI type

Using the reference solutions, it is possible to generate synthetic measurements that represent the behavior of MRI velocity type measurements. A 2D plane is chosen on which the velocity is measured in one specified direction $\boldsymbol{d} \in \mathbb{R}^2$, with $|\boldsymbol{d}| = 1$. Then, the measurement is given by

$$u_R = \boldsymbol{u}_R \cdot \boldsymbol{d}.$$

The MRI type velocity measurement data is represented in a mesh of uniform quadrilaterals of $2\,\text{mm} \times 2\,\text{mm}$. They are obtained by projecting u_R to the $\mathbb{Q}_0$ finite element space, given by piecewise constant discontinuous functions on the quadrilateral mesh. In practical applications, the input speed is unknown and must be estimated. Then, a direction $\boldsymbol{d}$ for this MRI can be chosen as that which is an inner normal to Γ_I. To determine U, the projection of u_R in $L_2(\Gamma_I)$ with respect to $Ux(2-x)$ is calculated by

$$U = \frac{\int_{\Gamma_I} u_R \left[x\,(2-x)\right]\, dS}{\int_{\Gamma_I} \left[x\,(2-x)\right]^2\, dS}.$$

Thus, U approaches in a least squares sense. Figure 4.6 shows the synthetic MRI generated from the reference solution.

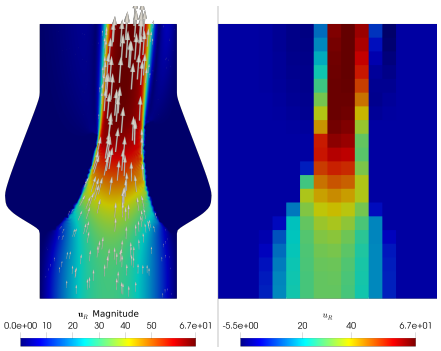

Figure 4.6: Reference $\boldsymbol{u}_R$ (left) and synthetic MRI type velocity measurement (u_R, right).

The new problem to solve is given by

$$\text{minimize} \quad J(\gamma, \boldsymbol{u}) = \frac{1}{2}\|(\boldsymbol{u}-\boldsymbol{u}_R)\cdot\boldsymbol{d}\|^2_{0,\Omega} + \frac{\alpha}{2}\|\gamma\|^2_{0,\Omega} + \frac{\beta}{2}|\gamma|^2_{1,\Omega} \tag{4.12}$$

$$\begin{aligned}
\text{subject to} \quad -\nu\triangle\boldsymbol{u} + (\nabla\boldsymbol{u})\,\boldsymbol{u} + \nabla p + \gamma\boldsymbol{u} &= \boldsymbol{0} && \text{in } \Omega \qquad (4.13)\\
\operatorname{div}\boldsymbol{u} &= 0 && \text{in } \Omega\\
\boldsymbol{u} &= \boldsymbol{u}_D && \text{on } \Gamma_I\\
\boldsymbol{u} &= \boldsymbol{0} && \text{on } \Gamma_W\\
-\nu\frac{\partial\boldsymbol{u}}{\partial\boldsymbol{n}} + p\boldsymbol{n} &= \boldsymbol{0} && \text{on } \Gamma_N\\
\boldsymbol{u} \in \boldsymbol{H}^1(\Omega)\,,\ \gamma \in H^1(\Omega)&\\
0 \le \gamma \le C \text{ a.e. in } \Omega.&
\end{aligned}$$

where the values $C = 10^3$, $\alpha = 10^{-4}$ and $\beta = 10^{-8}$ were used. It is possible to prove the existence of solution of this problem in the same way as in the proof of the theorem. Figure 4.7 shows the numerical results and the references. The parameter γ has some jumps that coincide with the vertical lines between the MRI voxels, while the polyline tends to have segments parallel to those vertical lines, but it acceptably approximates the space between the valves.

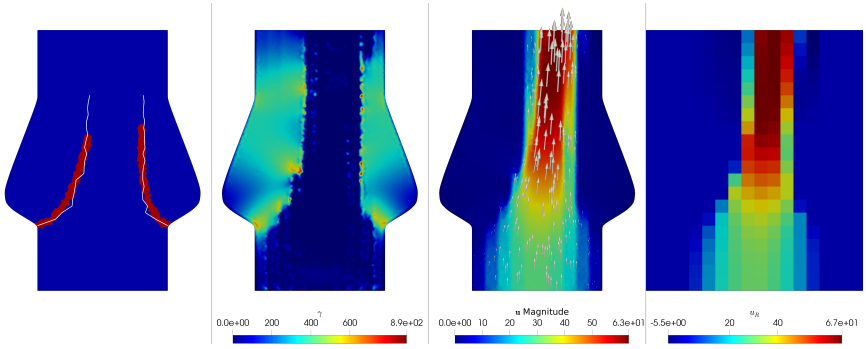

Figure 4.7: Real γ and reconstructed valve, optimal γ, optimal $\boldsymbol{u}$, and synthetic MRI (from left to right). MRI noiseless.

The white noise intensity in the velocity measurements from MRI is proportional to the velocity encoding parameter (also called VENC [40]) of the scan. This parameter is

configured with a value greater than the maximum expected velocity, in order to eliminate signal aliasing. Then, the noise in all voxels is proportional to the maximum velocity in the measurement area. In the clinical practice it can be expected that high-quality MRI contains a velocity noise of 10% of the maximum velocity in each voxel [40]. Gaussian noises were added to this MRI with a standard deviation of 5%, 10% and 20% of the maximum value of u_R.

Figure 4.8 shows the results of this experiment with a 5% of Guassian noise, but changing the weights to $\alpha = 10^{-4}$ and $\beta = 10^{-6}$ in terms to decrease the effects of noise. The results are similar to the experiment without noise in terms to the tendency of the polyline to approximate the valve shape and draw lines parallel to the voxels.

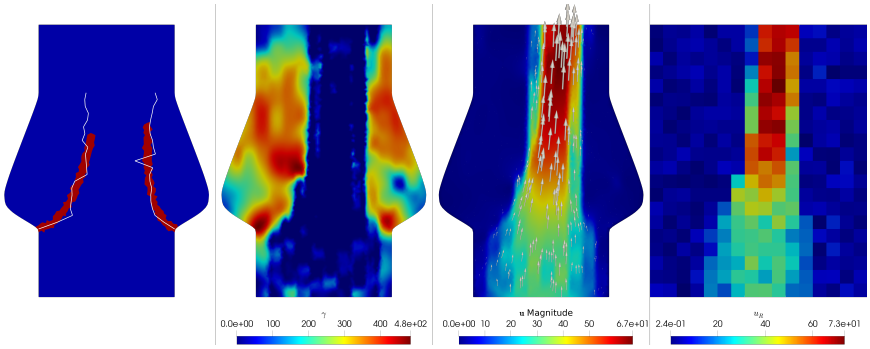

Figure 4.8: Real γ and reconstructed valve, optimal γ, optimal $\boldsymbol{u}$, and synthetic MRI (from left to right). MRI with 5% of noise.

This approximation seems weaker as noise increases, in the sense that the polyline has a lower quality in its approximation and that the gamma function tends to overfit the data. The following two figures show the result of the experiment with 10% and 20% of Gaussian noise, respectively. The noise is exactly the same than the 5% Gaussian noise case, but increasing the level noise.

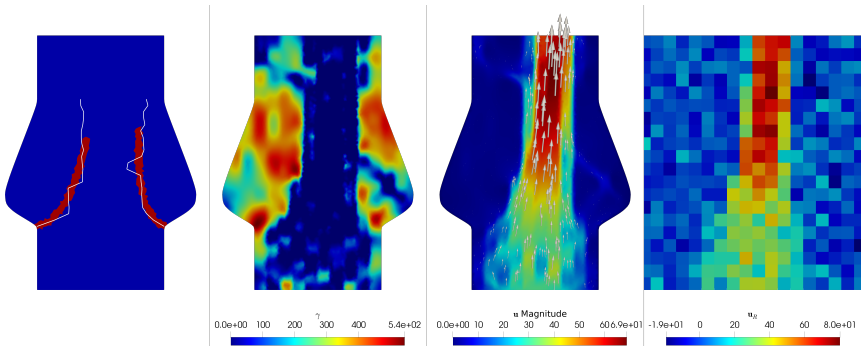

Figure 4.9: Real γ and reconstructed valve, optimal γ, optimal $\boldsymbol{u}$, and synthetic MRI (from left to right). MRI with 10% of noise.

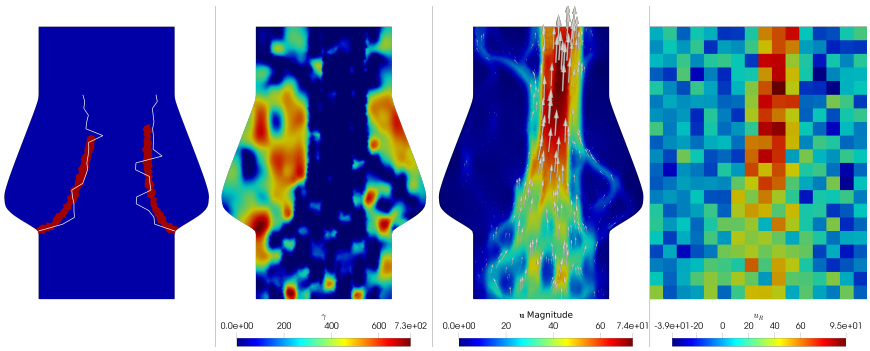

Figure 4.10: Real γ and reconstructed valve, optimal γ, optimal $\boldsymbol{u}$, and synthetic MRI (from left to right). MRI with 20% of noise.

Table 4.1 shows the mean square error (MSE) between the reconstructed valve given by the polylines obtained using MRI in Figures 4.7, 4.8, 4.9 and 4.10, and the polyline obtained in the reference test (see Figure 4.4). To quantify this error, we consider only the points of the polyline in Figure 4.4 that are at a distance less than or equal to 0.5 mm from $\mathcal{O}$. There are minor differences between the valve reconstructions for the cases with a noise level of 5% and 10%. However, the quality of the reconstruction decreases when the level noise increases up to 20%.

Noise level	MSE
0%	$4.4680 \cdot 10^{-3}$
5%	$8.6308 \cdot 10^{-3}$
10%	$8.1992 \cdot 10^{-3}$
20%	$1.5016 \cdot 10^{-2}$

Table 4.1: MSE of reconstructed valves using MRI with different noise levels.

Figure 4.11 shows the reconstructed polyline for three experiments with independent noises at same level of noise. Each polyline color represents the final result of this experiment with a Gaussian noise independent of the others, whose amplitude was adjusted for the noise level of 5%, 10% and 20%. We can see that the rebuilt valves are more irregular as the noise level increases, especially for 20% of level noise, which is consistent with Table 4.1.

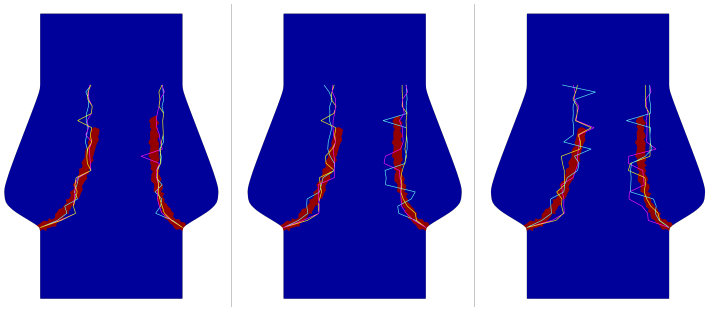

Figure 4.11: Comparison of reconstructed valves with three different noises, with 5%, 10% and 20% of noise (from left to right).

4.6.4 Measurements of ultrasound imaging type

It is possible to generate synthetic measurements similar to ultrasound images. From a given focal point, directional velocities are measured at each point in a domain with the form of a circular sector with center in the focal point. The chosen directions $\boldsymbol{d}(\boldsymbol{x})$ are given by unit vectors parallel to the vector that joins the measurement point with the focal point. Then, the measurement is given by

$$u_R = \boldsymbol{u}_R \cdot \boldsymbol{d}(x)$$

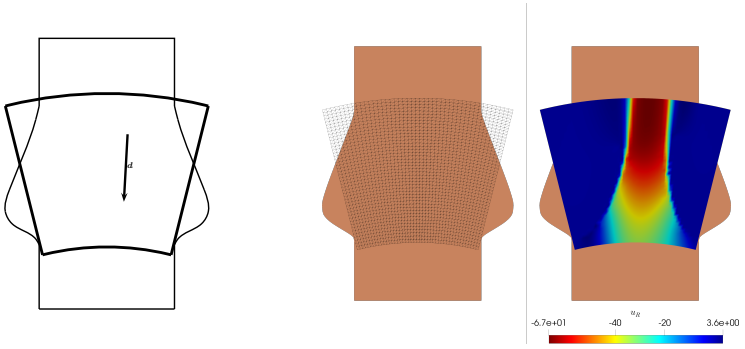

Figure 4.12: Ultrasound imaging domain, mesh and synthetic ultrasound imaging.

The measurement data is represented in a structured triangular mesh of 2116 nodes and 4050 triangles with $h = 0.067\,\text{cm}$ (see Figure 4.12). The measurements are obtained by interpolation of u_R to the $\mathbb{P}_1$ finite element space defined on the structured mesh. Again, the input speed is unknown and must be estimated from a preliminary measurement. To determine U, the projection of u_R in $L_2(\Gamma_I)$ with respect to $Ux(2-x)[\boldsymbol{n}\cdot\boldsymbol{d}(x)]$ is calculated by

$$U = \frac{\int_{\Gamma_I} u_R\left[x\left(2-x\right)\right]\left[\boldsymbol{n}\cdot\boldsymbol{d}\left(\boldsymbol{x}\right)\right]\ dS}{\int_{\Gamma_I}\left[x\left(2-x\right)\right]^2\left[\boldsymbol{n}\cdot\boldsymbol{d}\left(\boldsymbol{x}\right)\right]^2\ dS}$$

The new problem to solve is given by

$$\text{minimize} \quad J(\gamma,\boldsymbol{u}) = \frac{1}{2}\left\|(\boldsymbol{u}-\boldsymbol{u}_R)\cdot\boldsymbol{d}(\boldsymbol{x})\right\|^2_{0,\omega} + \frac{\alpha}{2}\left\|\gamma\right\|^2_{0,\Omega} + \frac{\beta}{2}\left|\gamma\right|^2_{1,\Omega} \tag{4.14}$$

$$\text{subject to} \quad -\nu\triangle\boldsymbol{u} + (\nabla\boldsymbol{u})\,\boldsymbol{u} + \nabla p + \gamma\boldsymbol{u} = \boldsymbol{0} \quad \text{in } \Omega \tag{4.15}$$

$$\operatorname{div}\boldsymbol{u} = 0 \quad \text{in } \Omega$$

$$\boldsymbol{u} = \boldsymbol{u}_D \quad \text{on } \Gamma_I$$

$$\boldsymbol{u} = \boldsymbol{0} \quad \text{on } \Gamma_W$$

$$-\nu\frac{\partial\boldsymbol{u}}{\partial\boldsymbol{n}} + p\boldsymbol{n} = \boldsymbol{0} \quad \text{on } \Gamma_N$$

$$\boldsymbol{u}\in\boldsymbol{H}^1(\Omega),\ \gamma\in H^1(\Omega)$$

$$0\le\gamma\le C \text{ a.e. in } \Omega$$

where ω is the subdomain on Ω covered by the ultrasound imaging and the values $C = 10^3$, $\alpha = 10^{-4}$ and $\beta = 10^{-8}$ were used. This problem has solution, and the proof of the

existence of solution is similar to the proof of the Theorem 4.3.1. Figure 4.13 presents the numerical results, the polyline and the references. The results obtained are very similar to those obtained in the reference tests with measurements in the entire domain and in a subdomain.

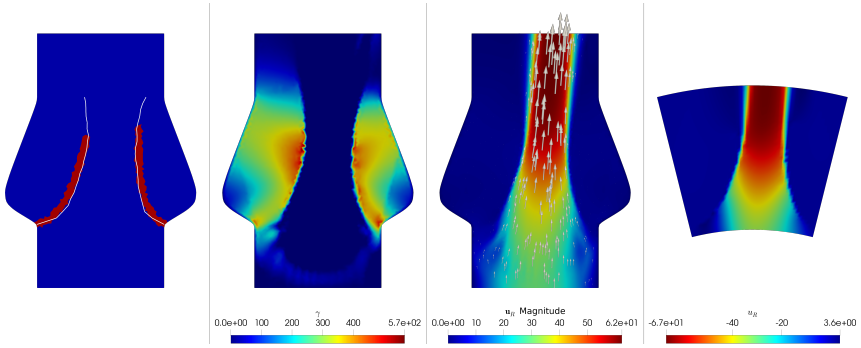

Figure 4.13: Real γ and reconstructed valve, optimal γ, optimal $\boldsymbol{u}$, and synthetic ultrasound imaging(from left to right).

There are multiple sources of noise in ultrasound images, such as reverberation, ghosting, or fake echo, among others. Therefore, it is not possible to define a simplified structure of noise in this type of images [21, 67]. In order to study the effect of the noise, we assume an additive Gaussian noise that is proportional to the maximum of $|u_R|$ in the measurement area. From [66], an experiment with a straight-vessel phantom had a 9.6% of standard deviation. Then, is acceptable to simulate an ultrasound imaging with a velocity noise of 10% of the maximum velocity in each node. Gaussian noises were added to this ultrasound imaging with a standard deviation of 10% and 20% of the maximum of $|u_R|$.

Figures 4.14 and 4.15 show the results of this experiment with a 10% and 20% of Guassian noise, respectively, but changing the weights to $\alpha = 10^{-4}$ and $\beta = 10^{-6}$ in terms to decrease the effects of noise. The results are similar to the experiment without noise in terms to the tendency of the polyline to approximate the valve shape.

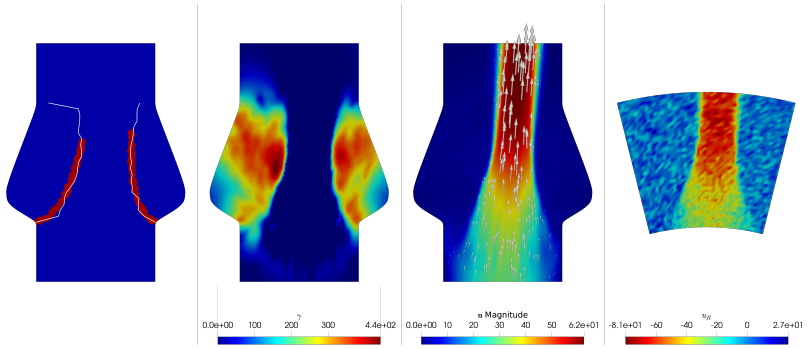

Figure 4.14: Real γ and reconstructed valve, optimal γ, optimal $\boldsymbol{u}$, and synthetic ultrasound imaging(from left to right) with 10% of noise.

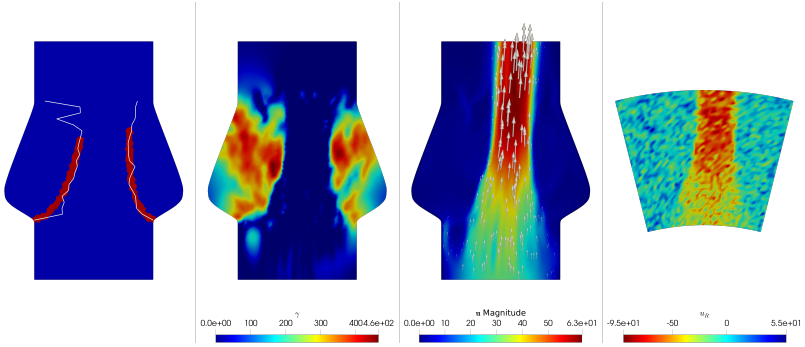

Figure 4.15: Real γ and reconstructed valve, optimal γ, optimal $\boldsymbol{u}$, and synthetic ultrasound imaging(from left to right) with 20% of noise.

Table 4.2 shows the mean square error (MSE) between the reconstructed valve given by the polylines obtained using MRI in Figures 4.13, 4.14 and 4.15, and the polyline obtained in the reference test with measurement in a subdomain (see Figure 4.5). The MSE was quantified by the same way as in Table 4.1. There are minor differences between the valve reconstructions for the cases with a noise level of 10% and 20%.

Noise level	MSE
0%	$3.0985 \cdot 10^{-3}$
10%	$8.1993 \cdot 10^{-3}$
20%	$8.6772 \cdot 10^{-3}$

Table 4.2: MSE of reconstructed valves using ultrasound imaging with different noise levels.

4.7 Conclusions

We have presented a new parameter identification problem for the Oseen equation, contributing to the detection of obstacles in fluid dynamic studies. For this problem, the existence of solution and optimality conditions were determined. The study of optimality conditions is necessary to validate the use of optimization algorithms. In particular, the second order optimality condition allowed to specify the H^s space where the parameter γ belongs.

The numerical experiments developed in this work allow us to conjecture that it would be possible to extend this analysis for the Navier-Stokes equation. Indeed, the numerical tests without noise had satisfactory results in terms of rebuilding the simulated valve. Furthermore, experiments with Gaussian noise show that disturbances in the reference image are reflected in bounded changes in the parameter and in the reconstructed valve. The quality of the solutions is worse as noise increases, as expected.

There are several ways to deepen this work. From an analytical perspective, it is necessary to repeat the theoretical analysis for Problem (4.9), in the same way as we worked with Problem (4.1), looking for obtaining similar results. Based on the favorable numerical results, the next step is to perform experiments with 3D domains, including structures and real images (both MRI and ultrasound imaging), whether obtained from phantoms or real patients. The 3D case is of medical interest, since it will contribute to simplify the detection of defects in

the function of aortic valves, among other structures. Therefore, designing an algorithm to recreate the aortic valve in 3D is also one of the future improvements.

Chapter 5

A distributed resistance inverse method for flow obstacle identification from internal velocity measurements: the Navier-Stokes problem

In this chapter we present a parameter identification problem for a scalar permeability parameter and the maximum velocity in an inflow, following a reference profile. We consider a modified version of the Navier-Stokes equations from global or local velocity measurements, where we add a permeability term given by the Brinkman's law to the momentum equation such that some subset of its boundary support represents obstacles. For the outflow, we consider a directional do-nothing condition as a backflow stabilization. From a reference velocity that could have some noise or be obtained in low resolution, we define a suitable quadratic cost functional with some stabilization terms. Existence of minimizers and first and second order optimality conditions are derived through the differentiability of the solutions of the Navier-Stokes equations with respect to the permeability and maximum velocity in the inflow. Finally, we present some synthetic numerical test based of recovering a 2D and 3D slope of a cardiac valve from total and local velocity measurements, inspired from 2D and 3D MRI type data.

5.1 Introduction

One of the most important challenges for Cardiology is to design safe ways to diagnose heart valve diseases. On the one hand, the valves are thin structures, the main non-invasive radiological examinations do not allow to obtain clear images of the valves when they are open. On the other hand, invasive procedures are only performed in the case of valve replacement surgery, requiring catheterization from the esophagus and compromising the integrity of the patient.

Previously, we proposed in [3] a technique that allows to recover obstacles and domain deformations by means of a virtual domain and a permeability parameter that follows Brinkham's law [24, 13] for the Oseen equations . In [4], we showed that there is an asymptotic relationship between the solutions of the Navier-Stokes equations with domains that consider

obstacles and virtual domains where the obstacles are replaced by a permeability parameter. The novelty of this new work is the theoretical development of the problem considering the Navier-Stokes equations, presenting techniques that relax the regularity assumptions, the inclusion of the directional do-nothing condition (see [22]) as a new boundary condition on the outflow and the maximum speed on the inflow, assuming a profile that complies with Poiseuille's Law (see [74]), as a new constant parameter to be determined.

The paper is structured as follows. In Section 2, a parameter identification problem is defined for the Navier-Stokes equations with a permeability term given by the Brinkman's law with the form $\gamma \boldsymbol{u}$, where $\boldsymbol{u}$ is the velocity field and $\gamma \geq 0$ is a function that takes large values in zones where is the obstacle should be located. In Section 3, we present some results of existence of solution for our direct problem and our minimization problem, considering the inclusion of the directional do-nothing condition (DDN). In Sections 4 and 5, we establish the first and second order optimality conditions for our suitable cost functional improving the proof techniques presented in [3]. Section 6 presents numerical tests that consist of recovering the shape of a heart valve from global or partial measurements of the velocity of the blood passing through the valves. For the 2D experiments, we emulate a cardiac valve and we recover its shape via estimating the permeability parameter from perturbed measurements as in [3]. The 3D examples are based on a tricuspid aortic valve. In both cases, 2D and 3D, we use total or partial velocity from a numerical reference test and we use that velocity to generate a synthetic 2D or 3D MRI. Finally, conclusions and future work are presented in Section 7.

5.2 Model problem

Consider a non-empty bounded domain $\Omega \subseteq \mathbb{R}^N$, $N \in \{2, 3\}$. The Lebesgue measure of Ω is denoted by $|\Omega|$, which extends to lesser dimension spaces. The norm and seminorms for Sobolev spaces $W^{m,p}(\Omega)$ is denoted by $\|\cdot\|_{m,p,\Omega}$ and $|\cdot|_{m,p,\Omega}$, respectively. For $p = 2$, the norm, seminorms and inner product of the space $W^{m,2}(\Omega) = H^m(\Omega)$ are denoted by $\|\cdot\|_{m,\Omega}$, $|\cdot|_{m,\Omega}$ and $(\cdot,\cdot)_{m,\Omega}$, respectively. Also, $\|\cdot\|_{\infty,\Omega}$ denotes the norm of $L^\infty(\Omega)$. The spaces $\boldsymbol{H}^m(\Omega)$ and $\boldsymbol{W}^{m,p}(\Omega)$ are defined by $\boldsymbol{H}^m(\Omega) = [H^m(\Omega)]^N$ and $\boldsymbol{W}^{m,p}(\Omega) = [W^{m,p}(\Omega)]^N$. The notation for norms, seminorms and inner products will be extended from $W^{m,p}(\Omega)$ or $H^m(\Omega)$.

Consider $\alpha_0 > 0$, $\alpha_1 > 0$, $\nu > 0$, $s \geq 0$, $M_1 > 0$, $M_2 > 0$, Ω with a Lipschitz boundary $\partial\Omega = \Gamma_D \cup \Gamma_N$ such that $\operatorname{int}(\Gamma_D) \cap \operatorname{int}(\Gamma_N) = \emptyset$, an open subset $\omega \subseteq \Omega$, $\boldsymbol{u}_R \in \boldsymbol{H}^{1/2}(\Gamma_D)$ and $\boldsymbol{n}$ the outer normal vector on $\partial\Omega$. The model problem is defined by

$$\text{minimize} \quad J(\gamma, \beta, \boldsymbol{u}) = \frac{1}{2}\|\boldsymbol{u} - \boldsymbol{u}_R\|_{0,\omega}^2 + \frac{\alpha}{2}\|\gamma\|_{s,\Omega}^2 \tag{5.1}$$

$$\begin{aligned} \text{subject to} \quad -\nu\triangle\boldsymbol{u} + (\nabla\boldsymbol{u})\,\boldsymbol{u} + \nabla p + \gamma\boldsymbol{u} &= \boldsymbol{0} && \text{in } \Omega \\ \operatorname{div}\boldsymbol{u} &= 0 && \text{in } \Omega \\ \boldsymbol{u} &= \beta\boldsymbol{u}_D && \text{on } \Gamma_D \\ -\nu\frac{\partial\boldsymbol{u}}{\partial\boldsymbol{n}} + p\boldsymbol{n} + \frac{1}{2}(\boldsymbol{u}\cdot\boldsymbol{n})_-\,\boldsymbol{u} &= \boldsymbol{0} && \text{on } \Gamma_N \end{aligned} \tag{5.2}$$

$$\boldsymbol{u} \in \boldsymbol{H}^1(\Omega),\ \gamma \in H^s(\Omega),\ \beta \in \mathbb{R},$$
$$0 \leq \beta \leq M_1,\ 0 \leq \gamma \leq M_2 \text{ a.e. in } \Omega.$$

where $(x)_- = \min\{x, 0\}$. The modified version of Navier-Stokes given by Equation (5.2) models the velocity $\boldsymbol{u}$ and pressure p of a fluid that passes through the control volume Ω. The term $\gamma\boldsymbol{u}$, with $\gamma \geq 0$, represents the distributed resistance that Ω imposes to the fluid. A zero value of γ represents that the fluid follows the Navier-Stokes equations. As the γ values increases in a certain area, the magnitude of $\boldsymbol{u}$ tends to decrease to 0. According to Brinkman's law [24, 13], $1/\gamma$ is an indicator of permeability. The media is completely permeable when $\gamma = 0$, while γ tends to $+\infty$ in zones where there are obstacles. Bounded values of γ model porous media, where porosity decreases as γ increases. In comparison with the traditional "do nothing" condition given by $-\nu\dfrac{\partial \boldsymbol{u}}{\partial \boldsymbol{n}} + p\boldsymbol{n}$, the "directional do nothing" condition imposed on Γ_N adds a correction term for backflow (see [22])

5.3 Existence of solution

In what follows, we suppose that $\boldsymbol{u}_D$ verifies the hypotheses of Theorem 1.2.3. Thus, (5.2) has a unique solution. For this hypothesis to be valid, M_1 is required to be small enough in order to verify the sufficient conditions of existence and uniqueness of solution given by $2M_1\kappa \|\boldsymbol{u}_D\|_{1/2,\Omega} \leq \nu$ and $\dfrac{3\kappa C_1}{2\nu^2}\left(\|\boldsymbol{g}\|_{1,\Omega} + \|\boldsymbol{g}\|_{1,\Omega}^2\right) < 1$. First of all, we need to define some new notations.

Definition 5.3.1. *The subsets $\Gamma_N^+ \subseteq \Gamma_N$ and $\Gamma_N^- \subseteq \Gamma_N$ are defined by*

$$\Gamma_N^+ = \{x \in \Gamma_N \mid \boldsymbol{u}\cdot\boldsymbol{n} > 0\} \quad \Gamma_N^- = \{x \in \Gamma_N \mid \boldsymbol{u}\cdot\boldsymbol{n} < 0\}$$

Definition 5.3.2. *Let $s \geq 0$. The set of admissible parameter functions is defined by*

$$\mathcal{A} = \{(\gamma, \beta) \in H^s(\Omega) \times \mathbb{R} \mid 0 \leq \beta \leq M_1 \text{ and } 0 \leq \gamma \leq M_2 \text{ a.e.}\}.$$

Definition 5.3.3. *The map $A : \mathcal{A} \to \boldsymbol{H}^1(\Omega) \times L_0^2(\Omega)$ is defined by $A(\gamma,\beta) = [A_1(\gamma,\beta), A_2(\gamma,\beta)] = [\boldsymbol{u}, p]$, where $\boldsymbol{u} \in \boldsymbol{H}^1(\Omega)$ and $p \in L_0^2(\Omega)$ are the unique variational solutions of the Problem (5.2).*

Remark 5.3.1. *The uniformly boundedness of $\boldsymbol{u}$ and p are obtained since $0 \leq \beta \leq M_1$ and $\|\gamma\|_{\infty,\Omega} \leq M_2$ for all $(\gamma,\beta) \in \mathcal{A}$.*

Now we can state the result of existence of solution.

Theorem 5.3.1. *Problem (4.3) has at least one solution $\gamma^* \in \mathcal{A}$ with optimal states $A(\gamma^*,\beta^*) = [\boldsymbol{u}^*, p^*]$, i.e.*

$$(\forall \gamma \in \mathcal{A}) \quad J(\gamma, \beta, A_1(\gamma,\beta)) \geq J(\gamma^*, \beta^*, \boldsymbol{u}^*).$$

Proof. First, $J(\gamma, \beta, A_1(\gamma,\beta))$ is bounded below by 0 and

$$(\forall (\gamma,\beta) \in \mathcal{A}) \quad J(\gamma, \beta, A_1(\gamma,\beta)) \geq \frac{\alpha}{2}\|\gamma\|_{s,\Omega}^2.$$

Thus, $m = \inf_{\gamma \in \mathcal{A}} J(\gamma)$ is well defined. Let $\{(\gamma_n, \beta_n)\}_{n\in\mathbb{N}} \subseteq \mathcal{A}$ and $\{[\boldsymbol{u}_n, p_n]\}_{n\in\mathbb{N}} \subseteq \boldsymbol{H}^1_{\Gamma_D}(\Omega) \times L^2_0(\Omega)$ such that $A(\gamma_n, \beta_n) = [\boldsymbol{u}_n, p_n]$, $\{J(\gamma_n, \beta_n)\}$ is decreasing and $J(\gamma_n, \beta_n) \to m$. It is clear that

$$(\forall n \in \mathbb{N}) \quad J(\gamma_n, \beta_n) \leq J(\gamma_1, \beta_1).$$

Then, $\{\gamma_n\}_{n\in\mathbb{N}}$ is uniformly bounded in $H^s(\Omega)$. Since $\mathcal{A}$ is weakly closed, there exists a subsequence (denoted by $\{(\gamma_n, \beta_n)\}_{n\in\mathbb{N}}$) such that $\gamma_n \rightharpoonup \gamma^*$ in $H^s(\Omega)$ and $\beta_n \to \beta^*$, with $(\gamma^*, \beta^*) \in \mathcal{A}$. In particular, $\gamma_n \rightharpoonup \gamma^*$ in $L^2(\Omega)$. Let $\boldsymbol{v}_n = \boldsymbol{u}_n - \beta_n \boldsymbol{g}$. The sequences $\{\boldsymbol{v}_n\}_{n\in\mathbb{N}}$ and $\{p_n\}_{n\in\mathbb{N}}$ are also uniformly bounded on $\boldsymbol{H}^1_{\Gamma_D}(\Omega)$ and $L^2_0(\Omega)$, respectively, because $|\beta_n| \leq M_1$ and $\|\gamma\|_{\infty,\Omega} \leq M_2$. Applying the Sobolev Embedding Theorem (see Section 6.6 in [36]), there exists a subsequence (also denoted by $\{\boldsymbol{v}_n\}_{n\in\mathbb{N}}$) such that $\boldsymbol{v}_n \rightharpoonup \boldsymbol{v}^*$ weakly in $\boldsymbol{H}^1_{\Gamma_D}(\Omega)$, with $\boldsymbol{v}^* \in \boldsymbol{H}^1_{\Gamma_D}(\Omega)$, and $\boldsymbol{v}_n \to \boldsymbol{v}^*$ in $\boldsymbol{L}^p(\Omega)$ for $p \in [2, 6)$ when $N \geq 3$, or for $p \geq 2$ when $N = 2$. In particular,

$$\boldsymbol{v}_n \to \boldsymbol{v}^* \text{ in } \boldsymbol{L}^4(\Omega) \text{ and } \boldsymbol{L}^2(\Omega).$$

Let $\boldsymbol{w} \in \boldsymbol{H}^1_{\Gamma_D}(\Omega)$. Since $d \in \{2, 3\}$, then $\boldsymbol{w} \in \boldsymbol{L}^4(\Omega)$. By the same way, $\boldsymbol{g} \in \boldsymbol{L}^4(\Omega)$. Thus, for every $\boldsymbol{w} \in \boldsymbol{H}^1_{\Gamma_D}(\Omega)$

$$(\gamma_n \boldsymbol{v}_n, \boldsymbol{w})_{0,\Omega} \to (\gamma^* \boldsymbol{v}^*, \boldsymbol{w})_{0,\Omega} \quad ((\nabla \boldsymbol{v}_n)\boldsymbol{a}, \boldsymbol{w})_{0,\Omega} \to ((\nabla \boldsymbol{v}^*)\boldsymbol{a}, \boldsymbol{w})_{0,\Omega}.$$

$$((\nabla \boldsymbol{g})\boldsymbol{v}_n, \boldsymbol{w})_{0,\Omega} \to ((\nabla \boldsymbol{g})\boldsymbol{v}^*, \boldsymbol{w})_{0,\Omega} \quad ((\nabla \boldsymbol{v}_n)\boldsymbol{g}, \boldsymbol{w})_{0,\Omega} \to ((\nabla \boldsymbol{v}^*)\boldsymbol{a}, \boldsymbol{w})_{0,\Omega}.$$

Analogously, the embedding from $\boldsymbol{H}^{1/2}(\Omega)$ to $\boldsymbol{L}^q(\Gamma_N)$ and the trace operator from $\boldsymbol{H}^1(\Omega)$ to $\boldsymbol{L}^q(\Gamma_N)$ are compacts for $q \in (1, 4)$ (see Section 6.6 in [36]). Then, $((\boldsymbol{v}_n + \boldsymbol{g}) \cdot \boldsymbol{n})_- (\boldsymbol{v}_n + \boldsymbol{g}) \rightharpoonup ((\boldsymbol{v}^* + \boldsymbol{g}) \cdot \boldsymbol{n})_- (\boldsymbol{v}^* + \boldsymbol{g})$ weakly in $\boldsymbol{L}^2(\Gamma_N)$. For every $\boldsymbol{w} \in \boldsymbol{H}^1_{\Gamma_D}(\Omega)$, we obtain

$$\left(((\boldsymbol{v}_n + \beta_n \boldsymbol{g}) \cdot \boldsymbol{n})_- (\boldsymbol{v}_n + \beta_n \boldsymbol{g}), \boldsymbol{w}\right)_{0,\Gamma_N} \to \left(((\boldsymbol{v}^* + \beta^* \boldsymbol{g}) \cdot \boldsymbol{n})_- (\boldsymbol{v}^* + \beta^* \boldsymbol{g}), \boldsymbol{w}\right)_{0,\Gamma_N}$$

Repeating this argument, there exists a subsequence also denoted by $\{p_n\}_{n\in\mathbb{N}}$ such that

$$p_n \rightharpoonup p^* \text{ in } L^2_0(\Omega).$$

In conclusion, $(\boldsymbol{v}^*, p^*) \in \mathcal{H}$ is the variational solution of Equation (5.2). Since $\boldsymbol{u}_n \rightharpoonup \boldsymbol{v}^* + \beta^* \boldsymbol{g}$, we obtain $A(\gamma^*, \beta^*) = [\boldsymbol{u}^*, p^*]$. Now, (γ^*, β^*) is optimal. Indeed,

$$\begin{aligned} m &= \lim_{n\to\infty} J(\gamma_n) \\ &\geq \lim_{n\to\infty} \frac{1}{2} \|\boldsymbol{u}_n - \boldsymbol{u}_R\|^2_{0,\omega} + \frac{\alpha}{2} \liminf_{n\to\infty} \|\gamma_n\|^2_{s,\Omega} \\ &\geq \frac{1}{2} \|\boldsymbol{u}^* - \boldsymbol{u}_R\|^2_{0,\omega} + \frac{\alpha}{2} \|\gamma^*\|^2_{s,\Omega} = J(\gamma^*) \geq m. \end{aligned}$$

Hence, $J(\gamma, \beta, A_1(\gamma, \beta)) \geq J(\gamma^*, \beta^*, \boldsymbol{u}^*)$ for every $(\gamma, \beta) \in \mathcal{A}$, proving this theorem.

□

5.4 First order necessary optimality condition

In order to implement a descent method to numerically solve this problem, it is necessary to establish the differentiability of functional J. However, this directly depends on the differentiability of map A. From this result, it is possible to establish necessary optimality conditions. First, it is necessary to verify a technical result.

Lemma 5.4.1. *Let $(\gamma,\beta);(h,\varepsilon)\in\mathcal{A}$, such that $A(\gamma,\beta)=[\boldsymbol{u},p]$ and $A(\gamma+h,\beta+\varepsilon)=[\boldsymbol{u}_*,p_*]$. Then, there exists $C>0$, independent of $\boldsymbol{u}$, (γ,β) and (h,ε) such that $|\boldsymbol{u}_h-\boldsymbol{u}|_{1,\Omega}\leq C\|h\|_{\infty,\Omega}$.*

Proof. Let $(\boldsymbol{w},q)=(\boldsymbol{u}_*-\boldsymbol{u},p_*-p)$ and $\boldsymbol{v}\in H^1_{\Gamma_D}(\Omega)$ such that $\boldsymbol{w}=\boldsymbol{v}+\varepsilon\boldsymbol{g}$. Subtracting the equations of $A(\gamma+h,\beta+\varepsilon)$ and $A(\gamma,\beta)$, it is obtained

$$\begin{aligned}
-\nu\triangle\boldsymbol{w}+(\nabla\boldsymbol{w})\,\boldsymbol{u}_*+(\nabla\boldsymbol{u})\,\boldsymbol{w}+\nabla q+\gamma\boldsymbol{w}&=-h\boldsymbol{u}_* && \text{in } \Omega\\
\operatorname{div}\boldsymbol{w}&=0 && \text{in } \Omega\\
\boldsymbol{w}&=\varepsilon\boldsymbol{g} && \text{on } \Gamma_D\\
-\nu\frac{\partial\boldsymbol{w}}{\partial\boldsymbol{n}}+q\boldsymbol{n}+\frac{1}{2}(\boldsymbol{u}_*\cdot\boldsymbol{n})_-\,\boldsymbol{u}_*-\frac{1}{2}(\boldsymbol{u}\cdot\boldsymbol{n})_-\,\boldsymbol{u}&=\boldsymbol{0} && \text{on } \Gamma_N
\end{aligned}$$

Replacing $\boldsymbol{w}$ by $\boldsymbol{v}+\varepsilon\boldsymbol{g}$ and testing the equations with $\boldsymbol{v}$ and q, respectively, we deduce

$$\begin{aligned}
&\nu|\boldsymbol{v}|^2_{1,\Omega}+(\gamma\boldsymbol{v},\boldsymbol{v})_{0,\Omega}+((\nabla\boldsymbol{v})\,\boldsymbol{u}_*,\boldsymbol{v})_{0,\Omega}+((\nabla\boldsymbol{u})\,\boldsymbol{v},\boldsymbol{v})_{0,\Omega}\\
&\quad+\frac{1}{2}\int_{\Gamma_N}\left[(\boldsymbol{u}\cdot\boldsymbol{n})_-\,\boldsymbol{u}-(\boldsymbol{u}_*\cdot\boldsymbol{n})_-\,\boldsymbol{u}_*\right]\cdot\boldsymbol{v}\;dS\\
=&-(h\boldsymbol{u}_*,\boldsymbol{v})_{0,\Omega}-\varepsilon\nu(\nabla\boldsymbol{v},\nabla\boldsymbol{g})_{0,\Omega}\\
&\quad-\varepsilon(\gamma\boldsymbol{g},\boldsymbol{v})_{0,\Omega}-\varepsilon((\nabla\boldsymbol{g})\,\boldsymbol{u}_*,\boldsymbol{v})_{0,\Omega}-((\nabla\boldsymbol{u})\,\boldsymbol{g},\boldsymbol{v})_{0,\Omega}
\end{aligned}$$

where, applying Theorems 1.2.2 and 1.2.1, and Lemmas 1.2.2 and 1.2.3, we can obtain

$$((\nabla\boldsymbol{u})\,\boldsymbol{v},\boldsymbol{v})_{0,\Omega}\geq-\kappa|\boldsymbol{u}|_{1,\Omega}|\boldsymbol{v}|^2_{1,\Omega}$$

and

$$\begin{aligned}
&((\nabla\boldsymbol{v})\,\boldsymbol{u}_*,\boldsymbol{v})_{0,\Omega}+\frac{1}{2}\int_{\Gamma_N}\left[(\boldsymbol{u}\cdot\boldsymbol{n})_-\,\boldsymbol{u}-(\boldsymbol{u}_*\cdot\boldsymbol{n})_-\,\boldsymbol{u}_*\right]\cdot\boldsymbol{v}\;dS\\
=&\frac{1}{2}\int_{\Gamma_N}(\boldsymbol{u}_*\cdot\boldsymbol{n})\,|\boldsymbol{v}|^2\;dS+\frac{1}{2}\int_{\Gamma_N}\left[(\boldsymbol{u}\cdot\boldsymbol{n})_-\,\boldsymbol{u}-(\boldsymbol{u}_*\cdot\boldsymbol{n})_-\,\boldsymbol{u}_*\right]\cdot\boldsymbol{v}\;dS\\
=&\frac{1}{2}\int_{\Gamma_N}(\boldsymbol{u}_*\cdot\boldsymbol{n})_+\,|\boldsymbol{v}|^2\;dS-\frac{1}{2}\int_{\Gamma_N}(\boldsymbol{u}_*\cdot\boldsymbol{n})_-\,(\boldsymbol{u}+\varepsilon\boldsymbol{g})\cdot\boldsymbol{v}\;dS+\frac{1}{2}\int_{\Gamma_N}(\boldsymbol{u}\cdot\boldsymbol{n})_-\,\boldsymbol{u}\cdot\boldsymbol{v}\;dS\\
=&\frac{1}{2}\int_{\Gamma_N}(\boldsymbol{u}_*\cdot\boldsymbol{n})_+\,|\boldsymbol{v}|^2\;dS-\frac{1}{2}\int_{\Gamma_N}\left((\boldsymbol{u}\cdot\boldsymbol{n})_-(\boldsymbol{u}_*\cdot\boldsymbol{n})_-\right)\boldsymbol{u}\cdot\boldsymbol{v}\;dS\\
&\quad-\frac{1}{2}\varepsilon\int_{\Gamma_N}(\boldsymbol{u}_*\cdot\boldsymbol{n})_-\,\boldsymbol{g}\cdot\boldsymbol{v}\;dS,
\end{aligned}$$

where $\frac{1}{2}\int_{\Gamma_N}(\boldsymbol{u}_*\cdot\boldsymbol{n})_+\,|\boldsymbol{v}|^2\;dS\geq0$ and $\left|(\boldsymbol{u}\cdot\boldsymbol{n})_--(\boldsymbol{u}_*\cdot\boldsymbol{n})_-\right|\leq\left|(\boldsymbol{u})_--(\boldsymbol{u}_*\cdot\boldsymbol{n})_-\right|$. Thus,

$$\begin{aligned}
&((\nabla\boldsymbol{v})\,\boldsymbol{u}_*,\boldsymbol{v})_{0,\Omega}+\frac{1}{2}\int_{\Gamma_N}\left[(\boldsymbol{u}\cdot\boldsymbol{n})_-\,\boldsymbol{u}-(\boldsymbol{u}_*\cdot\boldsymbol{n})_-\,\boldsymbol{u}_*\right]\cdot\boldsymbol{v}\;dS\\
\geq&-\frac{1}{2}\kappa|\boldsymbol{w}|_{1,\Omega}|\boldsymbol{u}|_{1,\Omega}|\boldsymbol{v}|_{1,\Omega}-\frac{1}{2}\varepsilon\kappa|\boldsymbol{u}_*|_{1,\Omega}\|\boldsymbol{g}\|_{1,\Omega}|\boldsymbol{v}|_{1,\Omega}\\
\geq&-\frac{1}{2}\kappa|\boldsymbol{v}|^2_{1,\Omega}|\boldsymbol{u}|_{1,\Omega}-\frac{1}{2}\varepsilon\kappa\left(|\boldsymbol{u}|_{1,\Omega}+|\boldsymbol{u}_*|_{1,\Omega}\right)\|\boldsymbol{g}\|_{1,\Omega}|\boldsymbol{v}|_{1,\Omega}
\end{aligned}$$

Then, there exists a constant $C_1 > 0$ independent of $\boldsymbol{u}$, $\boldsymbol{u}_*$, (γ, β) and (h, ε) such that such that

$$\begin{aligned}&\nu \left|\boldsymbol{v}\right|_{1,\Omega}^2 - \frac{3}{2}\kappa \left|\boldsymbol{u}\right|_{1,\Omega} \left|\boldsymbol{v}\right|_{1,\Omega}^2 \\ \leq & C_1 \left|\boldsymbol{v}\right|_{1,\Omega} \left(\left\|h\right\|_{\infty,\Omega} \left|\boldsymbol{u}_*\right|_{1,\Omega} + \varepsilon(\left\|h\right\|_{\infty,\Omega} + \left\|\boldsymbol{g}\right\|_{1,\Omega} + \left|\boldsymbol{u}\right|_{1,\Omega} + \left|\boldsymbol{u}_*\right|_{1,\Omega})\right)\end{aligned}$$

Since $\left|\boldsymbol{u}\right|_{1,\Omega}$ ard $\left|\boldsymbol{u}_*\right|_{1,\Omega}$ are uniformly bounded and Theorem 1.2.3, there exists a constant c_1, independent of $\boldsymbol{u}$, $\boldsymbol{u}_*$, (γ, β) and (h, ε) such that $0 < c_1 \leq \nu - \frac{3}{2}\kappa \left|\boldsymbol{u}\right|_{1,\Omega}$ and

$$\begin{aligned}c_1 \left|\boldsymbol{v}\right|_{1,\Omega}^2 &= \nu \left|\boldsymbol{v}\right|_{1,\Omega}^2 - \frac{3}{2}\kappa \left|\boldsymbol{u}\right|_{1,\Omega} \left|\boldsymbol{v}\right|_{1,\Omega}^2 \\ &\leq C_1 \left|\boldsymbol{v}\right|_{1,\Omega} \left(\left\|h\right\|_{\infty,\Omega} \left|\boldsymbol{u}_*\right|_{1,\Omega} + \varepsilon \left(\left\|h\right\|_{\infty,\Omega} + \left\|\boldsymbol{g}\right\|_{1,\Omega} + \left|\boldsymbol{u}\right|_{1,\Omega} + \left|\boldsymbol{u}_*\right|_{1,\Omega}\right)\right)\end{aligned}$$

but $\left|\boldsymbol{u}\right|_{1,\Omega}$ and $\left|\boldsymbol{u}_*\right|_{1,\Omega}$ are uniformly bounded by a constant $c_4 > 0$ independent of (γ, β) and (h, ε) (see Remark 5.3.1). Then, due to $\left\|h\right\|_{\infty,\Omega} \leq M_2$, there exists a constant $C_2 > 0$, independent of independent of $\boldsymbol{u}$, $\boldsymbol{u}_*$, (γ, β) and (h, ε) such that

$$\left|\boldsymbol{w}\right|_{1,\Omega} \leq C_2 \left(\left\|h\right\|_{\infty,\Omega} + \varepsilon\right)$$

and

$$\left|\boldsymbol{v}\right|_{1,\Omega} \leq \left|\boldsymbol{w}\right|_{1,\Omega} + \varepsilon \left|\boldsymbol{g}\right|_{1,\Omega} \leq \left(C_2 + \left|\boldsymbol{g}\right|_{1,\Omega}\right) \left(\left\|h\right\|_{\infty,\Omega} + \varepsilon\right)$$

Taking $C = C_2 + \left|\boldsymbol{g}\right|_{1,\Omega}$, the lemma is proved.

□

Theorem 5.4.1. *The map A is Fréchet-differentiable for every $\gamma \in \mathcal{A}$ where A is well defined. For each $(\gamma, \beta), (h, \varepsilon) \in \mathcal{A}$, if $A(\gamma, \beta) = [\boldsymbol{u}, p]$, then the Fréchet derivative $A(\gamma, \beta)[(h, \varepsilon)] = [\boldsymbol{u}', p']$ can be described by the weak solution of the following problem*

$$\begin{aligned}-\nu \triangle \boldsymbol{u}' + (\nabla \boldsymbol{u}')\,\boldsymbol{u} + (\nabla \boldsymbol{u})\,\boldsymbol{u}' + \nabla p' + \gamma \boldsymbol{u}' &= -h\boldsymbol{u} && \text{in } \Omega \\ \operatorname{div} \boldsymbol{u}' &= 0 && \text{in } \Omega \\ \boldsymbol{u}_1' &= \varepsilon \boldsymbol{g} && \text{on } \Gamma_D \\ -\nu \frac{\partial \boldsymbol{u}'}{\partial \boldsymbol{n}} + p'\boldsymbol{n} + \frac{1}{2} f(\boldsymbol{u}, \boldsymbol{u}') &= \boldsymbol{0} && \text{on } \Gamma_N.\end{aligned} \tag{5.3}$$

where

$$f(\boldsymbol{v}, \boldsymbol{v}') = \begin{cases} \boldsymbol{0} & \text{on } \Gamma_N^+ \\ (\boldsymbol{u}' \cdot \boldsymbol{n})\,\boldsymbol{u} + (\boldsymbol{u} \cdot \boldsymbol{n})\,\boldsymbol{u}' & \text{on } \Gamma_N^- \end{cases}$$

Proof. Let $(\gamma, \beta), (h, \varepsilon) \in \mathcal{A}$, it will be proved that there is a linear application $D : \mathcal{A} \to \mathcal{H}$ such that

$$A(\gamma + h, \beta + \varepsilon) - A(\gamma, \beta) = D(h, \varepsilon) + r((\gamma, \beta); (h, \varepsilon)),$$

where

$$\left(\left\|h\right\|_{\infty,\Omega} + \varepsilon\right) \to 0 \Rightarrow \frac{\left\|r((\gamma, \beta); (h, \varepsilon))\right\|_{\mathcal{H}}}{\left(\left\|h\right\|_{\infty,\Omega} + \varepsilon\right)} \to 0.$$

Let $[\boldsymbol{u}_*, p_*] = A(\gamma + h, \beta + \varepsilon)$. Taking $D(\gamma_1) = [\boldsymbol{u}', p']$ and $r((\gamma, \beta); (h, \varepsilon)) = [\delta\boldsymbol{u}, \delta p] = [\boldsymbol{u}_* - \boldsymbol{u} - \boldsymbol{u}', p_* - p - p']$, it is possible to see that $D(\gamma_1)$ is linear. Also, $[\delta\boldsymbol{u}, \delta p]$ is solution of the problem

$$\begin{aligned} -\nu\triangle(u) + (\nabla\delta\boldsymbol{u})\,\boldsymbol{u} + (\nabla\boldsymbol{u})\,\delta\boldsymbol{v} + \nabla(\delta p) + \gamma(\delta\boldsymbol{u}) &= \boldsymbol{f} && \text{in } \Omega \\ \operatorname{div}(\delta\boldsymbol{u}) &= 0 && \text{in } \Omega \\ (\delta\boldsymbol{u}) &= \boldsymbol{0} && \text{on } \Gamma_D \\ -\nu\frac{\partial(\delta\boldsymbol{u})}{\partial\boldsymbol{n}} + (\delta p)\,\boldsymbol{n} + \frac{1}{2}f_1(\delta\boldsymbol{u}, \boldsymbol{u}) &= \frac{1}{2}f_2(\boldsymbol{u}, \boldsymbol{u}_1) && \text{on } \Gamma_N. \end{aligned}$$

where

$$\boldsymbol{f} = h(\boldsymbol{u} - \boldsymbol{u}_*) - (\nabla(\boldsymbol{u}_* - \boldsymbol{u}))(\boldsymbol{u}_* - \boldsymbol{u})$$

$$f_1(\delta\boldsymbol{v}, \boldsymbol{v}) = \begin{cases} \boldsymbol{0} & \text{in } \Gamma_N^+ \\ (\delta\boldsymbol{u}\cdot\boldsymbol{n})\,\boldsymbol{u} + (\boldsymbol{u}\cdot\boldsymbol{n})\,\delta\boldsymbol{u} & \text{in } \Gamma_N^- \end{cases}$$

$$f_2(\boldsymbol{v}, \boldsymbol{v}_1) = \begin{cases} (\boldsymbol{u}\cdot\boldsymbol{n})_-\,\boldsymbol{u} - (\boldsymbol{u}_*\cdot\boldsymbol{n})_-\,\boldsymbol{u}_* & \text{in } \Gamma_N^+ \\ (\boldsymbol{u}\cdot\boldsymbol{n})_-\,\boldsymbol{u} - (\boldsymbol{u}_*\cdot\boldsymbol{n})_-\,\boldsymbol{u}_* + ((\boldsymbol{u}_* - \boldsymbol{u})\cdot\boldsymbol{n})\,\boldsymbol{u} + (\boldsymbol{u}\cdot\boldsymbol{n})_-(\boldsymbol{u}_* - \boldsymbol{u}) & \text{in } \Gamma_N^- \end{cases}$$

Thus, testing the first equation with $\delta\boldsymbol{u}$ and the second equation with δp, we obtain

$$\begin{aligned} &\nu|\delta\boldsymbol{u}|_{1,\Omega}^2 + (\gamma(\delta\boldsymbol{u}), \delta\boldsymbol{u})_{0,\Omega} + ((\nabla\boldsymbol{u})\,\delta\boldsymbol{u}, \delta\boldsymbol{u})_{0,\Omega} \\ &+ \frac{1}{2}\left((\boldsymbol{u}\cdot\boldsymbol{n}), |\delta\boldsymbol{u}|^2\right)_{0.\Gamma_N} - \frac{1}{2}(f_1(\delta\boldsymbol{u}, \boldsymbol{u}), \delta\boldsymbol{u})_{0.\Gamma_N} \\ &= (h(\boldsymbol{u} - \boldsymbol{u}_*) - (\nabla(\boldsymbol{u}_* - \boldsymbol{u}))(\boldsymbol{u}_* - \boldsymbol{u}), \delta\boldsymbol{u}) - \frac{1}{2}(f_2(\boldsymbol{u}, \boldsymbol{u}_*), \delta\boldsymbol{u})_{0.\Gamma_N} \end{aligned}$$

where, applying Lemmas 1.2.2, 1.2.3, 1.2.1 and 1.2.2, we can deduce that

$$\begin{aligned} &((\nabla\boldsymbol{u})\,\delta\boldsymbol{u}, \delta\boldsymbol{u})_{0,\Omega} + \frac{1}{2}\left((\boldsymbol{u}\cdot\boldsymbol{n}), |\delta\boldsymbol{u}|^2\right)_{0.\Gamma_N} - \frac{1}{2}(f_1(\delta\boldsymbol{u}, \boldsymbol{u}), \delta\boldsymbol{u})_{0.\Gamma_N} \\ &= ((\nabla\boldsymbol{u})\,\delta\boldsymbol{u}, \delta\boldsymbol{u})_{0,\Omega} - \frac{1}{2}((\delta\boldsymbol{u}\cdot\boldsymbol{n})\,\boldsymbol{u}, \delta\boldsymbol{u})_{0.\Gamma_N} + \frac{1}{2}\left((\boldsymbol{u}\cdot\boldsymbol{n})_+, |\delta\boldsymbol{u}|^2\right)_{0.\Gamma_N} \\ &\geq ((\nabla\boldsymbol{u})\,\delta\boldsymbol{u}, \delta\boldsymbol{u})_{0,\Omega} - \frac{1}{2}((\delta\boldsymbol{u}\cdot\boldsymbol{n})\,\boldsymbol{u}, \delta\boldsymbol{u})_{0.\Gamma_N} \\ &\geq -\frac{3\kappa}{2}|\boldsymbol{u}|_{1,\Omega}|\delta\boldsymbol{u}|_{1,\Omega}^2 \end{aligned}$$

Since sufficient condition of uniqueness of solution (see Theorem 1.2.3) and uniformly boundedness of $|\boldsymbol{u}|_{1,\Omega}$ (see Remark 5.3.1) imply that there exists a constant $c_1 > 0$ such that $\frac{3}{2}\kappa|\boldsymbol{u}|_{1,\Omega} \leq c_1 < \nu$. Then, there exists a constant $c_2 = \nu - c_1 > 0$, independent of $\boldsymbol{u}$, $\boldsymbol{u}_*$, (γ, β), (h, ε) and $(\gamma_1, \varepsilon_1)$ such that

$$\begin{aligned} &\nu|\delta\boldsymbol{u}|_{1,\Omega}^2 + ((\nabla\boldsymbol{u})\,\delta\boldsymbol{u}, \delta\boldsymbol{u})_{0,\Omega} + \frac{1}{2}\left((\boldsymbol{u}\cdot\boldsymbol{n}), |\delta\boldsymbol{u}|^2\right)_{0.\Gamma_N} - \frac{1}{2}(f_1(\delta\boldsymbol{u}, \boldsymbol{u}), \delta\boldsymbol{u})_{0.\Gamma_N} \\ &\geq \left(\nu - \frac{3\kappa}{2}|\boldsymbol{u}|_{1,\Omega}\right)|\delta\boldsymbol{u}|_{1,\Omega}^2 = c_2|\delta\boldsymbol{u}|_{1,\Omega}^2 \end{aligned}$$

Applying Hölder inequality, Theorem 1.2.2, Sobolev Embedding Theorem, Lemmas 1.2.1, 1.2.2 and 1.2.3, there exist constants $c_3 > 0$ and $c_4 > 0$, independents of $\boldsymbol{u}$, $\boldsymbol{u}_*$, (γ, β), (h, ε) and $(\gamma_1, \varepsilon_1)$ such that

$$-\frac{1}{2}(f_2(\boldsymbol{v}, \boldsymbol{v}_1), \delta\boldsymbol{v})_{0.\Gamma_N} \leq \left|((\boldsymbol{u}_* - \boldsymbol{u})\cdot\boldsymbol{n}, (\boldsymbol{u}_* - \boldsymbol{u})\cdot\delta\boldsymbol{u})_{0.\Gamma_N}\right|$$

$$\leq c_3 \left(\left(|\boldsymbol{u}_* - \boldsymbol{u}|_{1,\Omega} + \varepsilon \right)^2 |\delta \boldsymbol{u}|_{1,\Omega} \right)$$

and

$$\begin{aligned} &\left(h\left(\boldsymbol{u}-\boldsymbol{u}_*\right)-\left(\nabla\left(\boldsymbol{u}_*-\boldsymbol{u}\right)\right)\left(\boldsymbol{u}_*-\boldsymbol{u}\right), \delta \boldsymbol{u}\right) \\ \leq & c_4 |\delta \boldsymbol{u}|_{1,\Omega} \left(\|h\|_{\infty,\Omega} \left(|\boldsymbol{u}_* - \boldsymbol{u}|_{1,\Omega} + \varepsilon \right) + \left(|\boldsymbol{u}_* - \boldsymbol{u}|_{1,\Omega} + \varepsilon \right)^2 \right) \end{aligned}$$

Applying Lemma 5.4.1, there exist constant $c_5 > 0$, independent of $\boldsymbol{u}$, $\boldsymbol{u}_*$, (γ, β), (h, ε) and $(\gamma_1, \varepsilon_1)$ such that

$$\begin{aligned} c_2 |\delta \boldsymbol{u}|_{1,\Omega}^2 &\leq |\delta \boldsymbol{u}|_{1,\Omega} \left((c_3 + c_4) \left(|\boldsymbol{u}_* - \boldsymbol{u}|_{1,\Omega} + \varepsilon \right)^2 + c_4 \|h\|_{\infty,\Omega} \left(|\boldsymbol{u}_* - \boldsymbol{u}|_{1,\Omega} + \varepsilon \right) \right) \\ &\leq c_5 |\delta \boldsymbol{u}|_{1,\Omega} \left(\|h\|_{\infty,\Omega} + \varepsilon \right)^2 \end{aligned}$$

Thus, there exists a constant $C_1 > 0$, independent of $\boldsymbol{u}$, $\boldsymbol{u}_*$, (γ, β), (h, ε) and $(\gamma_1, \varepsilon_1)$ such that

$$|\delta \boldsymbol{u}|_{1,\Omega} \leq C_1 \left(\|h\|_{\infty,\Omega} + \varepsilon \right)^2$$

Repeating the same arguments, we obtain that there exists a constant $C_2 > 0$, independent of $\boldsymbol{u}$, $\boldsymbol{u}_*$, (γ, β), (h, ε) and $(\gamma_1, \varepsilon_1)$ such that

$$\|\delta p\|_{0,\Omega} = \beta_1 \sup_{|\boldsymbol{w}|_{1,\Omega}=1,\ \boldsymbol{w} \in \boldsymbol{H}^1_{\Gamma_D}(\Omega)} \left| (\delta p, \operatorname{div} \boldsymbol{w})_{0,\Omega} \right| \leq C_1 \left(\|h\|_{\infty,\Omega} + \varepsilon \right)^2$$

Then, there exists $C > 0$, independent of $\boldsymbol{u}$, $\boldsymbol{u}_*$, (γ, β), (h, ε) and $(\gamma_1, \varepsilon_1)$ such that

$$\|r\left((\gamma, \beta); (h, \varepsilon)\right)\|_{\mathcal{H}} = \nu |\delta \boldsymbol{u}|_{1,\Omega} + \|\delta p\|_{0,\Omega} \leq C \left(\|h\|_{\infty,\Omega} + \varepsilon \right)^2$$

Therefore,

$$\frac{\|r\left((\gamma, \beta); (h, \varepsilon)\right)\|_{\mathcal{H}}}{\left(\|h\|_{\infty,\Omega} + \varepsilon \right)} \leq C \left(\|h\|_{\infty,\Omega} + \varepsilon \right) \overset{\left(\|h\|_{\infty,\Omega} + \varepsilon\right) \to 0}{\longrightarrow} 0,$$

proving the theorem.

□

Defining $B(\boldsymbol{u}) = \dfrac{1}{2} \|\boldsymbol{u} - \boldsymbol{u}_R\|_{0,\omega}^2$ and $C(\gamma) = \dfrac{\alpha}{2} \|\gamma\|_{s,\Omega}^2$, an expression for Frechét derivatives of B and C is given by

$$B'(\boldsymbol{v})[\boldsymbol{w}] = (\boldsymbol{u} - \boldsymbol{u}_R, \boldsymbol{w})_{0,\omega} \quad C'(\gamma)[h] = \alpha (\gamma, h)_{s,\Omega}.$$

Applying chain rule, it is obtained that

$$\begin{aligned} J'(\gamma, \beta)[(h, \varepsilon)] &= B'(\boldsymbol{v}) \left[A_1'(\gamma, \beta)[(h, \varepsilon)] \right] + C'(\gamma)[h] \\ &= (\boldsymbol{u} - \boldsymbol{u}_R, \boldsymbol{u}')_{0,\omega} + \alpha (\gamma, h)_{s,\Omega}. \end{aligned}$$

In order to reduce this expression, the following definition is introduced similarly to [1].

Definition 5.4.1. *Let $\gamma \in \mathcal{A}$ and $A(\gamma,\beta) = [\boldsymbol{u}, p]$. The adjoint states $A^*(\gamma,\beta) = [\boldsymbol{\varphi}, \xi]$ are defined as the unique weak solution of the problem*

$$\begin{aligned} -\nu\triangle\boldsymbol{\varphi} - (\nabla\boldsymbol{\varphi})\,\boldsymbol{u} + (\nabla\boldsymbol{u})^T\,\boldsymbol{\varphi} + \nabla\xi + \gamma\boldsymbol{\varphi} &= \chi_\omega(\boldsymbol{u}-\boldsymbol{u}_R) && \text{in } \Omega \\ \operatorname{div}\boldsymbol{\varphi} &= 0 && \text{in } \Omega \\ \boldsymbol{\varphi} &= \boldsymbol{0} && \text{on } \Gamma_D \\ -\nu\frac{\partial\boldsymbol{\varphi}}{\partial\boldsymbol{n}} + \xi\boldsymbol{n} - (\boldsymbol{u}\cdot\boldsymbol{n})\,\boldsymbol{\varphi} + \frac{1}{2}\phi(\boldsymbol{v},\boldsymbol{\varphi}) &= \boldsymbol{0} && \text{on } \Gamma_N. \end{aligned} \tag{5.4}$$

where χ_ω is the indicator function of ω and

$$\phi(\boldsymbol{v},\boldsymbol{\varphi}) = \begin{cases} 0 & \text{on } \Gamma_N^+ \\ (\boldsymbol{u}\cdot\boldsymbol{\varphi})\,\boldsymbol{n} + (\boldsymbol{u}\cdot\boldsymbol{n})\,\boldsymbol{\varphi} & \text{on } \Gamma_N^- \end{cases}$$

Using this defintion, it is possible to rewrite $J'(\gamma,\beta)$ depending of the adjoint state. That expression is simpler to analyze, since it depends on the adjoint state, allowing a simple form of a first order optimality condition using a variational inequality.

Theorem 5.4.2. *Let $\gamma, \gamma_1 \in \mathcal{A}$ and $s \geq 0$. Then,*

$$J'(\gamma,\beta)[(h,\varepsilon)] = -(h\boldsymbol{u},\boldsymbol{\varphi})_{0,\Omega} + \varepsilon\int_{\Gamma_D}\boldsymbol{u}_D\cdot\left[-\nu\frac{\partial\boldsymbol{\varphi}}{\partial\boldsymbol{n}} + \xi\boldsymbol{n}\right]\,dS + \alpha(\gamma,h)_{s,\Omega},$$

where $A(\gamma,\beta) = [\boldsymbol{u}, p]$. If $(\gamma^*,\varepsilon^*) \in \mathcal{A}$ is an optimal for Problem (4.3), then for all $\gamma,\beta \in \mathcal{A}$

$$-((\gamma-\gamma^*)\,\boldsymbol{u},\boldsymbol{\varphi})_{0,\Omega} + (\varepsilon-\varepsilon^*)\int_{\Gamma_D}\boldsymbol{u}_D\cdot\left[-\nu\frac{\partial\boldsymbol{\varphi}}{\partial\boldsymbol{n}} + \xi\boldsymbol{n}\right]\,dS + \alpha(\gamma^*,\gamma-\gamma^*)_{s,\Omega} \geq 0$$

where $A(\gamma^*) = [\boldsymbol{v}^*, p^*]$ and $A^*(\gamma^*) = [\boldsymbol{\varphi},\xi]$ are the states and adjont states of γ^*, respectively.

Proof. First, using integration by parts with the adjoint states $[\boldsymbol{\varphi},\xi]$ as tests functions, it is obtained that

$$\begin{aligned} -\nu\int_\Omega \triangle\boldsymbol{u}'\cdot\boldsymbol{\varphi}\,d\boldsymbol{x} &= -\nu\int_\Omega\triangle\boldsymbol{\varphi}\cdot\boldsymbol{u}'\,d\boldsymbol{x} + \int_{\partial\Omega}\boldsymbol{\varphi}\cdot\left(-\nu\frac{\partial\boldsymbol{u}'}{\partial\boldsymbol{n}}\right) - \boldsymbol{u}'\cdot\left(-\nu\frac{\partial\boldsymbol{\varphi}}{\partial\boldsymbol{n}}\right)\,dS \\ \int_\Omega[(\nabla\boldsymbol{u}')\,\boldsymbol{u}]\cdot\boldsymbol{\varphi}\,d\boldsymbol{x} &= -\int_\Omega[(\nabla\boldsymbol{\varphi})\,\boldsymbol{u}]\cdot\boldsymbol{u}'\,d\boldsymbol{x} + \int_{\partial\Omega}(\boldsymbol{u}\cdot\boldsymbol{n})\,(\boldsymbol{\varphi}\cdot\boldsymbol{u}')\,dS \\ \int_\Omega\nabla p'\cdot\boldsymbol{\varphi}\,d\boldsymbol{x} &= -\int_\Omega p'\operatorname{div}\boldsymbol{\varphi}\,d\boldsymbol{x} + \int_{\partial\Omega}\boldsymbol{\varphi}\cdot(p'\boldsymbol{n})\,dS \\ -\int_\Omega\xi\operatorname{div}\boldsymbol{u}'\,d\boldsymbol{x} &= \int_\Omega\nabla\xi\cdot\boldsymbol{u}'\,d\boldsymbol{x} - \int_{\partial\Omega}\boldsymbol{u}'\cdot(\xi\boldsymbol{n})\,dS. \end{aligned}$$

and also

$$\int_\Omega[(\nabla\boldsymbol{u})\,\boldsymbol{u}']\cdot\boldsymbol{\varphi}\,d\boldsymbol{x} = \int_\Omega\left[(\nabla\boldsymbol{u})^T\,\boldsymbol{\varphi}\right]\cdot\boldsymbol{u}'\,d\boldsymbol{x}$$

Then,

$$-(h\boldsymbol{u},\boldsymbol{\varphi})_{0,\Omega} = -\nu\int_\Omega\triangle\boldsymbol{u}'\cdot\boldsymbol{\varphi}\,d\boldsymbol{x} + \int_\Omega[(\nabla\boldsymbol{u}')\,\boldsymbol{u}]\cdot\boldsymbol{\varphi}\cdot\boldsymbol{\varphi}\,d\boldsymbol{x} + \int_\Omega[(\nabla\boldsymbol{u})\,\boldsymbol{u}']\cdot\boldsymbol{\varphi}\,d\boldsymbol{x}$$

$$
\begin{aligned}
&+\int_\Omega \nabla p'\cdot\boldsymbol{\varphi}\,d\boldsymbol{x}+\int_\Omega \gamma\boldsymbol{u}'\cdot\boldsymbol{\varphi}\,d\boldsymbol{x}-\int_\Omega \xi\,\mathrm{div}\,\boldsymbol{u}'\,d\boldsymbol{x}\\
=&-\nu\int_\Omega \triangle\boldsymbol{\varphi}\cdot\boldsymbol{u}'\,d\boldsymbol{x}-\int_\Omega[(\nabla\boldsymbol{\varphi})\,\boldsymbol{u}]\cdot\boldsymbol{u}'\,d\boldsymbol{x}+\int_\Omega\left[(\nabla\boldsymbol{u})^T\,\boldsymbol{\varphi}\right]\cdot\boldsymbol{u}'\,d\boldsymbol{x}\\
&+\int_\Omega \nabla\xi\cdot\boldsymbol{u}'\,d\boldsymbol{x}+\int_\Omega\gamma\boldsymbol{u}'\cdot\boldsymbol{\varphi}\,d\boldsymbol{x}-\int_\Omega p'\,\mathrm{div}\,\boldsymbol{\varphi}\,d\boldsymbol{x}\\
&+\int_{\Gamma_N}\boldsymbol{\varphi}\cdot\left(-\nu\frac{\partial\boldsymbol{u}'}{\partial\boldsymbol{n}}+p'\boldsymbol{n}\right)-\int_{\partial\Omega}\boldsymbol{u}'\cdot\left(-\nu\frac{\partial\boldsymbol{\varphi}}{\partial\boldsymbol{n}}+\xi\boldsymbol{n}-(\boldsymbol{u}\cdot\boldsymbol{n})\,\boldsymbol{\varphi}\right)\,dS\\
=&\,(\boldsymbol{u}-\boldsymbol{u}_R,\boldsymbol{u}_1')_{0,\omega}-\int_{\Gamma_N^-}\boldsymbol{\varphi}\cdot((\boldsymbol{u}'\cdot\boldsymbol{n})\,\boldsymbol{u}+(\boldsymbol{u}\cdot\boldsymbol{n})\,\boldsymbol{u}')\\
&-\int_{\partial\Omega}\boldsymbol{u}'\cdot\left(-\nu\frac{\partial\boldsymbol{\varphi}}{\partial\boldsymbol{n}}+\xi\boldsymbol{n}-(\boldsymbol{u}\cdot\boldsymbol{n})\,\boldsymbol{\varphi}\right)\,dS
\end{aligned}
$$

where

$$
\begin{aligned}
&\int_{\partial\Omega}\boldsymbol{u}'\cdot\left(-\nu\frac{\partial\boldsymbol{\varphi}}{\partial\boldsymbol{n}}+\xi\boldsymbol{n}-(\boldsymbol{u}\cdot\boldsymbol{n})\,\boldsymbol{\varphi}\right)\,dS\\
=&\varepsilon\int_{\Gamma_D}\boldsymbol{g}\cdot\left(-\nu\frac{\partial\boldsymbol{\varphi}}{\partial\boldsymbol{n}}+\xi\boldsymbol{n}\right)\,dS-\int_{\Gamma_N^-}\boldsymbol{u}'\cdot((\boldsymbol{u}\cdot\boldsymbol{\varphi})\,\boldsymbol{n}+(\boldsymbol{u}\cdot\boldsymbol{n})\,\boldsymbol{\varphi})\,dS\\
=&\varepsilon\int_{\Gamma_D}\boldsymbol{g}\cdot\left(-\nu\frac{\partial\boldsymbol{\varphi}}{\partial\boldsymbol{n}}+\xi\boldsymbol{n}\right)\,dS-\int_{\Gamma_N^-}\boldsymbol{\varphi}\cdot((\boldsymbol{u}'\cdot\boldsymbol{n})\,\boldsymbol{u}+(\boldsymbol{u}\cdot\boldsymbol{n})\,\boldsymbol{u}')
\end{aligned}
$$

Thus,

$$
\begin{aligned}
(\boldsymbol{u}-\boldsymbol{u}_R,\boldsymbol{u}_1')_{0,\omega}=&-(h\boldsymbol{u},\boldsymbol{\varphi})_{0,\Omega}+\int_{\Gamma_N^-}\boldsymbol{\varphi}\cdot((\boldsymbol{u}'\cdot\boldsymbol{n})\,\boldsymbol{u}+(\boldsymbol{u}\cdot\boldsymbol{n})\,\boldsymbol{u}')\\
&-\int_{\partial\Omega}\boldsymbol{u}'\cdot\left(-\nu\frac{\partial\boldsymbol{\varphi}}{\partial\boldsymbol{n}}+\xi\boldsymbol{n}-(\boldsymbol{u}\cdot\boldsymbol{n})\,\boldsymbol{\varphi}\right)\,dS\\
=&-(h\boldsymbol{u},\boldsymbol{\varphi})_{0,\Omega}+\varepsilon\int_{\Gamma_D}\boldsymbol{g}\cdot\left(-\nu\frac{\partial\boldsymbol{\varphi}}{\partial\boldsymbol{n}}+\xi\boldsymbol{n}\right)\,dS
\end{aligned}
$$

proving that

$$
J'(\gamma,\beta)\,[(h,\varepsilon)]=-(h\boldsymbol{u},\boldsymbol{\varphi})_{0,\Omega}+\varepsilon\int_{\Gamma_D}\boldsymbol{g}\cdot\left(-\nu\frac{\partial\boldsymbol{\varphi}}{\partial\boldsymbol{n}}+\xi\boldsymbol{n}\right)\,dS+\alpha\,(\gamma,h)_{s,\Omega}\,.
$$

Later, if $\gamma^*\in\mathcal{A}$ is optimal for the problem, then

$$
(\forall\gamma\in\mathcal{A})\quad J(\gamma)\geq J(\gamma^*)\,.
$$

Finally, it is obtained that

$$
J'(\gamma,\beta)\,[(\gamma-\gamma^*,\varepsilon-\varepsilon^*)]=\lim_{t\to0^+}\frac{J(\gamma^*+t\,(\gamma-\gamma^*))-J(\gamma^*)}{\varepsilon}\geq0,
$$

proving this theorem.

□

5.5 Second order sufficient optimality condition

The stability results of the optimization algorithms depend, for the most part, on the existence of the second derivative of J. Likewise, it is possible to establish second order sufficient optimality conditions. First, it is necessary to introduce some techincal results.

Lemma 5.5.1. *Let* $(\gamma,\beta);(\gamma_1,\varepsilon_1)\in\mathcal{A}$ *such that* $[\boldsymbol{u}',p']=A'(\gamma,\beta)[(\gamma_1,\varepsilon_1)]$. *There exist* $C_1>0$ *and* $C_2>0$, *independents of* $\boldsymbol{u}$, γ, β, h *and* ε *such that* $|\boldsymbol{u}'|_{1,\Omega}\leq C_1\left(\|\gamma_1\|_{\infty,\Omega}+\varepsilon_1\right)$ *and* $|\boldsymbol{u}'|_{1,\Omega}\leq C_2\left(\|\gamma_1\|_{s,\Omega}+\varepsilon_1\right)$.

Proof. Let $\boldsymbol{v}'\in\boldsymbol{H}^1_{\Gamma_D}(\Omega)$ such that $\boldsymbol{u}'=\boldsymbol{v}'+\varepsilon_1\boldsymbol{g}$. Testing the equations of $A'(\gamma,\beta)$ with $\boldsymbol{v}'$ and p', respectively, we obtain

$$\begin{aligned}
&\nu|\boldsymbol{v}'|^2_{1,\Omega}+(\gamma\boldsymbol{v}',\boldsymbol{v}')_{0,\Omega}+((\nabla\boldsymbol{v}')\,\boldsymbol{u},\boldsymbol{v}')_{0,\Omega}+((\nabla\boldsymbol{u})\,\boldsymbol{v}',\boldsymbol{v}')_{0,\Omega}\\
&-\frac{1}{2}\int_{\Gamma_N^-}(\boldsymbol{v}'\cdot\boldsymbol{n})\,\boldsymbol{u}\cdot\boldsymbol{v}'+(\boldsymbol{u}\cdot\boldsymbol{n})\,|\boldsymbol{v}'|^2\;dS\\
=&-(\gamma_1\boldsymbol{u},\boldsymbol{v}')_{0,\Omega}-\varepsilon_1\left(\nu(\nabla\boldsymbol{v}',\nabla\boldsymbol{g})_{0,\Omega}+(\gamma\boldsymbol{v}',\boldsymbol{v}')_{0,\Omega}+((\nabla\boldsymbol{g})\,\boldsymbol{u},\boldsymbol{v}')_{0,\Omega}+((\nabla\boldsymbol{u})\,\boldsymbol{g},\boldsymbol{v}')_{0,\Omega}\right)\\
&+\frac{1}{2}\varepsilon_1\int_{\Gamma_N^-}(\boldsymbol{g}\cdot\boldsymbol{n})\,\boldsymbol{u}\cdot\boldsymbol{v}'+(\boldsymbol{u}\cdot\boldsymbol{n})\,(\boldsymbol{g}\cdot\boldsymbol{v}')\;dS
\end{aligned}$$

where

$$\begin{aligned}
&(\gamma\boldsymbol{v}',\boldsymbol{v}')_{0,\Omega}+((\nabla\boldsymbol{v}')\,\boldsymbol{u},\boldsymbol{v}')_{0,\Omega}-\frac{1}{2}\int_{\Gamma_N^-}(\boldsymbol{u}\cdot\boldsymbol{n})\,|\boldsymbol{v}'|^2\;dS\\
&=(\gamma\boldsymbol{v}',\boldsymbol{v}')_{0,\Omega}+\frac{1}{2}\int_{\Gamma_N}(\boldsymbol{u}\cdot\boldsymbol{n})_+\,|\boldsymbol{v}'|^2\;dS\geq 0
\end{aligned}$$

and

$$((\nabla\boldsymbol{u})\,\boldsymbol{v}',\boldsymbol{v}')_{0,\Omega}-\frac{1}{2}\int_{\Gamma_N^-}(\boldsymbol{v}'\cdot\boldsymbol{n})\,\boldsymbol{u}\cdot\boldsymbol{v}'dS\geq-\frac{3}{2}\kappa\,|\boldsymbol{u}|_{1,\Omega}\,|\boldsymbol{v}'|^2_{1,\Omega}$$

Since sufficient condition of uniqueness of solution (see Theorem 1.2.3) and uniformly boundedness of $|\boldsymbol{u}|_{1,\Omega}$ (see Remark 5.3.1) imply that there exists a constant $c_1>0$ such that $\frac{3}{2}\kappa\,|\boldsymbol{u}|_{1,\Omega}\leq c_1<\nu$. Then, there exists a constant $c_2=\nu-c_1>0$, independent of $\boldsymbol{u}$, γ, β, h and ε such that

$$\begin{aligned}
c_2\,|\boldsymbol{v}'|^2_{1,\Omega}\leq&-\varepsilon_1\left(\nu(\nabla\boldsymbol{v}',\nabla\boldsymbol{g})_{0,\Omega}+(\gamma\boldsymbol{v}',\boldsymbol{v}')_{0,\Omega}+((\nabla\boldsymbol{g})\,\boldsymbol{u},\boldsymbol{v}')_{0,\Omega}+((\nabla\boldsymbol{u})\,\boldsymbol{g},\boldsymbol{v}')_{0,\Omega}\right)\\
&+\frac{1}{2}\varepsilon\int_{\Gamma_N^-}(\boldsymbol{g}\cdot\boldsymbol{n})\,\boldsymbol{u}\cdot\boldsymbol{v}'+(\boldsymbol{u}\cdot\boldsymbol{n})\,(\boldsymbol{g}\cdot\boldsymbol{v}')\;dS-(\gamma_1\boldsymbol{u},\boldsymbol{v}')_{0,\Omega}
\end{aligned}$$

By the same way as in Lemma 5.4.1, there exists $c_3>0$, independent of $\boldsymbol{u}$, γ, β, h and ε such that

$$c_2\,|\boldsymbol{v}'|^2_{1,\Omega}\leq-(\gamma_1\boldsymbol{u},\boldsymbol{v}')_{0,\Omega}+\varepsilon_1c_3\,|\boldsymbol{v}'|_{1,\Omega}$$

Applying Hölder inequality for $q,r\in[2,+\infty]$ such that $\dfrac{1}{q}+\dfrac{2}{r}=1$, we obtain

$$-(h\boldsymbol{u},\boldsymbol{v}')_{0,\Omega}\leq\|\gamma_1\|_{0,q,\Omega}\,\|\boldsymbol{u}\|_{0,r,\Omega}\,\|\boldsymbol{v}'\|_{0,r,\Omega}$$

First, choosing $q = +\infty$ and $r = 2$, and applying Theorem 1.2.2, there exists a constant $c_4 > 0$, only depending of Ω and Γ_D, such that

$$c_2 \left|\boldsymbol{v}'\right|_{1,\Omega}^2 \leq \varepsilon_1 c_3 \left|\boldsymbol{v}'\right|_{1,\Omega} + c_4 \left\|\gamma_1\right\|_{\infty,\Omega} \left(\left|\boldsymbol{u}\right|_{1,\Omega} + \beta \left\|\boldsymbol{u}_D\right\|_{0,\Gamma_D}\right) \left|\boldsymbol{v}'\right|_{1,\Omega}$$

where $\left|\boldsymbol{u}\right|_{1,\Omega} + \beta \left\|\boldsymbol{u}_D\right\|_{0,\Gamma_D}$ is uniformly bounded (see Remark 5.3.1). Then, there exists $c_5 > 0$ such that

$$\left|\boldsymbol{v}'\right|_{1,\Omega} \leq c_5 \left(\left\|\gamma_1\right\|_{\infty,\Omega} + \varepsilon_1\right)$$

Taking $C_1 = c_5 + \left|\boldsymbol{g}\right|_{1,\Omega}$, we obtain

$$\left|\boldsymbol{u}'\right|_{1,\Omega} \leq \left|\boldsymbol{v}'\right|_{1,\Omega} + \varepsilon_1 \left|\boldsymbol{g}\right|_{1,\Omega} \leq C_1 \left(\left\|\gamma_1\right\|_{\infty,\Omega} + \varepsilon_1\right)$$

Second, choosing $q = 2$ and $r = 4$, applying Sobolev Embedding Theorem and Theorem 1.2.2, there exists $c_4 > 0$ such that

$$c_2 \left|\boldsymbol{v}'\right|_{1,\Omega}^2 \leq \varepsilon_1 c_3 \left|\boldsymbol{v}'\right|_{1,\Omega} + c_6 \left\|\gamma_1\right\|_{s,\Omega} \left(\left|\boldsymbol{u}\right|_{1,\Omega} + \beta \left\|\boldsymbol{u}_D\right\|_{0,\Gamma_D}\right) \left|\boldsymbol{v}'\right|_{1,\Omega}$$

Repeating the previous argument, there exists $C_2 > 0$ independent of γ, γ_1 and h such that

$$\left|\boldsymbol{v}'\right|_{1,\Omega} \leq c_5 \left(\left\|\gamma_1\right\|_{s,\Omega} + \varepsilon_1\right)$$

proving this lemma.

□

Lemma 5.5.2. *There exists $C > 0$ such that*

$$\left|\boldsymbol{\varphi}\right|_{1,\Omega} \leq C \left(\left|\boldsymbol{u}\right|_{1,\Omega} + \left\|\boldsymbol{u}_R\right\|_{0,\omega}\right)$$

Furthermore, $\left|\boldsymbol{\varphi}\right|_{1,\Omega}$ is uniformly bounded.

Proof. Testing the two equations of (5.4) with $\boldsymbol{\varphi}$ and ξ, respectively, and integrating by parts some terms, we obtain

$$\nu \left|\boldsymbol{\varphi}\right|_{1,\Omega}^2 + \frac{1}{2} \int_{\Gamma_N} \left(\boldsymbol{u} \cdot \boldsymbol{n}\right)_+ \left|\boldsymbol{\varphi}\right|^2 \, dS + \left(\gamma \boldsymbol{\varphi}, \boldsymbol{\varphi}\right)_{0,\Omega} + \left(\left(\nabla \boldsymbol{u}\right) \boldsymbol{\varphi}, \boldsymbol{\varphi}\right)_{0,\Omega}$$
$$- \frac{1}{2} \int_{\Gamma_N^-} \left(\boldsymbol{u} \cdot \boldsymbol{\varphi}\right) \left(\boldsymbol{\varphi} \cdot \boldsymbol{n}\right) \, dS = \left(\boldsymbol{u} - \boldsymbol{u}_R, \boldsymbol{\varphi}\right)_{0,\omega}$$

where

$$\frac{1}{2} \int_{\Gamma_N} \left(\boldsymbol{u} \cdot \boldsymbol{n}\right)_+ \left|\boldsymbol{\varphi}\right|^2 \, dS + \left(\gamma \boldsymbol{\varphi}, \boldsymbol{\varphi}\right)_{0,\Omega} \geq 0$$

Proceeding in the same way as in the proof of Lemma 5.5.1, there exists $c_1 \in (0, \nu)$ and $c_2 = \nu - c_1 > 0$ such that

$$c_2 \left|\boldsymbol{\varphi}\right|_{1,\Omega}^2 \leq \left(\boldsymbol{u} - \boldsymbol{u}_R, \boldsymbol{\varphi}\right)_{0,\omega}$$

Applying Hölder inequality and Theorem 1.2.2, there exists $c_3 > 0$ such that

$$c_2 \left|\boldsymbol{\varphi}\right|_{1,\Omega}^2 \leq \left(\boldsymbol{u} - \boldsymbol{u}_R, \boldsymbol{\varphi}\right)_{0,\omega} \leq \left(\left\|\boldsymbol{u}\right\|_{0,\omega} + \left\|\boldsymbol{u}_R\right\|_{0,\omega}\right) \left\|\boldsymbol{\varphi}\right\|_{0,\omega}$$

$$\leq \left(\|\boldsymbol{v}\|_{0,\Omega} + \|\boldsymbol{u}_R\|_{0,\omega}\right) \|\boldsymbol{\varphi}\|_{0,\Omega}$$
$$\leq c_3 \left(|\boldsymbol{v}|_{1,\Omega} + \|\boldsymbol{u}_R\|_{0,\omega}\right) |\boldsymbol{\varphi}|_{0,\Omega}$$

Then,

$$|\boldsymbol{\varphi}|_{1,\Omega} \leq \frac{c_3}{c_2} \left(|\boldsymbol{u}|_{1,\Omega} + \|\boldsymbol{u}_R\|_{0,\omega}\right)$$

The uniformly boundedness of $|\boldsymbol{\varphi}|_{1,\Omega}$ is consecuence of the uniformly boundedness of $|\boldsymbol{u}|_{1,\Omega}$. Taking $C = \dfrac{c_3}{c_2} > 0$, the lemma is proved.

□

Lemma 5.5.3. *Let* $(\gamma, \beta); (h, \varepsilon); (\gamma_1, \varepsilon_1) \in \mathcal{A}$ *such that*

$$[\boldsymbol{u}_1', p_1'] = A'(\gamma, \beta)[(\gamma_1, \varepsilon_1)] \text{ and } [\boldsymbol{u}_{*1}', p_{*1}'] = A'(\gamma + h, \beta + \varepsilon)[(\gamma_1, \varepsilon_1)]$$

There exist $C > 0$, *independent of* $\boldsymbol{v}$, γ, γ_1 *and* h, *such that* $|\boldsymbol{u}_{*1}' - \boldsymbol{u}_1'|_{1,\Omega} \leq C_1 \left(\|h\|_{\infty,\Omega} + \varepsilon\right) \left(\|\gamma_1\|_{s,\Omega} + \varepsilon_1\right)$.

Proof. Proceeding in the same way as in the previous lemma, denoting $[\boldsymbol{u}, p] = A(\gamma, \beta)$, $[\boldsymbol{u}_*, p_*] = A(\gamma + h, \beta + \varepsilon)$, $\boldsymbol{w} = \boldsymbol{u}_* - \boldsymbol{u}$, $\boldsymbol{w}' = \boldsymbol{u}_{*1}' - \boldsymbol{u}_1' \in \boldsymbol{H}^1_{\Gamma_D}(\Omega)$ and $q = p_{*1}' - p_1'$, we verify

$$\begin{aligned}
&\nu |\boldsymbol{w}'|^2_{1,\Omega} + (\gamma \boldsymbol{w}', \boldsymbol{w}')_{0,\Omega} + ((\nabla \boldsymbol{w}')\, \boldsymbol{u}_*, \boldsymbol{w}')_{0,\Omega} + ((\nabla \boldsymbol{u}_*)\, \boldsymbol{w}', \boldsymbol{w}')_{0,\Omega} \\
&\quad - \frac{1}{2} \int_{\Gamma_N} (\boldsymbol{u}_* \cdot \boldsymbol{n})_- |\boldsymbol{w}'|^2 \, dS - \frac{1}{2} \int_{\Gamma_N} |\boldsymbol{w}' \cdot \boldsymbol{n}| \, |\boldsymbol{u}_* \cdot \boldsymbol{w}'| \, dS \\
&\leq - (h \boldsymbol{u}_{*1}', \boldsymbol{w}')_{0,\Omega} - (\gamma_1 \boldsymbol{w}, \boldsymbol{w}')_{0,\Omega} - ((\nabla \boldsymbol{w})\, \boldsymbol{u}_1', \boldsymbol{w}')_{0,\Omega} - ((\nabla \boldsymbol{u}_1')\, \boldsymbol{w}, \boldsymbol{w}')_{0,\Omega} \\
&\quad + \frac{1}{2} \int_{\Gamma_N} |\boldsymbol{w} \cdot \boldsymbol{n}| \, |\boldsymbol{u}_1' \cdot \boldsymbol{w}'| \, dS + \frac{1}{2} \int_{\Gamma_N} |\boldsymbol{u}_1' \cdot \boldsymbol{n}| \, |\boldsymbol{w} \cdot \boldsymbol{w}'| \, dS
\end{aligned}$$

where

$$((\nabla \boldsymbol{w}')\, \boldsymbol{u}_*, \boldsymbol{w}')_{0,\Omega} - \frac{1}{2} \int_{\Gamma_N} (\boldsymbol{u}_* \cdot \boldsymbol{n})_- |\boldsymbol{w}'|^2 \, dS = \frac{1}{2} \int_{\Gamma_N} (\boldsymbol{u}_* \cdot \boldsymbol{n})_+ |\boldsymbol{w}|^2 \, dS \geq 0$$

and

$$((\nabla \boldsymbol{u}_*)\, \boldsymbol{w}', \boldsymbol{w}')_{0,\Omega} - \frac{1}{2} \int_{\Gamma_N} |\boldsymbol{w}' \cdot \boldsymbol{n}| \, |\boldsymbol{u}_* \cdot \boldsymbol{w}'| \, dS \geq -\frac{3\kappa}{2} |\boldsymbol{u}_*|_{1,\Omega} |\boldsymbol{w}'|^2_{1,\Omega}$$

Since sufficent condition of uniqueness of solution (see Theorem 1.2.3) and uniformly boundedness of $|\boldsymbol{u}|_{1,\Omega}$ (see Remark 5.3.1) imply that there exists a constant $c_1 > 0$ such that $\dfrac{3}{2}\kappa |\boldsymbol{u}|_{1,\Omega} \leq c_1 < \nu$. Then, there exists a constant $c_2 = \nu - c_1 > 0$, independent of $\boldsymbol{u}$, $\boldsymbol{u}_*$, (γ, β), (h, ε) and $(\gamma_1, \varepsilon_1)$ such that

$$\begin{aligned}
c_2 |\boldsymbol{w}'|^2_{1,\Omega} \leq &- (h \boldsymbol{u}_{*1}', \boldsymbol{w}')_{0,\Omega} - (\gamma_1 \boldsymbol{w}, \boldsymbol{w}')_{0,\Omega} - ((\nabla \boldsymbol{w})\, \boldsymbol{u}_1', \boldsymbol{w}')_{0,\Omega} - ((\nabla \boldsymbol{u}_1')\, \boldsymbol{w}, \boldsymbol{w}')_{0,\Omega} \\
&+ \frac{1}{2} \int_{\Gamma_N} |\boldsymbol{w} \cdot \boldsymbol{n}| \, |\boldsymbol{u}_1' \cdot \boldsymbol{w}'| \, dS + \frac{1}{2} \int_{\Gamma_N} |\boldsymbol{u}_1' \cdot \boldsymbol{n}| \, |\boldsymbol{w} \cdot \boldsymbol{w}'| \, dS
\end{aligned}$$

Applying Hölder inequality, Theorem 1.2.2, Lemma 1.2.2 and Sobolev Embedding Theorem, there exists $c_3 > 0$ independent of $\boldsymbol{u}$, $\boldsymbol{u}_*$, (γ, β), (h, ε) and $(\gamma_1, \varepsilon_1)$ such that

$$\begin{aligned}
&-\left(h\boldsymbol{u}'_{*1}, \boldsymbol{w}'\right)_{0,\Omega} - \left(\gamma_1 \boldsymbol{w}, \boldsymbol{w}'\right)_{0,\Omega} - \left(\left(\nabla \boldsymbol{w}\right)\boldsymbol{u}'_1, \boldsymbol{w}'\right)_{0,\Omega} - \left(\left(\nabla \boldsymbol{u}'_1\right)\boldsymbol{w}, \boldsymbol{w}'\right)_{0,\Omega} \\
\leq & c_3 \left|\boldsymbol{w}'\right|_{1,\Omega} \left(\left\|h\right\|_{\infty,\Omega} \left|\boldsymbol{u}'_{*1}\right|_{1,\Omega} + \left\|\gamma_1\right\|_{s,\Omega} \left|\boldsymbol{w}\right|_{1,\Omega} + \left|\boldsymbol{u}'_1\right|_{1,\Omega} \left|\boldsymbol{w}\right|_{1,\Omega}\right) \\
\leq & c_3 \left|\boldsymbol{w}'\right|_{1,\Omega} \left(\left\|h\right\|_{\infty,\Omega} \left|\boldsymbol{u}'_{*1}\right|_{1,\Omega} + \left\|\gamma_1\right\|_{s,\Omega} \left|\boldsymbol{w}\right|_{1,\Omega} + \left|\boldsymbol{u}'_1\right|_{1,\Omega} \left|\boldsymbol{w}\right|_{1,\Omega}\right) \\
\leq & c_3 \left\|\gamma_1\right\|_{s,\Omega} \left|\boldsymbol{v}_1 - \boldsymbol{v}\right|_{1,\Omega} \left|\boldsymbol{w}\right|_{1,\Omega}
\end{aligned}$$

Then, using Lemmas 5.4.1 and 5.5.1, there exists $c_4 > 0$ such that

$$\begin{aligned}
&-\left(h\boldsymbol{u}'_{*1}, \boldsymbol{w}'\right)_{0,\Omega} - \left(\gamma_1 \boldsymbol{w}, \boldsymbol{w}'\right)_{0,\Omega} - \left(\left(\nabla \boldsymbol{w}\right)\boldsymbol{u}'_1, \boldsymbol{w}'\right)_{0,\Omega} - \left(\left(\nabla \boldsymbol{u}'_1\right)\boldsymbol{w}, \boldsymbol{w}'\right)_{0,\Omega} \\
\leq & c_4 \left|\boldsymbol{w}'\right|_{1,\Omega} \left(\left\|h\right\|_{\infty,\Omega} + \varepsilon\right) \left(\left\|\gamma_1\right\|_{s,\Omega} + \varepsilon_1\right)
\end{aligned}$$

Now, applying Hölder inequality, Theorems 1.2.2 and 1.2.1, Lemma 1.2.3 and Sobolev Embedding Theorem, there exists $c_5 > 0$ such that

$$\frac{1}{2}\int_{\Gamma_N} \left|\boldsymbol{w}\cdot\boldsymbol{n}\right| \left|\boldsymbol{u}'_1 \cdot \boldsymbol{w}'\right| \ dS + \frac{1}{2}\int_{\Gamma_N} \left|\boldsymbol{u}'_1\cdot\boldsymbol{n}\right| \left|\boldsymbol{w}\cdot\boldsymbol{w}'\right| \ dS \leq c_5 \left|\boldsymbol{w}'\right|_{1,\Omega} \left|\boldsymbol{w}\right|_{1,\Omega} \left|\boldsymbol{u}'_1\right|_{1,\Omega}$$

Applying Lemmas 5.4.1 and 5.5.1 again, there exists $c_6 > 0$ such that

$$\begin{aligned}
&\frac{1}{2}\int_{\Gamma_N} \left|\boldsymbol{w}\cdot\boldsymbol{n}\right| \left|\boldsymbol{u}'_1 \cdot \boldsymbol{w}'\right| \ dS + \frac{1}{2}\int_{\Gamma_N} \left|\boldsymbol{u}'_1\cdot\boldsymbol{n}\right| \left|\boldsymbol{w}\cdot\boldsymbol{w}'\right| \ dS \\
\leq & c_6 \left|\boldsymbol{w}'\right|_{1,\Omega} \left(\left\|h\right\|_{\infty,\Omega} + \varepsilon\right) \left(\left\|\gamma_1\right\|_{s,\Omega} + \varepsilon_1\right)
\end{aligned}$$

In conclusion,

$$\begin{aligned}
c_2 \left|\boldsymbol{w}'\right|^2_{1,\Omega} &\leq \left(c_4 + c_6\right) \left|\boldsymbol{w}'\right|_{1,\Omega} \left(\left\|h\right\|_{\infty,\Omega} + \varepsilon\right) \left(\left\|\gamma_1\right\|_{s,\Omega} + \varepsilon_1\right) \\
\left|\boldsymbol{w}'\right|_{1,\Omega} &\leq \left(\frac{c_4 + c_6}{c_2}\right) \left(\left\|h\right\|_{\infty,\Omega} + \varepsilon\right) \left(\left\|\gamma_1\right\|_{s,\Omega} + \varepsilon_1\right)
\end{aligned}$$

proving the lemma.

□

Theorem 5.5.1. *The map $(\gamma, \beta) \longmapsto A'(\gamma, \beta)[(\gamma_1, \varepsilon_1)]$ from $\mathcal{A}$ to $\mathcal{H}$ is Fréchet-differentiable for each $(\gamma_1, \varepsilon_1) \in \mathcal{A}$. Let $(\gamma, \beta); (\gamma_1, \varepsilon_1); (\gamma_1, \varepsilon_1) \in \mathcal{A}$, the Fréchet derivative of $A'(\gamma, \beta)[(\gamma_1, \varepsilon_1)]$ on $(\gamma_2, \varepsilon_2)$ direction is given by $A''(\gamma, \beta)[(\gamma_1, \varepsilon_1); (\gamma_2, \varepsilon_2)] = [\boldsymbol{u}'', p'']$, where $[\boldsymbol{u}'', p'']$ is the unique weak solution of the problem*

$$\begin{aligned}
-\nu\triangle \boldsymbol{u}'' + \left(\nabla \boldsymbol{u}''\right)\boldsymbol{u} + \left(\nabla \boldsymbol{u}\right)\boldsymbol{u}'' + \nabla p'' + \gamma \boldsymbol{u}'' &= \boldsymbol{f}\left(\boldsymbol{u}'_1, \boldsymbol{u}'_2, \boldsymbol{u}''\right) && \text{in } \Omega \\
\operatorname{div} \boldsymbol{u}'' &= 0 && \text{in } \Omega \\
\boldsymbol{u}'' &= \boldsymbol{0} && \text{on } \Gamma_D \\
-\nu\frac{\partial \boldsymbol{u}''}{\partial \boldsymbol{n}} + p''\boldsymbol{n} + \frac{1}{2} g\left(\boldsymbol{v}, \boldsymbol{v}', \boldsymbol{v}''\right) &= \boldsymbol{0} && \text{on } \Gamma_N,
\end{aligned}$$

where $\boldsymbol{f}$ *and* $\boldsymbol{g}$ *are defined by*

$$\begin{aligned}\boldsymbol{f}\left(\boldsymbol{u}_1', \boldsymbol{u}_2', \boldsymbol{u}''\right) &= -\left[\left(\gamma_2 \boldsymbol{u}_1' + \gamma_1 \boldsymbol{u}_2'\right) + \left(\nabla \boldsymbol{u}_1'\right) \boldsymbol{u}_2' + \left(\nabla \boldsymbol{u}_2'\right) \boldsymbol{u}_1'\right] \\ \boldsymbol{g}\left(\boldsymbol{u}, \boldsymbol{u}_1', \boldsymbol{u}_2', \boldsymbol{u}''\right) &= \begin{cases} \boldsymbol{0} & \text{on } \Gamma_N^+ \\ \left(\boldsymbol{u}'' \cdot \boldsymbol{n}\right) \boldsymbol{u} + \left(\boldsymbol{u}_1' \cdot \boldsymbol{n}\right) \boldsymbol{u}_2' + \left(\boldsymbol{u}_2' \cdot \boldsymbol{n}\right) \boldsymbol{u}_1' + \left(\boldsymbol{u} \cdot \boldsymbol{n}\right) \boldsymbol{u}'' & \text{on } \Gamma_N^- \end{cases}\end{aligned}$$

and $A'\left(\gamma, \beta\right)\left[\left(\gamma_j, \varepsilon_j\right)\right] = \left[\boldsymbol{u}_j', p_j'\right]$, *for* $j \in \{1, 2\}$.

Proof. Let $\gamma, \gamma_1 \in \mathcal{A}$, it will be proved that there is a linear application $D_2 : \mathcal{A} \to \mathcal{H}$ such that

$$\begin{aligned}&A'\left(\gamma + \gamma_2, \beta + \varepsilon_2\right)\left[\left(\gamma_1, \varepsilon_1\right)\right] - A'\left(\gamma\right)\left[\left(\gamma_1, \varepsilon_1\right)\right] \\ =&D\left(\left(\gamma, \beta\right); \left(\gamma_2, \varepsilon_2\right)\right)\left[\left(\gamma_1, \varepsilon_1\right)\right] + r\left(\left(\gamma, \beta\right); \left(\gamma_1, \varepsilon_1\right); \left(\gamma_2, \varepsilon_2\right)\right),\end{aligned}$$

where

$$\left(\left\|\gamma_2\right\|_{\infty,\Omega} + \varepsilon_2\right) \to 0 \Rightarrow \frac{\left\|r\left(\left(\gamma, \beta\right); \left(\gamma_1, \varepsilon_1\right); \left(\gamma_2, \varepsilon_2\right)\right)\right\|_{\mathcal{H}}}{\left(\left\|\gamma_2\right\|_{\infty,\Omega} + \varepsilon_2\right)} \to 0.$$

Let $A'\left(\gamma + \gamma_2, \beta + \varepsilon_2\right)\left[\gamma_1, \varepsilon_1\right] = \left[\boldsymbol{u}_{*1}', p_{*1}'\right]$, (see Theorem 5.4.1), $A\left(\gamma, \beta\right) = \left[\boldsymbol{u}, p\right]$ and $A\left(\gamma + \gamma_2, \beta + \varepsilon_2\right) = \left[\boldsymbol{u}_*, p_*\right]$ (see Definition 5.3.3). Defining

$$D\left(\left(\gamma, \beta\right); \left(\gamma_1, \varepsilon_1\right)\right)\left[\left(\gamma_2, \varepsilon_2\right)\right] = \left[\boldsymbol{u}'', p''\right]$$

as function of $\left(\gamma_2, \varepsilon_2\right)$ and

$$r\left(\left(\gamma, \beta\right); \left(\gamma_1, \varepsilon_1\right); \left(\gamma_2, \varepsilon_2\right)\right) = \left[\delta \boldsymbol{u}, \delta p\right] = \left[\boldsymbol{u}_{*1}' - \boldsymbol{u}_1' - \boldsymbol{u}'', p_{*1}' - p_1' - p''\right],$$

it is possible to see that $D\left(\left(\gamma, \beta\right); \left(\gamma_1, \varepsilon_1\right)\right)$ is a linear application and $r\left(\left(\gamma, \beta\right); \left(\gamma_1, \varepsilon_1\right); \left(\gamma_2, \varepsilon_2\right)\right)$ is solution of the problem

$$\begin{aligned}-\nu \triangle\left(\delta \boldsymbol{u}\right) + \nabla\left(\delta p\right) + \gamma\left(\delta \boldsymbol{u}\right) + \left(\nabla \delta \boldsymbol{u}\right) \boldsymbol{u} + \left(\nabla \boldsymbol{u}\right) \delta \boldsymbol{u} &= \boldsymbol{f}_1\left(\boldsymbol{u}, \boldsymbol{u}_1', \boldsymbol{u}_{*1}', \boldsymbol{u}_2', \right) && \text{in } \Omega \\ \operatorname{div}\left(\delta \boldsymbol{u}\right) &= 0 && \text{in } \Omega \\ \left(\delta \boldsymbol{u}\right) &= \boldsymbol{0} && \text{on } \Gamma_D \\ -\nu \frac{\partial\left(\delta \boldsymbol{u}\right)}{\partial \boldsymbol{n}} + \left(\delta p\right) \boldsymbol{n} + \frac{1}{2} g_1\left(\boldsymbol{u}, \boldsymbol{u}_*, \boldsymbol{u}_1', \boldsymbol{u}_2', \boldsymbol{u}_{*1}', \boldsymbol{u}''\right) &= \boldsymbol{0} && \text{on } \Gamma_N,\end{aligned}$$

where

$$\begin{aligned}\boldsymbol{f}_1\left(\boldsymbol{u}, \boldsymbol{u}_1', \boldsymbol{u}_{*1}', \boldsymbol{u}_2', \right) =& \gamma_2\left(\boldsymbol{u}_1' - \boldsymbol{u}_{*1}'\right) + \left(\nabla \boldsymbol{u}_2'\right)\left(\boldsymbol{u}_1' - \boldsymbol{u}_2'\right) + \left(\nabla\left(\boldsymbol{u}_1' - \boldsymbol{u}_2'\right)\right) \boldsymbol{u}_2' \\ &+ \gamma_1\left(\boldsymbol{u}_2' + \boldsymbol{u} - \boldsymbol{u}_*\right) + \left(\nabla \boldsymbol{u}_{*1}'\right)\left(\boldsymbol{u}_2' + \boldsymbol{u} - \boldsymbol{u}_*\right) + \left(\nabla\left(\boldsymbol{u}_2' + \boldsymbol{u}\right.\right. \\ &\left.\left. - \boldsymbol{u}_* \boldsymbol{u}_{*1}'\right.\right.\end{aligned}$$

and g_1 is an appropriate function. Testing the equations with $\delta \boldsymbol{u}$ and δp, respectively and integrating by parts, we obtain

$$\begin{aligned}&\nu\left|\delta \boldsymbol{u}\right|_{1,\Omega}^2 + \left(\gamma_1 \delta \boldsymbol{u}, \delta \boldsymbol{u}\right)_{0,\Omega} + \left(\left(\nabla \delta \boldsymbol{u}\right) \boldsymbol{u}, \delta \boldsymbol{u}\right)_{0,\Omega} + \left(\left(\nabla \boldsymbol{u}\right) \delta \boldsymbol{u}, \delta \boldsymbol{u}\right)_{0,\Omega} \\ &- \frac{1}{2} \int_{\Gamma_N} \left(\boldsymbol{u} \cdot \boldsymbol{n}\right)_- \left|\delta \boldsymbol{u}\right|^2 \, dS - \frac{1}{2} \int_{\Gamma_N} \left|\delta \boldsymbol{u} \cdot \boldsymbol{n}\right| \left|\boldsymbol{u} \cdot \delta \boldsymbol{u}\right| \, dS\end{aligned}$$

$$
\begin{aligned}
&\leq \left(\gamma_2\left(\boldsymbol{u}_1'-\boldsymbol{u}_{*1}'\right)+\left(\nabla\boldsymbol{u}_2'\right)\left(\boldsymbol{u}_1'-\boldsymbol{u}_2'\right)+\left(\nabla\left(\boldsymbol{u}_1'-\boldsymbol{u}_2'\right)\right)\boldsymbol{u}_2',\delta\boldsymbol{v}\right)_{0,\Omega}\\
&\quad+\left(\gamma_1\left(\boldsymbol{u}_2'+\boldsymbol{u}-\boldsymbol{u}_*\right)+\left(\nabla\boldsymbol{u}_{*1}'\right)\left(\boldsymbol{u}_2'+\boldsymbol{u}-\boldsymbol{u}_*\right)+\left(\nabla\left(\boldsymbol{u}_2'+\boldsymbol{u}-\boldsymbol{u}_*\right)\right)\boldsymbol{u}_{*1}',\delta\boldsymbol{u}\right)_{0,\Omega}\\
&\quad+\frac{1}{2}\int_{\Gamma_N}\left|\left(\boldsymbol{u}_1'-\boldsymbol{u}_2'\right)\cdot\boldsymbol{n}\right|\left|\boldsymbol{u}_2'\cdot\delta\boldsymbol{u}\right|\,dS+\frac{1}{2}\int_{\Gamma_N}\left|\boldsymbol{u}_2'\cdot\boldsymbol{n}\right|\left|\left(\boldsymbol{u}_1'-\boldsymbol{u}_2'\right)\cdot\delta\boldsymbol{u}\right|\,dS\\
&\quad+\frac{1}{2}\int_{\Gamma_N}\left|\left(\boldsymbol{u}_2'+\boldsymbol{u}-\boldsymbol{u}_*\right)\cdot\boldsymbol{n}\right|\left|\boldsymbol{u}_{*1}'\cdot\delta\boldsymbol{u}\right|\,dS+\frac{1}{2}\int_{\Gamma_N}\left|\boldsymbol{u}_{*1}'\cdot\boldsymbol{n}\right|\left|\left(\boldsymbol{u}_2'+\boldsymbol{u}-\boldsymbol{u}_*\right)\cdot\delta\boldsymbol{u}\right|\,dS
\end{aligned}
$$

Reasoning as in Lemma 5.5.3, there exists a constant $C_1>0$, independent of γ, γ_1 and γ_2 such that

$$
\left|\delta\boldsymbol{u}\right|_{1,\Omega}^2\leq C_1\left(A_1+A_2\right)
$$

where A_1 and A_2 are given by

$$
\begin{aligned}
A_1=&\left(\gamma_1\left(\boldsymbol{u}_2'+\boldsymbol{u}-\boldsymbol{u}_*\right)+\left(\nabla\boldsymbol{u}_{*1}'\right)\left(\boldsymbol{u}_2'+\boldsymbol{u}-\boldsymbol{u}_*\right)+\left(\nabla\left(\boldsymbol{u}_2'+\boldsymbol{u}-\boldsymbol{u}_*\right)\right)\boldsymbol{u}_{*1}',\delta\boldsymbol{u}\right)_{0,\Omega}\\
&+\frac{1}{2}\int_{\Gamma_N}\left|\left(\boldsymbol{u}_2'+\boldsymbol{u}-\boldsymbol{u}_*\right)\cdot\boldsymbol{n}\right|\left|\boldsymbol{u}_{*1}'\cdot\delta\boldsymbol{u}\right|\,dS+\frac{1}{2}\int_{\Gamma_N}\left|\boldsymbol{u}_{*1}'\cdot\boldsymbol{n}\right|\left|\left(\boldsymbol{u}_2'+\boldsymbol{u}-\boldsymbol{u}_*\right)\cdot\delta\boldsymbol{u}\right|\,dS\\
A_2=&\left(\gamma_2\left(\boldsymbol{u}_1'-\boldsymbol{u}_{*1}'\right)+\left(\nabla\boldsymbol{u}_2'\right)\left(\boldsymbol{u}_1'-\boldsymbol{u}_2'\right)+\left(\nabla\left(\boldsymbol{u}_1'-\boldsymbol{u}_2'\right)\right)\boldsymbol{u}_2',\delta\boldsymbol{v}\right)_{0,\Omega}\\
&+\frac{1}{2}\int_{\Gamma_N}\left|\left(\boldsymbol{u}_1'-\boldsymbol{u}_2'\right)\cdot\boldsymbol{n}\right|\left|\boldsymbol{u}_2'\cdot\delta\boldsymbol{u}\right|\,dS+\frac{1}{2}\int_{\Gamma_N}\left|\boldsymbol{u}_2'\cdot\boldsymbol{n}\right|\left|\left(\boldsymbol{u}_1'-\boldsymbol{u}_2'\right)\cdot\delta\boldsymbol{u}\right|\,dS
\end{aligned}
$$

Applying Hölder inequality, Theorem 1.2.2, Sobolev Embedding Theorem, Lemmas 1.2.1, 1.2.2 and 1.2.3, there exist constants $c_1>0$ and $c_2>0$ (γ,β), (γ_1,ε_1) and (γ_2,ε_2) such that

$$
\begin{aligned}
A_1=&\left(\gamma_1\left(\boldsymbol{u}_2'+\boldsymbol{u}-\boldsymbol{u}_*\right)+\left(\nabla\boldsymbol{u}_{*1}'\right)\left(\boldsymbol{u}_2'+\boldsymbol{u}-\boldsymbol{u}_*\right)+\left(\nabla\left(\boldsymbol{u}_2'+\boldsymbol{u}-\boldsymbol{u}_*\right)\right)\boldsymbol{u}_{*1}',\delta\boldsymbol{u}\right)_{0,\Omega}\\
&+\frac{1}{2}\int_{\Gamma_N}\left|\left(\boldsymbol{u}_2'+\boldsymbol{u}-\boldsymbol{u}_*\right)\cdot\boldsymbol{n}\right|\left|\boldsymbol{u}_{*1}'\cdot\delta\boldsymbol{u}\right|\,dS+\frac{1}{2}\int_{\Gamma_N}\left|\boldsymbol{u}_{*1}'\cdot\boldsymbol{n}\right|\left|\left(\boldsymbol{u}_2'+\boldsymbol{u}-\boldsymbol{u}_*\right)\cdot\delta\boldsymbol{u}\right|\,dS\\
&\leq\left|\delta\boldsymbol{u}\right|_{1,\Omega}\left(c_1\left\|\gamma_1\right\|_{\infty,\Omega}\left|\boldsymbol{u}_2'+\boldsymbol{u}-\boldsymbol{u}_*\right|_{1,\Omega}+c_2\left|\boldsymbol{u}_2'+\boldsymbol{u}-\boldsymbol{u}_*\right|_{1,\Omega}\left|\boldsymbol{u}_{*1}'\right|_{1,\Omega}\right)
\end{aligned}
$$

and, using Lemmas 5.5.1 and 5.5.3, there exists a constant $c_3>0$ such that

$$
\begin{aligned}
A_2=&\left(\gamma_2\left(\boldsymbol{u}_1'-\boldsymbol{u}_{*1}'\right)+\left(\nabla\boldsymbol{u}_2'\right)\left(\boldsymbol{u}_1'-\boldsymbol{u}_2'\right)+\left(\nabla\left(\boldsymbol{u}_1'-\boldsymbol{u}_2'\right)\right)\boldsymbol{u}_2',\delta\boldsymbol{v}\right)_{0,\Omega}\\
&+\frac{1}{2}\int_{\Gamma_N}\left|\left(\boldsymbol{u}_1'-\boldsymbol{u}_2'\right)\cdot\boldsymbol{n}\right|\left|\boldsymbol{u}_2'\cdot\delta\boldsymbol{u}\right|\,dS+\frac{1}{2}\int_{\Gamma_N}\left|\boldsymbol{u}_2'\cdot\boldsymbol{n}\right|\left|\left(\boldsymbol{u}_1'-\boldsymbol{u}_2'\right)\cdot\delta\boldsymbol{u}\right|\,dS\\
&\leq\left|\delta\boldsymbol{u}\right|_{1,\Omega}\left(c_1\left\|\gamma_2\right\|_{\infty,\Omega}\left|\boldsymbol{u}_1'-\boldsymbol{u}_{*1}'\right|_{1,\Omega}+c_2\left|\boldsymbol{u}_1'-\boldsymbol{u}_{*1}'\right|_{1,\Omega}\left|\boldsymbol{u}_2'\right|_{1,\Omega}\right)\\
&\leq c_3\left|\delta\boldsymbol{u}\right|_{1,\Omega}\left(\left\|\gamma_2\right\|_{\infty,\Omega}+\varepsilon_2\right)^2
\end{aligned}
$$

Repeating the reasoning of the proof of the Theorem 5.4.1, it is possible to prove that there exists $c_4>0$, independent of γ, γ_1 and γ_2, such that

$$
\left|\left(\boldsymbol{v}_2'+\boldsymbol{v}-\boldsymbol{w}\right)\right|_{1,\Omega}\leq c_4\left(\left\|\gamma_2\right\|_{\infty,\Omega}+\varepsilon_2\right)
$$

Thus, there exists $C_2>0$, independent of γ, γ_1 and γ_2, such that

$$
\left|\delta\boldsymbol{v}\right|_{1,\Omega}^2\leq C_1\left(A_1+A_2\right)\leq C_2\left(\left\|\gamma_2\right\|_{\infty,\Omega}+\varepsilon_2\right)^2\left|\delta\boldsymbol{v}\right|_{1,\Omega}
$$

Repeating the same arguments, it is possible to prove that there exists $C_3 < 0$ such that

$$\|\delta p\|_{0,\Omega} \leq C_3 \left(\|\gamma_2\|_{\infty,\Omega} + \varepsilon_2 \right)^2$$

In conclusion,

$$\|r\left((\gamma,\beta);(\gamma_1,\varepsilon_1);(\gamma_2,\varepsilon_2)\right)\|_{\mathcal{H}} = (C_2 + C_3) \left(\|\gamma_2\|_{\infty,\Omega} + \varepsilon_2 \right)^2$$

Therefore,

$$\frac{\|r\left((\gamma,\beta);(\gamma_1,\varepsilon_1);(\gamma_2,\varepsilon_2)\right)\|_{\mathcal{H}}}{\left(\|\gamma_2\|_{\infty,\Omega} + \varepsilon_2 \right)^2} \leq (C_2 + C_3) \left(\|\gamma_2\|_{\infty,\Omega} + \varepsilon_2 \right) \overset{(\|\gamma_2\|_{\infty,\Omega}+\varepsilon_2)\to 0}{\longrightarrow} 0,$$

proving the theorem.

□

Let $(\gamma,\beta);(\gamma_1,\varepsilon_1);(\gamma_2,\varepsilon_2) \in \mathcal{A}$. An expresion for the Fréchet second derivative of $J(\gamma)$ on directions (γ_1,ε_1) and (γ_2,ε_2) is given by

$$\begin{aligned} J''(\gamma,\beta)\left[(\gamma_1,\varepsilon_1);(\gamma_2,\varepsilon_2)\right] =& B''\left(A(\gamma,\beta)\right)\left[A_1'(\gamma,\beta)\left[(\gamma_1,\varepsilon_1)\right], A_1'(\gamma,\beta)\left[(\gamma_2,\varepsilon_2)\right]\right] \\ &+ B'\left(\left(A(\gamma,\beta)\right)\right)\left[A_1''(\gamma,\beta)\left[(\gamma_1,\varepsilon_1);(\gamma_2,\varepsilon_2)\right]\right] \\ &+ C''(\gamma)\left[\gamma_1,\gamma_2\right] \\ =& \left(\boldsymbol{u}_1', \boldsymbol{u}_2'\right)_{0,\Omega} + \left(\boldsymbol{u} - \boldsymbol{u}_R, \boldsymbol{u}''\right)_{0,\omega} + \alpha\left(\gamma_1,\gamma_2\right)_{s,\Omega}, \end{aligned}$$

where, reasoning as in the proof of Theorem 5.4.2,

$$\begin{aligned} \left(\boldsymbol{u} - \boldsymbol{u}_D, \boldsymbol{u}''\right)_{0,\omega} =& -\left(\gamma_1 \boldsymbol{u}_2' + \gamma_2 \boldsymbol{u}_1' + \left(\nabla \boldsymbol{u}_1'\right)\boldsymbol{u}_2' + \left(\nabla \boldsymbol{u}_2'\right)\boldsymbol{u}_1', \boldsymbol{\varphi}\right)_{0,\Omega} \\ &+ \frac{1}{2}\int_{\Gamma_N^-} \left(\left(\boldsymbol{u}_1' \cdot \boldsymbol{n}\right)\boldsymbol{u}_2 + \left(\boldsymbol{u}_2' \cdot \boldsymbol{n}\right)\boldsymbol{u}_1\right) \cdot \boldsymbol{\varphi}\, dS. \end{aligned}$$

In consequence,

$$\begin{aligned} J''(\gamma,\beta)\left[(\gamma_1,\varepsilon_1);(\gamma_2,\varepsilon_2)\right] &= \left(\boldsymbol{u}_1', \boldsymbol{u}_2'\right)_{0,\Omega} + \left(\boldsymbol{u} - \boldsymbol{u}_R, \boldsymbol{u}''\right)_{0,\omega} + \alpha\left(\gamma_1,\gamma_2\right)_{s,\Omega} \\ &= \left(\boldsymbol{u}_1', \boldsymbol{u}_2'\right)_{0,\Omega} - \left(\gamma_1 \boldsymbol{u}_2' + \gamma_2 \boldsymbol{u}_1' + \left(\nabla \boldsymbol{u}_1'\right)\boldsymbol{u}_2' + \left(\nabla \boldsymbol{u}_2'\right)\boldsymbol{u}_1', \boldsymbol{\varphi}\right)_{0,\Omega} \\ &\quad + \alpha\left(\gamma_1,\gamma_2\right)_{s,\Omega} + \frac{1}{2}\int_{\Gamma_N^-} \left(\left(\boldsymbol{u}_1' \cdot \boldsymbol{n}\right)\boldsymbol{u}_2 + \left(\boldsymbol{u}_2' \cdot \boldsymbol{n}\right)\boldsymbol{u}_1\right) \cdot \boldsymbol{\varphi}\, dS. \end{aligned}$$

In what follows, a second order optimality condition is proved. For this, a series of technical results are required. Let $(\gamma,\beta),(\gamma_1,\varepsilon_1),(\gamma_2,\varepsilon_2),(h,\varepsilon) \in \mathcal{A}$, consider $A(\gamma,\beta) = [\boldsymbol{u},p]$, $A(\gamma+h,\beta+\varepsilon) = [\boldsymbol{u}_*,p_*]$, with respective adjoint states $[\boldsymbol{\varphi},\xi]$ and $[\boldsymbol{\varphi}_*,\xi_*]$, $A'(\gamma,\beta)\left[(\gamma_k,\varepsilon_k)\right] = [\boldsymbol{u}_k', p_k']$ and $[\boldsymbol{u}_{*k}', p_{*k}'] = A'(\gamma+h,\beta+\varepsilon)\left[(\gamma_k,\varepsilon_k)\right]$ for $k \in \{1,2\}$. Using this, it is possible to obtain the following estimations.

Lemma 5.5.4. *There exists $C > 0$ such that*

$$\begin{aligned} \left|\left(\boldsymbol{u}_{*1}' - \boldsymbol{u}_1', \boldsymbol{u}_2'\right)_{0,\Omega}\right| &\leq C\left(\|\gamma_1\|_{s,\Omega} + \varepsilon_1\right)\left(\|\gamma_2\|_{s,\Omega} + \varepsilon_2\right)\left(\|h\|_{\infty,\Omega} + \varepsilon\right) \\ \left|\left(\boldsymbol{u}_{*1}', \boldsymbol{u}_{2*}' - \boldsymbol{u}_2'\right)_{0,\Omega}\right| &\leq C\left(\|\gamma_1\|_{s,\Omega} + \varepsilon_1\right)\left(\|\gamma_2\|_{s,\Omega} + \varepsilon_2\right)\left(\|h\|_{\infty,\Omega} + \varepsilon\right). \end{aligned}$$

Proof. Applying Cauchy-Schwartz inequality and Theorem 1.2.2, since $\boldsymbol{u}'_{*1} - \boldsymbol{u}'_1 \in \boldsymbol{H}^1_{\Gamma_D}(\Omega)$, there exists $c_1 > 0$ such that

$$\left|(\boldsymbol{u}'_{*1} - \boldsymbol{u}'_1, \boldsymbol{u}'_2)_{0,\Omega}\right| \leq \|\boldsymbol{u}'_{*1} - \boldsymbol{u}'_1\|_{0,\Omega} \|\boldsymbol{u}'_2\|_{0,\Omega} \leq c_1 |\boldsymbol{u}'_{*1} - \boldsymbol{u}'_1|_{1,\Omega} |\boldsymbol{u}'_2|_{1,\Omega}$$

Using Lemma 5.5.1 and Lemma 5.5.3, there exist $c_2 > 0$ and $c_3 > 0$ such that

$$\begin{aligned}\left|(\boldsymbol{u}'_{*1} - \boldsymbol{u}'_1, \boldsymbol{u}'_2)_{0,\Omega}\right| &\leq c_1 |\boldsymbol{u}'_{*1} - \boldsymbol{u}'_1|_{1,\Omega} |\boldsymbol{u}'_2|_{1,\Omega} \\ &\leq c_1 \left(c_2 \left(\|h\|_{\infty,\Omega} + \varepsilon\right) \left(\|\gamma_1\|_{s,\Omega} + \varepsilon_1\right)\right) \left(c_3 \left(\|\gamma_2\|_{s,\Omega} + \varepsilon_2\right)\right) \\ &\leq C \left(\|\gamma_1\|_{s,\Omega} + \varepsilon_1\right) \left(\|\gamma_2\|_{s,\Omega} + \varepsilon_2\right) \left(\|h\|_{\infty,\Omega} + \varepsilon\right)\end{aligned}$$

where $C = c_1 c_2 c_3$. The second estimate is analogous.

□

Lemma 5.5.5. *There exist $C > 0$ such that $|\boldsymbol{\varphi}_* - \boldsymbol{\varphi}|_{1,\Omega} \leq C \|h\|_{\infty,\Omega}$.*

Proof. Analogous to the proof of Lemma 5.5.3. □

Lemma 5.5.6. *Let $k, j \in \{1, 2\}$, with $j \neq k$. There exists $C > 0$ such that*

$$\left|(\gamma_j \boldsymbol{u}'_{*k}, \boldsymbol{\varphi}_* - \boldsymbol{\varphi})_{0,\Omega}\right| \leq C \left(\|\gamma_1\|_{s,\Omega} + \varepsilon_1\right) \left(\|\gamma_2\|_{s,\Omega} + \varepsilon_2\right) \left(\|h\|_{\infty,\Omega} + \varepsilon\right).$$

Proof. First, applying Hölder inequality, Sobolev Embedding Theorem and Theorem 1.2.2, there exists $c_1 > 0$ such that

$$\begin{aligned}\left|\left(\gamma_j \boldsymbol{v}'_{h,k}, \boldsymbol{\varphi}_h - \boldsymbol{\varphi}\right)_{0,\Omega}\right| &\leq \|\gamma_j\|_{0,\Omega} \left\|\boldsymbol{v}'_{h,k}\right\|_{0,4,\Omega} \|\boldsymbol{\varphi}_h - \boldsymbol{\varphi}\|_{0,4,\Omega} \\ &\leq c_1 \|\gamma_j\|_{s,\Omega} \left|\boldsymbol{v}'_{h,k}\right|_{1,\Omega} |\boldsymbol{\varphi}_h - \boldsymbol{\varphi}|_{1,\Omega}.\end{aligned}$$

Applying Lemmas 5.5.1 and 5.5.5, there exists $c_2 > 0$ and $c_3 > 0$ such that

$$\begin{aligned}\left|\left(\gamma_j \boldsymbol{v}'_{h,k}, \boldsymbol{\varphi}_h - \boldsymbol{\varphi}\right)_{0,\Omega}\right| &\leq c_1 \|\gamma_j\|_{s,\Omega} \left|\boldsymbol{v}'_{h,k}\right|_{1,\Omega} |\boldsymbol{\varphi}_h - \boldsymbol{\varphi}|_{1,\Omega} \\ &\leq c_1 \|\gamma_j\|_{s,\Omega} \left(c_2 \|\gamma_k\|_{s,\Omega}\right) \left(c_3 \|h\|_{\infty,\Omega}\right) \\ &\leq C \|\gamma_j\|_{s,\Omega} \|\gamma_k\|_{s,\Omega} \|h\|_{\infty,\Omega}\end{aligned}$$

where $C = c_1 c_2 c_3$. Thus, the lemma is proved. □

First, applying Hölder inequality, Sobolev Embedding Theorem and Theorem 1.2.2, there exists $c_1 > 0$ such that

$$\begin{aligned}\left|(\gamma_j \boldsymbol{u}'_{*k}, \boldsymbol{\varphi}_* - \boldsymbol{\varphi})_{0,\Omega}\right| &\leq \|\gamma_j\|_{0,\Omega} \|\boldsymbol{u}'_{*k}\|_{0,4,\Omega} \|\boldsymbol{\varphi}_* - \boldsymbol{\varphi}\|_{0,4,\Omega} \\ &\leq c_1 \|\gamma_j\|_{s,\Omega} \left(|\boldsymbol{u}'_{*k}|_{1,\Omega} + \varepsilon \|\boldsymbol{u}_D\|_{1/2,\Gamma_D}\right) |\boldsymbol{\varphi}_h - \boldsymbol{\varphi}|_{1,\Omega}.\end{aligned}$$

Applying Lemmas 5.5.1 and 5.5.5, there exists $c_2 > 0$ and $c_3 > 0$ such that

$$\left|(\gamma_j \boldsymbol{u}'_{*k}, \boldsymbol{\varphi}_* - \boldsymbol{\varphi})_{0,\Omega}\right| \leq c_1 \|\gamma_j\|_{s,\Omega} \left(|\boldsymbol{u}'_{*k}|_{1,\Omega} + \varepsilon \|\boldsymbol{u}_D\|_{1/2,\Gamma_D}\right) |\boldsymbol{\varphi}_h - \boldsymbol{\varphi}|_{1,\Omega}$$

$$\begin{aligned}&\leq c_1 \|\gamma_j\|_{s,\Omega} \left(c_2 \left(\|\gamma_k\|_{s,\Omega} + \varepsilon_k\right)\right) \left(c_3 \left(\|h\|_{\infty,\Omega} + \varepsilon\right)\right)\\ &\leq C \left(\|\gamma_1\|_{s,\Omega} + \varepsilon_1\right) \left(\|\gamma_2\|_{s,\Omega} + \varepsilon_2\right) \left(\|h\|_{\infty,\Omega} + \varepsilon\right)\end{aligned}$$

where $C = c_1 c_2 c_3$. Thus, the lemma is proved.

Lemma 5.5.7. *Let $k, j \in \{1, 2\}$, with $j \neq k$. There exists $C > 0$ such that*

1. $\left|\left(\left(\nabla \boldsymbol{u}'_{*j}\right) \boldsymbol{u}'_{*k}, \boldsymbol{\varphi}_h - \boldsymbol{\varphi}\right)_{0,\Omega}\right| \leq C \left(\|\gamma_1\|_{s,\Omega} + \varepsilon_1\right) \left(\|\gamma_2\|_{s,\Omega} + \varepsilon_2\right) \left(\|h\|_{\infty,\Omega} + \varepsilon\right)$
2. $\left|\left(\left(\nabla \boldsymbol{u}'_{*j} - \boldsymbol{u}'_j\right) \boldsymbol{u}'_{*k}, \boldsymbol{\varphi}\right)_{0,\Omega}\right| \leq C \left(\|\gamma_1\|_{s,\Omega} + \varepsilon_1\right) \left(\|\gamma_2\|_{s,\Omega} + \varepsilon_2\right) \left(\|h\|_{\infty,\Omega} + \varepsilon\right)$
3. $\left|\left(\left(\nabla \boldsymbol{u}'_{*j}\right) \left(\boldsymbol{u}'_{*k} - \boldsymbol{u}'_k\right), \boldsymbol{\varphi}\right)_{0,\Omega}\right| \leq C \left(\|\gamma_1\|_{s,\Omega} + \varepsilon_1\right) \left(\|\gamma_2\|_{s,\Omega} + \varepsilon_2\right) \left(\|h\|_{\infty,\Omega} + \varepsilon\right)$
4. $\left|\left(\boldsymbol{u}'_{*j} \cdot \boldsymbol{n}, \boldsymbol{u}'_{*k} \cdot \left(\boldsymbol{\varphi}_* - \boldsymbol{\varphi}\right)\right)_{0,\Gamma_N}\right| \leq C \left(\|\gamma_1\|_{s,\Omega} + \varepsilon_1\right) \left(\|\gamma_2\|_{s,\Omega} + \varepsilon_2\right) \left(\|h\|_{\infty,\Omega} + \varepsilon\right)$
5. $\left|\left(\left(\boldsymbol{u}'_{*j} - \boldsymbol{u}'_j\right) \cdot \boldsymbol{n}, \boldsymbol{u}'_{*k} \cdot \boldsymbol{\varphi}\right)_{0,\Gamma_N}\right| \leq C \left(\|\gamma_1\|_{s,\Omega} + \varepsilon_1\right) \left(\|\gamma_2\|_{s,\Omega} + \varepsilon_2\right) \left(\|h\|_{\infty,\Omega} + \varepsilon\right)$
6. $\left|\left(\boldsymbol{u}'_{*j} \cdot \boldsymbol{n}, \left(\boldsymbol{u}'_{*k} - \boldsymbol{u}'_k\right) \boldsymbol{\varphi}\right)_{0,\Gamma_N}\right| \leq C \left(\|\gamma_1\|_{s,\Omega} + \varepsilon_1\right) \left(\|\gamma_2\|_{s,\Omega} + \varepsilon_2\right) \left(\|h\|_{\infty,\Omega} + \varepsilon\right)$

Proof. Using Theorems 1.2.2 and 1.2.2, we obtain

$$\left|\left(\left(\nabla \boldsymbol{u}'_{*j}\right) \boldsymbol{u}'_{*k}, \boldsymbol{\varphi}_h - \boldsymbol{\varphi}\right)_{0,\Omega}\right| \leq \kappa \left|\boldsymbol{u}'_{*j}\right|_{1,\Omega} \left|\boldsymbol{v}'_{*k}\right|_{1,\Omega} \left|\boldsymbol{\varphi}_h - \boldsymbol{\varphi}\right|_{1,\Omega}$$

Applying Lemmas 5.5.3 and 5.5.5, there exists $c_1 > 0$ and $c_2 > 0$ such that

$$\begin{aligned}\left|\left(\left(\nabla \boldsymbol{u}'_{*j}\right) \boldsymbol{u}'_{*k}, \boldsymbol{\varphi}_h - \boldsymbol{\varphi}\right)_{0,\Omega}\right| &\leq \kappa c_1^2 c_2 \left(\left(\|\gamma_j\|_{s,\Omega} + \varepsilon_j\right)\right) \left(\left(\|\gamma_k\|_{s,\Omega} + \varepsilon_k\right)\right) \left(\left(\|h\|_{\infty,\Omega} + \varepsilon\right)\right)\\ &\leq C \left(\|\gamma_1\|_{s,\Omega} + \varepsilon_1\right) \left(\|\gamma_2\|_{s,\Omega} + \varepsilon_2\right) \left(\|h\|_{\infty,\Omega} + \varepsilon\right)\end{aligned}$$

where $C = \kappa c_1^2 c_2 > 0$, proving the first estimate. The proof of the following two estimates are similar. Finally, the last three estimates can be obtained using Theorem 1.2.3 instead of Theorem 1.2.2

□

Theorem 5.5.2. *Let $(\gamma, \beta); (h, \varepsilon) (\gamma_1, \varepsilon_1); (\gamma_2, \varepsilon_2) \in \mathcal{A}$. There exists $L > 0$ such that*

$$\begin{aligned}&\left|\left(J''(\gamma + h, \beta + \varepsilon) - J''(\gamma, \beta)\right) \left[(\gamma_1, \varepsilon_1); (\gamma_2, \varepsilon_2)\right]\right|\\ \leq &L \left(\|\gamma_1\|_{s,\Omega} + \varepsilon_1\right) \left(\|\gamma_2\|_{s,\Omega} + \varepsilon_2\right) \left(\|h\|_{\infty,\Omega} + \varepsilon\right).\end{aligned}$$

Proof. Applying triangular inequality, we obtain

$$\begin{aligned}&\left|\left(J''(\gamma + h, \beta + \varepsilon) - J''(\gamma, \beta)\right) \left[(\gamma_1, \varepsilon_1); (\gamma_2, \varepsilon_2)\right]\right|\\ \leq &\left|\left(\boldsymbol{u}'_{*,1}, \boldsymbol{u}'_{*,2} - \boldsymbol{u}'_2\right)_{0,\Omega}\right| + \left|\left(\boldsymbol{u}'_{*,1} - \boldsymbol{u}'_1, \boldsymbol{u}'_2\right)_{0,\Omega}\right|\\ &+ \left|\left(\gamma_1 \boldsymbol{u}'_{*,2}, \boldsymbol{\varphi}_* - \boldsymbol{\varphi}\right)_{0,\Omega}\right| + \left|\left(\gamma_1 \left(\boldsymbol{u}'_{*,2} - \boldsymbol{u}'_2\right), \boldsymbol{\varphi}\right)_{0,\Omega}\right|\\ &+ \left|\left(\gamma_2 \boldsymbol{u}'_{*,1}, \boldsymbol{\varphi}_* - \boldsymbol{\varphi}\right)_{0,\Omega}\right| + \left|\left(\gamma_2 \left(\boldsymbol{u}'_{*,1} - \boldsymbol{u}'_1\right), \boldsymbol{\varphi}\right)_{0,\Omega}\right|\end{aligned}$$

$$
\begin{aligned}
&+\left|\left(\left(\nabla \boldsymbol{u}'_{*,1}\right)\boldsymbol{u}'_{*,2},\boldsymbol{\varphi}_*-\boldsymbol{\varphi}\right)_{0,\Omega}\right|+\left|\left(\boldsymbol{u}'_{*1}\cdot\boldsymbol{n},\boldsymbol{u}'_{*2}\cdot\left(\boldsymbol{\varphi}_*-\boldsymbol{\varphi}\right)\right)_{0,\Gamma_N}\right|\\
&+\left|\left(\left(\nabla \boldsymbol{u}'_{*,1}-\boldsymbol{u}'_1\right)\boldsymbol{u}'_{*,2},\boldsymbol{\varphi}\right)_{0,\Omega}\right|+\left|\left(\left(\boldsymbol{u}'_{*1}-\boldsymbol{u}'_1\right)\cdot\boldsymbol{n},\boldsymbol{u}'_{*2}\cdot\boldsymbol{\varphi}\right)_{0,\Gamma_N}\right|\\
&+\left|\left(\left(\nabla \boldsymbol{u}'_{*,1}\right)\left(\boldsymbol{u}'_{*,2}-\boldsymbol{u}'_2\right),\boldsymbol{\varphi}\right)_{0,\Omega}\right|+\left|\left(\boldsymbol{u}'_{*1}\cdot\boldsymbol{n},\left(\boldsymbol{u}'_{*2}-\boldsymbol{u}'_2\right)\boldsymbol{\varphi}\right)_{0,\Gamma_N}\right|,
\end{aligned}
$$

where every term were bounded with estimations of the form $C\left(\|\gamma_1\|_{s,\Omega}+\varepsilon_1\right)\left(\|\gamma_2\|_{s,\Omega}+\varepsilon_2\right)\left(\|h\|_{\infty,\Omega}+\varepsilon\right)$ (see Lemmas 5.5.4, 5.5.6 and 5.5.7). In conclusion, there exists $L>0$ such that

$$
\left|\left(J''\left(\gamma+h\right)-J''\left(\gamma\right)\right)\left[\gamma_1,\gamma_2\right]\right|\leq L\left(\|\gamma_1\|_{s,\Omega}+\varepsilon_1\right)\left(\|\gamma_2\|_{s,\Omega}+\varepsilon_2\right)\left(\|h\|_{\infty,\Omega}+\varepsilon\right).
$$

□

Corollary 5.5.1. *Let $(\gamma,\beta);(\gamma^*,\beta^*)\in\mathcal{A}$. There exists $L>0$ such that, for every $\theta\in[0,1]$*

$$
\begin{aligned}
&\left|\left(J''\left(\theta\gamma^*+(1-\theta)\gamma,\theta\beta^*+(1-\theta)\beta\right)-J''\left(\gamma^*,\beta^*\right)\right)\left[\left(\gamma^*-\gamma,\beta^*-\beta\right),\left(\gamma^*-\gamma,\beta^*-\beta\right)\right]\right|\\
\leq& L\left(\|\gamma^*-\gamma\|_{\infty,\Omega}+|\beta-\beta^*|\right)\left(\|\gamma^*-\gamma\|_{s,\Omega}+|\beta-\beta^*|\right)^2.
\end{aligned}
$$

Finally, a second order sufficent optimality condition is presented and proved.

Theorem 5.5.3. *Let $(\gamma^*,\beta^*)\in\mathcal{A}$ such that (γ^*,β^*) verifies the first orden optimality condition. If there exists $\delta>0$ such that*

$$
\left(\forall\,(\gamma,\beta)\in\mathcal{A}\right)\quad J''\left(\gamma^*,\beta^*\right)\left[\left(\gamma^*-\gamma,\beta^*-\beta\right),\left(\gamma^*-\gamma,\beta^*-\beta\right)\right]\geq\delta\left(\|\gamma^*-\gamma\|_{s,\Omega}+|\beta-\beta^*|\right)^2
$$

Then, there exist $\sigma,\varepsilon>0$, independent of γ and γ^*, such that, if $\|\gamma^*-\gamma\|_{\infty,\Omega}+|\beta-\beta^*|\leq\varepsilon$, then

$$
J\left(\gamma,\beta\right)\geq J\left(\gamma^*,\beta^*\right)+\sigma\left(\|\gamma^*-\gamma\|_{s,\Omega}+|\beta-\beta^*|\right)^2.
$$

In consequence, J has a local minimum at (γ^*,β^*).

Proof. See Theorem 3.4 in [39].

□

Remark 5.5.1. *The result obtained in Theorem 5.5.3 depends of s, but is valid for every $s\geq 0$.*

5.6 Numerical Results

In this section, we present some numerical test for our minimization problem simulating a cardiac valve with 2D and 3D synthetic data in order to complement the theory presented in the previous sections. According to [4], it is possible to approximate the effect of the valves using an appropriate L^2 function in a virtual domain. For the 2D experiments, we propose a realistic domain with a piecewise smooth bicuspid valve which represent a longitudinal

section of the structure of a cardiac valve in an symmetric arbitrary position. We obtained our reference velocity from the numerical solutions of the Navier-Stokes equation with our real domain, extending by zero in the virtual domain used. For the 3D experiments, we used a cylinder as a virtual domain simulating a tricuspid cardiac valve with a realistic shape to obtain the reference velocity. In both cases, 2D and 3D, we used complete or partial information to numerically solve the following minimization problem.

$$\text{minimize} \quad J(\gamma, \beta, \boldsymbol{u}) = \frac{1}{2}\|\boldsymbol{u} - \boldsymbol{u}_{\text{OBS}}\|^2_{0,\omega} + \frac{\alpha}{2}\|\gamma\|^2_{s,\Omega} \tag{5.5}$$

$$\begin{aligned} \text{subject to} \quad -\nu\triangle\boldsymbol{u} + (\nabla\boldsymbol{u})\,\boldsymbol{u} + \nabla p + \gamma\boldsymbol{u} &= \boldsymbol{0} \quad \text{in } \Omega \\ \operatorname{div}\boldsymbol{u} &= 0 \quad \text{in } \Omega \\ \boldsymbol{u} &= \beta\boldsymbol{u}_D \quad \text{on } \Gamma_D \\ -\nu\frac{\partial\boldsymbol{u}}{\partial\boldsymbol{n}} + p\boldsymbol{n} + \frac{1}{2}(\boldsymbol{u}\cdot\boldsymbol{n})_-\,\boldsymbol{u} &= \boldsymbol{0} \quad \text{on } \Gamma_N \end{aligned} \tag{5.6}$$

$$\boldsymbol{u} \in \boldsymbol{H}^1(\Omega),\ \gamma \in H^s(\Omega),\ \beta \in \mathbb{R},$$
$$0 \le \beta \le M_1,\ 0 \le \gamma \le M_2 \text{ a.e. in } \Omega.$$

In the following subsections, the configurations of the reference case is explained, as well as the numerical solutions of the inverse problems associated with synthetic MRI.

5.6.1 2D reference test

To define a reference geometry, we use a domain Ω_0 that represents the area around the aortic valve with the valves (see Figure 5.1). The inflow Γ_I follows a Poiseuille's Law with parabolic profile given by

$$\boldsymbol{u}_D(x, y) = -Ux(d - x)\,\boldsymbol{n},$$

where $\boldsymbol{x} = (x, y)$ are the Cartesian coordinates of the domain, $\boldsymbol{n}$ is the outer normal vector and d is the diameter of the inflow. Later, we define the virtual domain Ω given for the realistic domain without the valves and the same boundary conditions.

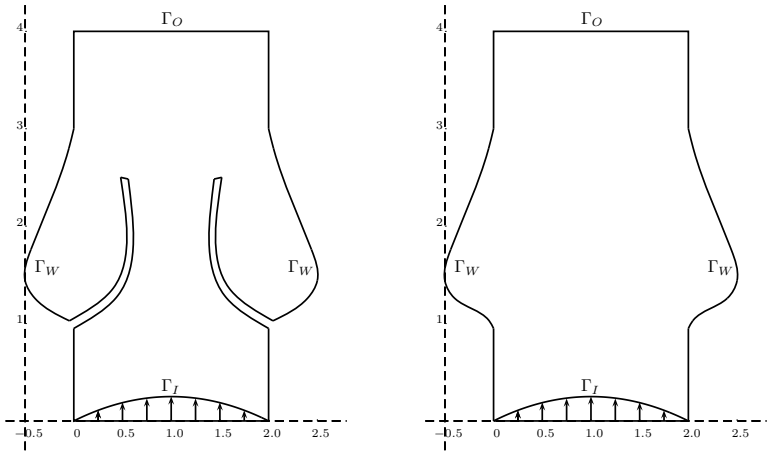

Figure 5.1: Realistic domain (Ω_0, left) and virtual domain (Ω, right).

The valves were generated with a rotated parabola with a thickness of 0.1 mm and can be recovered using the γ function. Indeed, according to [4], the valves are modeled on the resistance term $\gamma \boldsymbol{u}$ using the function γ. This function assumes a constant value $M \gg 1$ in the regions where the valve is and assumes the value 0 where the valve is not.

The parameters for the human blood flow are given by the kinematic viscosity equal to $\nu = 0.035\,\mathrm{cm}^2\,/\,\mathrm{s}$, the blood density given by $\rho = 1\,\mathrm{g}\,/\,\mathrm{cm}^3$, and the dimensions $d = 2\,\mathrm{cm}$ and $U = 30\,\mathrm{cm}\,/\,\mathrm{s}$, resulting in a peak Reynolds number on the inlet of

$$\mathrm{Re} = \frac{Ud}{\nu} = 1714.$$

The Navier-Stokes equations are discretized using the finite element method (FEM) with Taylor-Hood elements ($\mathbb{P}_2$ for the velocity $\boldsymbol{u}$ and $\mathbb{P}_1$ for the pressure) on an unstructured triangular mesh. To obtain the reference solution, we used a mesh for the realistic domain Ω_0 generated by domain triangulation with $h = 0.02\,\mathrm{cm}$, which corresponds to 37666 elements and 19209 nodes. We generated a second mesh for the virtual domain used in the minimization problem. That mesh were generated by domain triangulation of Ω with $h = 0.05\,\mathrm{cm}$, which corresponds to 9716 elements and 4986 nodes.

The solvers were implemented using the finite element library FEniCS [5] with the default configuration. To solve the nonlinear problems, the Newton method was used. We define the set $\mathcal{O}$, that represents the valve inside of Ω, that is, $\mathcal{O} = \Omega \setminus \Omega_0$. The reference velocity $\boldsymbol{u}_R$ is computed by the Lagrange intepolation on the virtual mesh of the velocity computed as the numerical solution of the Navier-Stokes in the realistic mesh, extended by $\mathbf{0}$ in $\mathcal{O}$.

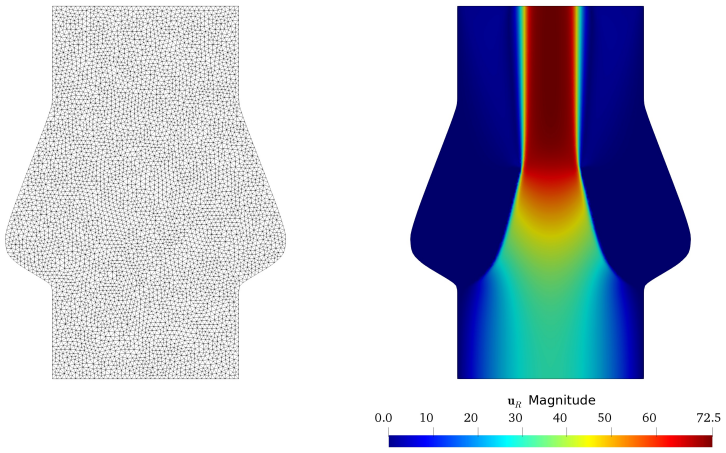

Figure 5.2: Plots of unstructured mesh for Ω (left) and reference solution $\boldsymbol{u}_R$ interpolated in Ω (right).

5.6.2 Numerical solution of the inverse problem in 2D

Using $\boldsymbol{u}_{\mathrm{OBS}} = \boldsymbol{u}_R$ as reference solution, the minimization problem (5.5) is numerically solved using FEniCS and dolfin-adjoint. For this first example, we considered a measurement area $\omega = \Omega$, $\gamma \in H^1(\Omega)$, and the values $M_1 = 50$, $M_2 = 10^4$, $\alpha_0 = 10^{-5}$ and $\alpha_1 = 10^{-8}$. The use of two different weights for the norm and seminorm is consistent with the theoretical analysis of the previous sections, so this problem has a solution. The dolfin-adjoint library [71] allows

to implement automatic derivation of the discrete adjoint equations for PDE models and implement minimization algorithms from the Python 3 libraries. In particular, the L-BFGS-B algorithm (see Section 4.3 in [39]) was used with the following stopping criteria on the step k

$$\frac{|J(\gamma_k) - J(\gamma_{k+1})|}{\max\{|J(\gamma_k)|, |J(\gamma_{k+1})|, 1\}} \leq 10^{-5}$$

To start the algorithm, $\gamma_0 = 0$ and $\beta = 0$ were used as the initial solution. The parameters γ and β were rescaled to the interval $[0, 1]$ for a correct implementation in dolfin-adjoint. As a way to define a valve reconstruction algorithm sketch, we follow the same steps we established in [3].

1. We defined an axis that crosses the domain from the inflow to the outflow.
2. For a uniform discretization of the axis, we defined perpendicular lines.
3. The solution γ^* obtained by the algorithm is interpolated on each of the lines. Three points are selected on each side of the axis. The first and second point are the limits of an interval where $\nabla\gamma^* \cdot \boldsymbol{n}$ has the maximum positive values with 1% of tolerance. The third point is the local maximum closest to the interval.
4. An average is obtained between the three points.
5. A polyline is drawn on each side of the axis. Each polyline passes through all the average points.

Numerical results are presented in Figure 5.3. The polyline is drawn in white, which presents a great approximation to the interface between the different values of the reference given by γ. The optimal γ^* has values close to 0 between the valves, above and below the valves. Likewise, the magnitude and direction of $\boldsymbol{u}^*$ is similar to $\boldsymbol{u}_R$, where $\boldsymbol{u}^*$ corresponds to the optimal state. The optimal $\beta^* = 31.854$ is very near to the reference value $\beta = 30$, showing empirically that the previously defined problem allows to obtain a good approximation of the maximum velocity magnitude in the inflow.

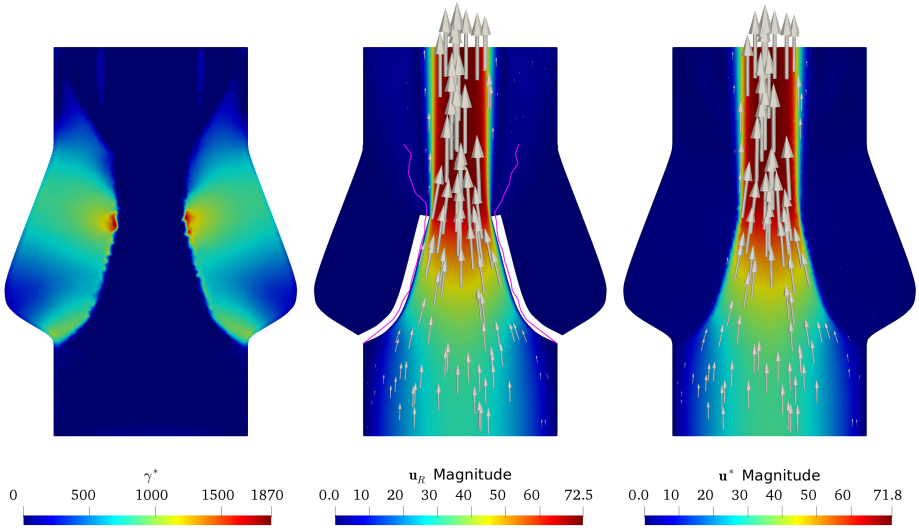

Figure 5.3: Optimal γ^*, reference solution $\boldsymbol{u}^*$ with reconstructed valve and optimal velocity $\boldsymbol{u}^*$ (from left to right). Reference test, 366 iterations, $\beta^* = 31,854$.

The second example were designed to corroborate that this algorithm is able to solve the inverse problem measuring only a part of $\boldsymbol{u}_R$ given by the reference velocity. In this case, choosing ω as the area where the valves should be (see Figure 4.5 center and right), given by

$$\omega = \Omega \cap \left\{(x, y) \in \mathbb{R}^2 \mid 1 \leq y \leq 3\right\},$$

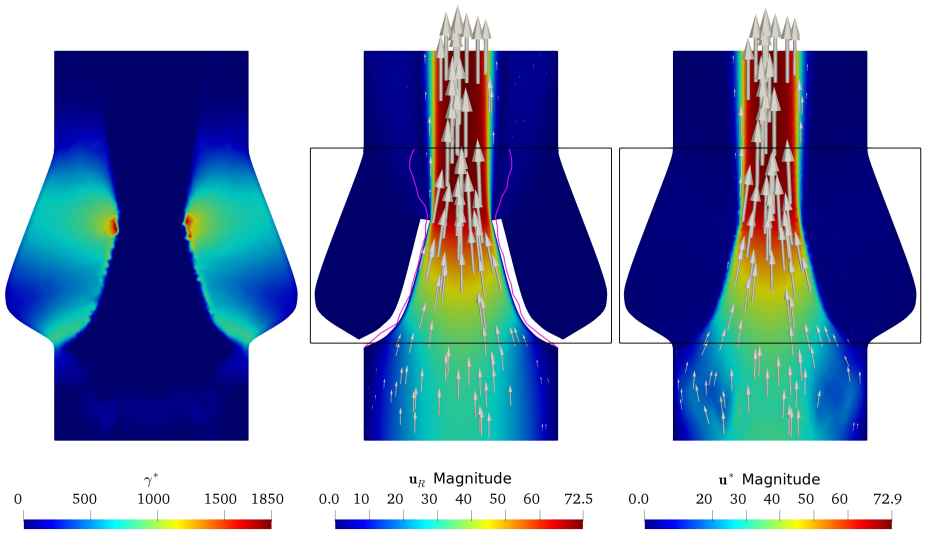

Figure 5.4: Optimal γ^*, reference solution $\boldsymbol{u}^*$ with reconstructed valve and optimal velocity $\boldsymbol{u}^*$ (from left to right). Reference test with subdomain, 320 iterations, $\beta = 32.2953$.

The expected result is similar to that found in the fist example. Figure 4.5 presents the numerical results, the polyline and the reference. In the case of the reference solution $\boldsymbol{u}_R$, a black rectangle was drawn that allows delimiting the measurement area ω. In particular, this problem required less iterations than the case with measurements on Ω, obtaining very similar results for γ and β. Although γ^* assumes small values below the valves, compared to its maximum value, these values are enough to generate a numerically significant resistance for the flux, which is compensated with a higher value for β.

5.6.3 Measurements of MRI type in 2D

In several medical applications, the 4D MRI allows to register the blood flow in a volume unit, also called voxel, which can be reinterpreted as the average blood velocity in the voxel. Inside each voxel, we can assume the blood velocity as a constant. Since our problem is stationary, an approximation to a synthetic MRI is to project $\boldsymbol{u}_R$, extended by zero outside the virtual domain Ω, to a $\mathbb{Q}_0$ FEM space (given by piecewise constant discontinuous functions on a quadrilateral mesh) using a new quadrilateral mesh that contains the virtual domain mesh obtaining our synthetic 2D MRI $\boldsymbol{u}_{\text{MRI}}$. That mesh were generated by uniform quadrilaterals of $1\,\text{mm} \times 1\,\text{mm}$. Unlike [3], where the authors used this synthetic MRI as an observation, we project it again to the original $\mathbb{P}_2$ space in order to obtain the new observation $\boldsymbol{u}_P$ that we can easily compare with the numerical states.

Figure 5.5 shows the synthetic MRI generated from the reference solution and the new reference solution $\boldsymbol{u}_{\text{P}}$, where we can verify that the reference is affected by the loss of resolution given by the MRI.

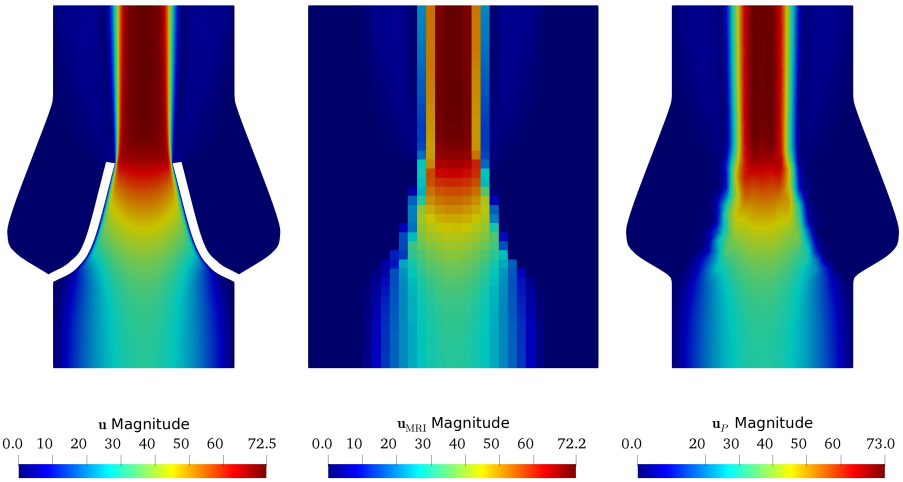

Figure 5.5: Original velocity $\boldsymbol{u}$ (left), synthetic MRI type velocity measurement $\boldsymbol{u}_{\text{MRI}}$ (center) and $\boldsymbol{u}_{\text{P}}$ (right).

Then, the new minimization problem is given by (5.5), but replacing $\boldsymbol{u}_{\text{OBS}}$ with $\boldsymbol{u}_{\text{P}}$, where the values $M_1 = 10^4$, $M_2 = 50$ $\alpha_0 = 10^{-5}$ and $\alpha_1 = 10^{-8}$ were used. It is possible to prove the existence of solution of this problem in the same way as in the proof of the theorem. Figure 5.6 shows the numerical results and the references. In comparison with Figure 5.3, the reconstructed valve in Figure 5.5 is located further from the center than in Figure 5.3 (see Figure 5.7), because of synthetic MRI sampling, but the optimal values β^* are similars.

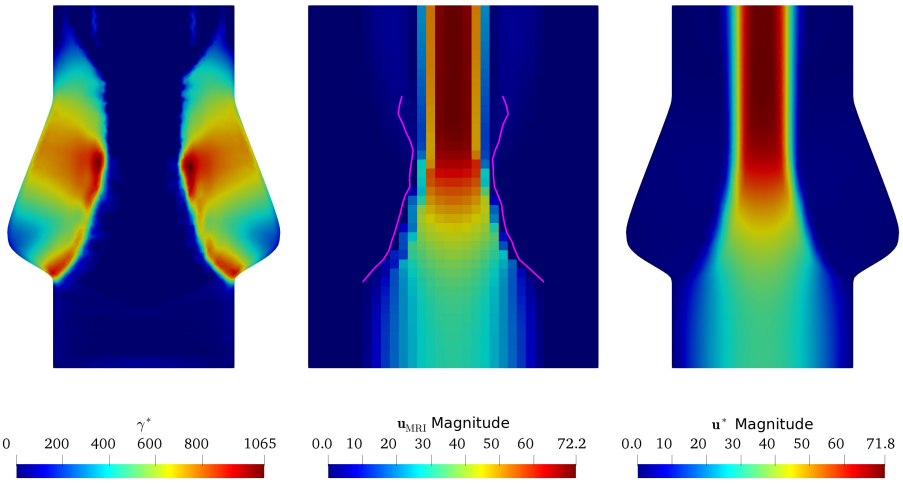

Figure 5.6: Optimal γ^*, synthetic MRI $\boldsymbol{u}_{\text{MRI}}$ with reconstructed valve and optimal velocity $\boldsymbol{u}^*$ (from left to right). Synthetic MRI, 373 iterations, $\beta = 31.6530$.

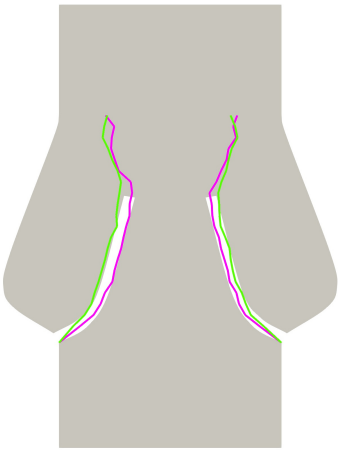

Figure 5.7: Comparison between reconstructed valves by reference solution (magenta) and synthetic 2D MRI (green).

The white noise intensity in the velocity measurements from MRI is proportional to the velocity encoding parameter (also called VENC [40]) of the scan. This parameter is configured with a value greater than the maximum expected velocity, in order to eliminate signal aliasing. Then, the noise in all voxels is proportional to the maximum velocity in the measurement area. In the clinical practice it can be expected that high-quality MRI contains a velocity noise of 10% of the maximum velocity in each voxel [40] in each direction. Gaussian noises were added to this MRI in every direction with a standard deviation of 5%, 10% and 20% of the maximum absolute value on each direction of u_R.

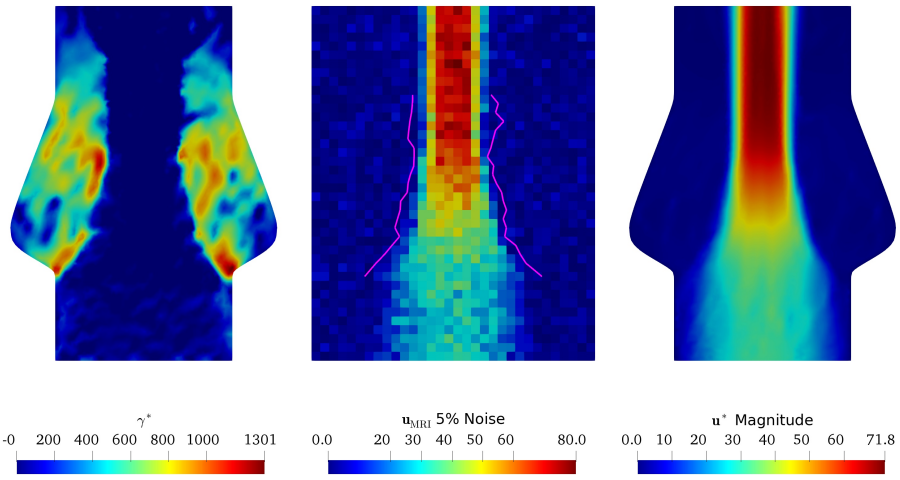

Figure 5.8: Optimal γ^*, synthetic MRI $\boldsymbol{u}_{\mathrm{MRI}}$ with reconstructed valve and optimal velocity $\boldsymbol{u}^*$ (from left to right). Synthetic MRI with 5% of noise, 298 iterations, $\beta = 31.4286$.

Figure 5.8 shows the results of this experiment with a 5% of Guassian noise. The results are similar to the experiment without noise in terms to the tendency of the polyline to approximate the valve shape and draw lines parallel to the voxels.

This approximation seems weaker as noise increases, in the sense that the polyline has a lower quality in its approximation and γ^* tends to overfit the data. Figures 5.9 and 5.10

show the result of the experiment with 10% and 20% of Gaussian noise, respectively. The noise is exactly the same than the 5% Gaussian noise case, but increasing the level noise.

Table 5.1 shows the mean square error (MSE) between the reconstructed valve given by the polylines obtained using MRI in Figures 5.5, 5.8, 5.9 and 5.10, and the polyline obtained in the reference test (see Figure 5.3). To quantify this error, we consider only the points of the polyline in Figure 5.3 that are at a distance less than or equal to 0.5 mm from $\mathcal{O}$. There are minor differences between the valve reconstructions for the cases with a noise level of 0% and 5%. However, the quality of the reconstruction decreases when the level noise increases up to 20%.

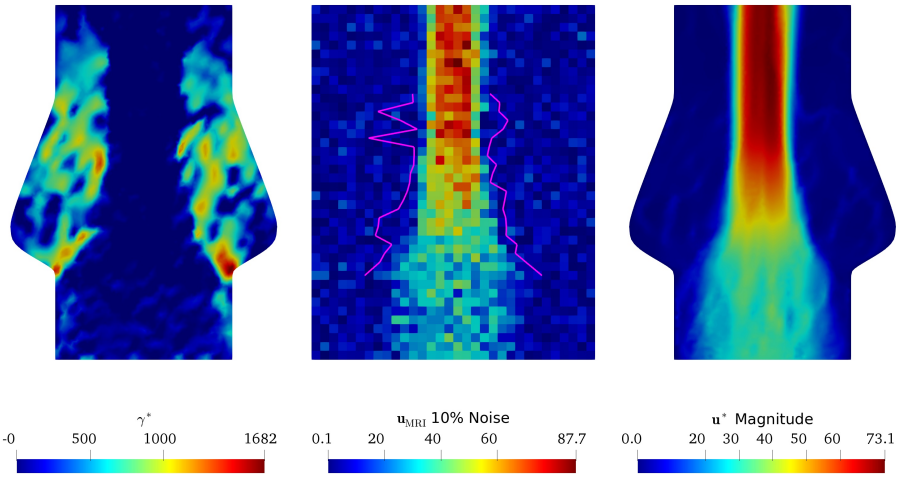

Figure 5.9: Optimal γ^*, synthetic MRI $\boldsymbol{u}_{\text{MRI}}$ with reconstructed valve and optimal velocity $\boldsymbol{u}^*$ (from left to right). Synthetic MRI with 10% of noise, 245 iterations, $\beta = 31.4040$.

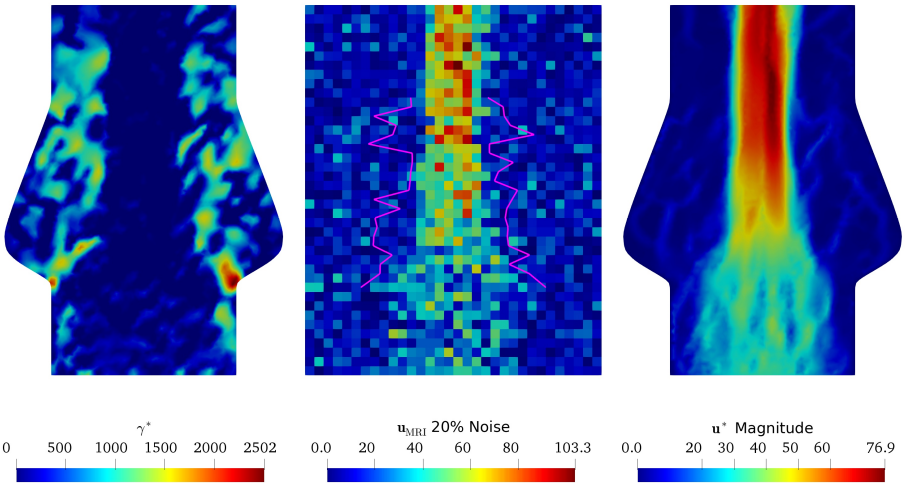

Figure 5.10: Optimal γ^*, synthetic MRI $\boldsymbol{u}_{\text{MRI}}$ with reconstructed valve and optimal velocity $\boldsymbol{u}^*$ (from left to right). Synthetic MRI with 20% of noise, 247 iterations, $\beta = 31.7620$.

Noise level	MSE
0%	$9.9098 \cdot 10^{-3}$
5%	$1.1720 \cdot 10^{-2}$
10%	$2.3320 \cdot 10^{-2}$
20%	$4.1661 \cdot 10^{-2}$

Table 5.1: MSE of reconstructed valves using MRI with different noise levels.

5.6.4 3D reference test

Here, the domain Ω is given by

$$\Omega = \left\{(x, y, z) \in \mathbb{R}^3 \mid x^2 + y^2 \leq R^2 \text{ and } x \in [0, L]\right\}$$

where $R = 1.305$ and $L = 4$, and a unstructured tetrahedral mesh with $h = 0.05$, with 59568 nodes and 329126 elements. The valves are modeled on the permeability term using the γ function. This function assumes the constant value $M \gg 1$ in the regions where the valve is and assumes the value 0 where the valve is not. We used a parametric model of the tricuspid valve inspired from [52] to define the γ function, where the support of γ lies in $\Omega \cap \{(x, y, z) \in \mathbb{R}^3 \mid x \in [1, 2]\}$. This function is modeled as a $\mathbb{P}_1$ function, where the nodal values of the function are given by $M = 10^{10}$ or 0, depending if the node lies or not in the valve. We still using the sames kinematic viscosity $\nu = 0.035\,\mathrm{cm}^2\,/\,\mathrm{s}$, density $\rho = 1\,\mathrm{g}\,/\,\mathrm{cm}^3$ and $U = 30\,\mathrm{cm}\,/\,\mathrm{s}$.

The inflow $\Gamma_I = \{(x, y, 0) \in \mathbb{R}^3 \mid x^2 + y^2 \leq R^2\}$ follows a Poiseuille's Law with parabolic profile given by

$$\boldsymbol{u}_D\,(x, y, z) = -\frac{U}{R^2}\left(R^2 - x^2 - y^2\right)\boldsymbol{n},$$

where $\boldsymbol{x} = (x, y)$ are the Cartesian coordinates of the domain, $\boldsymbol{n}$ is the outer normal vector and d is the diameter of the inflow, while the directional do-nothing conditions are imposed on the outflow $\Gamma_O = \{(x, y, 4) \in \mathbb{R}^3 \mid x^2 + y^2 \leq R^2\}$. The walls of the structure are represented by $\Gamma_W = \{(x, y, z) \in \mathbb{R}^3 \mid x^2 + y^2 = R^2 \text{ and } x \in [0, L]\}$.

Unlike the 2D case, due to computing efficiency, the Navier-Stokes equations were discretized using the finite element method (FEM) with the MINI element ($P_{1,\mathrm{bub}} = \mathbb{P}_1 \oplus V_{\mathrm{bub}}$ for the velocity $\boldsymbol{u}$ and $\mathbb{P}_1$ for the pressure p, where V_{bub} is the space of the bubble functions, see Section 3.6.1 in [62]). We still using FEniCS [5] with the default configuration with the Newton method. The numerical experiments in 3D were computed on 48 Intel Xeon 2.5 GHz cores. We define the set $\mathcal{O}$, that represents the valve inside of Ω, by

$$\mathcal{O} = \left\{\boldsymbol{x} \in \Omega \mid \gamma(\boldsymbol{x}) = 10^{10}\right\}.$$

Figures 5.11 and 5.12 show the reference valve and reference velocity field. The peak Reynolds number on the inlet is

$$\mathrm{Re} = \frac{Ud}{\nu} = 2237.$$

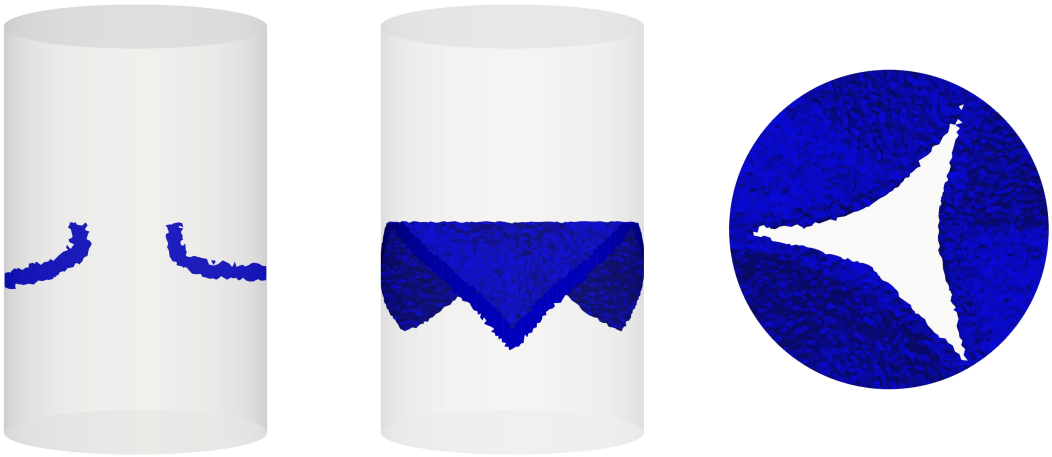

Figure 5.11: Plots of the valve region $\mathcal{O}$. Slice for $x = 0$ (left), frontal view (center) and outflow view (right).

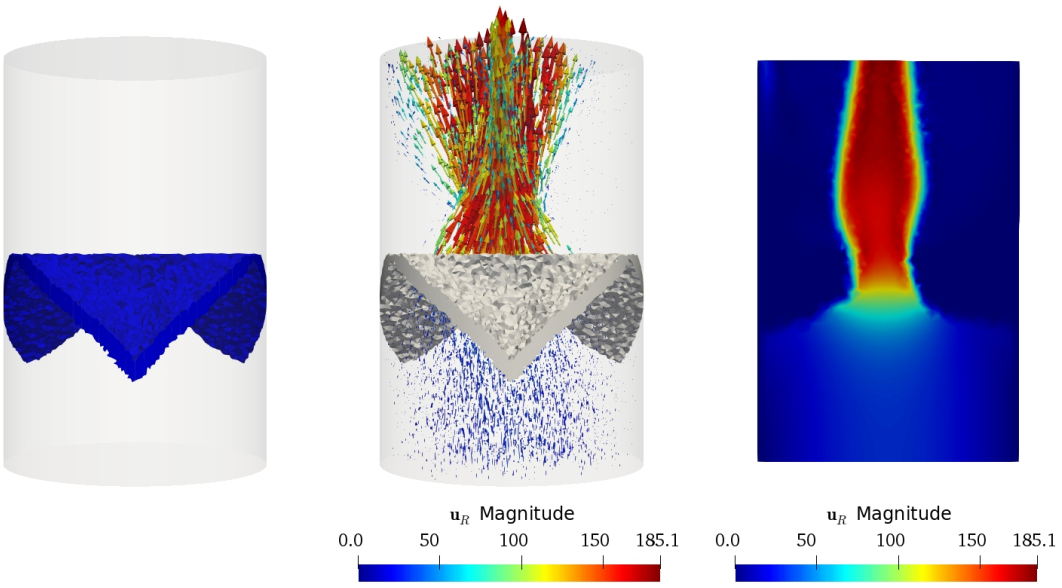

Figure 5.12: Plots of the valve (left), the reference velocity field (center) and isovalues of reference velocity for a $x = 0$ cut (right).

5.6.5 Numerical solution of the inverse problem in 3D

Using $\boldsymbol{u}_{\text{OBS}} = \boldsymbol{u}_R$ as reference solution, the minimization problem (5.5) is solved, but considering the new functional

$$J(\gamma, \boldsymbol{u}) = \frac{1}{2} \|(\boldsymbol{u})_{\mathbb{P}_1} - (\boldsymbol{u}_R)_{\mathbb{P}_1}\|^2_{0,\omega} + \frac{\alpha_0}{2} \|\gamma\|^2_{0,\Omega} + \frac{\alpha_1}{2} |\gamma|^2_{1,\Omega},$$

where $(\boldsymbol{u})_{\mathbb{P}_1}$ denotes the projection of $(\boldsymbol{u})$ on the $\mathbb{P}_1$ space. We decided to compare the velocity projections on $\mathbb{P}_1$ instead of the velocity in $P_{1,\text{bub}}$ since $\mathbb{P}_1$ are better approximations to the velocity than the one obtained in $P_{1,\text{bub}}$ (see Section 2 in [82]). This first example in 3D follows the same configuration of the first example in 2D, choosing the measurement area $\omega = \Omega$ and the values $M_1 = 50$, $M_2 = 10^4$, $\alpha_0 = 10^{-5}$ and $\alpha_1 = 10^{-8}$. We still using the dolfin-adjoint library [71] with the L-BFGS-B algorithm (see Section 4.3 in [39]) and stopping criteria on the step k given by

$$\frac{|J(\gamma_k) - J(\gamma_{k+1})|}{\max\{|J(\gamma_k)|, |J(\gamma_{k+1})|, 1\}} \leq 10^{-5}$$

To start the algorithm, $\gamma_0 = 0$ and $\beta = 0$ were used as the initial solution. The parameters γ and β were also rescaled to the interval $[0, 1]$ for a correct implementation in dolfin-adjoint. Numerical results are presented in Figure 5.13. The optimal γ^* has values close to 0 in zones before the valves and in the interior zone where there are no valves. If we choose the zones where γ^* has values greater or equal to the threshold $0.4 \max\{\gamma^*(\boldsymbol{x} \mid \boldsymbol{x} \in \Omega)\}$, we can see that region is able to recover the space between the valves. The magnitude and direction of $\boldsymbol{u}^*$ is similar to $\boldsymbol{u}_R$, where $\boldsymbol{u}^*$ corresponds to the optimal state. The optimal $\beta^* = 36,3068$ is near to the reference value $\beta = 30$, but the difference with respect the reference is greater than the 2D case.

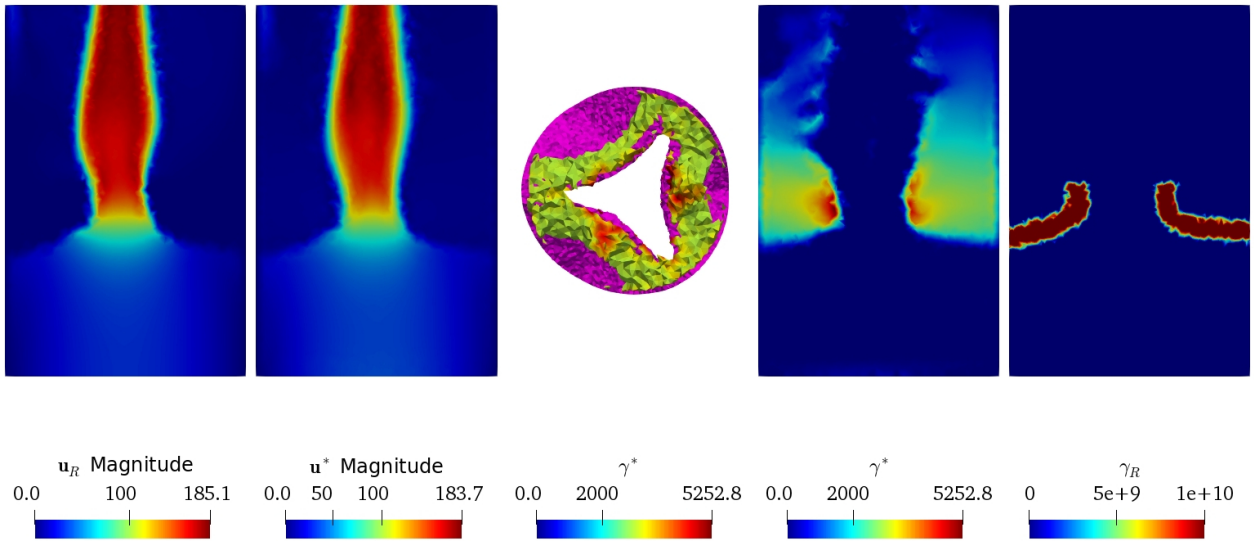

Figure 5.13: Slices of reference $\boldsymbol{u}_R$ and optimal $\boldsymbol{u}^*$, comparison between γ_R (magenta) and γ^*, slices of optimal γ^* and γ_R (from left to right). 3D Reference test, 460 iterations, $\beta = 36.3068$.

5.6.6 Measurements of MRI type in 3D

In this experiment, we present the covering of the γ function form a projection of $\boldsymbol{u}_R$, extended by zero outside the virtual domain Ω, on a $\mathbb{Q}_0$ FEM space using a new quadrilateral mesh that contains the virtual domain mesh obtaining our synthetic 3D MRI $\boldsymbol{u}_{\text{MRI}}$. That mesh were generated by uniform hexahedrons of $1\,\text{mm} \times 1\,\text{mm} \times 1\,\text{mm}$. Unlike [3], where the authors used this synthetic MRI as a reference, we project again to the $\mathbb{P}_1$ space in order to obtain the new velocity reference $\boldsymbol{u}_{\text{OBS}} = \boldsymbol{u}_P$ that we can easily compare with the projection of numerical states on $\mathbb{P}_1$ space.

Then, we solved Problem (5.5) considering this new functional

$$J(\gamma, \boldsymbol{u}) = \frac{1}{2} \|(\boldsymbol{u})_{\mathbb{P}_1} - \boldsymbol{u}_P\|^2_{0,\omega} + \frac{\alpha_0}{2} \|\gamma\|^2_{0,\Omega} + \frac{\alpha_1}{2} |\gamma|^2_{1,\Omega},$$

where the values $M_1 = 10^4$, $M_2 = 50$ $\alpha_0 = 10^{-5}$ and $\alpha_1 = 10^{-8}$ were used. It is possible to prove the existence of solution of this problem in the same way as in the proof of the theorem. Figure 5.14 shows the numerical results and the references similarly to Figure 5.13. We obtained similar results to the first 3D example, with a better prediction of the maximum velocity in the inflow β^* and a similar reconstruction of the space between the valves. However, the solver needed 106 more iterations in comparison with the original case.

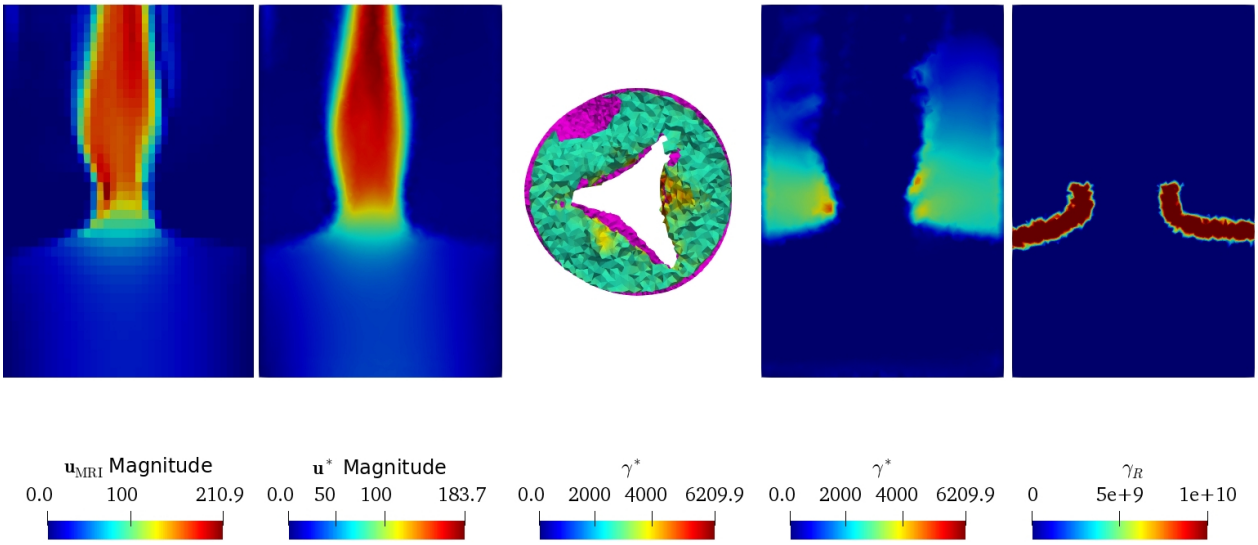

Figure 5.14: Slices of reference $\boldsymbol{u}_{\text{MRI}}$ and optimal $\boldsymbol{u}^*$, comparison between γ_R (magenta) and γ^*, slices of optimal γ^* and γ_R (from left to right). Synthetic 3D MRI, 566 iterations, $\beta = 35.6507$.

We also simulated a MRI with a velocity noise proportional to the maximum absolute velocity for each direction, following the same accepted medical parameters for a 4D flow MRI. Gaussian noises were added to this MRI in every direction with a standard deviation of 10% and 20% of the maximum absolute value on each direction of $\boldsymbol{u}_{\text{MRI}}$.

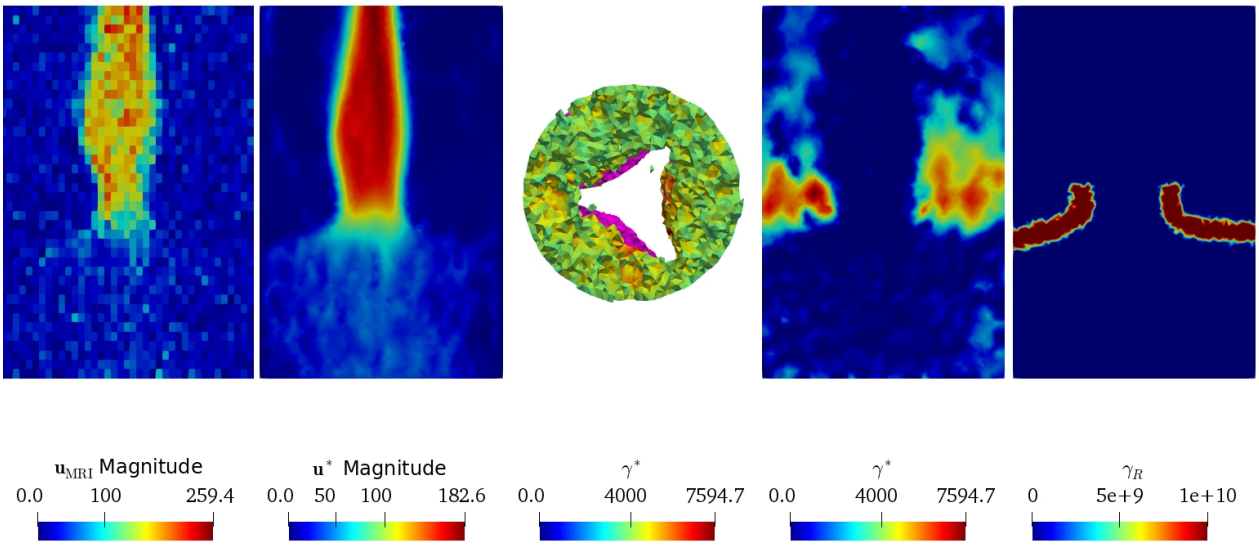

Figure 5.15: Slices of reference $\boldsymbol{u}_{\mathrm{MRI}}$ and optimal $\boldsymbol{u}^*$, comparison between γ_R (magenta) and γ^*, slices of optimal γ^* and γ_R (from left to right). Synthetic MRI with 10% of noise, 566 iterations, $\beta = 35.3435$.

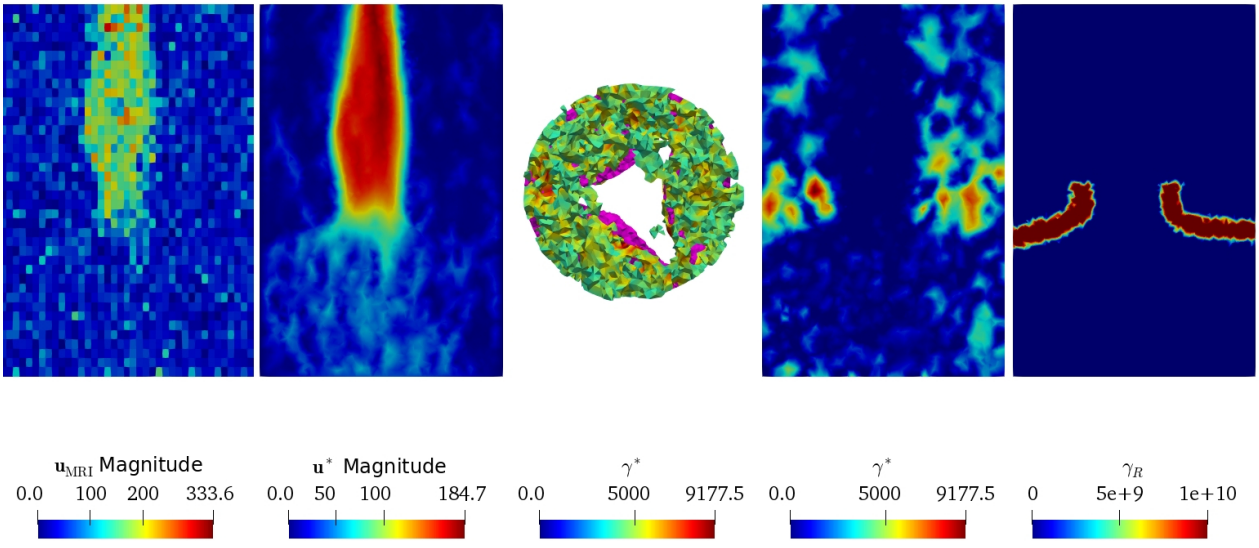

Figure 5.16: Slices of reference $\boldsymbol{u}_{\mathrm{MRI}}$ and optimal $\boldsymbol{u}^*$, comparison between γ_R (magenta) and γ^*, slices of optimal γ^* and γ_R (from left to right). Synthetic MRI with 20% of noise, 566 iterations, $\beta = 38.9662$.

Figures 5.15 and 5.16 show the results of this experiment with a 10% and 20% of Guassian noise, respectively. This approximation seems weaker as noise increases, following a similar tendency given in the 2D case. The valve reconstruction obtained in Figure 5.15 is similar to the one obtained in the previous 3D examples, but the γ^* has some numerical noise and is not so similar to γ_R. The results are worse when noise is increased up to 20%, where it is not possible to reconstruct the space between the valves (see Figure 5.16) and the γ^* is not comparable with the reference γ_R.

5.7 Conclusions

We have presented a new distributed parameter identification problem for the Navier-Stokes equations, contributing to the detection of obstacles and domain deformations in fluid dynamic studies. For this problem, we establish the existence of solution and optimality conditions, validating the use of some optimization algorithms for differentiable functionals. In comparison with [3], we could establish the same theorems for our problem with weaker smoothness hypotheses. One of the future improvements is to work towards the uniqueness of solution of this parameter identification problem using the results from Chapter 4 and another techniques.

The numerical experiments presented in this chapter show an improvement from the ones performed in [3] with a better precision and stability for the 2D experiments. The numerical tests without noise had satisfactory results in terms of rebuilding the simulated valve from data generate from a realistic domain. The experiments with Gaussian noise were improved adding a simple post-processing of the simulated MRI. The quality of the solutions is worse as noise increases, as expected. The 3D experiments presented similar results in comparison with the 2D experiments. However, the threshold criterion is not good enough to reconstruct the space between valves for higher noise levels and the execution time of the solver is high. Given the 3D case is interesting for the medical community, since it will contribute to simplify the detection of defects in the function of aortic valves, the design of a simplified algorithm that obtains numerical solutions for the parameter identification problem and a valve reconstruction is part of our future work.

Chapter 6

Conclusions and future work

In this thesis, new advances are presented in inverse problems of Fluid Mechanics in steady state, with direct applications in the recovery of domain deformations and obstacles. The search for non-invasive methods to detect valvular diseases is one of the medical challenges that where it is expected to apply 4D Flow MRI, which estimates the blood velocity circulating in the human body, particularly in the heart. One of the purpose of this thesis is to contribute to the detection of aortic valve conditions (such as insufficiency or stenosis) from a mathematical perspective, helping to model this problem and giving a first approach to the solution to this problem.

In Chapter 2, we presented the asymptotic equivalence between the problem of detecting obstacles an domain deformations and recovering a permeability function that is equal to a sufficiently large constant $R > 0$ in regions where there are obstacles or domain deformations or equal to 0 otherwise for the Stokes and Navier-Stokes equations. Using variational formulations and energy estimates, we obtained an asymptotic estimate between the velocities obtained by the real domain and the virtual domain with the permeability parameter. One of the advantages of working with virtual domains is that it is not necessary to modify meshes or subdomains to verify the effect of new changes in obstacles and domain deformations, since this contribution is reduced to analyzing the permeability parameter.

The results of the numerical test presented in Chapter 2 were better compared to the theoretical results, validating the use of this kind of functions and avoiding shape optimization methods when we work with penalization terms. That results also allow us to conjecture we could improve our energy estimate and increase the penalty error order from $R^{-3/4}$ to R^{-1} if we impose stronger hypotheses for the smoothness of the boundary data.

In Chapter 3, we could establish a stability result for the inverse problem of recovering a smooth scalar permeability parameter given by the Brinkman's law applied on steady Navier-Stokes equations with local observations of the fluid velocity and their vorticity on a fixed domain. Our estimate does not requiere pressure observations, but requires a weaker version of a non-degeneracy condition. Our strategy is based in techniques that allows to deduce Carleman estimates for the linearized steady Navier-Stokes equations can be extended to other equations.

We corroborate our estimate with a numerical test for recovering a smooth parameter, showing a slow convergence of the optimization solver. For the numerical test that recovered a discontinuous coefficient, we presented an adaptive refinement strategy with two a-posteroiri

predictors working together with satisfactory results. We can deduce that our estimates could be improved by relaxing the regularity hypotheses of our main theorem. We obtained some numerical noise in both experimental tests that could be caused by the numerical estimation of the curl. Then, one alternative is to consider mixed finite element formulations where the unknowns of the Navier-Stokes equations are the velocity, vorticity and pressure of the fluid.

Finally, we presented two different parameter identification problems for the Oseen and Navier-Stokes equations, respectively, when we recover the permeability parameter in order to reconstruct a realistic estimate of the aortic valve in Chapters 4 and 5. The proposed method in both chapters consists in adding the Brinkman's law permeability term, where the boundary of the scalar permeability parameter support represents the boundaries of the valves, thanks to the results obtained in the Chapter 2. We verified the existence of minimizers and first and second order optimality conditions are derived through the differentiability of the velocity and pressure of the fluid, following the Ossen and Navier-Stokes equations with respect of the parameters. Then, we can use a quadratic differentiable functional, based in the stability estimates given in Chapter 3, with some additional stabilization terms.

The numerical experiments presented in Chapters 4 and 5 validate the theory presented in Chapters 2 through 5. The 2D numerical tests without noise were successful in terms of recovering a permeability function and a valve shape that is similar to the reference shape. By the same way, the 3D numerical test without noise recovers a permeability function with a threshold such that the space between the valves can be detected. The experiments with Gaussian noise were improved adding a simple post-processing of the simulated MRI. The quality of the solutions is worse as noise increases, as expected, with similar performances in 2D and 3D experiments. However, the threshold criterion is not good enough to reconstruct the space between valves for higher noise levels. In that case, we need to develop more numerical test and the study of improved image recovering techniques in order to design a new algorithm that allows to obtain a high quality valve detection from the optimal permeability parameter. Another issue is the execution time of the 3D solver. One alternative to decrease the execution time is to simplify the problem adding more information about the permeability function, like a region of the domain where that function is equal to 0, or stabilized finite element formulations using $\mathbb{P}_1$ elements for the velocity.

Bibliography

[1] Feby Abraham, Marek Behr, and Matthias Heinkenschloss. The effect of stabilization in finite element methods for the optimal boundary control of the Oseen equations. *Finite Elements in Analysis and Design*, 41(3):229–251, dec 2004.

[2] Robert A. Adams and John J. F. Fournier. *Sobolev Spaces*. Elsevier Science Techn., June 2003.

[3] Jorge Aguayo, Cristóbal Bertoglio, and Axel Osses. A distributed resistance inverse method for flow obstacle identification from internal velocity measurements. *Inverse Problems*, 37(2):025010, jan 2021.

[4] Jorge Aguayo and Hugo Carrillo. Analysis of obstacles immersed in viscous fluids using Brinkman's law for steady Stokes and Navier-Stokes equations. *SIAM Journal on Applied Mathematics*, 2022.

[5] Martin Alnæs, Jan Blechta, Johan Hake, August Johansson, Benjamin Kehlet, Anders Logg, Chris Richardson, Johannes Ring, Marie E. Rognes, and Garth N. Wells. The FEniCS Project Version 1.5. *Archive of Numerical Software*, Vol 3, 2015.

[6] C. Alvarez, C. Conca, L. Friz, O. Kavian, and J. Ortega. Identification of immersed obstacles via boundary measurements. *Inverse Problems*, 21(5):1531, 2005.

[7] Catalina Alvarez, Carlos Conca, Rodrigo Lecaros, and Jaime H Ortega. On the identification of a rigid body immersed in a fluid: A numerical approach. *Engineering analysis with boundary elements*, 32(11):919–925, 2008.

[8] Philippe Angot. Analysis of singular perturbations on the Brinkman problem for fictitious domain models of viscous flows. *Mathematical Methods in the Applied Sciences*, 22(16):1395–1412, nov 1999.

[9] Philippe Angot, Charles-Henri Bruneau, and Pierre Fabrie. A penalization method to take into account obstacles in incompressible viscous flows. *Numerische Mathematik*, 81(4):497–520, feb 1999.

[10] Philippe Angot and JP Caltagirone. *New Graphical and Computational Architecture Concept for Numerical Simulation of Supercomputers*. CERFACS, 1990.

[11] Ute Aßmann and Arnd Rösch. Identification of an unknown parameter function in the main part of an elliptic partial differential equation. *Zeitschrift für Analysis und ihre Anwendungen*, 32, 01 2013.

[12] Matteo Astorino, Jeroen Hamers, Shawn C. Shadden, and Jean-Frédéric Gerbeau. A robust and efficient valve model based on resistive immersed surfaces. *International Journal for Numerical Methods in Biomedical Engineering*, 28(9):937–959, may 2012.

[13] Jean-Louis Auriault. On the domain of validity of Brinkman's Equation. *Transport in Porous Media*, 79(2):215–223, dec 2008.

[14] Mehdi Badra, Fabien Caubet, and Jérémi Dardé. Stability estimates for Navier-Stokes equations and application to inverse problems. *Discrete and Continuous Dynamical Systems - Series B*, 21(8):2379–2407, sep 2016.

[15] A. Ballerini. Stable determination of an immersed body in a stationary Stokes fluid. *Inverse Problems*, 26(12):125015, 2010.

[16] Lucie Baudouin, Maya de Buhan, Sylvain Ervedoza, and Axel Osses. Carleman-Based Reconstruction Algorithm for Waves. *SIAM Journal on Numerical Analysis*, 59(2):998–1039, jan 2021.

[17] Michel Bergmann, Giovanni Bracco, Federico Gallizio, Ermanno Giorcelli, Angelo Iollo, Giuliana Mattiazzo, and Maurizio Ponzetta. A two-way coupling CFD method to simulate the dynamics of a wave energy converter. In *OCEANS 2015 - Genova*, pages 1–6, 2015.

[18] Cristóbal Bertoglio, Alfonso Caiazzo, Yuri Bazilevs, Malte Braack, Mahdi Esmaily, Volker Gravemeier, Alison L. Marsden, Olivier Pironneau, Irene E. Vignon-Clementel, and Wolfgang A. Wall. Benchmark problems for numerical treatment of backflow at open boundaries. *International Journal for Numerical Methods in Biomedical Engineering*, 34(2):e2918, sep 2017.

[19] Cristóbal Bertoglio, Rodolfo Nuñez, Felipe Galarce, David Nordsletten, and Axel Osses. Relative pressure estimation from velocity measurements in blood flows: State-of-the-art and new approaches. *International Journal for Numerical Methods in Biomedical Engineering*, 34(2):e2925, nov 2017.

[20] Amneet Pal Singh Bhalla, Nishant Nangia, Panagiotis Dafnakis, Giovanni Bracco, and Giuliana Mattiazzo. Simulating water-entry/exit problems using eulerian–lagrangian and fully-eulerian fictitious domain methods within the open-source ibamr library. *Applied Ocean Research*, 94:101932, 2020.

[21] S. Bjærum, H. Torp, and K. Kristoffersen. Clutter filter design for ultrasound color flow imaging. *IEEE Transactions on Ultrasonics, Ferroelectrics and Frequency Control*, 49(2):204–216, feb 2002.

[22] Malte Braack and Piotr Boguslaw Mucha. Directional Do-Nothing Condition for the Navier-Stokes Equations. *Journal of Computational Mathematics*, 32(5):507–521, jun 2014.

[23] Haïm Brezis and Petru Mironescu. Gagliardo–Nirenberg inequalities and non-inequalities: The full story. *Annales de l'Institut Henri Poincaré C, Analyse non linéaire*, 35(5):1355–1376, aug 2018.

[24] H. C. Brinkman. A calculation of the viscous force exerted by a flowing fluid on a dense swarm of particles. *Flow, Turbulence and Combustion*, 1(1), dec 1949.

[25] HC Brinkman. On the permeability of media consisting of closely packed porous particles. *Flow, Turbulence and Combustion*, 1(1):81–86, 1949.

[26] Robert W Brown, Y-C Norman Cheng, E Mark Haacke, Michael R Thompson, and Ramesh Venkatesan. *Magnetic resonance imaging: physical principles and sequence design*. John Wiley & Sons, 2014.

[27] Eric Brown-Dymkoski, Nurlybek Kasimov, and Oleg V. Vasilyev. A characteristic based volume penalization method for general evolution problems applied to compressible viscous flows. *Journal of Computational Physics*, 262:344–357, apr 2014.

[28] Eric Brown-Dymkoski, Nurlybek Kasimov, and Oleg V Vasilyev. A characteristic based volume penalization method for general evolution problems applied to compressible viscous flows. *Journal of Computational Physics*, 262:344–357, 2014.

[29] Alfonso Caiazzo, Miguel A. Fernández, Jean-Frédéric Gerbeau, and Vincent Martin. Projection schemes for fluid flows through a porous interface. *SIAM Journal on Scientific Computing*, 33(2):541–564, jan 2011.

[30] T. Carleman. Sur un problème d'unicité pur les systèmes d'équations aux dérivées partielles à deux variables indépendantes. *Ark. Mat. Astr. Fys.*, 26:1–9, 01 1939.

[31] Hugo Carrillo and Alden Waters. Recovery of a Lamé parameter from displacement fields in nonlinear elasticity models. *Journal of Inverse and Ill-posed Problems*, 0(0), apr 2021.

[32] F. Caubet. Instability of an Inverse Problem for the Stationary Navier–Stokes Equations. *SIAM Journal on Control and Optimization*, 51(4):2949–2975, 2013.

[33] F. Caubet, M. Dambrine, D. Kateb, and C. Timimoun. A Kohn-Vogelius formulation to detect an obstacle immersed in a fluid. *Inverse Problems & Imaging*, 7:123, 2013.

[34] Mourad Choulli, Oleg Yu. Imanuvilov, Jean-Pierre Puel, and Masahiro Yamamoto. Inverse source problem for linearized Navier-Stokes equations with data in arbitrary subdomain. *Applicable Analysis*, 92(10):2127–2143, oct 2013.

[35] Mourad Choulli, Oleg Yu. Imanuvilov, and Masahiro Yamamoto. Inverse source problem for the Navier-Stokes equations. *Preprint Series, Graduate School of Mathematical Sciences, The University of Tokyo*, 2006.

[36] Philippe G. Ciarlet. *Linear and Nonlinear Functional Analysis with Applications*. Society for Industrial and Applied Mathematics, USA, 2013.

[37] Carlos Conca, Muslim Malik, and Alexandre Munnier. Detection of a moving rigid solid in a perfect fluid. *Inverse Problems*, 26(9):095010, 2010.

[38] Maya de Buhan and Marie Kray. A new approach to solve the inverse scattering problem for waves: combining the TRAC and the adaptive inversion methods. *Inverse Problems*, 29(8):085009, jul 2013.

[39] Juan Carlos de los Reyes. *Numerical PDE-Constrained Optimization*. Springer International Publishing, 2015.

[40] Petter Dyverfeldt, Malenka Bissell, Alex J. Barker, Ann F. Bolger, Carl-Johan Carlhääll, Tino Ebbers, Christopher J. Francios, Alex Frydrychowicz, Julia Geiger, Daniel Giese, Michael D. Hope, Philip J. Kilner, Sebastian Kozerke, Saul Myerson, Stefan Neubauer, Oliver Wieben, and Michael Markl. 4D flow cardiovascular magnetic resonance consensus statement. *Journal of Cardiovascular Magnetic Resonance*, 17(1), aug 2015.

[41] Lawrence Evans. *Partial Differential Equations*. American Mathematical Society, mar 2010.

[42] Jishan Fan, Michele Di Cristo, Yu Jiang, and Gen Nakamura. Inverse viscosity problem for the Navier-Stokes equation. *Journal of Mathematical Analysis and Applications*, 365(2):750–757, may 2010.

[43] K. Fattouch, P. Lancellotti, M. Vannan, and G. Speziale. *Advances in Treatments for Aortic Valve and Root Diseases*. Springer, 2018. doi.org/10.1007/978-3-319-66483-5.

[44] Marco Fedele, Elena Faggiano, Luca Dedè, and Alfio Quarteroni. A patient-specific aortic valve model based on moving resistive immersed implicit surfaces. *Biomechanics and Modeling in Mechanobiology*, 16(5):1779–1803, jun 2017.

[45] L. Fernandez, A. A. Novotny, and R. Prakash. Noniterative reconstruction method for an inverse potential problem modeled by a modified Helmholtz equation. *Numerical Functional Analysis and Optimization*, 39(9):937–966, feb 2018.

[46] L Fernandez, AA Novotny, and R Prakash. Noniterative reconstruction method for an inverse potential problem modeled by a modified helmholtz equation. *Numerical Functional Analysis and Optimization*, 39(9):937–966, 2018.

[47] A. V. Fursikov and O. Yu. Imanuvilov. *Controllability of Evolution Equations*. Lecture Notes Series - Seoul National University, Research Institute of Mathematics, Global Analysis Research Center. Seoul National University, 1996.

[48] Giovanni Paolo Galdi. *An Introduction to the Mathematical Theory of the Navier-Stokes Equations*. Springer New York, 2011.

[49] Christophe Geuzaine and Jean-François Remacle. Gmsh: A 3-D finite element mesh generator with built-in pre- and post-processing facilities. *International Journal for Numerical Methods in Engineering*, 79(11):1309–1331, may 2009.

[50] Vivette Girault and Pierre-Arnaud Raviart. *Finite Element Methods for Navier-Stokes Equations*. Springer Berlin Heidelberg, 1986.

[51] Konrad Gröger. A $W^{1,p}$-Estimate for solutions to mixed boundary value problems for second order elliptic differential eqution. *Mathematische Annalen*, 283(4):679–688, 1989.

[52] Rami Haj-Ali, Gil Marom, Sagit Ben Zekry, Moshe Rosenfeld, and Ehud Raanani. A general three-dimensional parametric geometry of the native aortic valve and root for biomechanical modeling. *Journal of Biomechanics*, 45(14):2392–2397, sep 2012.

[53] Baptiste Hardy, Juray De Wilde, and Grégoire Winckelmans. A penalization method for the simulation of weakly compressible reacting gas-particle flows with general boundary conditions. *Computers & Fluids*, 190:294–307, aug 2019.

[54] Mohammad Honarvar, Ramin S. Sahebjavaher, S. E. Salcudean, and R. Rohling. Sparsity regularization in dynamic elastography. *Physics in Medicine and Biology*, 57(19):5909–5927, sep 2012.

[55] O. Yu. Imanuvilov. Boundary controllability of parabolic equations. *Sb. Math.*, 186:879–900, 1995.

[56] O. Yu. Imanuvilov. On exact controllability for the Navier-Stokes equations. *ESAIM: Control, Optimisation and Calculus of Variations*, 3:97–131, 1998.

[57] Oleg Imanuvilov and Jean-Pierre Puel. Global carleman estimates for weak solutions of elliptic nonhomogeneous Dirichlet problems. *International Mathematics Research Notices*, 2003(16):883, 2003.

[58] Oleg Yu. Imanuvilov and Jean-Pierre Puel. Global Carleman estimates for weak solutions of elliptic nonhomogeneous Dirichlet problems. *Comptes Rendus Mathematique*, 335(1):33–38, jan 2002.

[59] Oleg Yu Imanuvilov and Masahiro Yamamoto. Determination of a coefficient in an acoustic equation with a single measurement. *Inverse Problems*, 19(1):157–171, jan 2003.

[60] B. Iung and A. Vahanian. Epidemiology of valvular heart disease in the adult. *Nature Reviews Cardiology*, 8(3):162–172, 2011.

[61] Clément Jause-Labert, Fabien S Godeferd, and Benjamin Favier. Numerical validation of the volume penalization method in three-dimensional pseudo-spectral simulations. *Computers & fluids*, 67:41–56, 2012.

[62] Volker John. *Finite Element Methods for Incompressible Flow Problems*. Springer International Publishing, 2016.

[63] Benjamin Kadoch, Dmitry Kolomenskiy, Philippe Angot, and Kai Schneider. A volume penalization method for incompressible flows and scalar advection–diffusion with moving obstacles. *Journal of Computational Physics*, 231(12):4365–4383, 2012.

[64] Khodor Khadra, Philippe Angot, Sacha Parneix, and Jean-Paul Caltagirone. Fictitious domain approach for numerical modelling of navier–stokes equations. *International journal for numerical methods in fluids*, 34(8):651–684, 2000.

[65] Raymond Y Kwong, Michael Jerosch-Herold, and Bobak Heydari. *Cardiovascular magnetic resonance imaging*. Springer, 2008.

[66] Chee Hau Leow, Eleni Bazigou, Robert J. Eckersley, Alfred C. H. Yu, Peter D. Weinberg, and Meng-Xing Tang. Flow Velocity Mapping Using Contrast Enhanced High-Frame-Rate Plane Wave Ultrasound and Image Tracking: Methods and Initial in-Vitro and in-Vivo Evaluation. *Ultrasound in Medicine & Biology*, 41(11):2913–2925, nov 2015.

[67] You Leo Li, Dongwoon Hyun, Lotfi Abou-Elkacem, Juergen Karl Willmann, and Jeremy J. Dahl. Visualization of Small-Diameter Vessels by Reduction of Incoherent Reverberation With Coherent Flow Power Doppler. *IEEE Transactions on Ultrasonics, Ferroelectrics, and Frequency Control*, 63(11):1878–1889, nov 2016.

[68] Nuno F. M. Martins. Identification results for inverse source problems in unsteady Stokes flows. *Inverse Problems*, 31(1):015004, jan 2015.

[69] John R. Mayo and Jonathon A. Leipsic. Radiation Dose in Cardiac CT. *American Journal of Roentgenology*, 192(3):646–653, mar 2009.

[70] Rajat Mittal and Gianluca Iaccarino. Immersed boundary methods. *Annu. Rev. Fluid Mech.*, 37:239–261, 2005.

[71] Sebastian Mitusch, Simon Funke, and Jørgen Dokken. dolfin-adjoint 2018.1: automated adjoints for FEniCS and Firedrake. *Journal of Open Source Software*, 4(38):1292, jun 2019.

[72] Hrizi Mourad, Maatoug Hassine, and Rakia Malek. A non-iterative reconstruction method for an inverse problem modeled by an Stokes-Brinkmann equations. *Journal of the Korean Mathematical Society*, 07 2020.

[73] David Nolte and Cristóbal Bertoglio. Reducing the impact of geometric errors in flow computations using velocity measurements. *International Journal for Numerical Methods in Biomedical Engineering*, page e3203, apr 2019.

[74] N. Riley P. G. Drazin. *The Navier-Stokes Equations: A Classification of Flows and Exact Solutions*. Cambridge University Press, May 2006.

[75] Charles Peskin. Flow patterns around heart valves: a numerical method. *Journal of Computational Physics*, 10(2):252–271, 1972.

[76] Charles Peskin. Numerical analysis of blood flow in the heart. *Journal of Computational Physics*, 25(3):220–252, 1977.

[77] Isabelle Ramière, Philippe Angot, and Michel Belliard. A fictitious domain approach with spread interface for elliptic problems with general boundary conditions. *Computer Methods in Applied Mechanics and Engineering*, 196(4-6):766–781, jan 2007.

[78] Isabelle Ramiere, Philippe Angot, and Michel Belliard. A fictitious domain approach with spread interface for elliptic problems with general boundary conditions. *Computer Methods in Applied Mechanics and Engineering*, 196(4-6):766–781, 2007.

[79] Teluo Sakurai, Katsunori Yoshimatsu, Naoya Okamoto, and Kai Schneider. Volume penalization for inhomogeneous Neumann boundary conditions modeling scalar flux in complicated geometry. *Journal of Computational Physics*, 390:452–469, aug 2019.

[80] Ramakrishnan Thirumalaisamy, Nishant Nangia, and Amneet Pal Singh Bhalla. Critique on "Volume penalization for inhomogeneous Neumann boundary conditions modeling scalar flux in complicated geometry". *Journal of Computational Physics*, 433:110163, may 2021.

[81] Ramakrishnan Thirumalaisamy, Neelesh A Patankar, and Amneet Pal Singh Bhalla. Handling neumann and robin boundary conditions in a fictitious domain volume penalization framework. *arXiv preprint arXiv:2101.02806*, 2021.

[82] R. Verfurth. A posteriori error estimators for the Stokes equations. *Numerische Mathematik*, 55(3):309–325, may 1989.

[83] R. Verfurth. A Posteriori Error Estimates for Nonlinear Problems. Finite Element Discretizations of Elliptic Equations. *Mathematics of Computation*, 62(206):445, apr 1994.